



HAL
open science

Synthesis of functionalized polyamide 6 by anionic ring-opening polymerization

Deniz Tunc

► **To cite this version:**

Deniz Tunc. Synthesis of functionalized polyamide 6 by anionic ring-opening polymerization. *Polymers*. Université de Bordeaux; Université de Liège, 2014. English. NNT : 2014BORD0178 . tel-01281327

HAL Id: tel-01281327

<https://theses.hal.science/tel-01281327>

Submitted on 2 Mar 2016

HAL is a multi-disciplinary open access archive for the deposit and dissemination of scientific research documents, whether they are published or not. The documents may come from teaching and research institutions in France or abroad, or from public or private research centers.

L'archive ouverte pluridisciplinaire **HAL**, est destinée au dépôt et à la diffusion de documents scientifiques de niveau recherche, publiés ou non, émanant des établissements d'enseignement et de recherche français ou étrangers, des laboratoires publics ou privés.

THÈSE PRÉSENTÉE
POUR OBTENIR LE GRADE DE
DOCTEUR DE
L'UNIVERSITÉ DE BORDEAUX
ET
DE L'UNIVERSITÉ DE LIEGE

ÉCOLE DOCTORALE DE SCIENCES CHIMIQUES (Université de Bordeaux)

ÉCOLE DOCTORALE DE CHIMIE (Université de Liège)

SPÉCIALITÉ POLYMERES

Par Deniz TUNC

**Synthesis of functionalized polyamide 6 by anionic ring-opening
polymerization**

Sous la direction de Stéphane CARLOTTI et Philippe LECOMTE

Soutenue le 30 octobre 2014

Membres du jury:

M. PERUCH, Frédéric
M. HOOGENBOOM, Richard
M. MONTEIL, Vincent
M. YAGCI, Yusuf
M. AMEDURI, Bruno
M. SERVANT, Laurent

Directeur de recherche, Université de Bordeaux
Professeur, Ghent University
Chargé de recherche, Université Claude Bernard
Professeur, Istanbul Technical University
Directeur de recherche, Institut Charles Gerhardt
Professeur, Université de Bordeaux

Président
Rapporteur
Rapporteur
Examineur
Examineur
Invité

Preamble

This PhD had been performed within the framework of the IDS FunMat joint doctoral programme. IDS-FunMat is “International Doctoral School in Functional Materials” funded by ERASMUS MUNDUS Programme of the European Union.

IDS FunMat PhD School offers PhD project in Functional Material Science which has to be carried out in co-supervision between universities from different countries. In most projects, an industrial partner is also involved. As one of the criteria, PhD candidate must spend at least 6 months in each university and ideally 1.5 year in each of the university.

In this PhD project, two partner universities were University of Bordeaux (LCPO, France) and University of Liège (CERM, Belgium), BASF (Ludwingshafen , Germany) was the industrial partner.



International Doctoral School
in Functional Materials
for Energy, Information Technology and Health



TABLE OF CONTENTS

Acknowledgment.....	i-ii
List of Abbreviations.....	iii-v
General Introduction.....	1

Chapter I. Literature Review: Synthesis and Functionalization of Polyamides

Introduction	13
1. Synthesis of aliphatic polyamides	14
1.1. Synthesis of aliphatic polyamides by polycondensation	14
1.2. Anionic ring-opening polymerization of cyclic amides (lactams)	14
1.2.1. Mechanism of the anionic polymerization of lactams	15
1.3. Anionic (co)polymerization of ϵ-caprolactam and ω-laurolactam.....	24
1.3.1. Homopolymerization of ϵ -caprolactam and ω -laurolactam	24
1.3.2. Copolymerization of ϵ -caprolactam and ω -laurolactam	26
1.3.3. Copolymerization of Lactams and Lactones.....	26
1.3.4. Polyamide-based copolymers with non-polyamide blocks.....	27
1.3.5. Industrial processes using AROP of ϵ -caprolactam and ω -laurolactam..	28
1.4. Anionic polymerization of other lactams	29
1.4.1. β -lactams	29
1.4.2. 2-pyrrolidone	30
1.4.3. 2-piperidone	31
1.4.4. Bicyclic lactams	31
2. Synthesis of aromatic polyamides.....	32
2.1. Step-growth condensation polymerization.....	33
2.2. Chain-growth condensation polymerization	34

2.2.1.	Mechanism of the polymerization: synthesis of aromatic polyamides ..	37
2.3.	Synthesis of copolymers based on aromatic polyamide by chain-growth polycondensation	42
2.3.1.	Sequential condensative chain polymerization.....	42
2.3.2.	Block copolymers by a coupling reaction	44
2.3.3.	Macro-initiator approach	47
2.4.	Complex architectures of aromatic polyamides	49
3.	Crosslinking of polyamide 6	50
3.1.	Radiation crosslinking of polyamide 6	50
3.2.	Crosslinked polyamide 6 by chemical modification.....	51
3.3.	Stimuli Responsive Polymers	53
3.3.1.	pH and thermo responsive groups	53
3.3.2.	Photoresponsive groups	54
3.4.	Photoreactions	55
3.4.1.	Photoisomerization	55
3.4.2.	Photocleavage	57
3.4.3.	Photodimerization	57
4.	Fluorinated aromatic and aliphatic polyamides.....	63
4.1.	Multilayered film preparation.....	64
4.2.	Blending hydrophilic and hydrophobic polymers	65
4.3.	Surface modification.....	65
4.4.	Incorporation of fluoro-monomer to polyamide by copolymerization	65
4.4.1.	Aromatic fluorinated polyamides.....	66
4.4.2.	Aliphatic fluorinated polyamides	67
	Conclusion.....	70
	References.....	71

Chapter II. Copolymerization of ϵ -caprolactam and fluorinated derivatives for increased surface hydrophobicity and thermal stability of polyamide 6

Introduction	86
1. Synthesis of polyamide 6 with fluorinated moieties	89
2. Rate of polymerization.....	94
3. Polymer characterization by NMR and ATR-IR	95
4. Thermal characteristics of modified polyamide 6 and investigation of degradation mechanism	98
5. Hydrophobicity and Water Uptake Determination	106
Conclusion	109
Experimental and supporting informations	111
Annexe: Supporting Information	114
References.....	121

Chapter III. Synthesis of reversible and irreversible crosslinked polyamide 6

Introduction	128
1. Synthesis of irreversible crosslinked polyamide 6	129
1.1. Synthesis of polyamide 6	130
1.2. Synthesis of bis-caprolactam from cyclic lysine.....	131
1.3. Synthesis of crosslinked polyamide 6	133
1.4. Characterization of crosslinked polyamide 6	136
2. Toward Reversible Crosslinked Polyamide 6.....	141
2.1. Synthesis of α-cinnamoylamido-ϵ-caprolactam	143

2.2. Copolymerization and crosslinking	144
2.3. Reversibility: De-crosslinking and re-crosslinking.....	154
Conclusion	157
Experimental and supporting information	159
Annexe: Supporting Information	165
References.....	178

Chapter IV. Synthesis of Aliphatic-Aromatic Copolyamides by Combination of Anionic Ring Opening Polymerization and Chain- Growth Condensation Polymerization

Introduction	186
1. Tuning the conditions for aliphatic-aromatic copolyamide synthesis	187
1.1. Effect of reaction temperature on chain growth condensation polymers	188
1.2. Effect of the activator on polymerization of ϵ -caprolactam.....	193
1.3. Effect of the initiator on polymerization of ϵ -caprolactam	195
2. Synthesis of aliphatic-aromatic copolyamide.....	197
3. Thermo-mechanical properties of polyamide 6 containing aromatic units	204
Conclusion	209
Experimental and supporting information.....	211
Annexe: Supporting Information	214
References.....	220

General Conclusion and Perspectives.....	223
--	-----

Acknowledgment

First of all, I would like to thank my thesis supervisors, Prof. Stéphane Carlotti and Dr. Philippe Lecomte, for giving me the great opportunity to work in their groups, encouraging my research and also for allowing me to grow as a research scientist. Stéphane, I thank you very much for giving me positive view on many things, your enthusiasm and motivation. Philippe, I want to thank you for your advices, help, support and for taking the time to guide me in scientific aspects.

I also want to express my thanks to our industrial collaborator Dr. Philippe Desbois for his kindness, help, providing professional advice on my thesis and also for giving me the opportunity to work with BASF chemical company.

I would also like to thank my committee members, Prof. Yusuf Yagci, Prof. Richard Hoogenboom, Dr. Bruno Ameduri, Dr. Frederic Peruch, Dr. Vincent Monteil and Prof. Laurent Servant for being as my committee members. I also want to thank you for letting my defense be an enjoyable moment, and for your brilliant comments and suggestions, thanks to you.

I want to deeply thank to Prof. Daniel Taton and Prof. Henri Cramail for being kind, helpful and supportive to me. I am also thankful to Mr. Gérard Dimier, Mr. Emmanuel Ibarboure and Mr. Cedric Le Coz for performing several number of DMA and AFM analyses throughout my research.

During my thesis, I had the opportunity to work in a multinational environment with friendly people. I wish to thank all the past and present members of “LCPO” and “CERM” groups for their help, friendship and the nice environment they created not only inside, but also outside the lab. Thus, my warm thanks will go to my friends from old generation Axel, Anna-Louise, Samira, Nico and Christos for their kindness and for making me forget about living far from home. I thank to Ozlem, Vusale and Mamatimin for their help, being so supportive and for their unique friendship.

In particular, I would like to thank to Eleni, Efthycia, Dimitri, Hassen, Océane, Geoffrey, An, Camille, Audrey, Kevin, Mikaél, Edgar and Anne-Louise for being so helpful, supportive and positive. I want to say thanks to Catherine Roulinat, strongest woman and mother of the lab, for being so nice, helpful, kind and for encouraging me always.

Especially, I also would like to thank to Prof. Christine Jérôme, Dr. Mikael Alexandre, Dr. Christophe Detrembleur, Dr. Antoine Debuigne, Dr. Benoît Clément, Dr. Bruno Grignard, Dr. Farid Ouhib, Dr. Raphaël Riva, Dr. Jean-Michel Thomassin, Dr. Florence Croisier, Daniela Cordella, Veronica Collard, Mirco Tomasetti, Pierino Malizia, Stéphanie Vanslambrouck, Mathilde Weiss-Maurin, Grégory Cartigny, Valérie Collard, Charlotte Dannemark, Laetitia de Fays, Martine Dejeneffe, Sophie Boulanger and Enza Esposito for being so helpful and kind to me during the great times in Liege.

I would also like to thank to IDS-FunMat international doctoral school with all members, especially to Prof. Jean Etourneau, Prof. Laurent Servant, Audrey Sidobre and Marianne

Acknowledgment

Delmas, for giving me chance to have international work experience with different working cultures and a great opportunity to meet all nice people from all around the world: Henu, Maryna, Begum, Mariel, Daniel, Jaroslaw, Marie and all IDS people.

Special thanks to Mathilde, Mercedes, Zeynep and Hanbin for being wonderful and unforgettable true friends to me and sharing these three years with me not only in good times but also in tough times. I thank to you for your kindness, supporting and great unique friendship. I wish to express my warm thanks to my BFF Winnie for being with me, helping and supporting.

I would also like to thank all of my old and new friends from Turkey who supported me during writing, and encouraged me to strive towards my goal; Gokhan, Songul, Zeynep, Gulsah, Burcin, Tugba, Doruk, Damla, Ibrahim and Gizem.

A special thanks to my family. Words cannot express my thanks to my mother, my father and my sisters for all of the sacrifices that you've made on my behalf. Your supports for me was what sustained me thus far. I am deeply grateful to my mother Nurhayat Tunc, my father Ibrahim Halil Tunc and the sparkling of my eyes, my little sisters, Duygu Tunc and Aleyna Dilek Tunc for their endless love, care, faith, support and understanding throughout my life. At the end I would like express appreciation to my beloved husband (soul mate-friend-love..) Selim Beyazit who spent sleepless nights for me and was always my support with his unconditional love and care, confidence, patience, support and encouragement.

Finally, I would like to dedicate this thesis to my Family.

October, 2014

Deniz TUNC

List of Abbreviations

- AIBN: 2,2-azo-bis(isobutyronitrile)
AM: activated monomer
AROP: anionic ring-opening polymerization
ATRC: atom transfer radical coupling
CA: contact angle
CGCP: chain-growth condensation polymerization
CL: ϵ -caprolactam
C10: sodium ϵ -caprolactam
C20: hexamethylene-1, 6-dicarbamoylcaprolactam
CTA: chain transfer agent
 \bar{D} : dispersity
DCM: dichloromethane
 ΔH_m : melting enthalpy
 ΔH_c : crystallization enthalpy
diPA: diblockpolybenzamide
DP: degree of polymerization
DMA: dynamic mechanical analysis
DMSO: dimethyl sulfoxide
DSC: differential scanning calorimetry
 E' : storage modulus
 E'' : loss modulus
EDG: electron-donating group
EtONa: sodium ethoxide
EWG: electron withdrawing group
 G' : storage modulus
 G'' : loss modulus
HCl: hydrochloric acid

List of abbreviations

HFIP: hexafluoro isopropanol

I: inductive

KLCL: γ -ethylene ketal- ϵ -caprolactam

LG: leaving group

LiHMDS: lithium bis(trimethylsilyl)amide

MAS NMR: magic angle spinning nuclear magnetic resonance

MeONa: sodiummethoxide

Mn: number average molar mass

MI: macroinitiator

Mw: weight average molar mass

NaHMDS: sodium bis(trimethylsilyl)amide

NMR: nuclear magnetic resonance

P: poly

PA: polybenzamide homopolymer

PA6: polyamide 6

PA6-6: polyamide 6-6

PA6-10: polyamide 6-10

PMAA: poly (methylacrylate)

PMMA: poly (methylmethacrylate)

PNIPAM: polyacrylamides

R: resonance

RAFT: reversible addition-fragmentation chain transfer

RIM: reaction injection molding

RTM: resin transfer molding

SGCP: step-growth condensation polymerization

SEC: size exclusion chromatography

Tan δ : loss factor

tBuOK: potassium *ter*-butoxide

Tc: crystallization temperature

Td: degradation temperature

TEA: triethyl amine

Tg: glass transition temperature

TGA: thermogravimetric analysis

THF: tetrahydro furan

Tm: melting point

UV: ultraviolet

WCA: water contact angle

w-LL: w-lauro lactam

General Introduction

General Introduction

Today, emerging needs to advanced materials force to develop more complex materials. In particular, the improvements on all kind of thermal and mechanical properties of polymeric materials are still substantial issues of material science. Moreover, the recyclability of polymeric materials is a crucial solution for the prevention of environmental pollution.

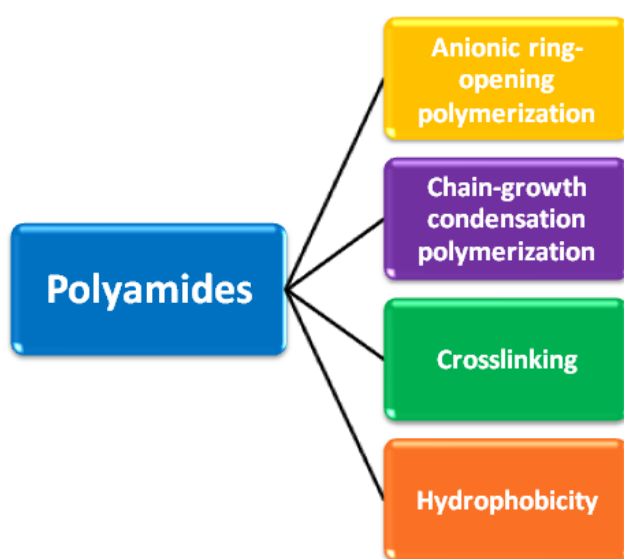
The reduction of the energy consumption and the implementation of new technologies dedicated to the production of green energy for a sustainable development are nowadays major priorities for governments all around the world and will have a steadily increasing impact in the everyday life of all human beings. Companies are more and more integrating this problematic in their research and development policies and are trying to propose new alternatives. This project is focused on the preparation of polyamides for composites in mainly Automotive and Wind Turbine applications. Many “plastic” parts are already used in cars but the next challenge for the car producers is to remove all heavy metal components by lighter materials in order to reduce consumption of energy and therefore release of CO₂. For the wind turbines, the blades are already built with composite materials which permit to precisely tune their mechanical characteristics such as profile or mass variation and optimize the conversion of the mechanical wind energy to electrical one. The majority of polymer resins used with glass, carbon, aramid and other fibers are Polyesters and Epoxy thermosets. It means that they are crosslinked and not recyclable. Thermoplastics appear today as the alternative as far as their processing remains simple permitting the production of pieces at low price.

Polyamide has also gained great interest in textile, building construction and furniture, electronic devices, and packaging areas by offering toughness and strength as well as heat and chemical resistance. Particularly, global production of polyamides reached to 6.5 million tons in 2006.

Since the discovery of aliphatic polyamides (nylons), the development of industrial processes based on polyamide 6 and polyamide 6-6 constitutes an important part of “engineering plastics” area today. Synthesis of polyamide 6 by anionic ring-opening polymerization provides good mechanical properties (stiffness/toughness balance), chemical resistance (automotive fluids), long term heat ageing performance, processability

(flowability, cycle time and recycling) and excellent cost. Interestingly enough, polyamide 6 is produced by the ring-opening polymerization of ϵ -caprolactam. Owing to the low price of this monomer as compared to epoxy resins (2.5 times cheaper) and to its recyclability, the use of polyamide 6 as a resin for composites becomes appealing. Tuning of its properties and processability will permit the replacement of epoxy and polyester resins and the use of new composites in the fields mentioned above. Ring-opening polymerization of lactams^{1, 2} was preferred for this project due to fast rates (few minutes) of polymerization between 100 and 200 °C as compared to polycondensation reactions, the other way to synthesize polyamides, where days at more than 220 °C are needed.

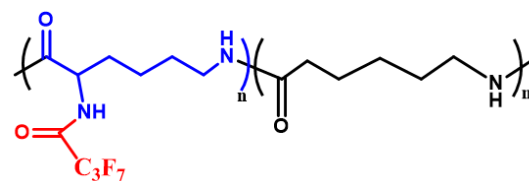
On the other hand, designing novel anionic polyamides and improving their current properties by controlling (co)polymerization reactions has achieved an important demand which must be improved and completed. Further developing and multiplying of the current material properties are still needed to compensate demands of today's and future's industry.



The goal of this thesis is to synthesize anionic aliphatic polyamides and their crosslinked, fluorinated and aromatic derivatives to decrease creep, improve surface hydrophobicity and improve thermal properties of anionic polyamide 6 and combine this challenging chemistry with different comonomers and methods. **Chapter I** provides a general bibliographic overview of

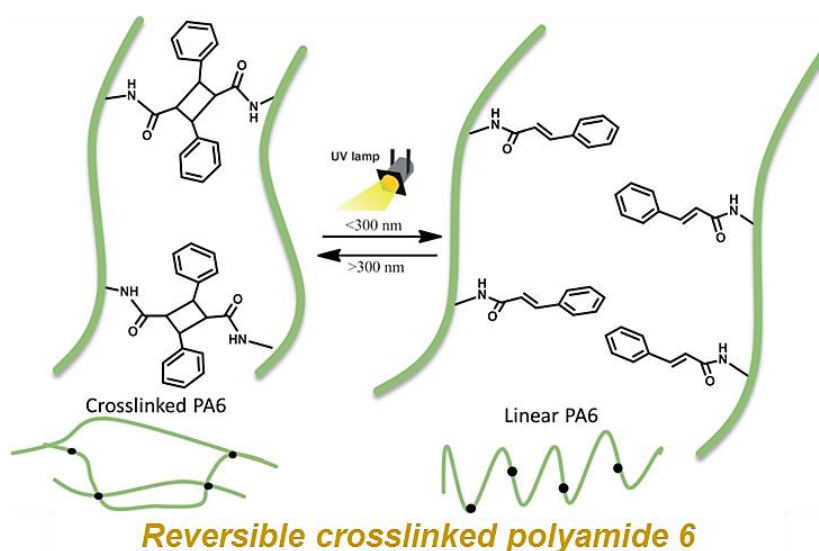
anionic ring-opening polymerization of ϵ -caprolactam (side reactions, copolymerizations and industrial processing) and other type of lactams, different type of aromatic polyamides syntheses such as linear, block, star and graft by chain-growth condensation polymerization, reversible or irreversible crosslinking systems via stimuli responsive functional groups, and fluorinated aromatic and/or aliphatic polyamides with hydrophobicity and thermal properties.

The study presented in the **Chapter II** of the thesis describes synthesis of polyamide 6 bearing pendant fluorinated groups by AROP of perfluorobutyryl-substituted α -amino- ϵ -caprolactam and ϵ -caprolactam to achieve hydrophobic polyamide surfaces. This fluorinated compound was obtained by the reaction between cyclic lysine (*i.e.* α -amino- ϵ -caprolactam) and perfluorobutyrylchloride. The effect of the fluorinated comonomer amount on AROP of ϵ -caprolactam was studied by following thermo-time changing and then the thermo-mechanical properties of the corresponding polymers were investigated.



*fluorinated polyamide 6
by anionic ring-opening polymerization*

Despite a possible loss of recyclability, crosslinked polyamide appeared attractive in order to limit the creep which is generally observed with linear structure. The first part of **Chapter III** is devoted to controlled synthesis of crosslinked polyamide 6 via using novel crosslinkers which are derivatives of α -amino- ϵ -caprolactam. Crosslinked polyamide 6 is investigated in term of rate of polymerization, thermal and rheological properties for an eventual processability at moderate temperature. Swelling degrees of crosslinked polymers with

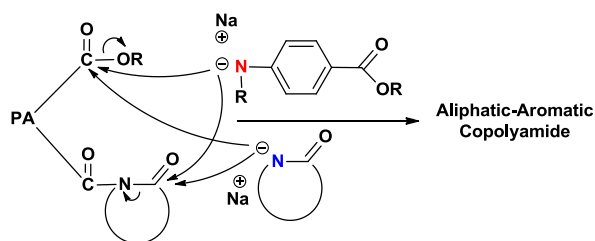


increasing amount of crosslinker are measured. Considering reversible crosslinking, polymers having cinnamoyl group exhibited excellent photoreactivity and crosslinking upon UV light irradiation or heating by dimerization reaction. The second part of **Chapter III**

states the synthesizing a novel photo- and thermosensitive polyamide 6 by anionic ring-opening copolymerization of ϵ -caprolactam and α -cinnamoylamido- ϵ -caprolactam (novel comonomer, derivative of α -amino- ϵ -caprolactam). The photochemical “reversible”

crosslinking of solutions and thermal crosslinking of spin-coated films made up of these new cinnamoyl-functionalized polyamides was monitored by UV-visible spectroscopy.

Finally, **Chapter IV** proposes a combination of chain-growth condensation polymerization³ (CGCP) and AROP in one-step reaction where both polymerization mechanisms are based on a nucleophilic



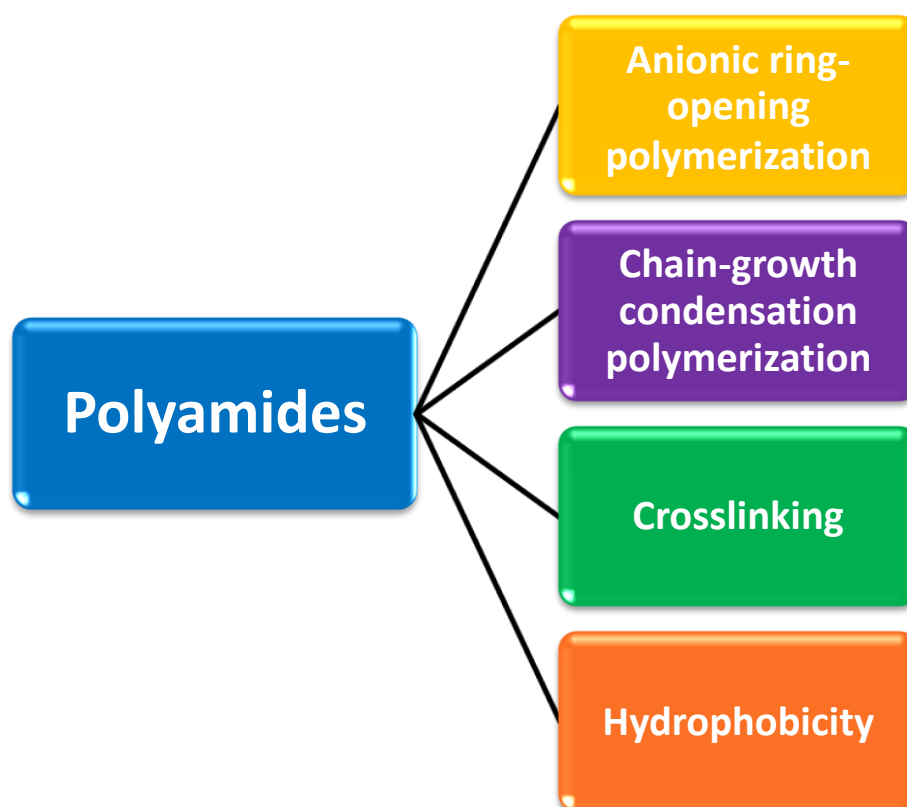
attack of the activated monomers onto chain ends. Preparing of high-performance aliphatic polyamide containing aromatic groups in the polymer backbone is conducted from ethyl 4-butylaminobenzoate in order to improve chemical stability and thermal performance.

References:

1. R. Puffr, in *Lactam-Based Polyamides*, ed. R. P. a. V. Kubánek, CRC Press, Boca Raton, FL, 1991, vol. 1.
2. K. Hashimoto, *Progress in Polymer Science*, 2000, **25**, 1411-1462.
3. T. Ohishi, R. Sugi, A. Yokoyama and T. Yokozawa, *Journal of Polymer Science Part A: Polymer Chemistry*, 2006, **44**, 4990-5003.

Chapter I

Literature Review: Synthesis and Functionalization of Polyamides



Keywords : *Anionic ring-opening polymerization, chain-growth condensation polymerization, step-growth polymerization, stimuli responsive polymers, crosslinked polyamide, hydrophobic polyamides.*

Summary: The theoretical part of this thesis provides a general overview of aliphatic and/or aromatic polyamides syntheses mechanisms.

Among reviewed methods, major attention is paid especially to anionic ring-opening (co)polymerization (AROP) of ϵ -caprolactam since every single chapter study of this thesis is based on AROP. Therefore, there is great importance of better understanding of the AROP mechanism, its side reactions, industrial processability, and copolymerization capability to shed light on our further investigations.

Another predominance of this chapter is the chain-growth condensation polymerization (CGCP) for aromatic polyamide synthesis. As well as CGCP strategy, all copolymerization possibilities are summarized.

As part of our continuing interest in developing copolymerization and functionalization of polyamide 6, crosslinking methods of polyamide 6, stimuli responsive polymers (which has a great potential to control polymer properties), and fluorinated aliphatic/aromatic polyamides are also reviewed. These all nicely studied and reviewed works are summarized here particularly over anionic mechanism of polyamide 6 synthesis.

Chapter I

Literature Review: Synthesis and Functionalization of Polyamides

TABLE OF CONTENTS

Introduction	13
1. Synthesis of aliphatic polyamides	14
1.1. Synthesis of aliphatic polyamides by polycondensation	14
1.2. Anionic ring-opening polymerization of cyclic amides (lactams)	14
1.2.1. Mechanism of the anionic polymerization of lactams	15
1.3. Anionic (co)polymerization of ϵ-caprolactam and ω-laurolactam.....	24
1.3.1. Homopolymerization of ϵ -caprolactam and ω -laurolactam	24
1.3.2. Copolymerization of ϵ -caprolactam and ω -laurolactam	26
1.3.3. Copolymerization of Lactams and Lactones.....	26
1.3.4. Polyamide-based copolymers with non-polyamide blocks.....	27
1.3.5. Industrial processes using AROP of ϵ -caprolactam and ω -laurolactam..	28
1.4. Anionic polymerization of other lactams	29
1.4.1. β -lactams	29
1.4.2. 2-pyrrolidone	30
1.4.3. 2-piperidone	31
1.4.4. Bicyclic lactams	31
2. Synthesis of aromatic polyamides.....	32
2.1. Step-growth condensation polymerization.....	33
2.2. Chain-growth condensation polymerization	34

2.2.1. Mechanism of the polymerization: synthesis of aromatic polyamides ..	37
2.3.Synthesis of copolymers based on aromatic polyamide by chain-growth polycondensation	42
2.3.1. Sequential condensative chain polymerization.....	42
2.3.2. Block copolymers by a coupling reaction	44
2.3.3. Macro-initiator approach	47
2.4. Complex architectures of aromatic polyamides	49
3. Crosslinking of polyamide 6	50
3.1. Radiation crosslinking of polyamide 6	50
3.2. Crosslinked polyamide 6 by chemical modification	51
3.3. Stimuli Responsive Polymers	53
3.3.1. pH and thermo responsive groups	53
3.3.2. Photoresponsive groups	54
3.4. Photoreactions	55
3.4.1. Photoisomerization	55
3.4.2. Photocleavage	57
3.4.3. Photodimerization	57
4. Fluorinated aromatic and aliphatic polyamides.....	63
4.1. Multilayered film preparation.....	64
4.2. Blending hydrophilic and hydrophobic polymers	65
4.3. Surface modification.....	65
4.4. Incorporation of fluoro-monomer to polyamide by copolymerization	65
4.4.1. Aromatic fluorinated polyamides.....	66
4.4.2. Aliphatic fluorinated polyamides	67
Conclusion	70
References.....	71

Introduction

Polyamides are well known polymers and present in markets such as fibers, engineering plastics and specialties, due to specific and various properties depending on their structures.

Polyamide 6 (PA6) is one of the most versatile engineering thermoplastic. Thermoplastic materials are very popular in broad range of markets. The excellent properties of PA6 such as impact strength, stiffness, solvent resistance owing to the strong interchain attraction derived from the polarity of amide (*CONH*) groups, PA6 is a remarkable candidate as a lightweight material for metal replacement applications. Even though these attractive properties, moisture absorption of the amide groups causes some drawbacks in PA6. Uptaken moisture has a plasticizing effect and reduces tensile strength and modulus. PA6 components are not used successfully in all engineering applications because of less rigidity. Lack of rigidity leads to difficult fabrication of PA6 components since it needs to be more moisture free before processing. Modification of the moisture absorbance of PA6 may result in anything from hard and stiff to soft and flexible material.

On the other hand, impact strength or toughness is a complex mechanical property. The toughening mechanisms are influenced by the properties of the matrix material and by the morphology of the blend. Mechanical and thermal properties of all aliphatic polyamides can be reinforced with different methods and various modifiers such as glass fibers, glass beads, and carbon fibers. An approach may require the changes in the functionality of the basic components before their polymerization, either early monomer preparation or modification of the polymer. This would end up in different types of polymer structures (block, random, crosslinked etc.).

PA6 has attained a massive interest due to its high strength, good fatigue resistance, excellent bend recovery rate and good resistance to most common solvents and weak acids¹. As well as those attractive properties, applications of polyamides often need to solve problems in their fabrication such as poor solubility, moisture absorption and high softening or melting temperatures caused by high crystallinity. Crosslinking is one of the methods to exceed these problems. On the other hand, the reversibility of their crosslinking has also significant potential to promote a wider range of applications of PA6 as a responsive polymer.

1. Synthesis of aliphatic polyamides

Synthesis of aliphatic polyamide can be divided into two ways: polycondensation (1) and anionic ring-opening polymerization (AROP) (2). Next paragraph is explaining the advantages of AROP over polycondensation and most common polyamide examples from both polymerization techniques.

1.1. Synthesis of aliphatic polyamides by polycondensation

Polycondensation is one of the methods to obtain aliphatic polyamides. Polycondensation is generally conducted at higher temperatures than the melting point of the resulting polymers to eliminate the released volatile products such as water or alcohol. Synthesis of aliphatic polyamides is carried out by reaction of difunctional carboxylic acids or acid chloride groups and amino groups. But resulting polymers have still some water in the polymerization atmosphere even though the polymerization is studied at higher temperature. The presence of water after polycondensation reduced the thermal and mechanical properties because of the plasticizing effect of water. Hydrolytic polyaddition/polycondensation reaction of ϵ -caprolactam at 250 °C for 72h gives PA6. For example, polyamide 6-6 (PA6-6) is synthesized via polycondensation reaction of adipic acid and hexamethylenediamine by eliminating water. Other polyamide examples are polyamide 6-10 (PA6-10) from hexamethylenediamine and sebacic acid and polyamide 4-6 (PA4-6) from butane-1,4-diamine and adipic acid. Even though all polyamides seem quite similar but their thermal and mechanical properties are very different. For example, PA6-6 has a higher crystallinity and a lower water uptake, therefore a higher chemical resistance, than PA6. However, PA6 has a lower melting temperature which makes it attractive for the easy processability in the industrial area.

1.2. Anionic ring-opening polymerization of cyclic amides (lactams)

Ring-opening polymerization of lactams (cyclic amides) initiated by water, referred to hydrolytic polymerization (i.e. reactions between the amine chain-end group and the lactam and/or carboxylic group of its hydrolyzed derivate), is carried out for industrial polymerization of ϵ -caprolactam (CL) to form PA6, though PA6-6, PA4-6, PA6-10 are

synthesized by stepwise reactions of a diacid monomer with a diamine monomer. Cationic initiation is also possible but not useful because of the low conversion and molar mass of the resulting polyamides². Anionic initiation following an activated monomer mechanism is mainly used for polymerization in molds in order to prepare polyamides (PA6, PA10, PA12) directly from the corresponding lactams³. Polymerization mechanism of lactams, their polymerizability and the properties of the resulting polymers were largely investigated. Fundamental reviews published by Reimschuessel^{4, 5}, Sebenda⁶, Sekiguchi², Hashimoto⁷, Roda⁸ and Russo⁹ can be found and precise this presented overview.

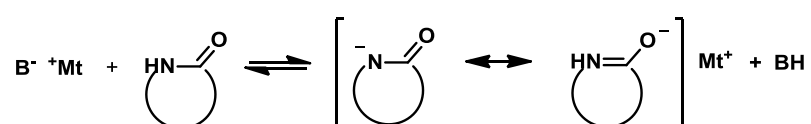
The anionic route is the fastest method for producing polyamides due to a low activation energy needed. This fast kinetic makes nowadays this route of high interest for industrial processes producing lightweight composite materials for automotive industry and wind energy. The anionic polymerization of lactams may be accomplished in solution or in bulk either below or above the melting point of the polymer for the latter.

1.2.1. Mechanism of the anionic polymerization of lactams

The mechanism differs from the anionic polymerization of most of the unsaturated and heterocyclic monomers because the growth center is not an anionically activated end group, but is represented by an *N*-acylated neutral chain. The anionic polymerization of lactams is initiated, under anhydrous conditions, by formation of the lactamate anion. Strong bases are able to deprotonate lactams and produce *N* anion of lactam effective for initiating the polymerization.

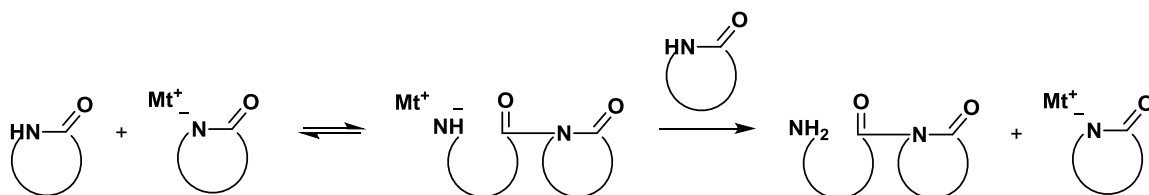
1.2.1.1. Initiating and activating systems

The anionically activated species is the monomer in the form of lactamate anion which is a very strong nucleophile (Scheme I-1). The negative charge is delocalized on the amide group due to resonance stabilization by conjugation with the carbonyl group.



Scheme I-1. Structures of the anionically activated monomer.

The lactamate anion is acylated by a lactam monomer, although the acylating ability of the latter is poor, with the amide group being stabilized by resonance. The lactamate anion reacts with the monomer by a ring-opening transamidation reaction forming *N*-acyl lactam structures carrying primary amine anions. Assuming a free ion mechanism⁶, the imide anion is formed, in the first slow step, by nucleophilic attack of the lactamate on the carbonyl of the lactam molecule (Scheme I-2). As it is not stabilized by resonance, rapid proton exchange undergoes with lactam monomer, yielding imide dimer (*N*-acyl lactam) and regenerating the lactamate. Result of these two combined reactions is the disproportionation between two amide groups (present in lactam monomer and in lactamate anion) to give amine and acyl lactam moieties (in the *N*-acyl lactam species) and the reaction rate dependent on factors like the nature of counter-ion and reaction medium, lactam ring size, substituents, and structure of the resulting linear monomeric unit. *N*-substituted lactams are observed to react with lactamate anion with a rate significantly higher than that of the initial reaction, depending on the size and the electrophilicity of the substituent, and are generally used as activators in the activated anionic polymerization. The use of high reaction temperatures (> 250 °C) is required in the absence of activator and only the more reactive lactams, such as CL, undergo polymerization in the presence of a strong base in a non-activated method.



Scheme I-2. Nucleophilic attack of lactamate anion to a lactam.

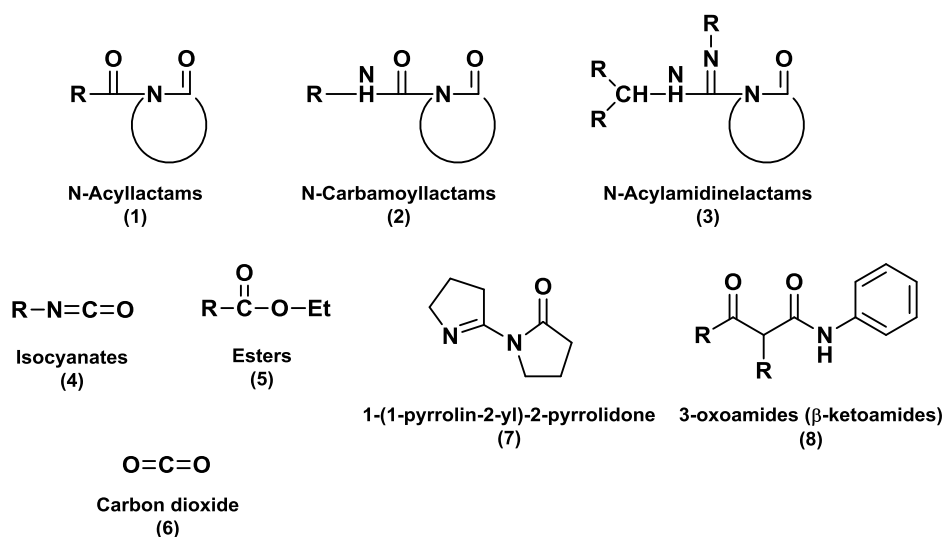
The initiators, which are the monomers carrying the anionic charge able to attack the chain end, are prepared by reaction of a lactam with strong bases such as mainly metal alkoxide¹⁰, metal halide¹¹, alkali metal², and grignard reagent¹², but also pentamethylene guanidine¹³, quaternary ammonium salts¹⁴, phosphazene¹⁵, bicyclic 'superbase' protophosphatranes^{16, 17} or carbene¹⁸. The association of a strong base (NaH, LiH, BuLi) with a reducing agent such metal dialkyl/dialkoxy aluminium hydrides^{19, 20} or metal dialkylboron hydride can be used also as precursors of lactamates. In this case, the nucleophilic species

obtained, *i.e.* the activated monomer, is a metal salt of 2-(dialkyoxyaluminoy)-1-azacycloheptane.

As usual in anionic polymerization, the nature and concentration of the initiator play a crucial role. The rate is directly related to the concentration of active species and in particular the dissociation constant yielding free ions. It is known that the concentration of free lactam anion increases with temperature, starting to be predominant above 150 °C, and the alkali metal lactamates are considered completely dissociated at higher temperatures. The rate of polymerization becomes here independent of the nature of the cation²¹. In general, the activity of alkali metals follows the order of electropositivity, except with Li and despite its highest ionization energy: $\text{Na}^+ < \text{Li}^+ < \text{K}^+ < \text{Cs}^+ = \text{R}_4\text{N}^+$. Lactamates of transition metals (e.g. Cr^{3+}) and other metals (e.g. Al^{3+}), which are exhibiting high values of electronegativity and having very low dissociation constants, hardly dissociate even at high temperatures. In the molten monomer medium, without solvating or complex species, the lactamate dissociation depends on both the lactam properties (*i.e.*, acidity, dielectric permittivity, donor-acceptor capability, substituents) and the electropositivity of the metal. For example, higher lactam permittivity, such as in ω -lauro lactam as compared to CL makes easier the salt dissociation²².

As an induction period and slow kinetics are observed with non-activated anionic polymerization of lactams, opposite behaviors are obtained when an activator is added. The induction period is absent and the AROP can be performed at much lower temperatures (130-180 °C for CL)⁶. Poorly reactive lactams, such as 2-pyrrolidone and 2-piperidone, can be polymerized by initial reaction of monomers with an acylating agent. In this activated mechanism, the slow self-initiation step is strongly minimized to the detriment of a fast acylation reaction and propagation step. The interest to work with milder conditions for shorter times is to strongly reduce side reactions, yielding more regular macromolecular chains. These observations are nevertheless dependent of the structure and concentration of the activators. Among the substances used, *N*-substituted lactams such as *N*-acyllactam (1)^{13, 23} and carbamoyl type (2)^{12, 24-27} with electronegative substituent (R) increasing the acylating ability of the cyclic acyl group, as well as compounds capable of producing *N*-substituted lactams, under the conditions of the anionic polymerization, by addition or substituent reactions (e.g. isocyanate (4), acidhalides or esters (5), carbon dioxide (6)^{23, 28-30})

and those derivatives from side reactions (C-, N-, O- Acylation) in low ring strain lactam monomers such as oxoamides type (8), *N*-acylamidine (3) and other types (7) (Scheme I-3).

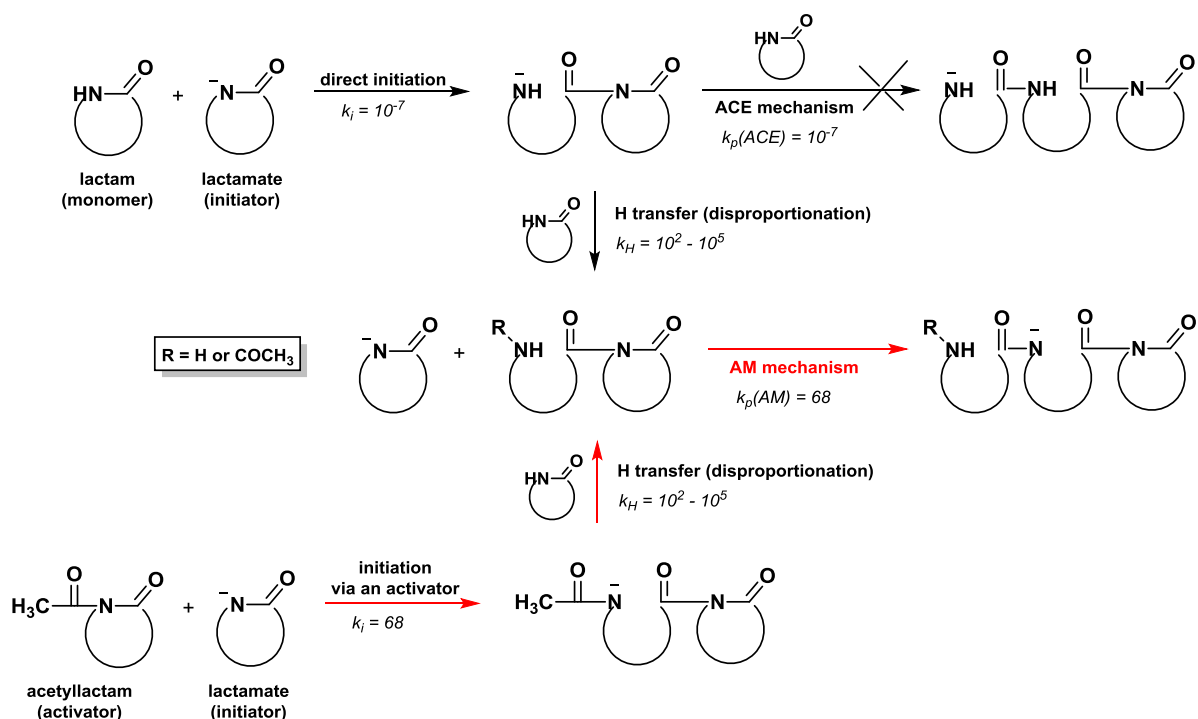


Scheme I-3. Main activators in anionic lactam ring-opening polymerization.

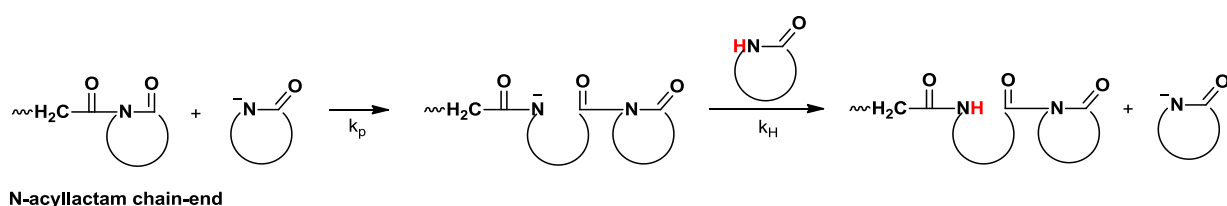
1.2.1.2. Propagation reaction

The slow formation of an *N*-acyllactam by reaction between monomer and lactamate ion ($k_i = 10^{-7} \text{ L}\cdot\text{mol}^{-1}\cdot\text{s}^{-1}$ for sodium ϵ -caprolactamate between 160-190 °C)³¹ is followed by an extremely fast neutralisation reaction, i.e. the monomer deprotonation. For pyrrolidone at 35 °C and lauro lactam at 160 °C, the rate constant of proton exchange (k_H) is $10^5 \text{ L}\cdot\text{mol}^{-1}\cdot\text{s}^{-1}$ ³² and $10^2 \text{ L}\cdot\text{mol}^{-1}\cdot\text{s}^{-1}$ ³³, respectively, which prevent the process of ring-opening of lactam via an Active Chain End mechanism (i.e. $k_{p(\text{ACE})} \sim k_i \sim 10^{-7} \text{ L}\cdot\text{mol}^{-1}\cdot\text{s}^{-1}$) (Scheme I-4). The nucleophilic attack of the lactamate anion on the carbonyl group of the monomer is much slower than that of the carbonyl group in a *N*-acyllactam-type chain end ($10^{-1} < k_{p(\text{AM})} < 10^3 \text{ L}\cdot\text{mol}^{-1}\cdot\text{s}^{-1}$, $k_{p(\text{AM})} = 68 \text{ L}\cdot\text{mol}^{-1}\cdot\text{s}^{-1}$ in the case of ϵ -caprolactam)³⁴, which refers to the process of ring-opening polymerization of lactam via Activated Monomer (AM) mechanism (Scheme I-5). The propagation step is therefore composed of a nucleophilic attack to the acyllactam-type growing chain end ($k_p < 10^3 \text{ L}\cdot\text{mol}^{-1}\cdot\text{s}^{-1}$) and a subsequent very fast proton transfer from the monomer to the amidate ($k_H \sim 10^2 - 10^5 \text{ L}\cdot\text{mol}^{-1}\cdot\text{s}^{-1}$) (Scheme I-5). The neutral *N*-acyllactam acts as the growth center at the chain end as the exocyclic carbonyl group in the *N*-acyllactam increases the electron deficiency of the amide group and, thus, the acylating ability. The polymerization rate is first order with respect to lactamate³⁵ and *N*-acyllactam

(Act) concentrations and zero order with respect to lactam monomer (L) concentration³¹ and can be written as follow: $-\frac{d[L]}{dt} = k_p \cdot [Act] \cdot [L^-]$



Scheme I-4. Formation of active species in anionic ring-opening polymerization of ϵ -caprolactam: Activated Monomer (AM) mechanism vs Active Chain-End mechanism.



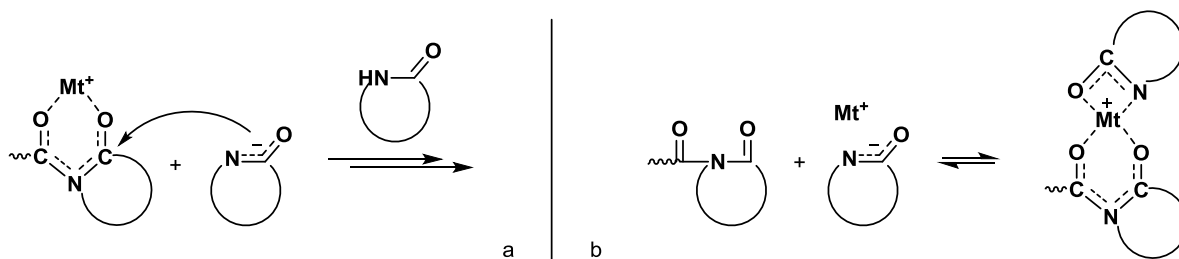
Scheme I-5. Propagation step in anionic ring-opening polymerization of lactams via activated monomer mechanism.

In the activated polymerization, the number average molar mass is determined by the concentration of the activator as compared to monomer concentration. Experimental values are generally higher than the theoretical ones. This is mainly due to the lowering of the number of growth centers due to the side reactions and to the crosslinking between polymer chains, for example, by Claisen-type condensation reactions, which are more and

more relevant as the medium basicity and the polymerization temperature increase³⁶. Such a polymerization is not living because of present side reactions in this lactam ring-opening chemistry. When the polymerization is run at temperatures below the melting point of the polyamide, side reactions are largely reduced and, even at equimolar concentrations of initiator and activator, the polymerization proceeds essentially by the reaction of lactam anions with a constant number of growth centers, resulting in a narrower molar mass distribution ($D < 2$)³⁷ and the formation of high molar masses^{12, 38}. In the non-activated polymerization, where the growth centers are both formed at the very beginning and in the final stage, the molar mass distribution is expected to be broader than the ones observed with the use of an activator.

The structure of the activators, in particular the nature of the exocyclic acyl group in *N*-acyl lactam, is shown to play a crucial role on the polymerization rates³⁹. The use of *N*-carbamoyl lactams in appropriate concentration, as "very fast" activators, allowed to drastically reduce the polymerization time^{12, 40} less than a minute and gets high polymer yield. It has the advantage to allow the decrease of polymerization temperature down to 140 °C minimizing the side reactions.

Aside from this mechanism, a lactamolytic mechanism proposed by Sekiguchi⁴¹⁻⁴³ (Scheme I-6-a) assumes the transfer of the alkali metal cation from the activated monomer species to the imide group at the end of the growing chain and its coordination to the carbonyl of the imide. The increase in conductivity was attributed to a higher concentration of free ions. The reaction proceeds via formation of an alkoxide-type anion by nucleophilic attack of the lactam anion on the endocyclic carbonyl, proton exchange with monomer, and rearrangement with ring-opening. Alternatively, Frunze et al.^{44, 45} proposed the participation of ion pairs of lactam salts in the propagation step and suggested an ion-coordination mechanism. According to this mechanism, a complex between the lactamate and the two carbonyl groups of the growing center is formed (Scheme I-6-b). As already mentioned, side reactions are observed whatever the assumed mechanisms. In any case, free ions play a decisive role at high temperatures and in media of high permittivity, while at low temperatures and in low polar media, the involvement of ion pairs is more expected.



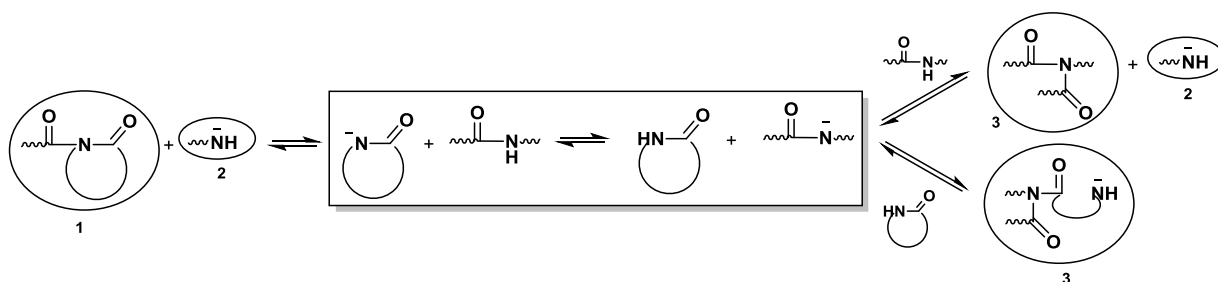
Scheme 6. Lactamolytic (a) and ion-coordinative (b) mechanisms.

1.2.1.3. Side Reactions

Species involved in anionic polymerization are in general highly reactive and lead to a series of side reactions, in particular when using high temperatures and long polymerization times. Reversible and irreversible side reactions can occur in which both the growth centers and the monomer anions are consumed. The strongly basic conditions in AROP of lactams promote mainly polymer branching and β -keto compounds, yielding to side products and chain irregularities. UV spectrometry was shown to be a tool for monitoring the occurrence of such side reactions^{10, 36, 46}.

Formation of acyllactams, amines and imides

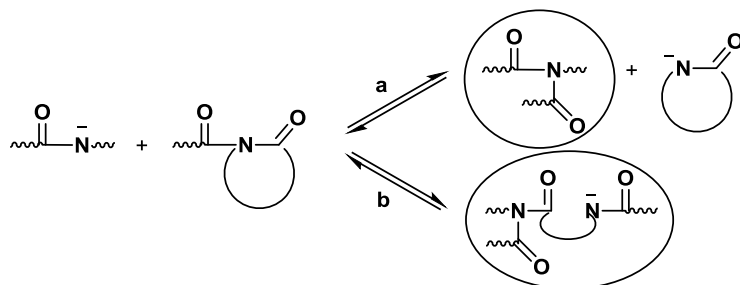
The polymer amide groups may be involved in disproportionation reactions, forming acyl lactams and amine end groups (Scheme I-7). The presence of amide *N* anions along the polymer chain, derived from equilibrium reactions with lactam anions in strongly basic medium, may produce imide groups and polymer branching (Scheme I-7).



Scheme 7. Formation of acyllactam (1), amine (2) and imide (3) groups during AROP of lactams.

Transacylation reactions between polymer amide anions and acyllactams (*N*-acylations) (Scheme I-8) may cause depolymerization or incorporation of a lactam unit when the

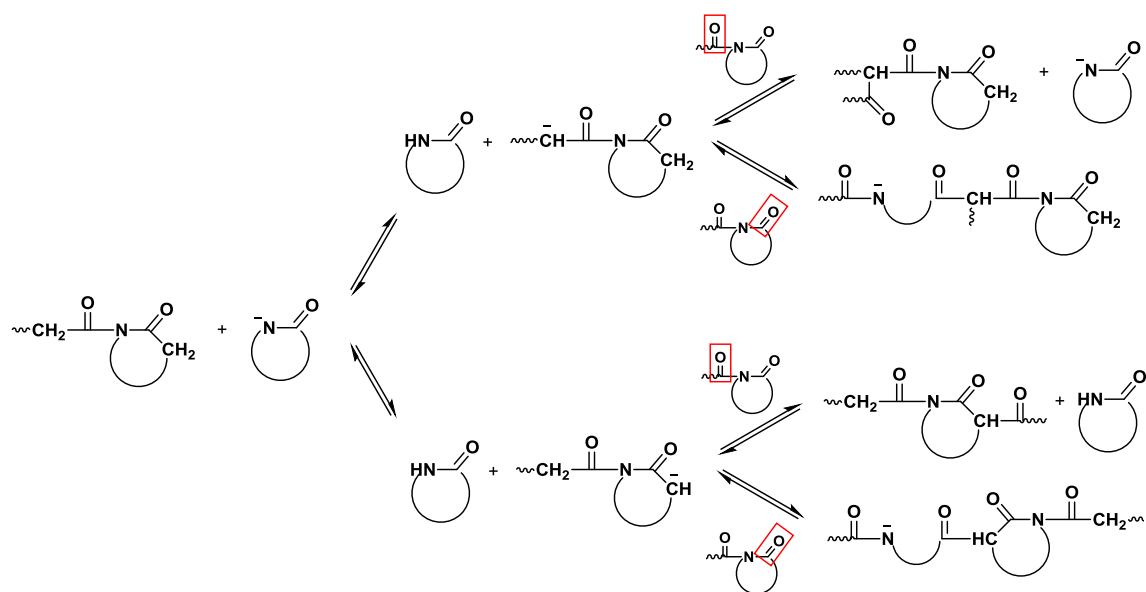
exocyclic (Scheme I-8-a) or the endo cyclic carbonyl groups (Scheme I-8-b) is involved. The nature of counter-ion affects not only the degree of dissociation of the corresponding lactamates but also the whole polymerization rate⁴⁷.



Scheme I-8. Formation of imide groups by *N*-acylation.

Formation of β -ketoimides and β -ketoamides

The acidity of the hydrogen atoms in α position of the carbonyl of the imide group in the *N*-acyl lactam chain end is comparable to that of hydrogen in an amide group. As a consequence, in the presence of lactamate, deprotonation may occur by leading to the formation of two distinct carbanions (Scheme I-9). The Claisen-type condensation reactions on exo- and endocarbonyl then happen, giving four different β -ketoimide structures. The concentration of these carbanions is generally low meaning that C-acylations and, only in some specific cases, O-acylations are competitive reactions with regard to the propagation step⁴⁸. One can also consider the formation of carbanion in the α -position of the carbonyl of a branched structure. Reactivities are related to the lactam size and their substituents, the nature of the activator, the initial ratio of initiator and activator concentrations, the permittivity of the reaction medium, and the reaction temperature as well as the nature of the counter-ion⁴⁸⁻⁵⁰.



Scheme-9. Formation of carbanions followed by β -ketoimides during AROP of lactams.

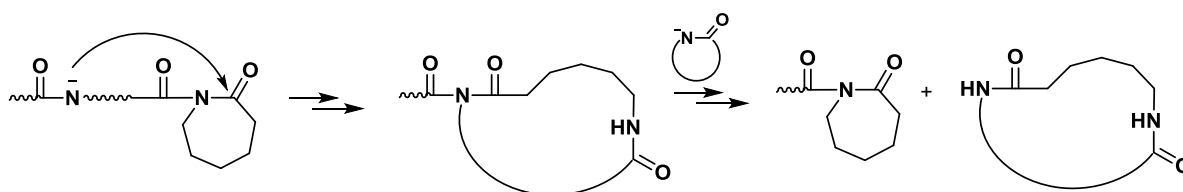
Neutral β -ketoimides are strong acylating agents and maybe involved in reactions, acting as growth centers and leading to either linear or branched chains. β -Ketoimides may be converted to β -ketoamides (2-oxoamides) by nucleophilic attack of the N- anion on the carbonyl of the imide group (Scheme-10). These keto derivatives decrease the concentration of active species and influence kinetics for instance. They are also very reactive under basic conditions or at high temperatures and responsible for complex secondary reactions, i.e. formation of water, carbondioxide, amines, and heterocyclic structures are able to act as branching and crosslinking points⁴⁸. The thermal or base-catalyzed decomposition of β -ketoamides can afford ketones and isocyanates. The latter reactive functions can also reform *N*-acyllactams capable to react in the expected polymerization way. Formation of water can contribute to the deactivation of lactamate and to the hydrolysis of *N*-acyllactams, β -keto compounds and imide branching points leading to carboxylates, amine groups, ketones, carbondioxide, or carbonates⁶.



Scheme-10. Formation of a β -ketoamide from acylation of β -ketoimide.

Formation of Cyclic Oligomers

The formation of cyclic oligomers was particularly investigated by Russo et al. for CL^{46, 51}, and the amount depends particularly on the polymerization temperature (e.g. 3.5% at 280 °C). The main reaction leading to cyclic oligomers is a back-biting reaction which is an intramolecular reaction of the neutral end groups with amidic groups inside the chain (Scheme I-11). The counter-ion involved in the polymerization is also directly influencing the occurrence of such a side reaction⁵². Using magnesium salts of CL, cyclization reactions are strongly reduced both below and above the melting temperature of the polymer formed as compared with sodium systems. The existence of coordination between magnesium-based compounds with end groups of polyamides is suggested. Cyclic structures can have a negative influence on processing or applications as they are able to modify the crystalline structure in the solid phase^{53, 54}.



Scheme I-11. Formation of cyclic oligomers by intramolecular reactions.

1.3. Anionic (co)polymerization of ϵ -caprolactam and ω -lauro lactam

1.3.1. Homopolymerization of ϵ -caprolactam and ω -lauro lactam

The polymerization of CL, a 7-membered ring, is usually conducted in bulk conditions, above the melting temperature of the monomer (80 °C) in the presence of initiator and activator. Initially liquid, the mixture turns turbid and then solidifies in the course of the polymerization which can be as fast as few tens of seconds for “very fast” systems. The beginning of solidification is considered as the moment at which the growing chains attain a critical length that enables their crystallization, forming spherulites insoluble in the monomer.

As discussed previously, playing with the structure and concentrations of both activator and initiator allows tuning the polymerization rate of CL. The initial polymerization

temperature as well as isothermal, non isothermal, or adiabatic conditions is also considered as tools to modify the time of reaction. "Very fast", "fast", or "slow" processes affect structure and properties of the resultant anionic PA6. For a very fast bulk polymerization of CL at 155°C, conditions close to adiabatic ones can be obtained due to high rate and poor heat exchange with the surroundings. A temperature increase of 50 °C is observed with a resulting polymer with high molar mass, low residual monomer content and low content in cyclic oligomers^{4, 12}. To decrease even more side reactions, quasi-isothermal conditions near 150-160°C were proposed²⁴.

Similar polymerization systems and conditions were proposed for the synthesis of polyamide 12 obtained by ring-opening of ω -laurolactam (ω -LL), a 13-membered ring. The polymer gained attention for its low level of absorbed moisture, easily removable during heating and melting of the monomer at 150 °C. Moreover, it possesses an excellent ductility, good electrical properties and significant chemical resistance. However, due to the long methylene sequences between the amide linkages, it has a lower melting point (172 °C) compared to PA6 (210 °C). To get a low content of residual monomer due to favorable monomer-polymer equilibrium, temperatures above 150 °C are generally required^{38, 55}. Some specific polymerization systems, based on alicyclic carbodiimide as an activator and sodium caprolactamate as an initiator, were also developed to allow for instance a long-term storage of the initiating species, an efficient control of the polymerization rate, and an accurate tailoring of polyamide molar masses⁵⁶. As for CL, initiation and activation influence also polymerization kinetics and thermodynamics but also the degree of crystallinity⁵⁷.

As discussed in the previous paragraph, the AROP of lactams suffers from numbers of side reactions, reversible or not, varying with the experimental conditions. The usual kinetic law depending on activator and initiator concentration ($R_p = -d[M]/dt = k_p f[\text{Activator}][\text{Initiator}]_0$) appears not efficient to get right values but might be sufficient to compare polymerization systems. The autocatalytic model of Malkin, based on a phenomenological approach, seems the most successful to follow that activated polymerization in bulk⁵⁸. It describes the non-isothermal kinetics of both CL and ω -laurolactam, monitoring the temperature rise inside the reactor:

$$-\frac{d[\lambda]}{dt} = k \frac{[A]^2}{[M]_0} (1 - \lambda) \left(1 + \frac{b\lambda}{[A]}\right) \exp\left(-\frac{Ea}{RT}\right)$$

with λ the conversion, $[A]$ the activator concentration, $[M]_0$ the initial monomer concentration, k the reaction rate constant, E_a the activation energy, and b the autocatalytic term characterizing the intensity of the self-acceleration effect during chain growth. Both k and b depend on the chosen activator. The rate constant can be evaluated for low conversions where polymerization and crystallization are not overlapped.

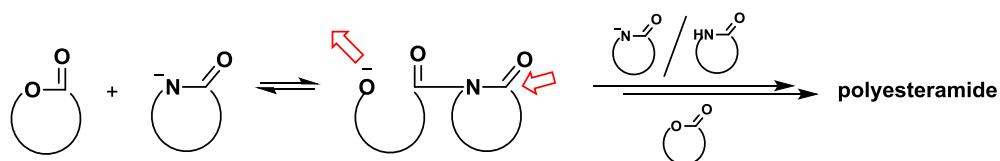
1.3.2. Copolymerization of ϵ -caprolactam and ω -lauro lactam

Anionic polymerization is well known and used for the synthesis of copolymers, in particular blocks, due to its living character. Despite the non-living character of lactams polymerization, copolymers based on polyamide can be synthesized and offers interesting and specific properties. ω -Lauro lactam is in general used as a co-monomer of CL in order to extend the range of PA6 properties, in particular by increasing the notched Izod impact strength at low temperature, and by decreasing water absorption¹³. Roda and coworkers showed the influence of the initiator toward the copolymers structures and therefore their properties^{55, 59}. As compared to ϵ -caprolactam magnesium bromide, sodium caprolactamate exhibits higher polymerization activity especially in copolymerization with a high content of ω -LL and at high polymerization temperatures. The copolymers have only one melting endotherm in the whole range of monomers feed, and one single crystalline form, when two melting endotherms (140 °C and 210 °C) and two types (α and β) of crystalline forms are observed from 30 to 70 mol% of CL with the magnesium-based initiator. This is explained by a copolymer microstructure composed of PA6 blocks linked to sequences of CL/ ω -LL random copolymer. PA6 is preferentially formed at the beginning of the polymerization, due to the much higher reactivity of CL as compared to ω -lauro lactam. Random copolymers are then formed from the remaining CL and slowly reacting with ω -LL. In the case of sodium caprolactamate which is a strong base as compared to the magnesium derivative, transamidation reactions cause full randomization of the sequences.

1.3.3. Copolymerization of lactams and lactones

The interest of preparing degradable polyamides through the synthesis of polyesteramides enabled researchers to think to the copolymerization of lactams and lactones even though other anionic ring-opening mechanisms were necessary for their

homopolymers formation⁸. Some lactones were shown to act both as activator of lactam polymerization and as co-monomer for the synthesis of a polyester block^{28, 60-62}. The initiation step corresponds to the acylation reaction between a lactamate and the reactive lactone (Scheme I-12). The oxyanion formed is then able to initiate the rapid ring-opening polymerization of some cyclic esters such as ϵ -caprolactone or δ -valerolactone by usual chain growth mechanism (active chain-end).



Scheme I-12. Parallel initiation of lactams and lactones in the presence of lactamate.

Playing with ϵ -caprolactam and ϵ -caprolactone ratios as well as experimental conditions, various random or multiblock copolymers were prepared. Fast transacylation reactions between ester and amide groups in the copolymer chains were proposed as responsible for the observed copolymer randomness. Using reactive processing like a twin-screw extruder, diblock or triblock copolymers were prepared from various lactams and lactones using suitable sequential monomer feeding and specific temperature profiles⁶³⁻⁶⁵. The block lengths can be adjusted by controlling the feed rate.

The use of poly(ϵ -caprolactone) (PCL) was also proposed as an additive to the polymerization of ϵ -caprolactone with ϵ -caprolactam magnesium bromide as an initiator and with or without activator. PCL was shown to act as an activator and random copolymers were prepared⁶⁶.

1.3.4. Polyamide-based copolymers with non-polyamide blocks

The main route leading to lactam-based block copolymers aims at using macroactivators obtained from appropriately terminated prepolymers. In general, hydroxyltelechelic polymers are reacted with diisocyanates and then blocked with CL. Combination of properties is the driving force of reacting various non-polyamide blocks as activators of anionic lactam polymerization. The toughness improvement of PA6 being a key issue, soft polymers such as polybutadiene⁶⁷⁻⁷⁰, polyethers⁷¹⁻⁷⁵, and polysiloxanes^{75, 76} were particularly

used. Following a similar approach, Styrene-Butadiene Rubber was also introduced into PA6 with the aim to also tune the mechanical properties⁷⁷. Graft copolymers were also designed for a compatibilization use. Polypropylene or polystyrene grafted with PA6 chains were easily obtained^{27, 78-81}.

1.3.5. Industrial processes using AROP of ϵ -caprolactam and ω -lauro lactam

Ring-opening polymerization of ϵ -caprolactam initiated by water, i.e. the hydrolytic mechanism, is carried out for industrial cast Nylon-6. Nowadays, due to fast kinetics of the “activated” anionic ring-opening polymerizations, this approach is more and more envisaged for the preparation of PA6 and PA6-co-PA12 in newly developed industrial applications using mainly powdered materials and molding or extrusion approaches.

1.3.5.1. Powdered polyamides

As compared to techniques industrially utilized so far, i.e. low-temperature grinding and polymer dissolution/precipitation, AROP yielding PA6 and PA6-co-PA12 offers some advantages such as a much higher particle porosity, a total absence of irregular edges and sinterized zones, and a controlled and narrow particle size. Polymerizations by dispersion⁸²⁻⁸⁷, suspension⁸⁸ and mini emulsion⁸⁹ are generally proposed. More recently, the use of phase inversion in PA6/PS blends were shown to prepare microspheres with controlled diameters⁹⁰. Fast polymerization systems have to be selected with such processes. The suspension method has the advantage to be the faster but suffers from difficult and expensive purification. Such materials are of great interest for cosmetic formulations, coating and graphic art applications, protein or enzyme immobilization techniques, rotational molding and sintering processes, chromatography applications, as well as filtration devices in food and beverage industry.

1.3.5.2. Molding and extrusion

Reaction Injection Molding (RIM), Resin Transfer Molding (RTM), Rotational molding and Reactive extrusion are the main processes used with an in situ activated anionic polymerization of CL^{91, 92}. Due to its high crystallinity and high molar mass, anionic PA6 exhibits for instance better thermo-mechanical properties or lower water uptake as compared to the extruded or molded PA6. The short polymerization times in the order of

minutes, as compared to hours for hydrolytic polymerization, the very low cyclic oligomer content, and the much lower initial polymerization temperature (130-170 °C vs 230-280 °C) are the main advantages of this activated AROP.

Soft polymers bearing terminal *N*-acyl lactam groups are used in RIM processes as activators of CL polymerization yielding PA6 with good impact strength. Usual initiators such as sodium ϵ -caprolactamate or magnesium bromide ϵ -caprolactamate are efficient in that process⁹³. RTM enables the injection of the melted monomeric reactants of low viscosity into a mold filled with reinforcing materials like fibers. Reactive extrusion processes regain also attention for the easy preparation of nanocomposites and nanoblends^{92, 94-97}. Single- or multiwallecarbon nanotubes and nanosilica are also shown to be dispersed in PA6 modifying its initial properties^{98, 99}. Nevertheless, it has to be mentioned that anhydrous conditions are required and may sometimes be considered as a limitation. Deactivation of the anionic groups is known to occur when some clay are used as reinforcing agents.

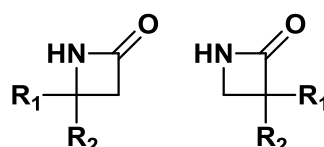
1.4. Anionic polymerization of other lactams

β -Lactams, 2-pyrrolidone, and 2-piperidone are the three main unsubstituted lactams available and studied by AROP. They are respectively yielding polyamide-3, polyamide-4, and polyamide-5. It has to be noticed that *N*-substituted polyamide-1 as well as polyamide-2 (polypeptide) are not obtained from lactams but from oxadiazolinones and *N*-carboxyanhydride, respectively.

1.4.1. β -lactams

Living anionic polymerization can be reached when substituted β -lactams (or β -propiolactams) (Scheme I-13) which are highly reactive, so possess a high ring strain, enabling the use of low polymerization temperatures and rates. The review of Hashimoto published in 2000 describes in detail the specificities of the ring-opening polymerization of such monomers⁷. Sebenda et al. showed first that the activated anionic polymerization of a bulky β -lactam, i.e. 3-butyl-3-methyl-2-azetidinone, has a living character giving a monodispersepolyamide of molar mass very close to the theoretical value^{100, 101}. Other substituted monomers were also polymerized in a controlled manner in homogeneous solution, using aprotic and apolar solvents like *N,N*-dimethyl acetamide, DMF, or DMSO, and

in the presence of lithium salts¹⁰²⁻¹⁰⁴. Depolymerization and transamidation reactions both at the acyl lactam chain end and on the polyamide chain are known to occur and therefore broadening the molar mass distribution⁷. Stopping the reaction before complete conversion minimizes transamidation reactions enabling the preparation of block and graft copolymers, or other structures taking advantage of the living character of the polymerization. The possibilities to play with substituents offer nowadays PA3 materials with amphiphilic character and exhibiting bioactivity for instance¹⁰⁵.



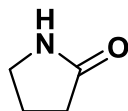
Scheme I-13. Structures of β -lactams.

1.4.2. 2-pyrrolidone

The particularity of the polymerization of 2-pyrrolidone (Scheme I-14), leading to polyamide-4, can be found in a rather low ceiling temperature (70 °C) limiting the reaction temperature to 50 °C¹⁰⁶. In bulk conditions, economically more interesting than in solution, polymerization rate decreases with time and partial conversion are obtained due to a phase separation, nucleation and crystallization with occlusion of the growth centers in this solid phase^{42, 107, 108}. Despite some potential industrial interests in textile for its good mechanical properties and hydrophilic behavior similar to cotton, synthesis difficulties are one main reason for its non-development.

Similar to CL polymerization, CO₂ was also proposed as an activator to successfully prepare PA4 with an improved thermal stability^{30, 109}. But depolymerization still remains a major drawback. Using quaternary ammonium salts of 2-pyrrolidone as initiators, instead of sodium or potassium ones, and *N*-acetyl-2-pyrrolidone as an activator, yields up to 80% could be obtained after 24h at 30 °C¹⁴. It is assumed that a bulky counter-ion allows the breaking of hydrogen bonds between polymer chains and creates local irregularities of the crystalline structure, enabling the contact between lactamates and reactive chain ends. Suspension polymerization can also be used¹¹⁰ and whatever the process used, polyamide-4 was obtained free of structural irregularities thanks to the low polymerization temperature

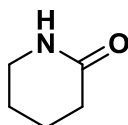
and limited conversions. Block copolymers containing PA4 segments could be obtained using the macroactivator approach¹¹¹, the synthesis of PA4 with a terminal azide function¹¹², or with CL as co-monomer above the ceiling temperature of 2-pyrrolidone^{113, 114}.



Scheme I-14. Structure of 2-pyrrolidone.

1.4.3. 2-piperidone

The ring-opening polymerization of 2-piperidone, also called 2-piperidinone or δ -valerolactam, piperidin-2-one, is kinetically slow due to its stable 6-membered ring² (Scheme I-15). Moreover, crystallization and side reactions contribute also to the slowness of the reaction. The use of activators is mandatory and relatively high molar masses of PA5, with a melting temperature of 283°C, were obtained with quaternary ammonium salts of monomers used as initiators^{108, 115}.



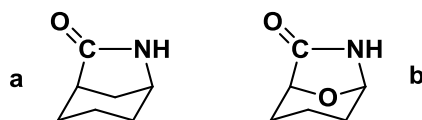
Scheme I-15. Structure of 2-piperidone.

The use of bicyclic lactams is proposed as an alternative, the ring strain being favorable to a faster AROP.

1.4.4. Bicyclic lactams

The key point in the AROP of bicyclic lactams is indeed the ring strain, coming for instance from the repulsion of hydrogen atoms, and its release. At first, Hall reported in the sixties the polymerization of a bicyclic lactam, i.e. the 6-azabicyclo[3.2.1]octan-7-one (Scheme I-16-a), in the presence of sodium hydride^{116, 117}. Hashimoto proposed a detailed review in 2000 relative to bicyclic and heterobicyclic lactams⁷. High temperatures are generally required limiting the livingness of such polymerizations. For the case of bicyclic oxalactams (Scheme I-16-b), the polymerization could be run at 25°C in DMSO due to a high kinetic polymerizability

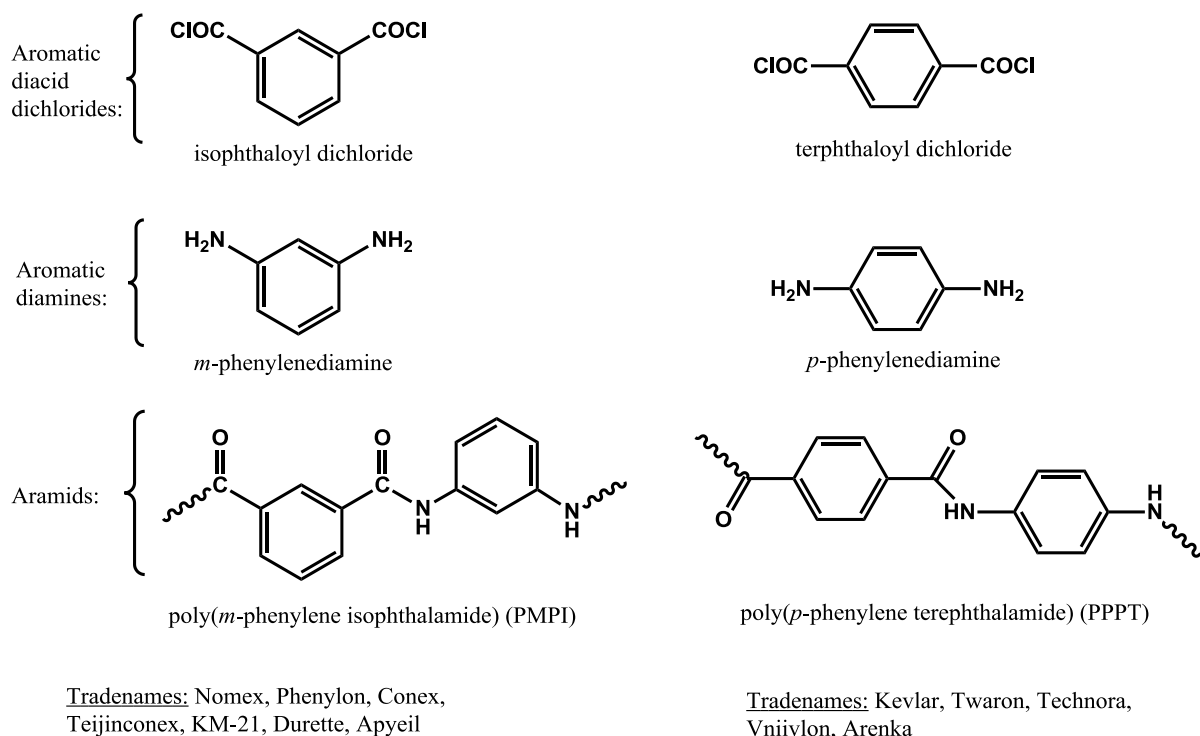
related to the high strain of internal bond angles^{118, 119}. A living character was observed till 60% of conversion.



Scheme I-16. Structures of a bicyclic lactam, i.e. 6-azabicyclo[3.2.1]octan-7-one (a) and of abicyclic oxalactam, i.e. 8-oxa-6-azabicyclo[3.2.1]octan-7-one (b).

2. Synthesis of aromatic polyamides

Wholly aromatic polyamides (aramids) differ from the aliphatic polyamides. Both aliphatic and aromatic polyamides are considered as engineering materials. However, the aromatic structure of the main chain of the aramids gives some specific properties which make them less sensitive to oxidation, higher solvent resistant, and higher thermal and mechanical performance¹²⁰⁻¹²⁷ than aliphatic polyamides. Owing to their superior properties, aramids have broad range of application areas such as in bulletproof jackets, automotive, electrical, and electronic fields^{35, 125, 128-131}. Nonetheless, the aramids have some limitation such as poor solubility in common organic solvents and very high transition temperature (even above their thermal decomposition temperature). Therefore, these drawbacks restrict their applicability and lead to processing difficulties. Many researches are dedicated to exceeding these shortcomings of the aramids and one of the ways is the addition of aliphatic polyamides to the aramids. By far most commercialized aromatic polyamides are poly(*p*-phenylene terephthalamide) (PPPT) or generally called poly(*para*-benzamide) (PPBA) and poly(*m*-phenylene isophthalamide) (PMPI) shown in Scheme I-17. *Meta*-substituted aromatic polyamides (PMPI) have a better solubility compare to *para*-substituted one (PPPT) due to the less symmetric structure of polymer¹²⁸.



Scheme I-17. Tradenames and chemical structures of diacids and diamines in commercial *meta* and *para*-aramids¹²⁸.

In general, the aramids have been synthesized by two major ways:

- (1) Polycondensation reaction via an aromatic diacid chloride and a diamine
- (2) Direct polycondensation reaction of a dicarboxylic acid and a diamine

Following parts will introduce and focus mainly on chain-growth condensation polymerization which exhibits a living character and a specific interest for a part of my research.

2.1. Step-growth condensation polymerization

A polycondensation reaction involves several additions of two functional groups with elimination of a side molecule. Engineering plastics such as polyamides, polyesters, polyimides, and polyurethanes are obtained from conventional step-growth condensation or addition polymerization. Polyamides have usually been synthesized by classical step-growth condensation polymerization (SGCP) method which is obeying Flory's statistical treatment¹³² and Carother's equation¹³³. By this method, polyamides have uncontrolled molar mass and a dispersity index approaches to 2 at high conversion which are not related

to living polymerization because of the polymerization occurs between monomers and all types of oligomers and monomers without any control. Step-growth condensation polymerization mechanism involves the initiation by the reaction of monomers with each other, and propagation of all formed oligomers between their chain ends and the monomer. The controlling of the macromolecular dimension as well as the synthesis of particular structures such as block, graft or star polymers has gained more and more attention by polymer research areas. Szwarc developed such a system by chain-growth condensation polymerization of styrene¹³⁴. But application of living polymerization has been restricted with addition polymerization of vinyl monomers as well as ring-opening polymerization of some cyclic monomers.

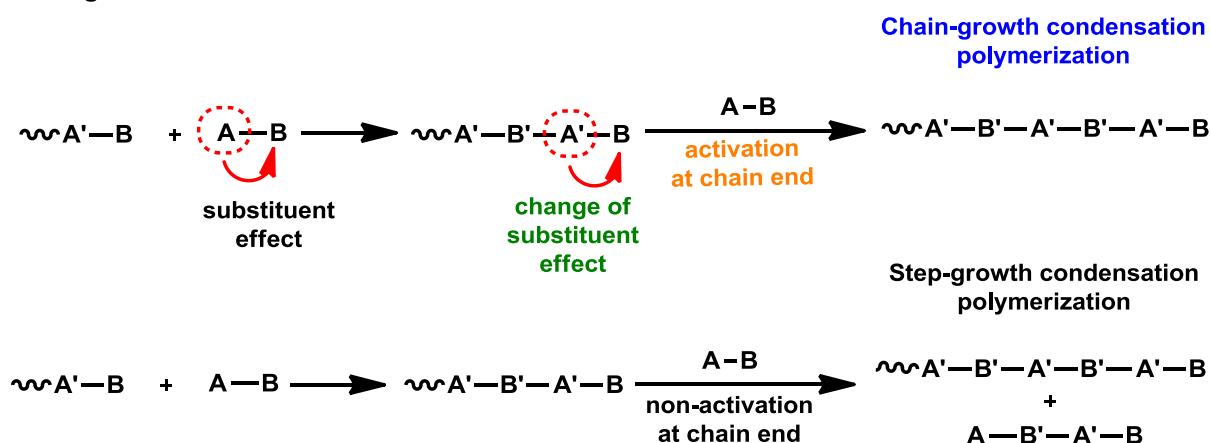
Combination of the chain-growth and condensation polymerization for the aromatic polyamide synthesis will be discussed in the following paragraph.

2.2. Chain-growth condensation polymerization

Chain-growth condensation polymerization working principle is based on substituent effects that can be either resonance or inductive effect depending on the substituent position on the monomer structure *para*-(*p*) or *meta*-(*m*). These both two possibilities are providing controlled molar mass as well as narrow dispersity of obtained polyamides. The change of the substituent effect occurred by a new bond formation between the monomer and initiator and keeps the reactivity at the polymer chain end (Scheme I-18). The polymer chain end has higher reactivity than monomers which prevents step-growth condensation polymerization¹³⁵.

In chain-growth condensation polymerization, the selective activation of polymer end groups is the controlling of substituent effects between the monomer functional groups. Schematic demonstration of condensation polymerization of AB type monomers is depicted in Scheme I-18. B site reactivity of monomer is increased by the substituent effect of A site as well as avoiding undesired step-growth reaction between monomers. On the other hand, once monomer reacts with an initiator having a reactive site, the substituent effect shifts to end group. As long as substituent efficiency is actively presence on formed bond, next monomer could attack selectively to the propagating chain end by obeying chain-growth condensation polymerization rather than step-growth condensation polymerization¹³⁶.

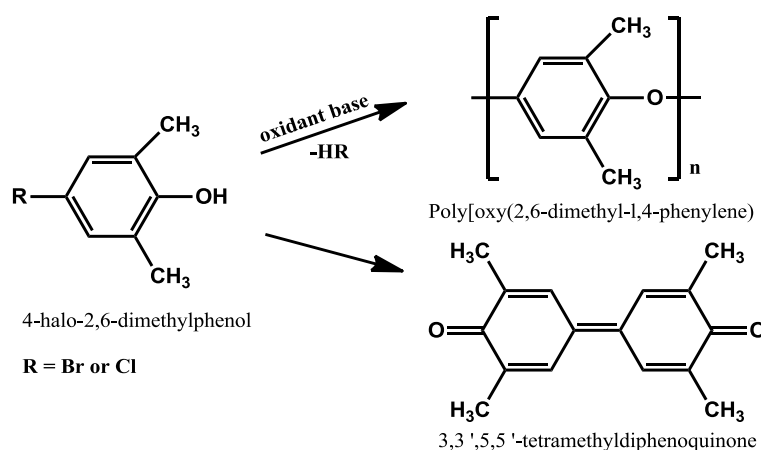
Change of substituent effect



Scheme I-18. Substituent effect on chain growth condensation polymerization. Adapted from¹³⁵.

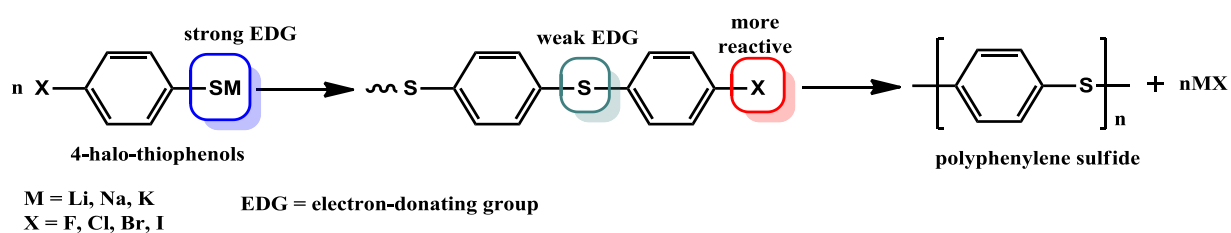
In the literature several studies of condensation polymerizations in a chain-growth polymerization way were reported such as 4-halo-thiophenols¹³⁷, 4-halo-2,6-dimethylphenol¹³⁸ and 4-fluorobenzenesulfinate¹³⁹. These all works and more are reviewed by Yokozawa and Yokoyama¹⁴⁰.

Synthesis of poly(2,6-dimethyl-1,4-phenylene oxide) from 4-halo-2,6-dimethylphenol yields 3,3',5,5'-tetramethyldiphenone as a by-product. The halogen displacement polymerization of 4-halo-2,6-dimethylphenols, which is catalyzed by various oxidants such as $K_3Fe(CN)_6$, I_2 , PbO_2 or cupric salts in combination with bases (Scheme I-19)¹³⁷.



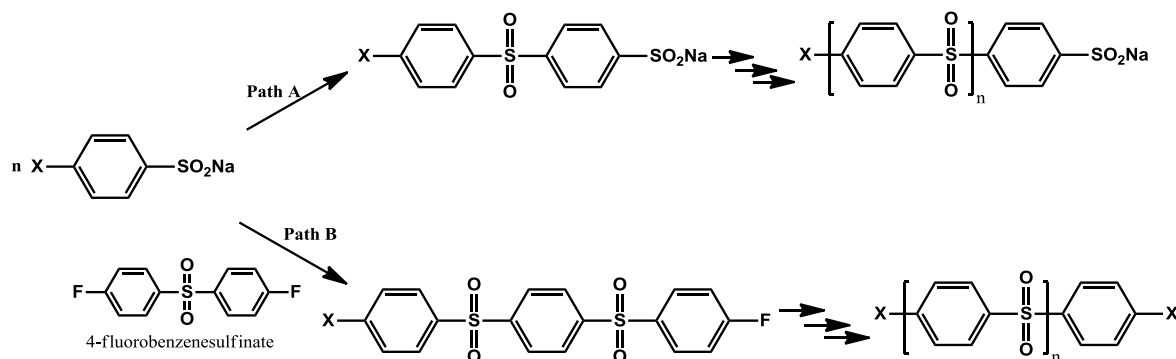
Scheme I-19. Synthesis of poly(oxy(2,6-dimethyl-1,4-phenylene)).

Polyphenylene sulfide was synthesized by condensation polymerization of alkali metal salts of the *p*-halothiophenols by Lenz et al., as depicted in Scheme I-20. The order of reactivities of the sodium salts was $I > Br > F > Cl$, and in the polymerization reaction, the order of reactivities of the alkali metal salts of *p*-bromothiophenol was $K < Na < Li$. They also reported that this comparison indicated that for the chloro and fluoro derivatives, the polymer chain end groups were more reactive than the monomers¹³⁷. Weak electron-donating of sulfide linkage in the polymer increases the reactivity of polymer chain end compared to the strong electron-donating effect of the thiophenoxide anion in the monomer. They called this effect “preferential polymer formation”.



Scheme I-20. Synthesis of polyphenylene sulfide.

Self-condensation of sodium 4-halobenzenesulfinate by using a small amount of 4-fluorophenyl sulfone which is assisting to increasing polymer yield were studied by Robello et al.¹³⁹. As reported by Lenz as a “preferential polymer formation”, aromatic halogen is much more strongly activated toward nucleophilic displacement by a para sulfone group than a negatively charged para-sulfone group. Therefore, path B is more effective than path A with a chain mechanism (Scheme I-21).



Scheme I-21. Synthesis of poly(*p*-phenylsulfone).

These all resulting polymers end with contamination of step-growth polymerization and insolubility in reaction media, therefore they cannot achieve narrow dispersity and controlled molar mass.

Recently, Yokozawa and coworkers investigated chain-growth polycondensation for typical condensation polymers such as aromatic polyamides, polyesters, polyethers, poly(ether sulfone)s and poly(ether ketone)s to control molar mass and polydispersity¹⁴¹. Between these condensation polymers, they mainly focused on the aromatic polyamide synthesis by chain-growth condensation polymerization due to slower transamidation reactions than the transesterification reactions and manipulation ability over the *N*-alkyl group on the polybenzamide or benzamide monomer by changing the alkyl- group.

2.2.1. Mechanism of the polymerization: synthesis of aromatic polyamides

As mentioned above, the solubility issue of aramids¹⁴² could be overcome with a pendant alkyl group (*N*-Alkyl) on monomer without strong hydrogen bonds and less intermolecular packing that can be easily removed upon treatment of the polyamide with the proper reagent under mild conditions.

Chain-growth polycondensation is in a competition with step-growth polycondensation in a condensation system. Successful synthesis of chain-growth polycondensation is based on having special activated polymer chain end group^{135, 141, 143, 144}. For this purpose, two different substituent effects have been used: *para*- and *meta*- substituent effects.

2.2.1.1. Para-substituted monomers

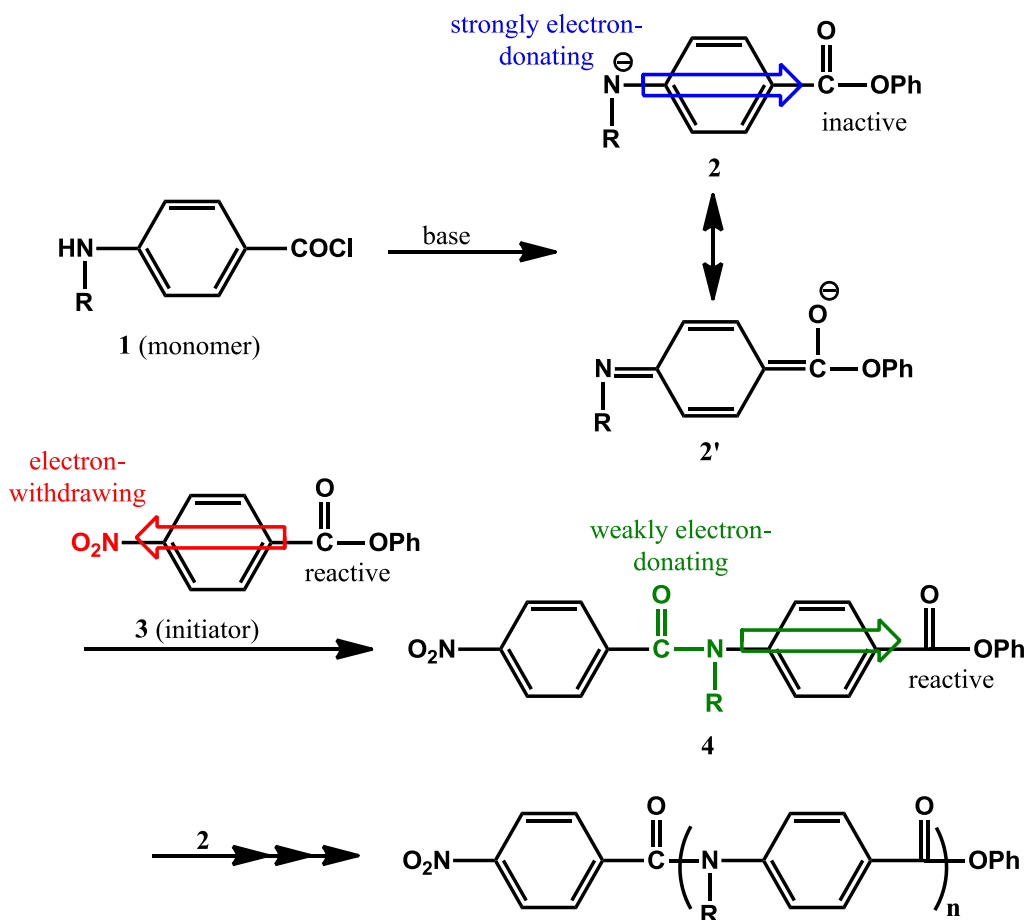
Para-substituted aromatic condensation polymers have generally less solubility in organic solvents because of strong intermolecular interaction based on the high symmetry of the polymers. The solubility limitation is surpassed at the same time keeping the mechanical properties by introducing long alkyl chains into the *para*-substituted monomers, or copolymerizing the *para*-substituted monomers with *meta*-substituted ones. Strategic parameter of *para*-substituted monomer is the resonance effect (*+R effect*).

Resonance effect of substituent on condensation polymerization assists to obtain chain-growth condensation polymerization by suppressing the step-growth condensation

polymerization. It was reported for the first time on the synthesis of *N*-alkylated poly(*p*-benzamide)s by polymerization of 4-(alkylamino)benzoic acid phenyl esters (**1**)¹⁴³.

In this system, more reactive ester linkage at chain end (**4**) than the activated monomer (**2**) owing to different resonance effects was used to control the reactivity of the electrophilic ester unit. Briefly, Scheme I-22 exemplifies the chain-growth condensation polymerization system over the resonance effect differences of monomers and polymer chain end¹⁴³.

Deprotonation of the monomer amino group by the strong base generates a strongly electron-donating amide anion. This amide anion is deactivating the electrophilic site at the *para*-position with the resonance effect of **2** and **2'**. During the polymerization of *para*-substituted monomer, the strong electron donating resonance effect of the amide anion is deactivating the electrophilic ester at the *para* position and preventing the self-condensation of the monomer. Once an initiator **3** is added, a reactive ester carbonyl group on the initiator leads to the reaction with **2** due to the presence of a strong electron-withdrawing substituent (-NO₂) at the *para* position of the initiator **3**. Thus, the next activated monomer reacts selectively with the phenyl ester moiety of the amide **4** when the ester function of **2** is deactivated by EDG. Propagation follows in "a chain polymerization" by the selective reaction of the amide monomer with the more reactive polymer terminal phenyl ester moiety. Polymerization of *para* substituted monomer **1** is conducted by chain-growth polymerization to yield aromatic polyamide with low dispersity and controlled molecular mass¹⁴¹.



Scheme I-22. Chain-growth condensation polymerization mechanism. Adapted from¹⁴¹.

In detailed studies, trials of different polymerization conditions show that specific reaction parameters such as moderate temperature, monomer type and strong base are necessary to gain chain-growth condensation polymerization.

As a successful *para*-substituent example, condensation polymerization of phenyl 4-(octylamino) benzoate (monomer) can be taken into account to explain main points of chain-growth condensation polymerization. Phenyl 4-nitrobenzoate (initiator) is used as an initiator in THF solution at ambient temperature. Polymerization is carried out in the presence of a strong base. Results of this work show that well-defined aromatic polyamides with very low dispersities ($\overline{M}_w/\overline{M}_n(D) \leq 1.1$) (Figure I-1)¹⁴³ and the controlled molar mass (\overline{M}_n) of polymer up to 22 000 g/mol by the feed ratio of monomer to initiator (Figure I-1). Additionally, the \overline{M}_n values and monomer conversion showed linear increasing which indicates the chain growth condensation polymerization (Figure I-1B)

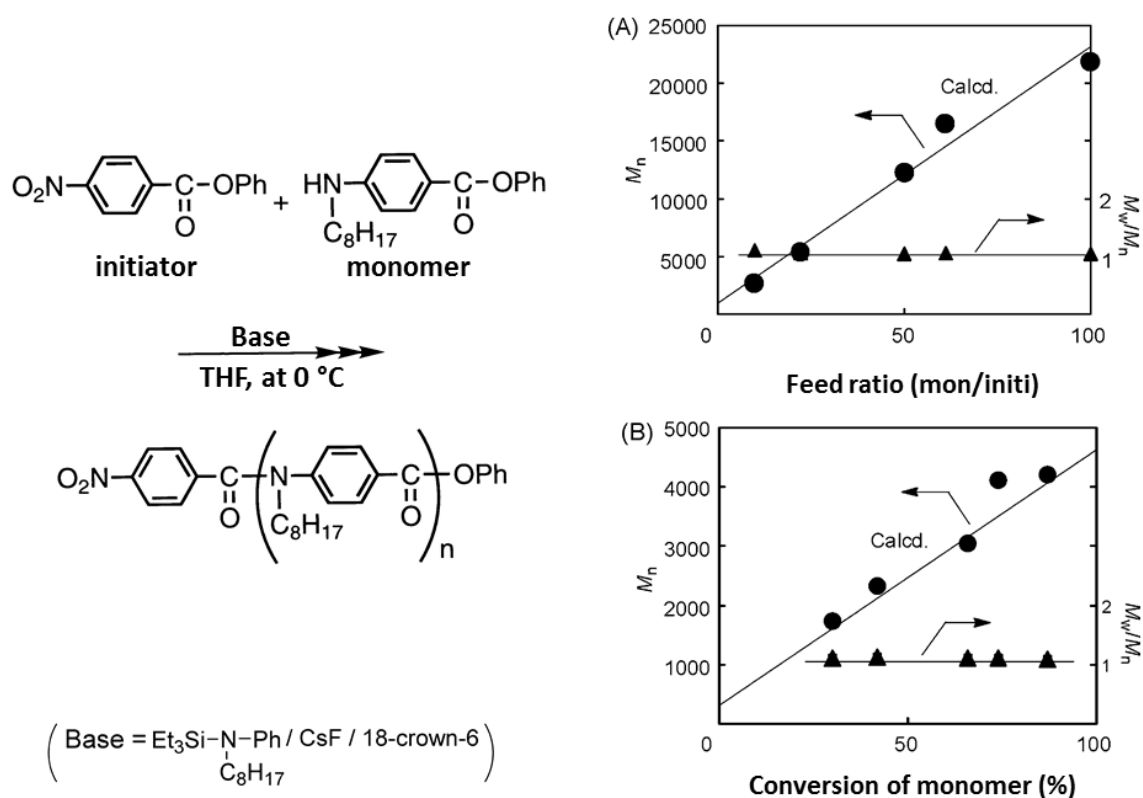


Figure I-1. Chain-growth condensation polymerization of phenyl 4-(octylamino) benzoate (monomer): (A) \overline{M}_n and $\overline{M}_w/\overline{M}_n$, as a function of the molar feed ratio of monomer to initiator, conversion = 100%. (B) \overline{M}_n and $\overline{M}_w/\overline{M}_n$, as a function of monomer conversion. The lines indicate the calculated \overline{M}_n values assuming one polymer chain per initiator unit¹⁴³.

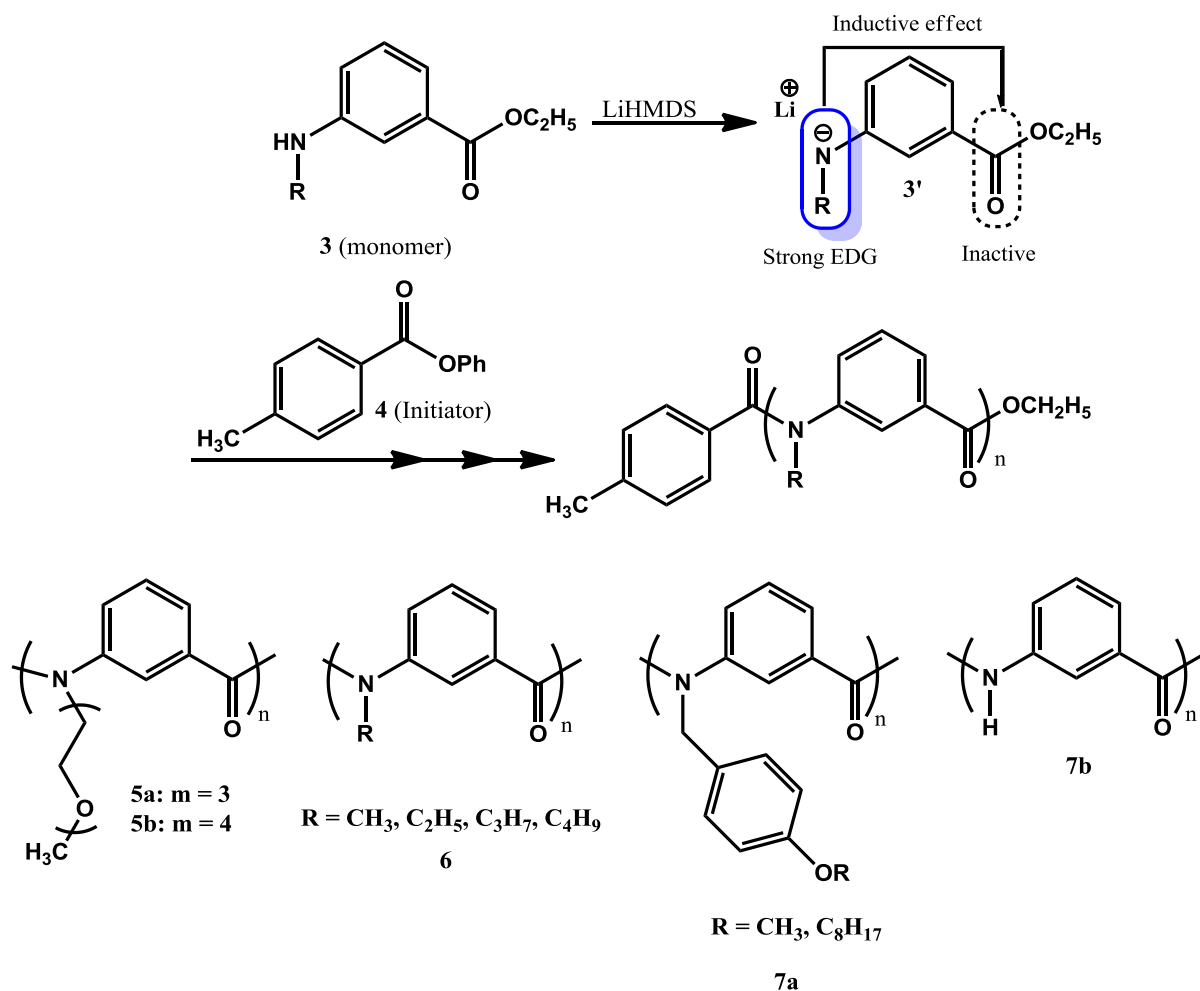
2.2.1.2. *Meta*-substituted monomers

Poly(*m*-benzamide)s have higher solubility in organic solvents than poly(*p*-benzamide)s due to their non-symmetric structure contrast to *para*-substituted one¹⁴⁵. Essential substituent effect of *meta*-substituted monomer chain-growth condensation polymerization is the inductive (+I) effect. As it is mentioned above, chain-growth condensation polymerization of *p*-substituted monomer is triggered by deactivation of electrophilic site from the anionic nucleophilic site through the +R effect.

+I effect of *m*-substituted monomer is triggering the chain-growth condensation polymerization rather than self-condensation. This formula is based on the acidity of benzoic acid derivatives. The pK_a s of *m*-nitrobenzoic acid and *p*-nitrobenzoic acid are 3.45 and 3.44,

respectively¹⁴⁶. This fact makes inductive effect of electrophilic site of *m*-substituent monomer as active as resonance effect of *p*-substituent one.

Chain-growth condensation polymerization of *m*-substituted monomers and their *N*-alkylated derivatives was reported by Yokozawa and coworkers (Scheme I-23)^{135, 145}.



Scheme I-23. *Meta*-substituent polybenzamide synthesis from different *N*-alkylated monomers¹³⁵.

One of them is the polymerization of ethyl 3-alkylaminobenzoate (**3**). After proton abstraction of monomer (**3**), deprotonated monomer's (**3'**) carbonyl site is deactivated by electron donating group (EDG). Following the deprotonation of the monomer, deprotonated monomer reacts with the initiator. Propagation of monomer increases the reactivity of carbonyl side by less electron donating effect compare to deprotonated one (**3'**). Therefore, the propagating monomer has a quite higher reactivity than the deprotonated one. In this polymerization, LiHMDS is used as a base and phenyl 4-methylbenzoate as an initiator in THF

at 0 °C to gain *N*-alkylated poly(*m*-benzamide)s with controlled molar masses up to 12 000 and narrow dispersities ($\overline{Mw}/\overline{Mn} \leq 1.1$) (Scheme I-64). Furthermore, poly(*m*-benzamide)s **5** bearing oligo(ethylene glycol) have solubility in water, (Scheme I-64)¹⁴⁷. For **5a** (DP = 29.8, $\overline{Mw}/\overline{Mn} = 1.19$)¹⁴⁸. Poly(*m*-benzamide)s with shorter alkyl groups (**6**) are insoluble in ether but soluble in polar solvents such as DMSO, CH₃CN or methanol in which poly(octyl *m*-benzamide) is not soluble. The effect of balance between the nonpolar alkyl groups and the polar amide linkage: the solubility of poly(octyl *m*-benzamide) with long alkyl group is dominated by nonpolar character of the alkyl group, while the solubilities of (**6**) are dominated by the polar character of amide linkage^{144, 149}. On the other hand, deprotection of (**7a**) via trifluoroacetic acid gives (**7b**) which has better solubility than *para*- counterpart due to the non-symmetric structure¹⁴⁹. Indeed, the solubility of poly(*m*-benzamide) bearing octyl- group is more soluble in ether and even in ethanol in which the *para*- form is insoluble¹⁴⁵.

2.3. Synthesis of copolymers based on aromatic polyamide by chain-growth polycondensation

Since investigation of chain-growth condensation polymerization, many efforts have been conducted to improve polybenzamide rigidity or solubility by combination of chain-growth condensation polymerization with different polymerization techniques such as ATRP, RAFT or coupling reactions. Here, these improvements will be explained in three groups for copolymers based on aromatic polyamides: (1) sequential condensative chain polymerization, (2) block copolymers by coupling reaction, and (3) macro-initiator approach by ATRP or RAFT.

2.3.1. Sequential condensative chain polymerization

Sequential polymerization method can support well-defined block copolymerization by taking advantage of substituent effect of monomers. In the literature, various polyamides studies have been dedicated to sequential condensation polymerization¹⁵⁰.

Recently, Oishi et al.¹⁵¹ reported the sequential condensation polymerization of *m*-substituted and *p*-substituted monomers with different combinations. They first synthesized *N*-alkyl poly(*m*-benzamide)-*b*-*N*-H poly(*m*-benzamide), *N*-alkyl poly(*m*-

benzamide)-b-*N*-H poly(*p*-benzamide), and *N*-alkyl poly(*p*-benzamide)-b-*N*-H poly(*m*-benzamide) by sequential chain-growth condensation polymerization of *N*-alkyl and *N*-octyloxybenzyl monomers, and then got rid of the octyloxybenzyl- group with trifluoroacetic acid to gain gelation properties on the resulting sequential copolymer.

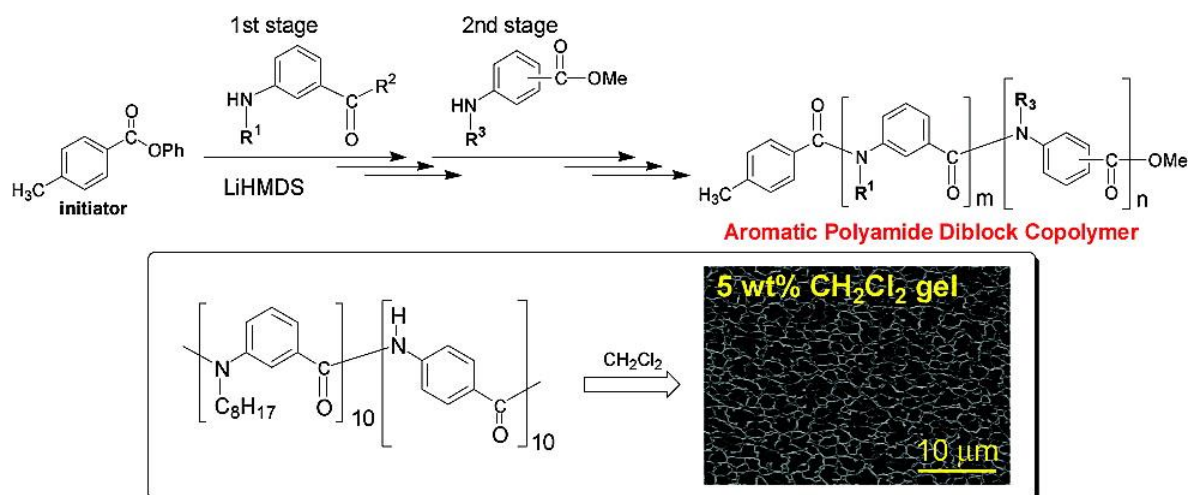


Figure I-2. Aromatic polyamide diblock copolymer synthesis and SEM analysis. Reprinted from ¹⁵¹.

The gelating property was analyzed by scanning electron microscopy (SEM) shown in Figure I-2. The SEM analysis of the dried CH₂Cl₂ gel demonstrated that the block copolymers self-assembled to form a three-dimensional network structure. The gelating properties are dependent on the substitution position (*meta* or *para*) and the composition ratio of the *N*-H poly(benzamide) segment in these block copolymers. Among them, the block copolymer containing *N*-H poly(*p*-benzamide) showed extensive gelating properties owing to high polar interactions and the aggregating nature of *N*-H aromatic polyamide units¹⁴⁵.

To the best of our knowledge, Sugi et al.¹⁴⁷ reported well-defined (controlled molar mass and low dispersity) thermo-sensitive and water soluble condensation aromatic polyamide (Figure I-3). The resulting poly(*m*-benzamide)s bearing a tri- or tetra(ethylene glycol) methyl ether unit on the amino group show reversible phase transitions in the aqueous solutions depending on the thermal changing. Compare to aliphatic polymers¹⁵²⁻¹⁵⁴ from living polymerizations, poly(*m*-benzamide)s demonstrated phase separations at lower temperature on cooling showing that there is a stronger intermolecular interaction as a result of the aromatic rings stacking in the aggregates¹⁴⁷.

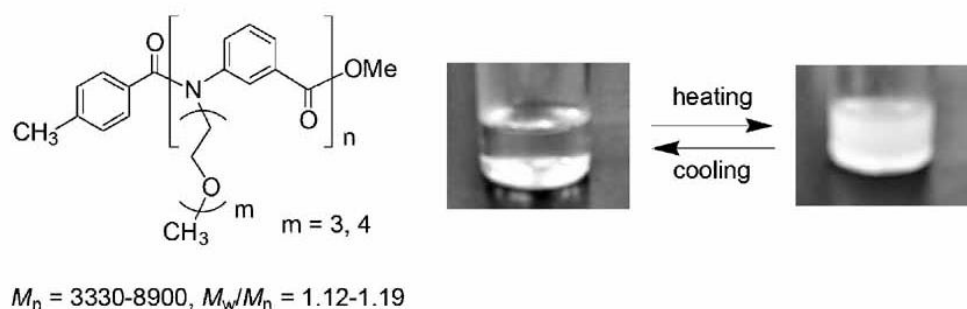
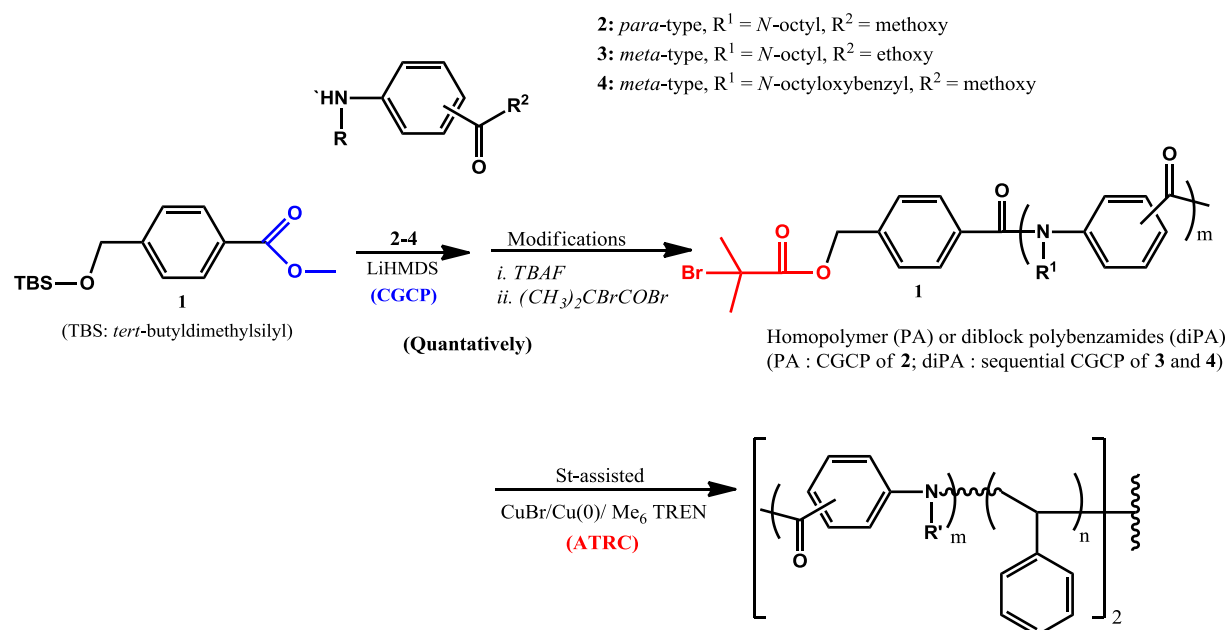


Figure I-3. Thermally sensitive water-soluble poly(*m*-benzamide)s. Adapted from¹⁴⁷.

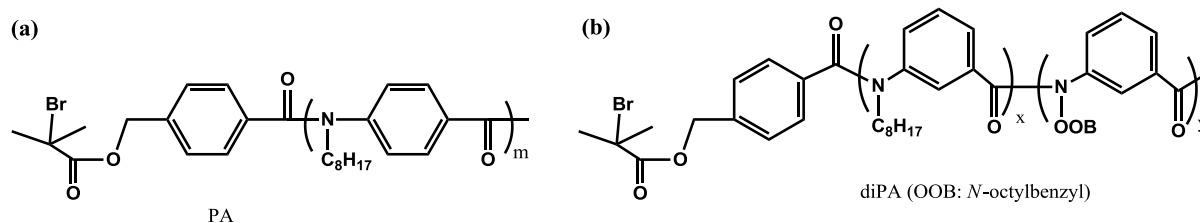
2.3.2. Block copolymers by a coupling reaction

Huang et al.¹⁵⁵ developed a combination of styrene-assisted atom transfer radical coupling (ATRC)¹⁵⁶ and CGCP for the synthesis of diblock and triblock copolyamides. Their strategy for combination with CGCP (polybenzamides) and styrene-assisted ATRC is depicted in Scheme I-24.



Scheme I-24. Synthesis of well-defined symmetrical polybenzamides by means of combination of styrene-assisted atom transfer radical coupling and chain-growth condensation polymerization. Adapted from¹⁵⁵.

They first synthesized two 2-bromoisobutyryl-terminated polybenzamide precursors, shown in Scheme I-25: poly(*N*-octyl-*p*-benzamide) (PA: \overline{Mn} = 3000, \mathcal{D} = 1.08) (a) and poly(*N*-octyl-*m*-benzamide)-block-poly(*N*-octyloxybenzyl-*m*-benzamide) (diPA: \overline{Mn} = 9300, \mathcal{D} = 1.09) (b).



Scheme I-25. Precursors of (a) polybenzamide homopolymer (PA) and (b) diblock polybenzamide (diPA) for coupling reactions. Adapted from¹⁵⁵.

After ATRC by styrene assisting, at 25 °C and completed only in 3 h, homo (\overline{Mn} = 3000) and diblock (\overline{Mn} = 9300) polybenzamides proceeded with a high extent of coupling, and the molar masses nearly doubled (\overline{Mn} ~ 6000 and \overline{Mn} ~ 18000) by keeping the narrow dispersity (\mathcal{D} < 1.18). Following the coupling reaction, size exclusion chromatography (SEC) of the resulting polybenzamides, (a) initial diblock polybenzamide (diPA), (b) crude triblock polybenzamide⁷⁴ after ATRC, and (c) purified triPA, with increased molar masses are shown in Figure I-4.

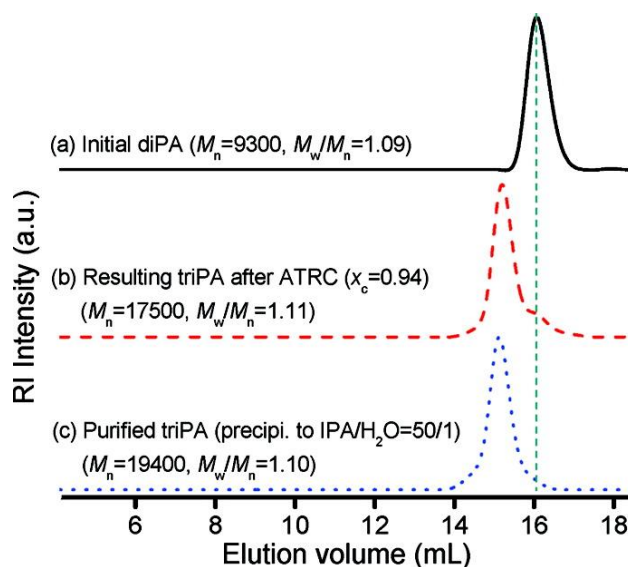
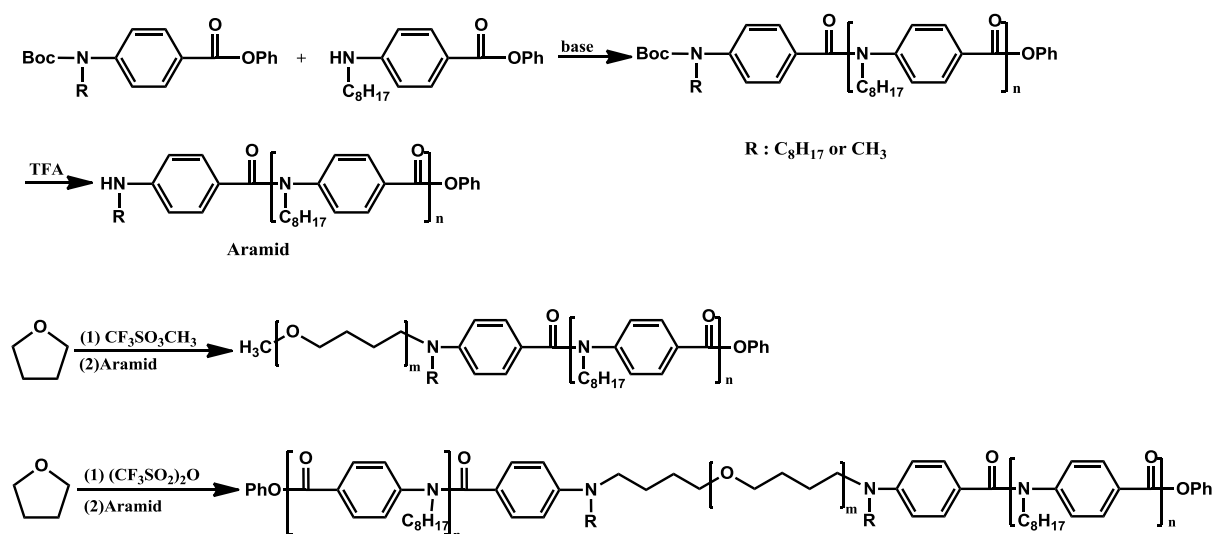


Figure I-4. SEC traces (RI detector) of diblock polybenzamide coupling products: (a) initial diblock polybenzamide (diPA), (b) crude triblock polybenzamide⁷⁴ after ATRC, and (c) purified triPA (precipitated into isopropylalcohol/H₂O = 50/1 (v/v)).

Furthermore, they studied the thermal properties of the obtained polybenzamides before and after selectively removing the pendant alkyl groups by trifluoroacetic acid for 3 days. Differential scanning calorimetry (DSC) measurements showed that the good thermal stability of the ester linkage resulted in the formation of poly-(*N*-H-polybenzamide) units. For the triblock polybenzamides, the T_g values are shifted from 45 to 62 °C which is probably related to the increasing intermolecular hydrogen-bonding after deprotection¹⁵⁵.

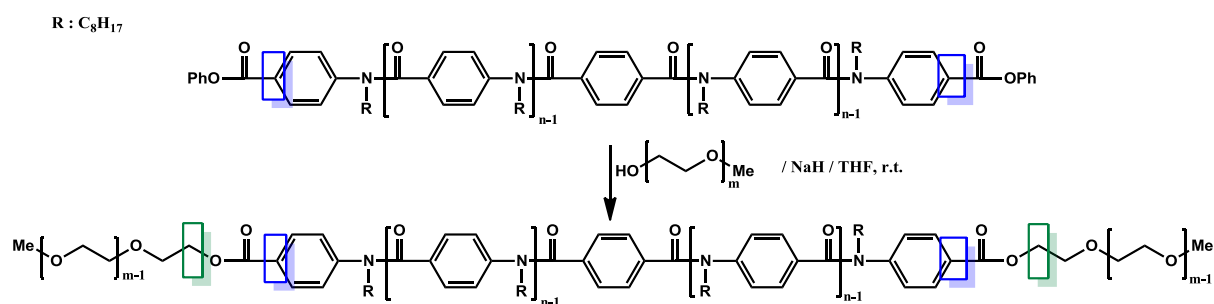
Block copolymers of aromatic polyamide and poly(tetrahydrofuran) were studied by Sugi et al.¹⁵⁷. First the polycondensation reaction of phenyl 4-(octylamino) benzoate was achieved with an initiator which has tert-butoxycarbonyl (Boc) substituent as a protecting group. After polycondensation, the initiator side of the resulting polymer was deprotected with trifluoroacetic acid and a telechelic aromatic polyamide with terminal amino group was obtained. Di- and triblock copolymers were obtained via the reaction of the terminal amino group of aromatic polyamides and living cationic propagating poly(tetrahydrofuran) (Scheme I-26).



Scheme I-26. Synthesis of block copolymers of polyamide and poly(tetrahydrofuran).

In another approach, the bidirectional propagation of chain-growth polycondensation and its application to poly(ethylene glycol)–aromatic polyamide–poly(ethylene glycol) (PEG–polyamide–PEG) triblock copolymer with low polydispersity were studied without contamination of step-growth condensation polymerization. First, the polycondensation of phenyl 4-(octylamino)benzoate was carried out in the presence of a difunctional initiator,

diphenyl terephthalate. Successfully synthesized well defined rodlike aromatic polyamides have phenyl ester moieties at both end side of the polymer¹⁵⁸. By taking advantage of the transesterification reaction of these phenyl ester end groups and the alkoxide part of PEG prepared by anionic living polymerization, PEG-polyamide-PEG triblock copolymers were synthesized (Scheme I-27).



Scheme I-27. Poly(ethylene glycol)–aromatic polyamide–poly(ethylene glycol) triblock copolymer synthesis.

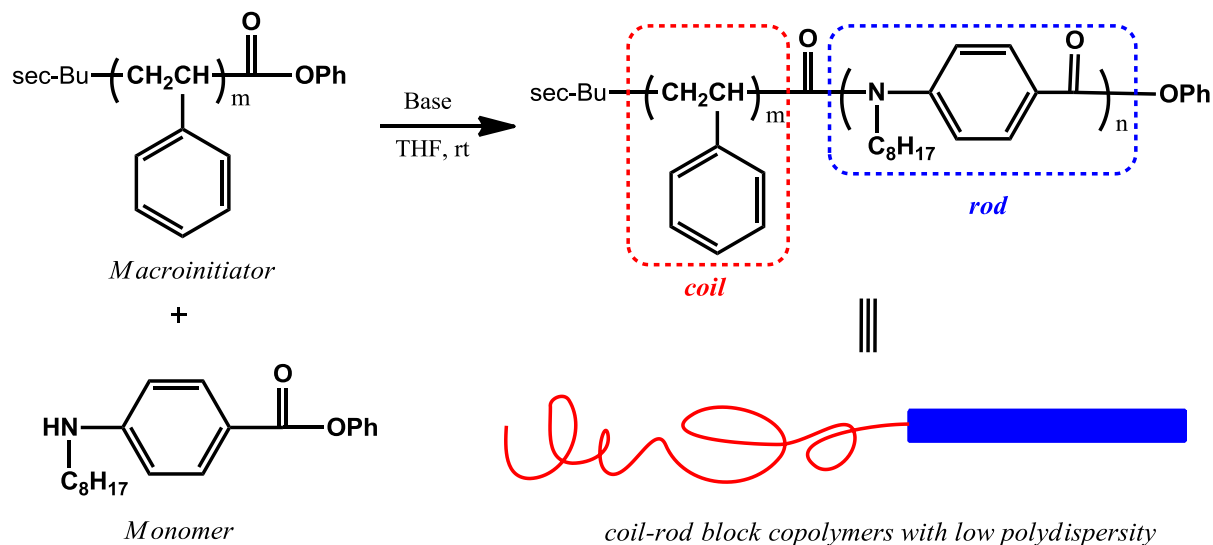
These methods were used to synthesize rod-coil like polymers owing to their interesting self-assembly behavior in solution and solid state. Rod-coil copolymers, including rigid rod segments and flexible coil segments, can have more precise self-assembly owing to controlled molar mass and low dispersity by CGCP.

2.3.3. Macro-initiator approach

Macro-initiator (MI) approach is one of the ways to gain rod-coil block copolymers. There are many methods including CGCP to achieve rod-coil block copolymers such as living anionic polymerization, atom transfer radical polymerization (ATRP), and reversible addition-fragmentation chain transfer (RAFT).

In this example, synthesis of well-defined rod-coil block copolymers of polystyrene and *N*-octyl poly(*p*-benzamide) were started with MI (Polystyrene) preparation from living anionic polymerization. Then, the chain-growth condensation polymerization of phenyl 4-(octylamino)benzoate was performed from polystyrene with a phenoxy carbonyl chain-end group in the presence of triethylsilane or *N*-octyl-*N*-triethylsilylaniline bases (Scheme I-28). They clearly observed SEC shifting with narrow dispersity. The obtained block copolymers

self-assembled in 2-propanol, which was a selective solvent for the polyamide unit, to give submicrometer-sized, spherical aggregates¹⁵².

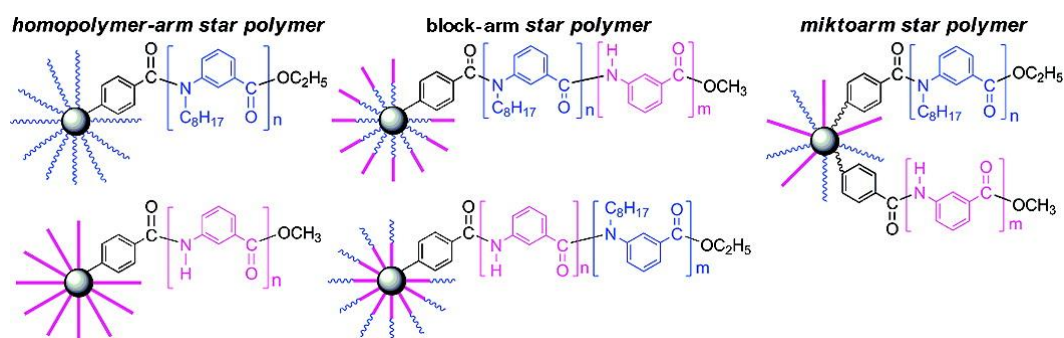


Scheme I-28. Chain-growth condensation polymerization of phenyl 4-(octylamino)benzoate from polystyrene macroinitiator. Adapted from¹⁵².

Synthesis of well-defined polybenzamide-block-polystyrene by combination of CGCP and RAFT polymerization with controlled molar mass and narrow dispersity was studied by Masukawa et al.¹⁵⁹. They have chosen this method owing to controlled radical polymerization because of its broad tolerance for functional groups including the amide bond. In this approach, polystyrene was synthesized from RAFT polymerization of styrene and polybenzamide was obtained by CGCP and used as a chain transfer agent (CTA) for RAFT polymerization. On the other hand, after RAFT-CGCP combination, CGCP and ATRP¹⁶⁰ combination was reported by the same group. However, this method was started from chain-growth polybenzamide as a MI to avoid hindrance problems which is sourced from the first using of high molar mass MI for CGCP by leading to self-condensation. Indeed, CGCP-ATRP combination also prevents from the tedious synthesis of macromolecular chain transfer agent of RAFT¹⁵⁹. CGCP was followed by chain end modification and then ATRP of St from this activated chain-end for the synthesis of well defined polybenzamide-b-polystyrene block copolymers. In this approach, they could obtain chain extensions with St and a linear increasing of molar mass by respecting to conversion, low dispersity, and monomodal SEC traces.

2.4. Complex architectures of aromatic polyamides

Since chain-growth polycondensation is investigated, this route was conducted to achieve various condensation polymer architectures such as block copolymers, hyperbranched and star polymers with controlled molar masses and narrow dispersities. As early mentioned above, linear aromatic polyamides (aramids) are known as important high-performance polymers because of their excellent thermal, mechanical, and chemical properties. Digressing from usual linear structure of polyamides leads to higher solubility and lower melting points due to the inhibition of strong hydrogen bonds of the amide group on polymer chain. However, these polyamides having spherical-like geometries introduce unique properties to conventional polyamide for novel applications such as their encapsulation characteristics, catalysis, chromatography, self-assembly, as well as medical and biological applications. Indeed, various number of hyperbranched and star polyamides are studied by conventional condensation polymerization without controlling of the molar mass and dispersity¹⁶¹. Among these complex structures, well-defined star¹⁶² and hyperbranched¹⁶³ polymers gained an important field in macromolecular chemistry due to their unique spatial shapes and rheological properties^{161, 162, 164, 165}. Recently, Ohishi et al.¹⁶² reported the synthesis of homopolymer-arm, block-arm, and miktoarm star polymers consisting of poly(*N*-octyl-*m*-benzamide) and poly(*N*-*H*-*m*-benzamide) by a core cross-linking method of macromonomers (condensation polymers of 3-(alkylamino)benzoic acid esters) with a divinyl terminal compound (Scheme I-29). These polymers have arms with different solubility and hydrogen-bonding capacity. Indeed, thermoresponsive ability of these novel star aromatic polyamides was studied due to changing of molecular geometry from semi-rigid to flexible coil.



Scheme I-29. Star polybenzamides¹⁶².

3. Crosslinking of polyamide 6

Crosslinking of numerous polymers is important on behalf of modifying a number of material properties. Only a few papers dealing with PA6 crosslinking have appeared in the scientific literature, and none of them are devoted to the reversible crosslinking of PA6 based composites even though it has a great potential. According to reported studies, PA6 can be crosslinked by radiation¹⁶⁶, high pressure-high temperature treatment¹⁶⁷, blending with different type of polymers, and copolymerization with crosslinkable groups^{168, 169}.

3.1. Radiation crosslinking of polyamide 6

Depending on the type of polymer, they may be crosslinked by using high-energy ionizing radiation, i.e. electron beam (or e-beam), gamma, or x-ray radiations. Electron beam is generally used for small parts, particularly low density parts, and linear product like aliphatic polyamide processed. Irradiation generates free radicals which chemically react in various ways, sometimes at slow reaction rates. The free radicals can reconnect to form the crosslinks. The benefits of this method are the crosslinking degree can be adjusted via the amount of radiation dose. However, irradiation oxidation can occur especially under gamma irradiation which is the faster method. Oxidation can continue after irradiation and changes in properties with time. This oxidation process can be hindered by adding antioxidants. E-beam irradiation crosslinking method is mostly preferred for PA6 crosslinking due to higher deterioration effect of gamma irradiation on mechanical properties than the e-beam irradiation^{170, 171}.

The effects of radiation crosslinking on PA6 and aliphatic polyamide family have been reported by many researchers^{166, 172-175}. E-beam crosslinked structures in PA6 are expected to vary physico-mechanical properties (hardness, tensile strength, flexural strength, and impact resistance) in irradiated polymer materials while reducing water absorption. Water absorption percent of PA6 was reduced substantially when irradiated by e-beam radiation in presence of triallyl isocyanurate as a crosslinking agent which reduces dose of radiation for crosslinking¹⁷⁵. Hardness, tensile strength, flexural strength, and impact resistance of PA6 were improved by adjusting the dose of e-beam radiation. Improvement of mechanical properties and reduction of water absorption were owing to the crosslinking of polyamide

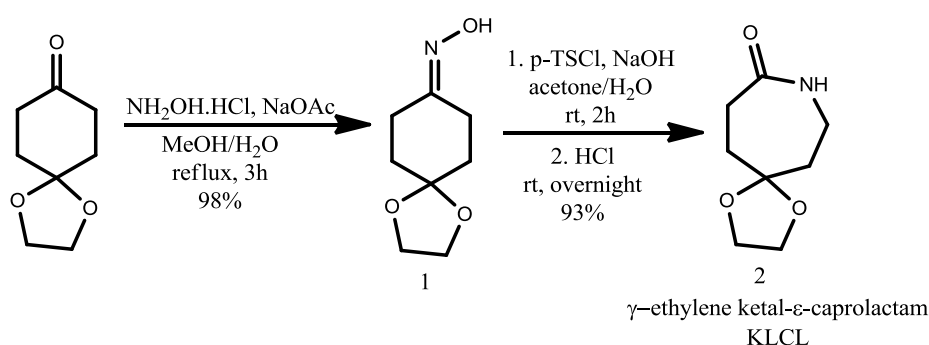
molecules in the presence of high-energy radiation. Increase of crosslinking with rising radiation dose was verified by gel content amount at higher doses¹⁷⁵.

Beside this advantages of radiation crosslinking on PA6 properties, high investment cost and equipment expertise make this way undesirable between crosslinking methods.

3.2. Crosslinked polyamide 6 by chemical modification

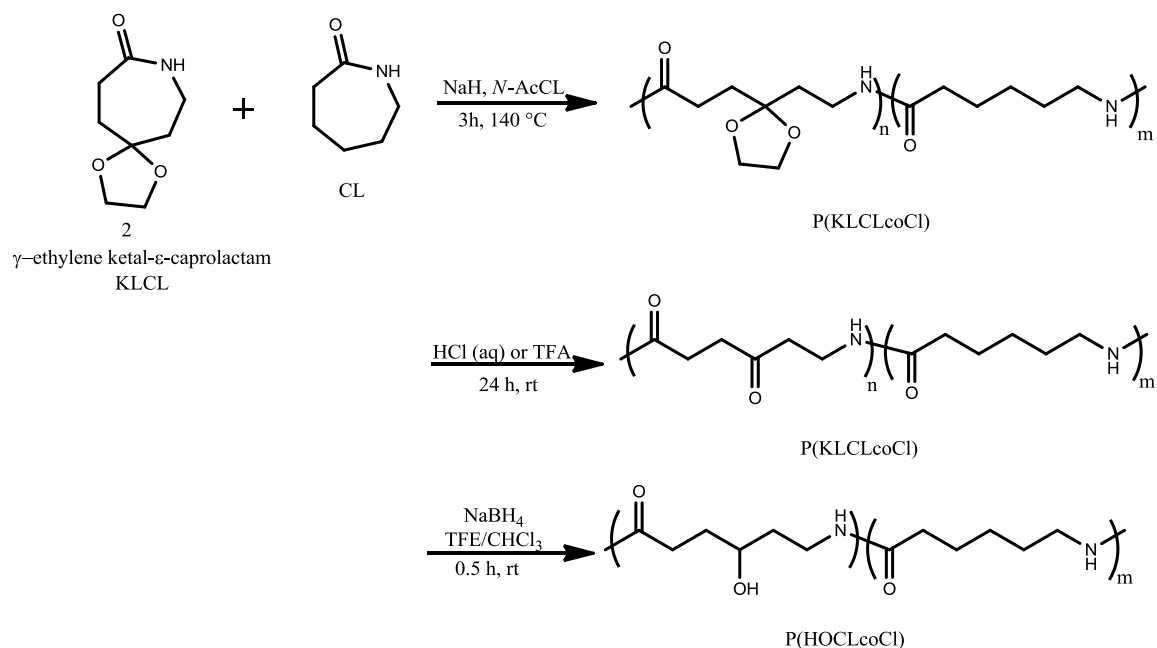
So far, crosslinked PA6 was explored in a restricted number of works that are obtained from homo- or copolymerization of CL with functional derivatives of CL either by anionic or hydrolytic ring-opening polymerization.

The functional groups must be selected or protected in such a way that they do not inhibit polymerization. The disadvantage of these studies is generally that they are obtained by either complex or time-consuming procedures. Recently, Mathias et al.¹⁶⁸ reported γ -ethylene ketal- ϵ -caprolactam (KLCL) synthesis and its polymerization by AROP. A new monomer KLCL was synthesized in two steps at room temperature and efficiently, Scheme I-30.



Scheme I-30. Monomer synthesis, ethylene ketal substituted ϵ -caprolactam (KLCL).

Following the monomer synthesis, AROP of KLCL was obtained in bulk at 140 °C under N₂ atmosphere. Even though solidification of P(KLCL) is completed in 5 min, yield was only 68% which is quite low compare to CL polymerization yield (98%) in the same conditions. Random copolymerization of KLCL and CL was achieved under the same polymerization conditions, Scheme I-31. In this first step, as can be seen from the polymer structure, the copolyamide has pendant ketone groups on the polymer chain. These ketone groups are deprotected by trifluoroacetic acid and then reduced to hydroxyl group by using sodium borohydride.

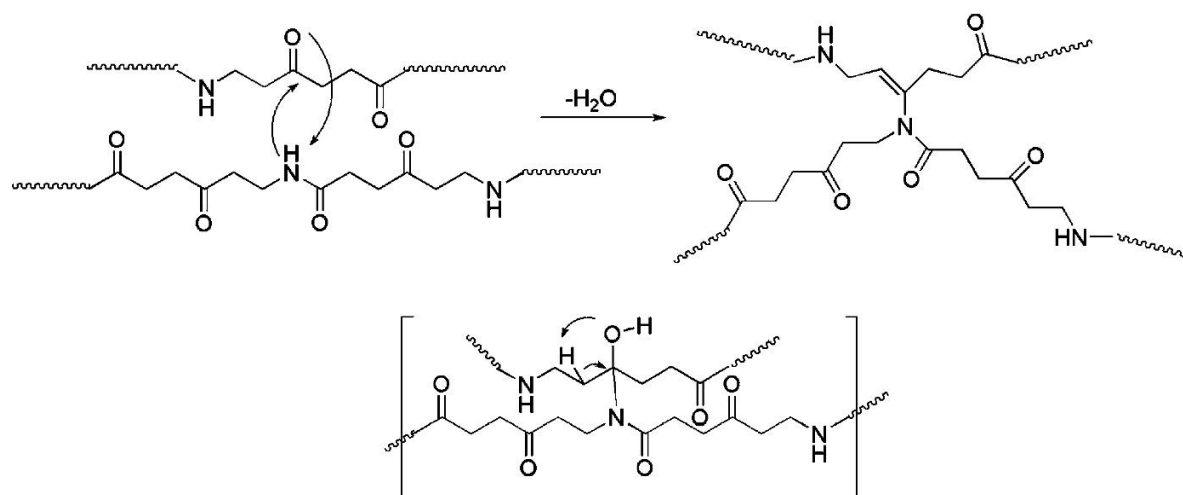


Scheme I-31. γ-ethylene ketal-ε-caprolactam monomer synthesis and its AROP¹⁶⁸.

According to thermal measurements from DSC (second scan), P(KLCL) and its copolymers have higher T_g than neat PA6. This new class of copolyamides has less crystallinity and lower melting temperatures than neat PA6. This result demonstrates that rigid ketal groups increase the T_g and inhibit close packing while decreasing the melting temperature and crystallinity.

Thermal- and photo-crosslinking sensitivity of the ketone content in the polymer is a special property of the ketone-containing polymers. By taking advantage of this property, crosslinked the “ketone groups” in the polymers were studied via either heating or UV irradiation. Crosslinking was detected by insolubility of these polymers in organic solvents and increasing T_g 's with increasing KCL content. On the other hand, the ketal- and hydroxyl-containing polymers are not crosslinked upon heating or UV irradiation.

Indeed, the crosslinking mechanism of this novel polymer suggested that the attack of amide nitrogen at the ketone carbonyl group was followed by the release of water and the formation of enamide linkages between chains (Scheme I-32).



Scheme I-32. Crosslinked structure of P(KLCL).

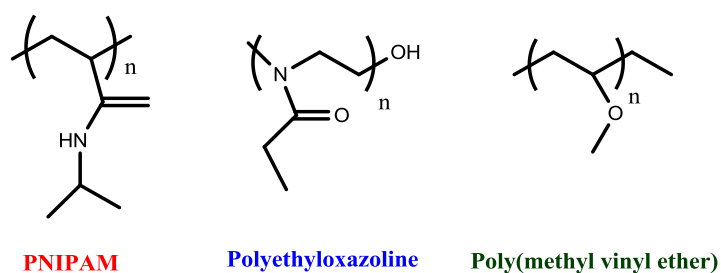
3.3. Stimuli Responsive Polymers

Stimuli-responsive polymers are affected by small changes in the environment such as temperature, light, pH and combination of two or more of them (two-multi stimuli). They gained a steadily increasing attention in materials science, nanotechnology, and biotechnology for the last two decades. Classifying these polymers according to their physical properties, free chains in solutions, chains grafted on a surface, covalently cross-linked gels and reversible or physical gels, are summarized. Indeed, double or multi-stimuli responsive polymers, the all-in-one^{176, 177} as well as pH, thermo and photoresponsive stimuli polymers, double or multi stimuli examples of them in one polymer also exist. Multi and double stimuli responsive systems were widely documented in order to obtain multiple responsive behavior by introducing newer application areas¹⁷⁸.

3.3.1. pH and thermoresponsive groups

pH responsive polymers containing ionizable functional sensitive groups can donate or accept protons relying on environmental pH changing¹⁷⁶. This donation or acceptance leads to the extension or collapse of the polymer chain in aqueous solution, induced by the electrostatic repulsion between generated charges. Recently, pH-sensitive polymers gained attention for applications in gene delivery and gene therapy research. Most common used pH sensitive polymers are polyacrylic acid¹⁷⁹, polymethacrylic acid (PMAA)¹⁸⁰, poly(ethylene imine)¹⁸¹ and poly(L-lysine)¹⁸².

Widening interest to thermoresponsive polymers was applied to smart material applications. Unique working principle of thermoresponsive polymers is showing fundamental changes in conformation by answering different temperatures. Thermoresponsive polymers have plenty of proposed applications, such as tissue engineering¹⁸³, drug delivery¹⁸⁴, catalysis¹⁸⁵, surface engineering¹⁸⁶, information processing¹⁸⁷ or shape memory polymers¹⁸⁸. Polyacrylamides(PNIPAM)¹⁸⁹, polyoxazolines¹⁹⁰, polyvinyl ethers¹⁹¹, and poly(ethylene oxide) methacrylates¹⁹² are largely examined polymers in this field are depicted in Scheme I-33.



Scheme I-33. Generally used thermoresponsive groups.

3.3.2. Photoresponsive groups

In recent decades, polymers containing photosensitive moieties have crucial interest because of their potential use in many range of application fields such as photolithography^{193, 194}, photo-curable coatings¹⁹⁵ and photoresists¹⁹⁶. Photoresponsive groups are also interesting to modify and develop some properties of PA6 which will be explained in one part of this thesis work.

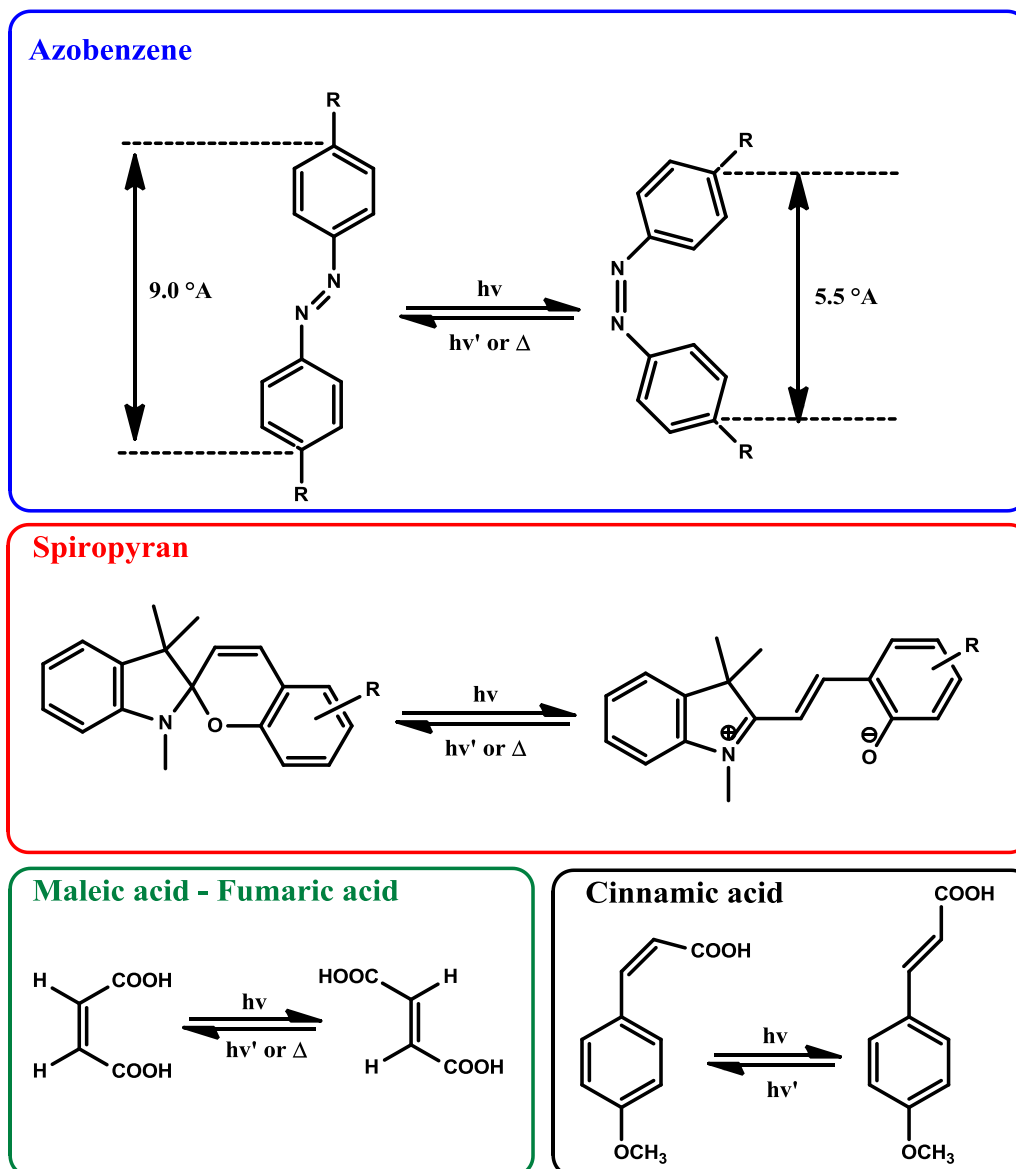
Photoresponsive systems can be associated to three reaction types: photoisomerization, photocleavage and photodimerization. Polymers, having photochromic molecules usually as the functional part on the polymer, first capture optical signal and then chromophore groups convert this signal to a chemical photoreaction as mentioned as isomerization, cleavage or dimerization. This chemical conversion can control its properties over the photoreactive groups. Reactivity and reversibility of these photo functional groups relies on the polymer structure (interaction between chromophore groups, flexibility and solubility during the irradiation).

3.4. Photoreactions

3.4.1. Photoisomerization

Photoisomerization of active units on the molecule occurs from trans (lower energy state) to cis (higher energy state) by photochemically or thermally and most often can go back to the original state by visible light irradiation or heating (Scheme I-34). Common used examples are the azobenzene, spiropyran, maleic acid, and cinnamic acid and in some reactions their reversibilities.

Among these examples azobenzene is mostly used as photoreactive group. Azobenzenes can switch from E form (trans form) to Z form (cis form) by UV irradiation and turn back to their thermodynamically stable trans configuration by irradiating visible light or thermally. Scarce studies were reported about polyamide containing azobenzene units. Aromatic polyamide having azobenzene groups in the polymer backbone and with a low molar mass model compound were studied as a photoresponsive polymer by Schnabel and coworkers¹⁹⁷. Conformational change of the azobenzene units via photoisomerization were followed by light scattering measurements.

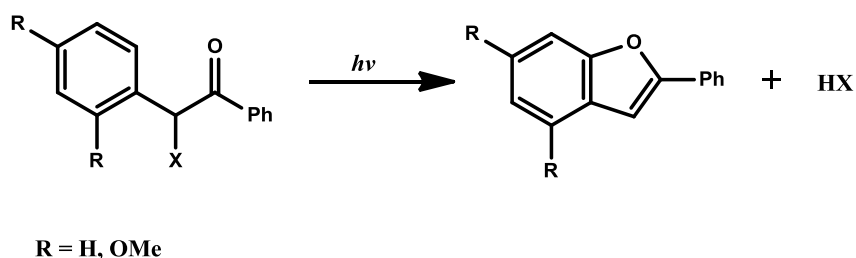


Scheme I-34. Photoisomerization of cinnamic acid, maleic acid-fumaric acid, spiropyran and azobenzene.

On the other hand, a series of novel comblike aromatic polyamide containing cinnamoyl side groups have been reported by conventional condensation polymerization¹⁹⁸. They characterized improved mechanical properties of the crosslinked aromatic polyamide after photoisomerization of these polymers in solution and solid state.

3.4.2. Photocleavage

Photo-cleavage reaction of triggering group via UV irradiation leads to the degradation of polymers by changing photochemical and chemical properties of polymer such as swelling property of hydrogels. *o*-nitrobenzyl¹⁹⁹, coumarin²⁰⁰, benzoin²⁰¹ and anthracene²⁰² are mostly used as photoreactive groups. As an example, photoreaction of the benzoin group is shown in Scheme I-35.



Scheme I-35. Photocleavage of benzoin.

3.4.3. Photodimerization

Cinnamoyl^{203, 204}, coumarin²⁰⁵ and anthracene^{202, 206} are mostly used photoreactive groups for the photodimerization reaction. Photoreversible approach of these groups in side or main-chain of polymer provides controlling of swelling properties of polymers as well as self-healing character. Photo-crosslinking method is preferred because of non-toxicity, economical and absence of by-products compare to other techniques.

3.4.3.1. Photodimerization of Anthracene

Anthracene is a well-known chromophore group²⁰⁷ that can be reversibly photo and thermodimerized through [4+4] cycloaddition reaction. This reversibility of anthracene dimerization can tune some properties such as swelling, degradation and diffusion properties in tissue engineering and drug delivery applications as a crosslinker²⁰⁸ or improve and/or modify physical or chemical properties of polymers by grafting. Although the dimerization of anthracene in polymer unit were extensively reported, reversible crosslinking studies are more scarce²⁰².

Lately, the creation of single-chain nanoparticles by intra-chain photodimerization of poly(methyl methacrylate) with pendant anthracene units was demonstrated as an efficient route to folded polymer structures by Frank et al.²⁰⁹. Single chain folding in dilute solution

and producing architecturally defined nanostructures in the sub-20 nm size regime were evidenced by decreasing UV absorbance and size exclusion chromatography (SEC) through shifting longer retention time as dimerization occurs (Figure I-5). This result is showing that large multichain aggregation occurs during the irradiation.

Retro-Diels-Alder reaction of aromatic polyamide containing anthracene²¹⁰ were also studied. First diels-alder reaction was carried out from monomers containing anthracene unit and then polycondensation of these monomers was obtained. After all, they could conduct thermal retro-Diels-Alder reactions at 220 °C.

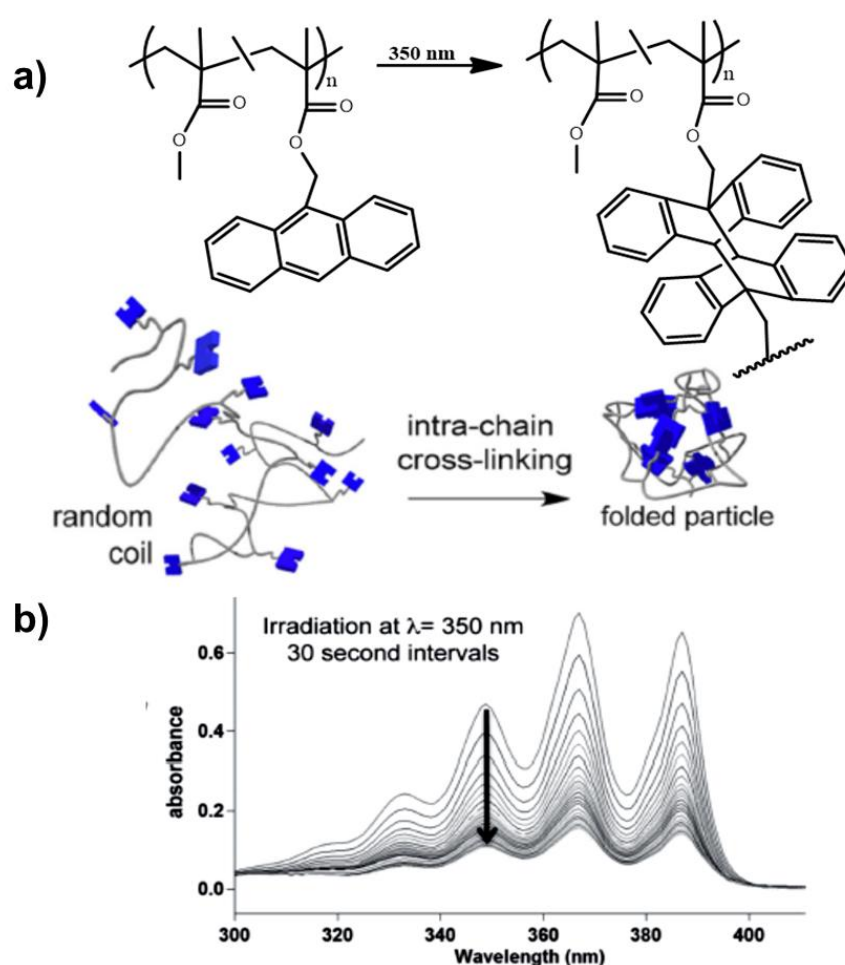
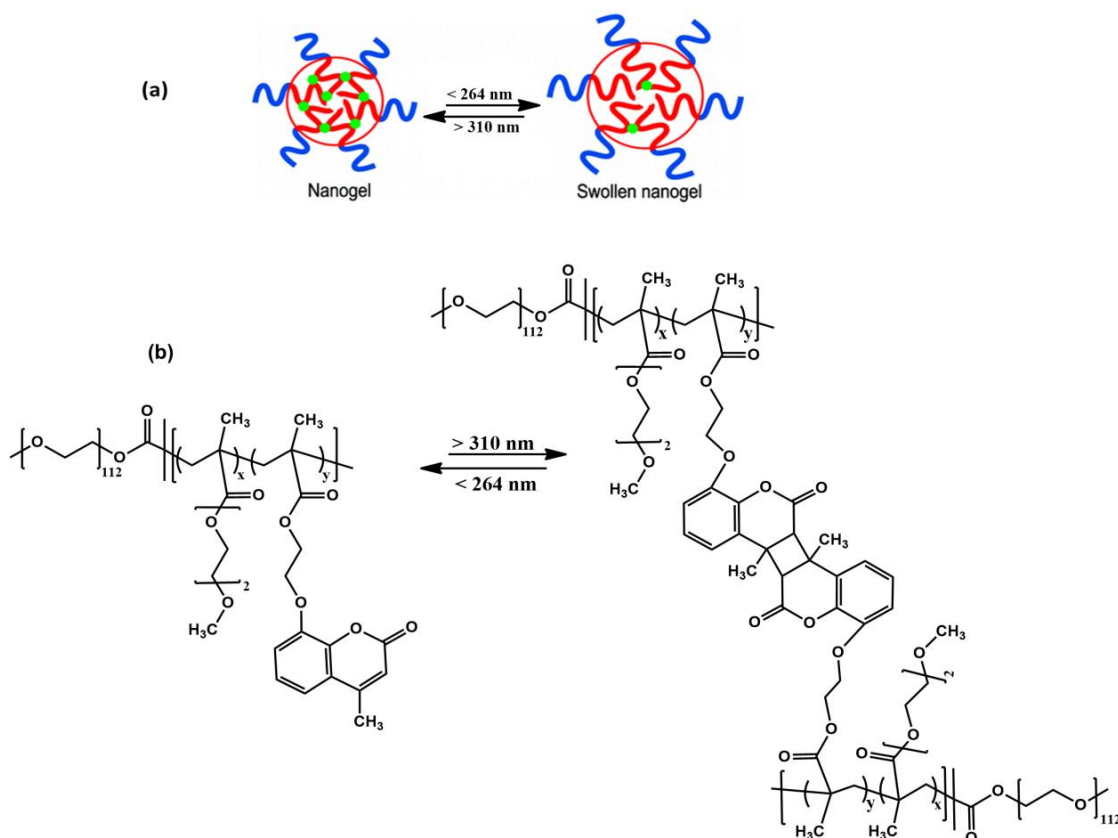


Figure I-5. a) Synthesis of anthracene-functionalized polymers. b) Overlay of UV-vis spectra for P1, confirming dimerization by monitoring the disappearance of the characteristic five-finger anthracene absorption. Exported from ref²⁰⁹.

3.4.3.2. Photodimerization of coumarin group

Unsophisticated coumarin derivatives are based on cinnamic acid which is a member of the benzopyrone family²¹¹. Incorporation of coumarin derivatives to macromolecules was widely used due to reversible dimerization by photocrosslinking (>300 nm) and photocleavage (<300 nm)²¹². Ji et al.²⁰⁵ reported the implementation of a reversible photo-crosslinking reaction for photoresponsive nanogels and for the control of the swelling degree of hydrogels.

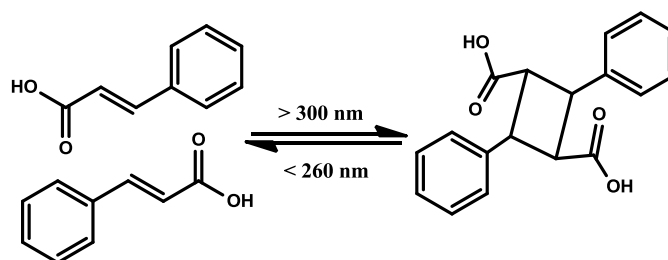
Photocleavage of the cyclobutane ring reduced the crosslinking density and led to an increase in nanogel's volume (up to 90%) at $\lambda < 260$ nm. Regaining initial hydrogel volume could be obtained by photo-crosslinking and the photoinduced volume transition could be repeated²⁰⁵. This system is depicted in Scheme I-36.



Scheme I-36. (a) Schematic illustration of the preparation and photocontrolled volume change of nanogel. (b) Designed diblock copolymer bearing coumarin side groups for the reversible photo-cross-linking reaction. Adapted from²⁰⁵.

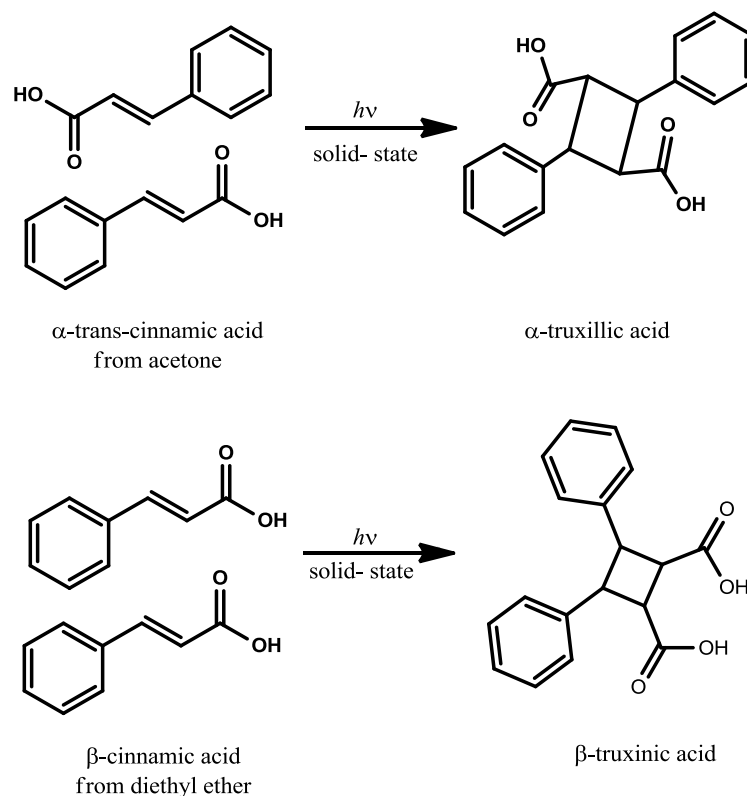
3.4.3.3. Photodimerization of cinnamoyl group

Photo-responsive cinnamoyl group either in the polymer backbone or as side chain can undergo crosslinking via [2+2] cycloaddition through the carbon-carbon double bond by thermo or photodimerization with UV light: photocleavage under 260 nm and photodimerization above 300 nm as shown in Scheme I-37 for the cinnamic acid.



Scheme I-37. Reversible photodimerization of trans-cinnamic acid.

The packing of *trans*-cinnamic acid and its derivatives in three different forms: an α -form (where monomers are arranged in a head-to-tail manner), β -form (with the monomers arranged head-to-head), and a γ -form (where the monomers are unfavorably aligned) were classified by Schmidt²¹³. The α - and β -forms the reactive double bonds approach each other by less than approximately 4 Å and which are photoactive yielding head-to-tail and head-to-head dimers, respectively (Scheme I-38), the γ -form is photostable^{214, 215}.



Scheme I-38. α - and β -forms of trans-cinnamic acid to dimers via topochemical reactions. Adapted from²¹⁴.

Among photosensitive moieties, polymers containing photo-reactive cinnamoyl group are also known with their high photosensitivity²¹⁶, the ability to form films, resistance towards solvents, and good thermal stability^{217, 218}. The reversible polymeric systems have gained wide range of application areas such as self-healing²¹⁹.

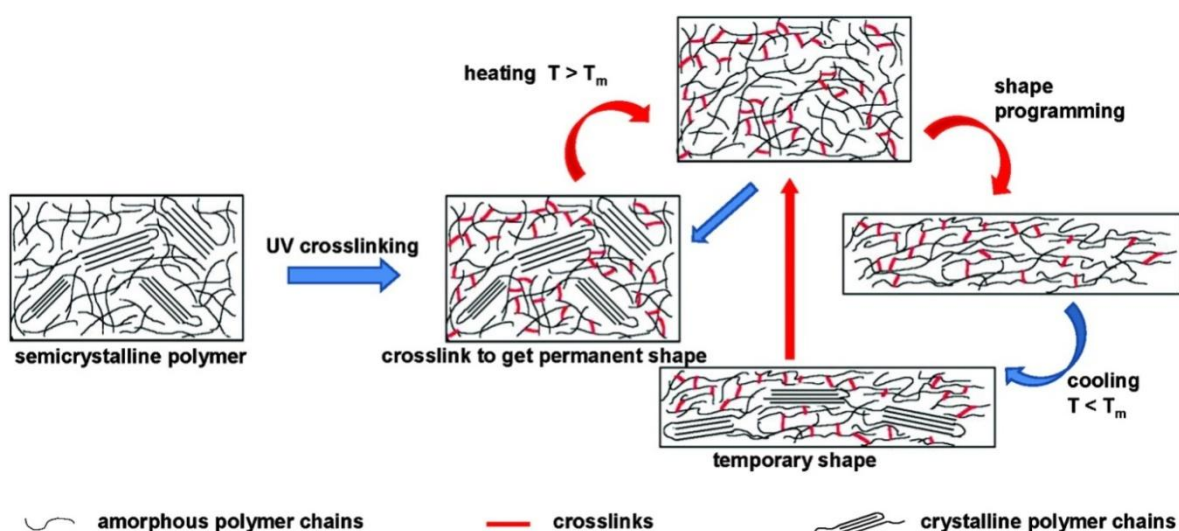
Wan Jae et al.²²⁰ reported the synthesis of healable poly (methacrylate) derivatives with photo-responsive cinnamoyl units into the side chain. They could also control the hardness of thermoplastic polymer films by reversible photo-cycloaddition reaction via UV irradiation.

As highlighted above, experimental conditions as well as size of polymer may also play an important role on the photodimerization. For example, the polymer bearing photosensitive groups shows a higher photoreactivity in solution compared to in the solid state as a coated film because photosensitive groups are not close enough together in the condensed state¹⁹⁸. Longer polymer chain has also less reactivity compare to shorter chains unit that leads to faster photoreaction due to better mobility²²¹. In the presence of [2+2] cinnamoyl

cycloaddition, the photodimerization generates crosslinking in the polymer via cyclobutane ring formation, ending to the insolubilization of the polymer in many organic solvents²²².

Quite recently, Garle et al.¹⁸⁸ reported the synthesis of semicrystalline poly(ϵ -caprolactone) (PCL) copolymer networks with stimuli-responsive shape memory behavior by investigating cinnamoyl moiety as a thermo-responsive group. Advantage of this system is that no initiator or chemical crosslinker is required for the crosslinking of semi-crystalline copolymers by UV irradiation¹⁸⁸.

Crosslinks formed from [2 + 2] cycloadditions of cinnamoyl units can be reversibly cleaved by UV irradiation at $\lambda < 260$ nm, leading to the recovery of the original shape. Therefore, crosslinking was used to establishing the permanent shape, and the melting transition could be used for shape memory programming and recovery (Scheme I-39). Indeed, adjusting of the glass transition temperature at which shape memory occurs can be accomplished by varying the molar mass of PCL. On the other hand, modification of ϵ -caprolactone monomer with a cinnamate functional group, and then copolymerizing with ϵ -caprolactone improved mechanical properties such as hardness¹⁸⁸.



Scheme I-39. Proposed structural changes during shape memory transformation of polymer. Adapted from ¹⁸⁸.

[2+2] photoinduced dimerization of cinnamic acid and its derivatives has gained great interest, as mentioned above. In particular, the reason of such a big interest is solid-state behavior and its versatility in a numerous number of applications such as healing²²³. The

photodimerization of cinnamate derivatives in solution has achieved less interest compare to solid state due to the long irradiation time needed to complete good conversion. Photodimerization of cinnamate in solid state are among the most extensively reported crystalline-state reaction. Indeed, solid state gets rid of any solvent effect during dimerization.

4. Fluorinated aromatic and aliphatic polyamides

Wettability is an important property of solid surfaces, the wettability control of a solid surface shows an enormous value in both fundamental research and practical applications²²⁴. Wetting of a liquid on a solid surface or material depends on the solid surface properties (hydrophobic or hydrophilic) as well as the liquid used. Therefore, manipulating the properties of surfaces can optimize the hydrophobicity of a solid surface or material for the purpose of interest. Surface hydrophobicity can be estimated by determining the contact angle. Hydrophobic character of polymer surfaces can be divided to three different types according to their contact angle to liquid: super hydrophobic (Contact angle (CA) higher than 150° , lotus leaf effect), hydrophobic (CA higher than 90°) and hydrophilic (CA less than 90°) polymer surfaces (Figure I-6). It is generally agreed that the measurement of CAs of liquid with known surface tension on a given solid polymer surface is the most practical way to measure surface energy. This is also known that surface energy can be effected by surface roughness, different chemical amount, polymer solution, swelling, molecular orientation and sorption layers²²⁵.

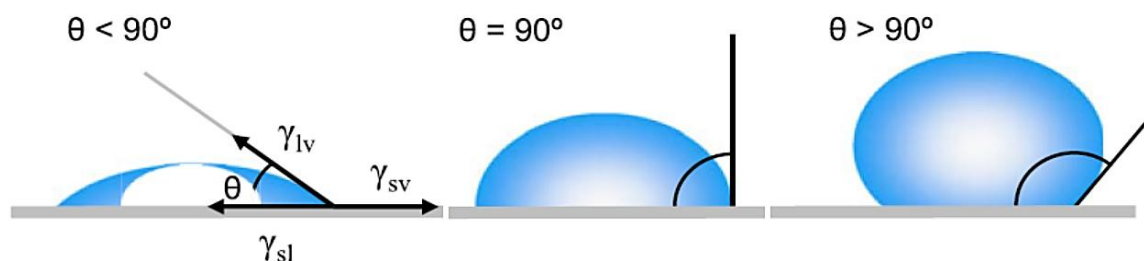


Figure I-6. Illustration of contact angles formed by sessile liquid drops on a smooth homogeneous solid surface. Reproduced from²²⁶.

Mimicking the hierarchical structure of lotus leaves, show super hydrophobicity (CA higher than 150°), has gained growing attention because of their unique structural and functional properties such as self-cleaning²²⁷, ice phobicity²²⁸, anti-corrosion²²⁹ and fluidic drag reduction²³⁰, transparency, anti-reflection and structural color.

In addition to discovering from nature, the progressively increasing requirements on high-performance materials and smart surfaces pushed forward the rapid development of multifunctional super hydrophobic surfaces. According to this basic principle, various hydrophobic surfaces were successfully prepared by combining hierarchical surface structures with low surface energy material coatings, such as fluorinated polymers or blends while keeping good thermal and mechanical properties of polymers.

PA6 is a semi crystalline thermoplastic material and has a broad range of application areas which include textile fibers, membranes, tapes, food packaging, electronics, and automotive parts. Indeed, hydrogen bonds of amide group (NH-CO) between adjacent chains of PA6 provide various attractive properties such as high crystalline structure, high melting point and chemical stability but high rate of water uptake is one of the main drawbacks of PA6 due to the hydrophilic character of amide group. To advance PA6s' performances, it is a necessary to induce specific functional groups on its surface in pre-determined locations, densities, and patterns. Low gas permeability and a high barrier to water vapor are expected properties, while PA6 is used for food packaging.

There is much interest in modifying the surface of polyamides to make them more hydrophobic. Several different methods were used for surface modification such as barrier coating layers, forming copolymers or blends, and use of nanofillers such as silica or clays for nanocomposite preparation.

4.1. Multilayered film preparation

Multilayered polyamide copolymer (aliphatic and aromatic) is one of the approaches to increase surface hydrophobicity of polyamides. Copolymers of PA6,6 and PA6 multilayered films were investigated with higher water permeability than neat PA6. Indeed, aromatic-aliphatic copolymers' water permeability was reported lower than the PA6. These results were related to aromatic repeating units in the copolymers. In particular, their wetting and thermal properties were not mentioned²³¹.

4.2. Blending hydrophilic and hydrophobic polymers

PA6/hydrophobic polyolefin blends gained a great importance for their application in food packaging, due to the good oxygen barrier of the polyamide and the excellent moisture barrier of the polyolefin²³². Valenza et al. studied on blending of PA6 and acrylic acid and showed improvement of the morphological, rheological and mechanical properties of the studied materials²³³.

4.3. Surface modification

To decrease the moisture absorption property of PA6-6 film, allyl pentafluorobenzene was incorporated on the argon plasma-pretreated nylon film by UV or thermally induced surface graft copolymerization²³⁴. Water contact angle of the product could increase only at mediocre level (around 55°).

4.4. Incorporation of fluoro-monomer to polyamide by copolymerization

To the best of our knowledge, among these approaches mentioned above, introduction of fluorine groups into the backbone or side chain of polyamides was considered as one of the most effective methods and attracted ever more attention from both academia and industry.

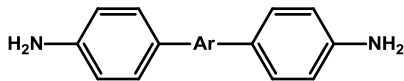
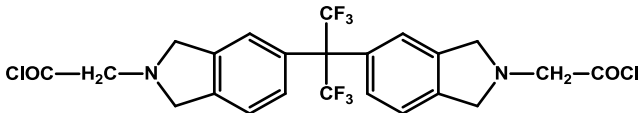
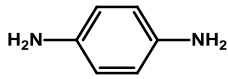
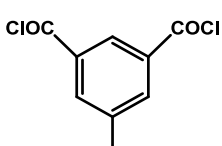
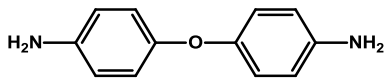
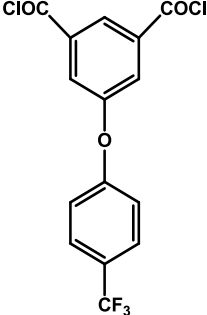
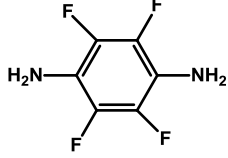
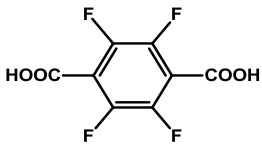
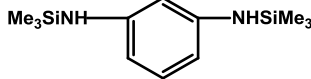
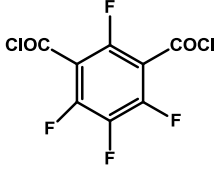
As a matter of fact, fluorinated polymers are known to exhibit peculiar properties such as high thermal stability, chemical inertness (to acids, bases, solvents and petroleum), low dielectric constants and dissipation factors, low water absorptivity, excellent weatherability and good resistances to flammability, oxidation and ageing, as well as low and specific surface properties²³⁵⁻²³⁸. These properties derive from the essential properties of fluorine atom: high electronegativity, high ionization potential, and low polarizability. Due to the very high electronegativity, C–F bonds are always strongly polarized. The strength of the C–F bond is due to its highly ionic character, which accounts for the thermal stability of perfluorocarbons. The high ionization potential, combined with the low polarizability, leads to weak intermolecular interactions, which in turn leads to low surface energy and low refractive indices for perfluorocarbons. Therefore, perfluorocarbons were used to create

non-stick and non-wettable surfaces with low surface energies (super hydrophobic character)²³⁹.

4.4.1. Aromatic fluorinated polyamides

Many efforts were performed to carry out hydrogen-fluorine substitution reactions in aromatic polyamides (the fluorine atoms or fluorinated groups are directly tethered to benzene ring such as F-, CF₃- and (CF₃)₃C- which are commonly prepared by polycondensation of acid chlorides or dicarboxylic acids and diamines. Such polyamides²⁴⁰⁻²⁴² exhibit higher thermal stability and lower surface energy than non-fluorinated polyamides (Table I-1).

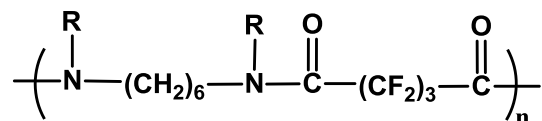
Table I-1. Structural formulas and codes of diacids, diamines, and diphenols used for fluorine containing aromatic polyamide preparation by polycondensation.

Monomer I (Amine)	Monomer II (Acid)	Ref
		243
		244
OR 	OR 	
		240
		242

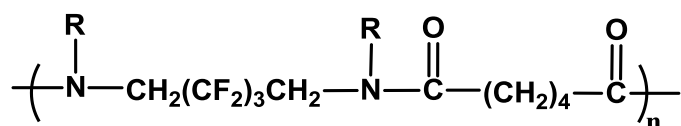
4.4.2. Aliphatic fluorinated polyamides

Preparing aliphatic polyamides with fluorine content is particularly expected to have better thermal stability, lower surface energy and water absorption. Three types of linear fluorine-containing aliphatic polyamides have been discovered by polycondensation reactions with four different combinations, (1) fluorinated diacid and fluorinated primary diamine, (2) fluorinated diacid and primary diamine, (3) diacid and fluorinated primary diamine²⁴⁵, and (4) hydrobromide salts of fluorinated diamine and acid chloride²⁴⁶. Type I (Scheme I-40) aliphatic fluorinated polyamides with high molar masses, where fluorine

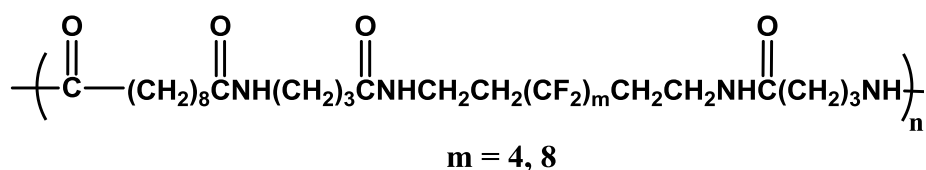
atoms are within the diacid portion of the polymer (1 and 2), suffer from hydrolytic degradation because of the inductive effect of the fluorine atoms weakening the amide linkages. On the other hand, type II (Scheme I-40) aliphatic fluorinated polyamides, where fluorine atoms are within the diamine portion of the polymer (3) have low molar masses due to the inductive effect of the fluorine atoms lowering the basicity, and therefore the reactivity of the diamines exhibit hydrolytic stability.



Type I



Type II



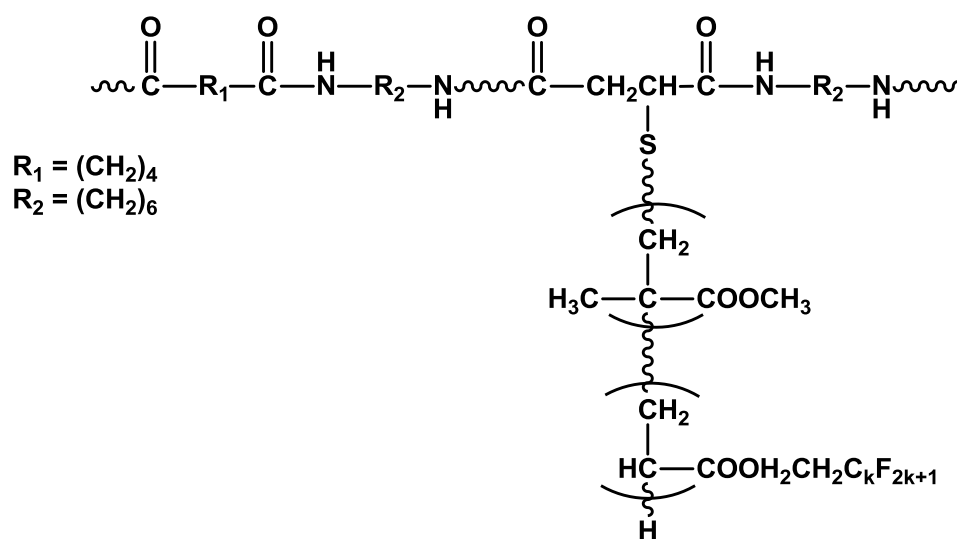
Type III

Scheme I-40. Type I, Type II and Type III of fluorinated aliphatic polyamides.

Type III aliphatic fluorinated polyamide (4), contrary to type I and II, is hydrolytically stable and has high molar mass but has less thermal stability than PA6-10 and even though it has higher water contact angle than PA6-10. Indeed, water uptake results were reported with higher values than PA6-10 because of fluoroaliphatic polyamides have less regular structure than PA6-10 that leads to less interchain hydrogen bonding therefore more free amide groups, which can then make hydrogen bondings to water by leading to larger water absorption values²⁴⁵⁻²⁴⁷.

Different from these type of aliphatic fluorinated polyamide, fluorine-containing graft copolyamides, dicarboxyl-terminated poly(perfluoroalkylethyl acrylate) were prepared by

radical chain transfer polymerization and copolycondensed with diamines and dicarboxylic acids (Scheme I-41)²⁴⁸. PA6 films containing various amounts of fluorine-containing graft copolyamides were obtained by heat pressing. 5wt % of graft copolymers enables making surfaces water repellent polyamide 6. Limitations of the polycondensation route, in particular the required long polymerization time and high polymerization temperatures, make the anionic ring-opening polymerization of interest for the synthesis of fluorinated polyamides.



Scheme I-41. Graft copolyamide structure containing fluorinated groups.

One of the most common approaches to increase solubility of is the introducing of fluorine unit in the polymer backbone and/or bulky pendent groups along the main chain such as hexafluoroisopropylidene groups and trifluoromethyl groups so to hinder interaction between neighboring molecules due to preventing molecular interactions^{246, 249}. Incorporation of geometrically non-symmetric units into the polymer backbone or graft copolymerization methods always increase the solubility because of less packing between polymer chains^{246, 249, 250}. Typically, it is more convenient first to synthesize modified monomers via incorporation of fluorinated monomers, followed by polycondensation with dicarboxylic acids or their derivatives (Table I-1, Schemes I-40 and I-41). It has also been shown that the incorporation of bulky trifluoromethyl- pendant groups generally into the aromatic polyamide backbone resulted in great benefits for improving polymer optical

transparency as well as solubility, which derived from the low polarizability of the C–F bond and the increase in free volume^{142, 251}.

Conclusion

Among the many produced polyamides by anionic ring-opening polymerization (AROP), polyamide 6 (PA6) is one the most common used type owing to its attractive properties and easy processability. PA6 continue to be one of the largest engineering polymer families.

Although anionic PA6 has gained impressive interest in engineering plastic field, some of the details of the mechanism and kinetics involved still remain unanswered. Therefore, these questions restrict further investigation and improvement.

In recent decades, many side groups on polyamide chain were investigated but generally by polycondensation reactions. Addition of crosslinking and hydrophobic character to PA6 needs long monomer synthesis steps or ends with lower polymerization yield than neat PA6 synthesis. Even though these limitations, researchers were trying to control or modify PA6 properties with challenging AROP.

As long as polyamide has a largest place in global market, particularly in automotive industry, PA6 keeps being one of the demanding high-performance material. Therefore, its improvement and tuned properties will be demanded. Polymer chemistry will be answering these expectations.

References

1. J. Roda, in *Handbook of Ring-Opening Polymerization*, Wiley-VCH Verlag GmbH & Co. KGaA, 2009, pp. 165-195.
2. H. Sekiguchi, ed. T. S. K.J. Ivin, Elsevier, London UK, 1984, vol. 2, p. 809.
3. R. Puffr, in *Lactam-Based Polyamides*, ed. R. P. a. V. Kubánek, CRC Press, Boca Raton, FL, 1991, vol. 1.
4. H. Reimschuessel, in *Ring-Opening Polymerizations*, ed. R. S. Frisch K., Dekker, New York, 1969, p. 303.
5. H. K. Reimschuessel, *Journal of Polymer Science: Macromolecular Reviews*, 1977, **12**, 65-139.
6. J. Sebenda, *Comprehensive Chemical Kinetics* Elsevier, Amsterdam, 1976.
7. K. Hashimoto, *Progress in Polymer Science*, 2000, **25**, 1411-1462.
8. J. Roda, in *Handbook of Ring-Opening Polymerization*, ed. C. O. Dubois P., Raquez J-M., Wiley-VCH, Weinheim Germany, 2009, p. 165.
9. E. C. S. Russo, in *Polymer Science: A Comprehensive Reference*, 2012, vol. 4, p. 331.
10. J. Sebenda, *J. Macromol. Sci., Chem.*, A6, 1972, 1145.
11. E. Sittler, *J. Poly. Sci., Part C* 1968, **33**, 270.
12. S. Russo, E. Biagini and G. Bonta, *Makromolekulare Chemie. Macromolecular Symposia*, 1991, **48-49**, 31-46.
13. L. Ricco, S. Russo, G. Orefice and F. Riva, *Macromolecular Chemistry and Physics*, 2001, **202**, 2114-2121.
14. H. Sekiguchi, P. R. Tsourkas and B. Coutin, *Journal of Polymer Science: Polymer Symposia*, 1973, **42**, 51-61.
15. R. Huisgen, H. Brade, H. Walz and I. Glogger, *Chemische Berichte*, 1957, **90**, 1437-1447.
16. R. Schwesinger, C. Hasenfratz, H. Schlemper, L. Walz, E.-M. Peters, K. Peters and H. G. von Schnering, *Angewandte Chemie International Edition in English*, 1993, **32**, 1361-1363.
17. J. Tang, J. Dopke and J. G. Verkade, *Journal of the American Chemical Society*, 1993, **115**, 5015-5020.
18. S. Naumann, F. G. Schmidt, M. Speiser, M. Böhl, S. Epple, C. Bonten and M. R. Buchmeiser, *Macromolecules*, 2013, **46**, 8426-8433.
19. N. Mougín, P. Rempp and Y. Gnanou, *Macromolecules*, 1992, **25**, 6739-6743.
20. N. Mougín, P. Rempp and Y. Gnanou, *Journal of Polymer Science Part A: Polymer Chemistry*, 1993, **31**, 1253-1260.
21. J. Sebenda, in *Lactam Based Polyamides*, ed. V. K. R. Puffr, CRC Press, Boca Raton, FL, 1991, vol. 1, p. 29.
22. J. Stehlíček and J. Šebenda, *European Polymer Journal*, 1987, **23**, 237-242.
23. D. Petit, R. Jerome and P. Teyssie, *Journal of Polymer Science: Polymer Chemistry Edition*, 1979, **17**, 2903-2916.
24. L. Ricco, S. Russo, G. Orefice and F. Riva, *Macromolecules*, 1999, **32**, 7726-7731.
25. R. Mateva, R. Filyanova, R. Velichkova and V. Gancheva, *Journal of Polymer Science Part A: Polymer Chemistry*, 2003, **41**, 487-496.
26. P. Petrov, R. Mateva, R. Dimitrov, S. Rousseva, R. Velichkova and M. Bourssukova, *Journal of Applied Polymer Science*, 2002, **84**, 1448-1456.

27. G.-H. Hu, H. Li and L.-F. Feng, *Journal of Applied Polymer Science*, 2006, **102**, 4394-4403.
28. J. Merna, D. Chromcová, J. Brožek and J. Roda, *European Polymer Journal*, 2006, **42**, 1569-1580.
29. J. Roda, J. Brožek and J. Králíček, *Die Makromolekulare Chemie, Rapid Communications*, 1980, **1**, 165-169.
30. L. Daniel, J. Brožek, J. Roda and J. Křílíček, *Die Makromolekulare Chemie*, 1982, **183**, 2719-2729.
31. J. S. E. Sittler, *J. Poly. Sci., Part C*, 1968, **33**, 3182.
32. M. L. S. Bazakay, D. Vofsi, *J. Polym. Sci., Part B* 1965, **3**, 601.
33. R. Rached, S. Hoppe, C. Fonteix, C. Schrauwen and F. Pla, *Chemical Engineering Science*, 2005, **60**, 2715-2727.
34. V. A. K. n. T. M. Frunze, V. V. Kurashev, A. Yu Arakyan, L. B. Danielevskaya, P. S. Davtyan, in *Macro 83*, Polymer Chemistry, Commun. I, Bucharest, 1983, vol. 72, p. 233.
35. P. Estévez, H. El-Kaoutit, F. C. García, F. Serna, J. L. de la Peña and J. M. García, *Journal of Polymer Science Part A: Polymer Chemistry*, 2010, **48**, 3823-3833.
36. C. C. G. Alfonso, S. Razore, S. Russo, in *ACS Symposium Series, No. 270*, ed. K. J., American Chemical Society, Washington, DC,, 1985, p. 163.
37. R. Mendichi, S. Russo, L. Ricco and A. Giacometti Schieronni, *Journal of Separation Science*, 2004, **27**, 637-644.
38. K. Udiipi, R. S. Davé, R. L. Kruse and L. R. Stebbins, *Polymer*, 1997, **38**, 927-938.
39. J. Stehlíček and T. Šebenda, *European Polymer Journal*, 1986, **22**, 5-11.
40. S. Russo, A. Imperato, A. Mariani and F. Parodi, *Macromolecular Chemistry and Physics*, 1995, **196**, 3297-3303.
41. G. Champetier and H. Sekiguchi, *Journal of Polymer Science*, 1960, **48**, 309-319.
42. H. Sekiguchi, *Bull. Soc. Chim. Fr.*, 1960, 1831.
43. H. Sekiguchi, *Journal of Polymer Science Part A: General Papers*, 1963, **1**, 1627-1633.
44. T. M. Frunze, V. A. Kotel'nikov, T. V. Volkova, V. V. Kurašev, S. P. Davtjan and I. V. Stankevič, *Acta Polymerica*, 1981, **32**, 31-35.
45. T. M. Frunze, V. A. Kotel'nikov, T. V. Volkova and V. V. Kurashov, *European Polymer Journal*, 1981, **17**, 1079-1084.
46. A. C. A. G. Bonta, S. Russo, in *ACS Symposium Series No. 59*, ed. G. E. Saegusa T., American Chemical Society, Washington, DC, 1977, p. 216.
47. J. S. a. J. S. P. Cefelín, *Collect. Czech. Chem. Commun.* , 1974, **39**, 2212-2220.
48. J. Sebenda, in *Comprehensive Polymer Science*, ed. A. L. A. G. Eastmond, S. Russo, P. Sigwalt, Pergamon Press, Oxford, UK, 1989, vol. 3, p. 511.
49. B. Coutin and H. Sekiguchi, *Journal of Polymer Science: Polymer Chemistry Edition*, 1977, **15**, 2539-2541.
50. J. S. J. P Cefelin P., J. Sebenda, *J. Polym. Sci. C.* , 1973, **42**, 79.
51. G. Carlo Alfonso, G. Cirillo, S. Russo and A. Turturro, *European Polymer Journal*, 1983, **19**, 949-953.
52. A. Greenberg, H.-J. Hsing and J. F. Liebman, *Journal of Molecular Structure: THEOCHEM*, 1995, **338**, 83-100.
53. K. J. Schneider B., Dybal J., Schmidt P., Suchoparek M., Prokopova I. , *Coll. Czech. Chem. Commun.*, 1993, **58**, 2403.

-
54. J. Dybal, B. Schneider, D. Doskočilová, J. Baldrian, H. Pavlíková, J. Kvarda and I. Prokopová, *Polymer*, 1997, **38**, 2483-2491.
 55. J. Budín, J. Brožek and J. Roda, *Polymer*, 2006, **47**, 140-147.
 56. A. Luisier, P. E. Bourban and J. A. E. Månson, *Journal of Polymer Science Part A: Polymer Chemistry*, 2002, **40**, 3406-3415.
 57. R. Mateva, O. Delev and S. Rousseva, *European Polymer Journal*, 1997, **33**, 1377-1382.
 58. A. Y. Malkin, S. L. Ivanova, V. G. Frolov, A. N. Ivanova and Z. S. Andrianova, *Polymer*, 1982, **23**, 1791-1800.
 59. J. Budín, J. Roda, J. Brožek and J. Kříř, *Macromolecular Symposia*, 2006, **240**, 78-82.
 60. I. Goodman and R. N. Vachon, *European Polymer Journal*, 1984, **20**, 529-537.
 61. X. Fang, R. Hutcheon and D. A. Scola, *Journal of Polymer Science Part A: Polymer Chemistry*, 2000, **38**, 1379-1390.
 62. D. Chromcová, L. Baslerová, J. Roda and J. Brožek, *European Polymer Journal*, 2008, **44**, 1733-1742.
 63. B. J. Kim and J. L. White, *Journal of Applied Polymer Science*, 2003, **88**, 1429-1437.
 64. I. Kim and J. L. White, *Journal of Applied Polymer Science*, 2003, **90**, 3797-3805.
 65. I. Kim and J. L. White, *Journal of Applied Polymer Science*, 2005, **96**, 1875-1887.
 66. A. Bernášková, D. Chromcová, J. Brožek and J. Roda, *Polymer*, 2004, **45**, 2141-2148.
 67. J. Roda, in *Block Copolymers*, ed. Z. R. F. Balta-Calleja, Marcel Dekker, New York, 2000, p. 93.
 68. V. Nováková, R. Sobotík, J. Matěnová and J. Roda, *Die Angewandte Makromolekulare Chemie*, 1996, **237**, 123-141.
 69. R. Sobotík, R. Šrubař and J. Roda, *Macromolecular Chemistry and Physics*, 1997, **198**, 1147-1163.
 70. P. Petrov, K. Jankova and R. Mateva, *Journal of Applied Polymer Science*, 2003, **89**, 711-717.
 71. F. M. B. Coutinho and A. A. B. Sobrinho, *European Polymer Journal*, 1991, **27**, 105-108.
 72. J. Stehlíček, G. S. Chauhan and M. Znášiková, *Journal of Applied Polymer Science*, 1992, **46**, 2169-2175.
 73. J.-L. Yeh, J.-F. Kuo and C.-Y. Chen, *Journal of Applied Polymer Science*, 1993, **50**, 1671-1681.
 74. D. H. K. Kim, A. Tripathy, T. Kyu *J. Appl. Polym. Sci.*, 1999, **73**, 285.
 75. S. Maier, T. Loontjens, B. Scholtens and R. Mülhaupt, *Macromolecules*, 2003, **36**, 4727-4734.
 76. R. Mateva, R. Filyanova, R. Dimitrov and R. Velichkova, *Journal of Applied Polymer Science*, 2004, **91**, 3251-3258.
 77. C. Macosko, *RIM Fundamentals of Reaction Injection Molding*, Hanser Publication, Munich, Germany, 1989.
 78. G.-H. Hu, H. Cartier, L.-F. Feng and B.-G. Li, *Journal of Applied Polymer Science*, 2004, **91**, 1498-1504.
 79. J. Teng, J. U. Otaigbe and E. P. Taylor, *Polymer Engineering & Science*, 2004, **44**, 648-659.
 80. G.-H. Hu, H. Li and L.-F. Feng, *Polymer*, 2005, **46**, 4562-4570.
 81. C.-L. Zhang, L.-F. Feng, S. Hoppe and G.-H. Hu, *Journal of Polymer Science Part A: Polymer Chemistry*, 2008, **46**, 4766-4776.
-

82. P. Biernacki, S. Chrzczonowicz and M. Wlodarczyk, *European Polymer Journal*, 1971, **7**, 739-747.
83. P. Biernacki and M. Wlodarczyk, *European Polymer Journal*, 1975, **11**, 107-109.
84. P. Biernacki and M. Wlodarczyk, *European Polymer Journal*, 1980, **16**, 843-848.
85. C. Vasiliu-Oprea and F. Dan, *Journal of Applied Polymer Science*, 1996, **62**, 1517-1527.
86. C. Vasiliu-Oprea and F. Dan, *Journal of Applied Polymer Science*, 1997, **64**, 2575-2583.
87. F. Dan and C. Vasiliu-Oprea, *Journal of Applied Polymer Science*, 1998, **67**, 231-243.
88. L. Ricco, O. Monticelli, S. Russo, A. Paglianti and A. Mariani, *Macromolecular Chemistry and Physics*, 2002, **203**, 1436-1444.
89. D. Crespy and K. Landfester, *Macromolecules*, 2005, **38**, 6882-6887.
90. A. Pei, A. Liu, T. Xie and G. Yang, *Macromolecules*, 2006, **39**, 7801-7804.
91. G. J. Hedrick R., Wohl M., in *Polymer Chemistry and Engineering*, ed. J. Kresta, ACS Symposium Series No. 270; American Chemical Society, Washington, DC, 1985, p. 135.
92. G. Illing, *Mod. Plastic*, 1969, **46**, 70.
93. C. Macosko, in *Hanser Publication*, Munich, Germany, 1989.
94. A. Wollny, H. Nitz, H. Faulhammer, N. Hoogen and R. Mülhaupt, *Journal of Applied Polymer Science*, 2003, **90**, 344-351.
95. G.-H. Hu, H. Cartier and C. Plummer, *Macromolecules*, 1999, **32**, 4713-4718.
96. B. Rothe, A. Elas and W. Michaeli, *Macromolecular Materials and Engineering*, 2009, **294**, 54-58.
97. L. Du and G. Yang, *Polymer Engineering & Science*, 2010, **50**, 1178-1185.
98. D. Yan and G. Yang, *Journal of Applied Polymer Science*, 2009, **112**, 3620-3626.
99. Y. G. M. Yang, J. P. He, H. M. Li, *express polymer letters*, 2007, **1**, 433-442.
100. J. Šebenda and J. Hauer, *Polymer Bulletin*, 1981, **5**, 529-534.
101. J. Šebenda, J. Hauer and J. Svetlik, *Journal of Polymer Science: Polymer Symposia*, 1986, **74**, 303-310.
102. K. Hashimoto, K. Hotta, M. Okada and S. Nagata, *Journal of Polymer Science Part A: Polymer Chemistry*, 1995, **33**, 1995-1999.
103. K. Hashimoto, T. Oi, J. Yasuda, K. Hotta and M. Okada, *Journal of Polymer Science Part A: Polymer Chemistry*, 1997, **35**, 1831-1838.
104. K. Hashimoto, J. Yasuda and M. Kobayashi, *Journal of Polymer Science Part A: Polymer Chemistry*, 1999, **37**, 909-915.
105. J. Zhang, S. H. Gellman and S. S. Stahl, *Macromolecules*, 2010, **43**, 5618-5626.
106. K. Tachibana, K. Hashimoto, N. Tansho and H. Okawa, *Journal of Polymer Science Part A: Polymer Chemistry*, 2011, **49**, 2495-2503.
107. G. Schirawski, *Die Makromolekulare Chemie*, 1972, **161**, 57-68.
108. J. Roda, Z. Votrubcová, J. Králíček, J. Stehlíček and S. Pokorný, *Die Makromolekulare Chemie*, 1981, **182**, 2117-2126.
109. , 1982.
110. G. Costa, M. Nencioni, S. Russo and G. L. Semeghini, *Die Makromolekulare Chemie*, 1981, **182**, 1399-1405.
111. K. Hashimoto, M. Sudo, T. Sugimura and Y. Inagaki, *Journal of Applied Polymer Science*, 2004, **92**, 3492-3498.
112. N. Kawasaki, N. Yamano, S. Takeda, H. Ando and A. Nakayama, *Journal of Applied Polymer Science*, 2012, **126**, E425-E432.

-
113. H. Komoto, *Die Makromolekulare Chemie*, 1968, **115**, 33-42.
 114. F. Chuchma, P. Trška, J. Roda and J. Králíček, *Polymer*, 1983, **24**, 1491-1494.
 115. J. Stehlíček and J. Šebenda, *European Polymer Journal*, 1986, **22**, 769-773.
 116. H. K. Hall, *Journal of the American Chemical Society*, 1958, **80**, 6412-6420.
 117. H. K. Hall, *Journal of the American Chemical Society*, 1960, **82**, 1209-1215.
 118. K. Hashimoto, H. Sumitomo and A. Washio, *Journal of Polymer Science Part A: Polymer Chemistry*, 1989, **27**, 1915-1923.
 119. K. Hashimoto, T. Sugata, S.-I. Imanishi and M. Okada, *Journal of Polymer Science Part A: Polymer Chemistry*, 1994, **32**, 1619-1625.
 120. J. M. García, F. C. García, F. Serna and J. L. de la Peña, *Progress in Polymer Science*, 2010, **35**, 623-686.
 121. P. E. Cassidy, in *Thermally stable polymers*, Dekker, New York, 1980.
 122. H. H. Yang, Wiley, New York, 1989.
 123. J. K. Fink, William Andrew Inc., New York, 2008.
 124. L. Vollbracht, in *Comprehensive polymer science*, ed. B. B. G. Allen, G.V. Eastmond, A. Ledwith, S. Russo, P. Sigwald, Pergamon Press, Oxford, 1989, vol. 5, pp. 373-383
 125. K. Marchildon, *Macromolecular Reaction Engineering*, 2011, **5**, 22-54.
 126. J. Preston, in *Encyclopedia of Polymer Science and Engineering*, ed. N. M. B. H. F. Mark, C. G. Overberger, G. Menges and J. I. Kroschwitz, John-Wiley & Sons, New York, 1988, vol. 11, p. 381.
 127. L. Vollbracht, in *Comprehensive Polymer Science*, ed. A. L. G. C. Eastmond, S. Russo and P. Sigwald, Pergamon Press, Oxford, England, 1989, vol. 5, p. 375.
 128. M. Trigo-López, P. Estévez, N. San-José, A. Gómez-Valdemoro, F. C. García, F. Serna, J. L. de la Peña and J. M. García, *Recent Patents on Materials Science*, 2009, **2**, 190-208.
 129. H.-M. Wang, S.-H. Hsiao, G.-S. Liou and C.-H. Sun, *Journal of Polymer Science Part A: Polymer Chemistry*, 2010, **48**, 4775-4789.
 130. H.-J. Yen, S.-M. Guo and G.-S. Liou, *Journal of Polymer Science Part A: Polymer Chemistry*, 2010, **48**, 5271-5281.
 131. J. M. García, F. C. García, F. Serna and J. L. de la Peña, in *Handbook of Engineering and Specialty Thermoplastics*, John Wiley & Sons, Inc., 2011, pp. 141-181.
 132. P. J. Flory, *Chemical Reviews*, 1946, **39**, 137-197.
 133. W. H. Carothers, *Transactions of the Faraday Society*, 1936, **32**, 39-49.
 134. M. Szwarc, M. Levy and R. Milkovich, *Journal of the American Chemical Society*, 1956, **78**, 2656-2657.
 135. T. Yokozawa and A. Yokoyama, *Chemical Reviews*, 2009, **109**, 5595-5619.
 136. T. Yokozawa and A. Yokoyama, *The Chemical Record*, 2005, **5**, 47-57.
 137. R. W. Lenz, C. E. Handlovits and H. A. Smith, *Journal of Polymer Science*, 1962, **58**, 351-367.
 138. W. Risse, W. Heitz, D. Freitag and L. Bottenbruch, *Die Makromolekulare Chemie*, 1985, **186**, 1835-1853.
 139. D. R. Robello, A. Ulman and E. J. Urankar, *Macromolecules*, 1993, **26**, 6718-6721.
 140. T. Yokozawa and A. Yokoyama, *Progress in Polymer Science*, 2007, **32**, 147-172.
 141. A. Yokoyama and T. Yokozawa, *Macromolecules*, 2007, **40**, 4093-4101.
 142. D.-J. Liaw, W.-H. Chen, C.-K. Hu, K.-R. Lee and J.-Y. Lai, *Polymer*, 2007, **48**, 6571-6580.
 143. T. Yokozawa, T. Asai, R. Sugi, S. Ishigooka and S. Hiraoka, *Journal of the American Chemical Society*, 2000, **122**, 8313-8314.
-

144. R. Sugi, A. Yokoyama, T. Furuyama, M. Uchiyama and T. Yokozawa, *Journal of the American Chemical Society*, 2005, **127**, 10172-10173.
145. T. Ohishi, R. Sugi, A. Yokoyama and T. Yokozawa, *Journal of Polymer Science Part A: Polymer Chemistry*, 2006, **44**, 4990-5003.
146. J. Hine, *Structural Effects on Equilibrium in Organic Chemistry*, Wiley, New York, 1975.
147. R. Sugi, T. Ohishi, A. Yokoyama and T. Yokozawa, *Macromolecular Rapid Communications*, 2006, **27**, 716-721.
148. S. Han, M. Hagiwara and T. Ishizone, *Macromolecules*, 2003, **36**, 8312-8319.
149. T. Yokozawa, M. Ogawa, A. Sekino, R. Sugi and A. Yokoyama, *Journal of the American Chemical Society*, 2002, **124**, 15158-15159.
150. M. Ueda, *Progress in Polymer Science*, 1999, **24**, 699-730.
151. T. Ohishi, R. Sugi, A. Yokoyama and T. Yokozawa, *Macromolecules*, 2008, **41**, 9683-9691.
152. S. Kim, Y. Kakuda, A. Yokoyama and T. Yokozawa, *Journal of Polymer Science Part A: Polymer Chemistry*, 2007, **45**, 3129-3133.
153. Y. Ohta, Y. Kamijyo, S. Fujii, A. Yokoyama and T. Yokozawa, *Macromolecules*, 2011, **44**, 5112-5122.
154. Q. Zhang, P. Schattling, P. Theato and R. Hoogenboom, *European Polymer Journal*, In press, doi:10.1016/j.eurpolymj.2014.06.029.
155. C.-F. Huang, Y. Ohta, A. Yokoyama and T. Yokozawa, *Macromolecules*, 2011, **44**, 4140-4148.
156. S. Yurteri, I. Cianga and Y. Yagci, *Macromolecular Chemistry and Physics*, 2003, **204**, 1771-1783.
157. R. Sugi, A. Yokoyama and T. Yokozawa, *Macromolecular Rapid Communications*, 2003, **24**, 1085-1090.
158. R. Sugi, Y. Hitaka, A. Sekino, A. Yokoyama and T. Yokozawa, *Journal of Polymer Science Part A: Polymer Chemistry*, 2003, **41**, 1341-1346.
159. T. Masukawa, A. Yokoyama and T. Yokozawa, *Macromolecular Rapid Communications*, 2009, **30**, 1413-1418.
160. C.-F. Huang, A. Yokoyama and T. Yokozawa, *Journal of Polymer Science Part A: Polymer Chemistry*, 2010, **48**, 2948-2954.
161. M. Jikei and M.-a. Kakimoto, *Journal of Polymer Science Part A: Polymer Chemistry*, 2004, **42**, 1293-1309.
162. T. Ohishi, T. Masukawa, S. Fujii, A. Yokoyama and T. Yokozawa, *Macromolecules*, 2010, **43**, 3206-3214.
163. Y. Ohta, Y. Kamijyo, A. Yokoyama and T. Yokozawa, *Polymers*, 2012, **4**, 1170-1182.
164. K. Yoshino, A. Yokoyama and T. Yokozawa, *Journal of Polymer Science Part A: Polymer Chemistry*, 2009, **47**, 6328-6332.
165. H. Shohi, M. Sawamoto and T. Higashimura, *Macromolecules*, 1991, **24**, 4926-4931.
166. N. K. Pramanik, R. Haldar, U. K. Niyogi and S. Alam, *Journal of Macromolecular Science, Part A*, 2014, **51**, 296-307.
167. J. Yu, B. Tonpheng and O. Andersson, *Macromolecules*, 2010, **43**, 10512-10520.
168. E. Tarkin-Tas and L. J. Mathias, *Macromolecules*, 2009, **43**, 968-974.
169. L. Chikh, X. Arnaud, C. Guillermain, M. Tessier and A. Fradet, *Macromolecular Symposia*, 2003, **199**, 209-222.

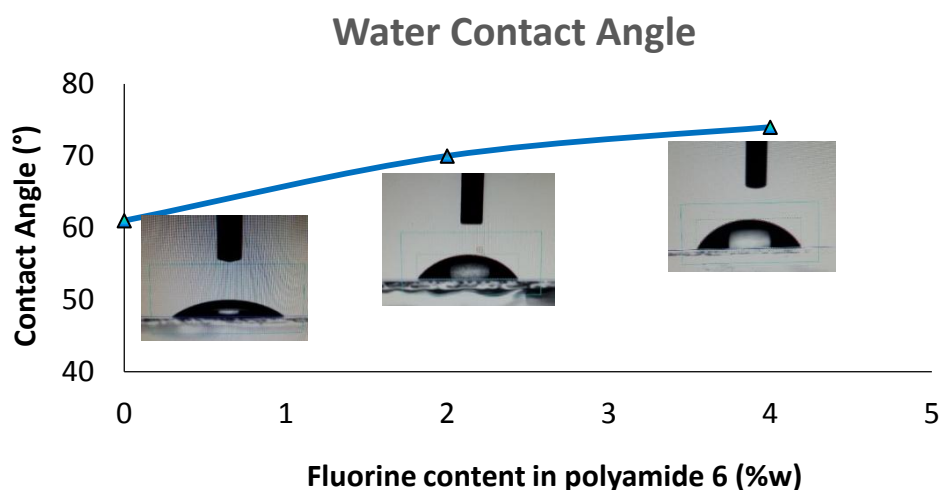
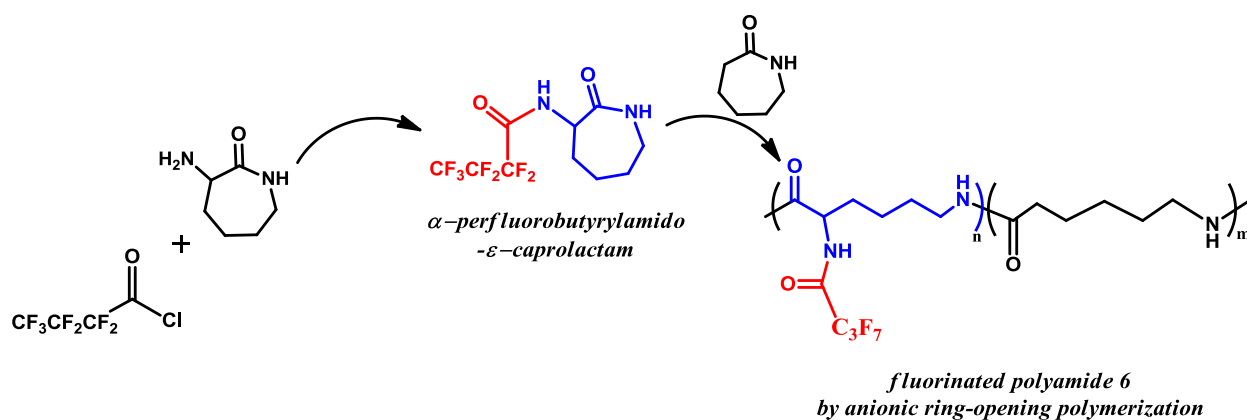
-
170. A. Aytaç, V. Deniz, M. Şen, E.-S. Hegazy and O. Güven, *Radiation Physics and Chemistry*, 2010, **79**, 297-300.
 171. A. Aytaç, M. Şen, V. Deniz and O. Güven, *Nuclear Instruments and Methods in Physics Research Section B: Beam Interactions with Materials and Atoms*, 2007, **265**, 271-275.
 172. N. K. Pramanik, R. S. Haldar, Y. K. Bhardwaj, S. Sabharwal, U. K. Niyogi and R. K. Khandal, *Radiation Physics and Chemistry*, 2009, **78**, 199-205.
 173. E. Adem, G. Burillo, L. F. del Castillo, M. Vásquez, M. Avalos-Borja and A. Marcos-Fernández, *Radiation Physics and Chemistry*, 2014, **97**, 165-171.
 174. A. Charlesby, *Nature*, 1953, **171**, 167-167.
 175. S. Dadbin, M. Frounchi and D. Goudarzi, *Polymer Degradation and Stability*, 2005, **89**, 436-441.
 176. F. Liu and M. W. Urban, *Progress in Polymer Science*, 2010, **35**, 3-23.
 177. P. Schattling, F. D. Jochum and P. Theato, *Polymer Chemistry*, 2014, **5**, 25-36.
 178. J. Xuan, D. Han, H. Xia and Y. Zhao, *Langmuir*, 2013, **30**, 410-417.
 179. G. Li, S. Song, L. Guo and S. Ma, *Journal of Polymer Science Part A: Polymer Chemistry*, 2008, **46**, 5028-5035.
 180. F. Liu and M. W. Urban, *Macromolecules*, 2008, **41**, 6531-6539.
 181. S. Xu, Y. Luo and R. Haag, *Macromolecular Bioscience*, 2007, **7**, 968-974.
 182. Y. Yan, J. Li, J. Zheng, Y. Pan, J. Wang, X. He, L. Zhang and D. Liu, *Colloids and Surfaces B: Biointerfaces*, 2012, **95**, 137-143.
 183. N. Zhang, S. Salzinger and B. Rieger, *Macromolecules*, 2012, **45**, 9751-9758.
 184. S. Su, H. Wang, X. Liu, Y. Wu and G. Nie, *Biomaterials*, 2013, **34**, 3523-3533.
 185. D. E. Bergbreiter, *Journal of Polymer Science Part A: Polymer Chemistry*, 2001, **39**, 2351-2363.
 186. T. Zhao, F.-Q. Nie and L. Jiang, *Journal of Materials Chemistry*, 2010, **20**, 2176-2181.
 187. F. D. Jochum, F. R. Forst and P. Theato, *Macromolecular Rapid Communications*, 2010, **31**, 1456-1461.
 188. A. Garle, S. Kong, U. Ojha and B. M. Budhlall, *ACS Applied Materials & Interfaces*, 2012, **4**, 645-657.
 189. M. Minoda, T. Shimizu, S. Miki and J. Motoyanagi, *Journal of Polymer Science Part A: Polymer Chemistry*, 2013, **51**, 786-792.
 190. R. Luxenhofer, S. Huber, J. Hytry, J. Tong, A. V. Kabanov and R. Jordan, *Journal of Polymer Science Part A: Polymer Chemistry*, 2013, **51**, 732-738.
 191. O. Confortini and F. E. Du Prez, *Macromolecular Chemistry and Physics*, 2007, **208**, 1871-1882.
 192. J. A. Yoon, T. Kowalewski and K. Matyjaszewski, *Macromolecules*, 2011, **44**, 2261-2268.
 193. L. Feng, J. Romulus, M. Li, R. Sha, J. Royer, K.-T. Wu, Q. Xu, N. C. Seeman, M. Weck and P. Chaikin, *Nat Mater*, 2013, **12**, 747-753.
 194. E. Reichmanis, O. Nalamasu, F. M. Houlihan and A. E. Novembre, *Polymer International*, 1999, **48**, 1053-1059.
 195. J. Jang, S. Nam, J. Hwang, J.-J. Park, J. Im, C. E. Park and J. M. Kim, *Journal of Materials Chemistry*, 2012, **22**, 1054-1060.
 196. D.-J. Liaw, K.-L. Wang, Y.-C. Huang, K.-R. Lee, J.-Y. Lai and C.-S. Ha, *Progress in Polymer Science*, 2012, **37**, 907-974.
 197. M. Irie and W. Schnabel, *Macromolecules*, 1981, **14**, 1246-1249.
-

198. H. J. Ommer and H. Ritter, *Macromolecular Chemistry and Physics*, 1996, **197**, 797-809.
199. N. Fomina, C. McFearin, M. Sermsakdi, O. Edigin and A. Almutairi, *Journal of the American Chemical Society*, 2010, **132**, 9540-9542.
200. D. Y. Wong, D. R. Griffin, J. Reed and A. M. Kasko, *Macromolecules*, 2010, **43**, 2824-2831.
201. J. W. Anna Paola Pelliccioli, *Photochem. Photobiol. Sci.*, 2002, **1**, 441-458.
202. Y. Zheng, M. Micic, S. V. Mello, M. Mabrouki, F. M. Andreopoulos, V. Konka, S. M. Pham and R. M. Leblanc, *Macromolecules*, 2002, **35**, 5228-5234.
203. D. Shi, M. Matsusaki and M. Akashi, *Bioconjugate Chemistry*, 2009, **20**, 1917-1923.
204. M. Sandholzer, S. Bichler, F. Stelzer and C. Slugovc, *Journal of Polymer Science Part A: Polymer Chemistry*, 2008, **46**, 2402-2413.
205. J. He, X. Tong and Y. Zhao, *Macromolecules*, 2009, **42**, 4845-4852.
206. Y. Sako and Y. Takaguchi, *Organic & Biomolecular Chemistry*, 2008, **6**, 3843-3847.
207. S. Grimme, C. Diedrich and M. Korth, *Angewandte Chemie International Edition*, 2006, **45**, 625-629.
208. L. A. Wells, M. A. Brook and H. Sheardown, *Macromolecular Bioscience*, 2011, **11**, 988-998.
209. P. G. Frank, B. T. Tuten, A. Prasher, D. Chao and E. B. Berda, *Macromolecular Rapid Communications*, 2014, **35**, 249-253.
210. M. A. Rabjohns, P. Hodge and P. A. Lovell, *Polymer*, 1997, **38**, 3395-3407.
211. G. J. O. K. Keating, R., *John Wiley & Sons: New York*, 1997.
212. S. R. Trenor, A. R. Shultz, B. J. Love and T. E. Long, *Chemical Reviews*, 2004, **104**, 3059-3078.
213. G. M. J. Schmidt, *Pure and Applied Chemistry*, 1971, **27**, 647-678.
214. M. Khan, G. Brunklaus, V. Enkelmann and H.-W. Spiess, *Journal of the American Chemical Society*, 2008, **130**, 1741-1748.
215. I. Abdelmoty, V. Buchholz, L. Di, C. Guo, K. Kowitz, V. Enkelmann, G. Wegner and B. M. Foxman, *Crystal Growth & Design*, 2005, **5**, 2210-2217.
216. X. Coqueret, *Macromolecular Chemistry and Physics*, 1999, **200**, 1567-1579.
217. J. Zhu, L.-P. Wu, Y.-Y. Zhang, X. Jin, S.-J. He, K.-Y. Shi, X. Guo, Z.-J. Du and B.-L. Zhang, *Journal of Applied Polymer Science*, 2006, **102**, 4565-4572.
218. N. Kawatsuki, H. Takatsuka, T. Yamamoto and O. Sengen, *Macromolecular Rapid Communications*, 1996, **17**, 703-712.
219. P. Froimowicz, D. Klinger and K. Landfester, *Chemistry – A European Journal*, 2011, **17**, 12465-12475.
220. W. Choi, J.-S. Chung, J.-j. Kim, S.-K. Kim, S.-H. Cha, M. Park and J.-C. Lee, *J Coat Technol Res*, 2014, **11**, 455-459.
221. S.-J. Sung, D.-H. Kim, M. Kim and K. Cho, *Macromol. Res.*, 2010, **18**, 614-617.
222. S. W. Lee, S. I. Kim, B. Lee, W. Choi, B. Chae, S. B. Kim and M. Ree, *Macromolecules*, 2003, **36**, 6527-6536.
223. D. M. Bassani, in *CRC Handbook of Organic Photochemistry and Photobiology, 2nd Edition*, CRC Press LLC, 2004, vol. 20, pp. 1-11.
224. Y.-L. Zhang, H. Xia, E. Kim and H.-B. Sun, *Soft Matter*, 2012, **8**, 11217-11231.
225. D. Li, M. Xie and A. W. Neumann, *Colloid Polym Sci*, 1993, **271**, 573-580.
226. Y. Yuan and T. R. Lee, *Surface Science Techniques*, 2013, **32p**, p3-34.

-
227. I. Sas, R. E. Gorga, J. A. Joines and K. A. Thoney, *Journal of Polymer Science Part B: Polymer Physics*, 2012, **50**, 824-845.
228. P. Tourkine, M. Le Merrer and D. Quéré, *Langmuir*, 2009, **25**, 7214-7216.
229. T. Ishizaki and M. Sakamoto, *Langmuir*, 2011, **27**, 2375-2381.
230. Y. Zhou, M. Li, B. Su and Q. Lu, *Journal of Materials Chemistry*, 2009, **19**, 3301-3306.
231. M. A. Del Nobile, G. G. Buonocore, L. Palmieri, A. Aldi and D. Acierno, *Journal of Food Engineering*, 2002, **53**, 287-293.
232. R. M. Holsti-Miettinen, K. P. Perttilä, J. V. Seppälä and M. T. Heino, *Journal of Applied Polymer Science*, 1995, **58**, 1551-1560.
233. A. Valenza, A. M. Visco and D. Acierno, *Polymer Testing*, 2002, **21**, 101-109.
234. J. Zhang, K. T. Khong and E. T. Kang, *Journal of Applied Polymer Science*, 2000, **78**, 1366-1373.
235. B. Ameduri, Boutevin, B., *Elsevier Science*, 2004, ISBN: 978-0-08-044388-1.
236. B. Ameduri, *Chemical Reviews*, 2009, **109**, 6632-6686.
237. F. Boschet and B. Ameduri, *Chemical Reviews*, 2014, **114**, 927-980.
238. Y. Y. Durmaz, E. L. Sahkulubey, Y. Yagci, E. Martinelli and G. Galli, *Journal of Polymer Science Part A: Polymer Chemistry*, 2012, **50**, 4911-4919.
239. D. Gan, A. Mueller and K. L. Wooley, *Journal of Polymer Science Part A: Polymer Chemistry*, 2003, **41**, 3531-3540.
240. T. Kiyotsukuri, N. Tsutsumi, K. Okada, K. Asai and M. Nagata, *Journal of Polymer Science Part A: Polymer Chemistry*, 1988, **26**, 2225-2234.
241. X.-L. Liu, D. Wu, R. Sun, L.-M. Yu, J.-W. Jiang and S.-R. Sheng, *Journal of Fluorine Chemistry*, 2013, **154**, 16-22.
242. Y. Oishi, S. Harada, M.-A. Kamimoto and Y. Imai, *Journal of Polymer Science Part A: Polymer Chemistry*, 1989, **27**, 3393-3403.
243. E. Hamciuc, C. Hamciuc, I. Sava and M. Bruma, *European Polymer Journal*, 2001, **37**, 287-293.
244. Z. Ge, S. Yang, Z. Tao, J. Liu and L. Fan, *Polymer*, 2004, **45**, 3627-3635.
245. B. S. Marks and G. C. Schweiker, *Journal of Polymer Science*, 1960, **43**, 229-239.
246. A. E. Mera and J. R. Griffith, *Journal of Fluorine Chemistry*, 1992, **59**, 81-89.
247. T. Kiyotsukuri, N. Tsutsumi, T. Sandan and M. Nagata, *Journal of Polymer Science Part A: Polymer Chemistry*, 1990, **28**, 315-322.
248. Y. Chujo, A. Hiraiwa, H. Kobayashi and Y. Yamashita, *Journal of Polymer Science Part A: Polymer Chemistry*, 1988, **26**, 2991-2996.
249. D.-J. Liaw and K.-L. Wang, *Journal of Polymer Science Part A: Polymer Chemistry*, 1996, **34**, 1209-1217.
250. P.-H. Li, C.-Y. Wang, G. Li and J.-M. Jiang, *Polymer Bulletin*, 2010, **64**, 127-140.
251. C.-X. Ma, S.-R. Sheng, M.-H. Wei, W. He and C.-S. Song, *Journal of Applied Polymer Science*, 2010, **118**, 2959-2968.
-

Chapter II

Copolymerization of ϵ -caprolactam and fluorinated derivatives for increased surface hydrophobicity and thermal stability of polyamide 6



Keywords : Anionic ring-opening polymerization, lysine, α -amino- ϵ -caprolactam, copolymerization, polyamide synthesis, fluorinated polyamides, hydrophobic surface and water uptake.

Summary: This chapter is dedicated to the use of novel perfluorobutyryl-substituted α -amino- ϵ -caprolactam comonomer for synthesis of polyamide (PA6) having a hydrophobic surface. PA6 bearing fluorinated groups was synthesized in bulk with perfluorobutyryl-substituted α -amino- ϵ -caprolactam and ϵ -caprolactam by anionic ring-opening polymerization (AROP). This fluorinated compound was obtained by reaction between cyclic lysine (i.e. α -amino- ϵ -caprolactam) and perfluorobutyrylchloride. The effect of the fluorinated monomer amount on AROP of ϵ -caprolactam was studied, exothermy of this polymerization was followed and the properties of the corresponding polymers were investigated with differential scanning calorimetry, thermogravimetric analysis, magic angle spinning (MAS) NMR, FT-IR, and contact angle analyses. PA6 bearing fluorinated groups exhibited better thermal stability as well as a higher hydrophobic character than PA6 as evidenced by surface tension measurements and despite low fluorine content.

Chapter II

Copolymerization of ϵ -caprolactam and fluorinated derivatives for increased surface hydrophobicity and thermal stability of polyamide 6

TABLE OF CONTENTS

Introduction	86
1. Synthesis of polyamide 6 with fluorinated moieties	89
2. Rate of polymerization.....	94
3. Polymer characterization by NMR and ATR-IR	95
4. Thermal characteristics of modified polyamide 6 and investigation of degradation mechanism	98
5. Hydrophobicity and Water Uptake Determination	106
Conclusion	109
Experimental and supporting informations	111
Annexe: Supporting Information	114
References.....	121

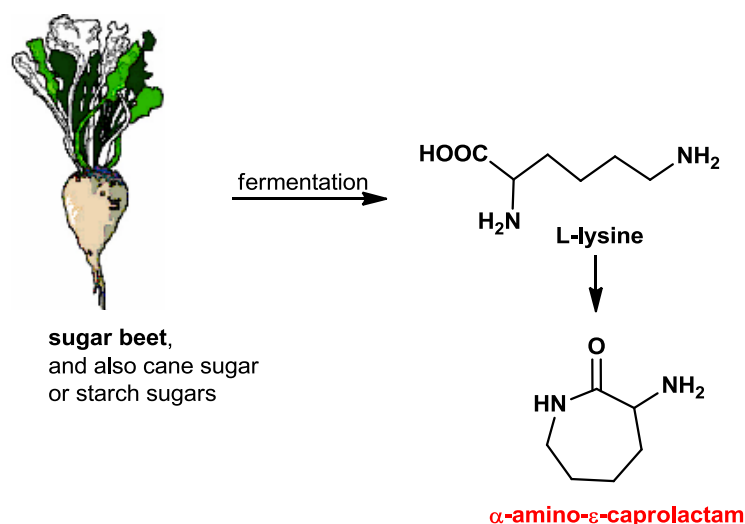
Introduction

Fluorination of polymers is particularly expected to impart better thermal stability, lower surface energy and water absorption¹⁻⁴. These properties are sourced from the essential characteristics of fluorine atom: high electronegativity, high ionization potential, and low polarizability⁵.

In the literature, there is less studies of fluorinated aliphatic polyamides⁶⁻⁹ than fluorinated aromatic polyamides¹⁰⁻¹⁴. Fluorinated copolyamide synthesis by condensation chemistry has some limitations such as long polymerization duration and high polymerization temperature. On the other hand, the anionic ring-opening polymerization (AROP) of ϵ -caprolactam (CL) has a potential to synthesize fluorinated aliphatic polyamide by eliminating those limitations. However, as it is well-known, there are some parameters of AROP that must be taken into account before considering the copolymerization of CL with a CL derivative.

As highlighted in the previous chapter, the AROP of CL is carried out by two reagents: the lactamate anion (C10) called as an initiator or catalyst (1) and *N*-acyllactam called as an activator. Initiation step involves an addition reaction of activator and initiator. Activator type has an effect both on the kinetics and on the obtained polyamide properties by increasing the polymerization rate and the monomer conversion while reducing molar mass of the polymer. Increasing initiator amount provides high of amount of free anions which can results in faster reaction rates^{15, 16}. In the literature, activator/initiator ratio is generally 1 to 1¹⁷. However, according to BASF protocols, activator/initiator ratio must be 1/4 or 1/8 which minimize side reactions therefore results in polymers with better properties.

Macromolecular materials based on renewable raw sources have gained increasing attention since they are environmentally friendly and have low cost compared to conventional methods and materials. α -amino- ϵ -caprolactam, derivative of CL, is obtained from the ring closure reaction of L-lysine, a renewable raw material. Lysine is an essential aminoacid present in plants, beet, cane, starch sugars via bacterial fermentation (Scheme II-1)^{18, 19}. L-lysine is usually manufactured by a fermentation process using *Corynebacterium glutamicum* for more than 40 years and the production exceeds 600,000 tons per year²⁰.

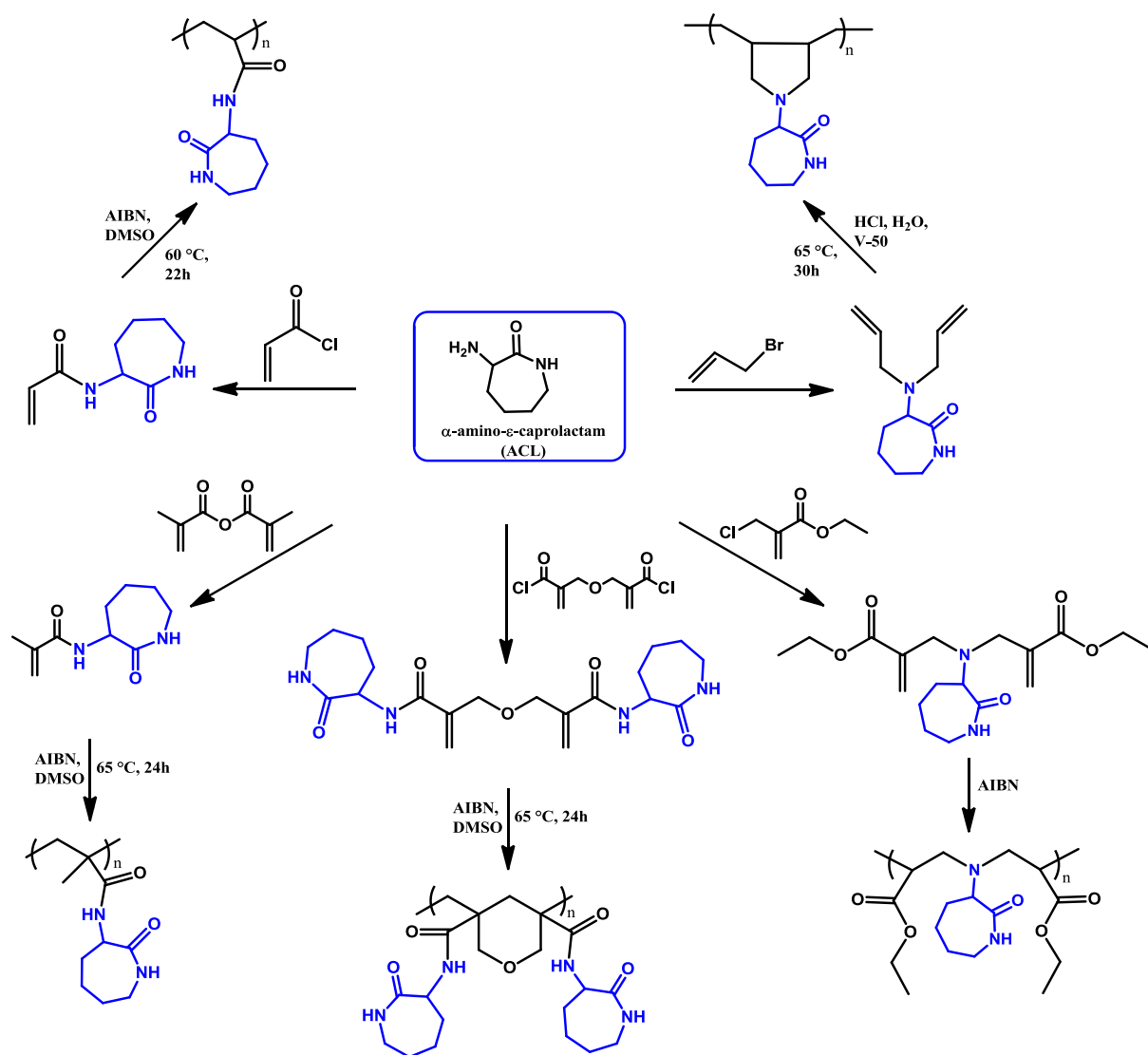


Scheme II-1. General synthesis of α -amino- ϵ -caprolactam.

Mathias et al.¹⁹ reported that vinyl derivatives of α -amino- ϵ -caprolactam from various diacid chlorides and diisocyanates (Scheme II-2) but not by AROP of CL ring. After series of monomer synthesis, polymers bearing pendant of α -amino- ϵ -caprolactam with multiple hydrogen bonding sites are obtained by the free radical polymerization in solution using 2,2-azo-bis(isobutyronitrile) (AIBN) and 2,2'-azo-bis(amidinopropane) hydrochloride as initiators.

Among these monomers, bis- and tetra-caprolactams derivatives are polymerized to form self-assembled polymers and networks via hydrogen bonding with good thermal properties.

On the other hand, obtained homopolymers from these monomers reveal high glass transition temperatures (T_g) owing to presence of the bulky pendant groups (cyclic) on the polymer backbone. This can be related to fact that bulky groups decrease chain mobility and increase rotational barrier via their intramolecular and/or intermolecular hydrogen bonding. They also studied that dynamic mechanical analysis of one example of the polymers bearing pendant cyclic group which demonstrates high storage modulus.



Scheme II-2. Modification and polymerization of the α -amino- ϵ -caprolactam¹⁹.

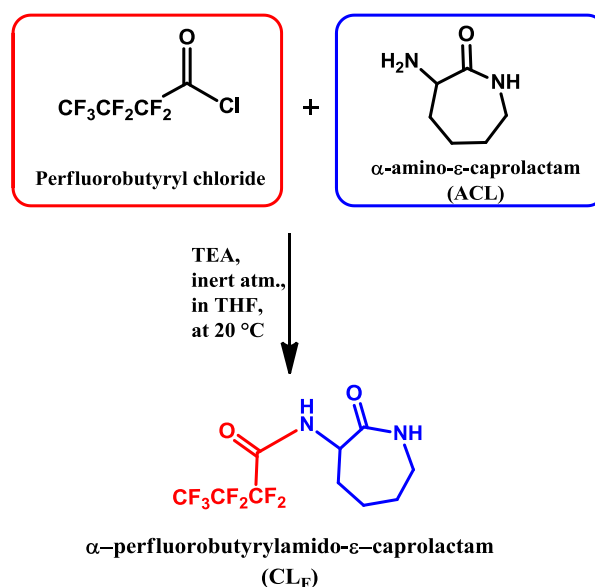
Besides, α -amino- ϵ -caprolactam has a great potential for modification and improving of PA6 structure and properties. In this case, side-reactions stemming from AROP of CL must be taken into account as well as the α -amino- ϵ -caprolactam structure and its primary amino group on the structure.

This thesis work aims at synthesizing novel PA6 with pendant fluorinated groups from a novel fluorinated monomer and CL by AROP, instead of common limited techniques as early mentioned in the first chapter. Furthermore, in this chapter work we report determining the possible side reactions during the AROP of CL in the presence of derivative of the α -amino- ϵ -caprolactam. Addition to, thermal properties, crystallinity, surface tension and

hydrophobicity are demonstrated as well as solubility tests on the novel structure of PA6 bearing fluorine units.

1. Synthesis of polyamide 6 with fluorinated moieties

A successful synthesis of novel α -perfluorobutyrylamido- ϵ -caprolactam monomer (CL_F) was achieved by a one-step amidation reaction from α -amino- ϵ -caprolactam and perfluorobutyrylchloride (Scheme II-3). To the solution of α -amino- ϵ -caprolactam in tetrahydrofuran (THF), triethylamine (TEA) was added to deprotonate a primary amine and quench HCl which is produced by amidation reaction. After 1h activation by TEA, perfluorobutyryl chloride was added dropwise while purging the reaction flask with argon because perfluorobutyryl chloride is sensitive to moisture it can easily exchange with $-OH$ and this would lead to more difficult nucleophilic attack of activated α -amino- ϵ -caprolactam. After 24h reaction and purification, white solid product was obtained with 85% yield.



Scheme II-3. One-step amidation reaction of perfluorobutyryl chloride with α -amino- ϵ -caprolactam.

The structure of the fluorinated monomer was confirmed by 1H NMR analysis. Figure II-1a exhibits the typical proton signals attributed to methylene groups ($-CH_2$; e, f, and g) of the α -amino- ϵ -caprolactam structure between 1.25-2.30 ppm. After reaction, the endocyclic amide proton on the ring was shifted from 6.70 to 6.03 ppm (Figure II-1b). $-NH$ proton of

fluorinated amide appears at 8.0 ppm. Integral ratios of obtained novel monomer show success of amidation reaction and purification. Integral ratios of d:c:a:b are 1:1:1:2 which are related to number of proton. Integral of CH_2 - protons (e, f, g) are 6.3 which is also correlated with the number of protons in that region (see Figure II-S1).

Pure PA6 was prepared by anionic ring-opening polymerization in the specific reactor system which provides better inert atmosphere and easy way to measure the exothermicity of the polymerization. For this reference PA6 synthesis, conventional AROP of ϵ -Caprolactam (CL, monomer) was carried out 5 time higher sodium ϵ -caprolactamate (C10, initiator) amount than usual method since copolymerization of CL and CL_F required higher amount of C10. Therefore, obtained homo- and copolyamides could be compared in the same conditions. The polymerization of CL was carried out in bulk at 140 °C. CL and C10 were added to a glass reactor (Figure II-S2) at 140 °C under nitrogen atmosphere to activate the monomer and were molten with continuous stirring and then hexamethylene-1, 6-dicarbamoylcaprolactam (C20, activator) was added to the mixture to start the polymerization. Anionic ring opening polymerization (AROP) of CL was completed within 15 minutes. After reaction, PA6 were refluxed in water to remove unreacted reagents and then dried in an oven overnight at 90 °C under vacuum before any analysis because moisture has a plasticizing effect on PA6. Conversion of the monomer (98%) was determined gravimetrically. Characterization of resulting PA6 was followed by 1H NMR and characteristic PA6 peaks was observed and shown in Figure II-S3. After polymerization, $-NH$ protons were shifted from 6.7 ppm to 6.0 ppm. Addition to, $CH_2-C=O$ protons were appeared at 2.2 ppm.

For the synthesis of PA6 bearing fluorine pendant groups, CL_F was added in the same moment with CL and the same way was followed like PA6 synthesis and purification. Additionally, polymers bearing fluorine groups were washed with CH_2Cl_2 after washing with water to remove unreacted CL_F and other reagents as well. Synthesis of PA6 bearing fluorinated groups was carried out in bulk at 140 °C by AROP (Scheme II-4) and the results are summarized in Table II-1.

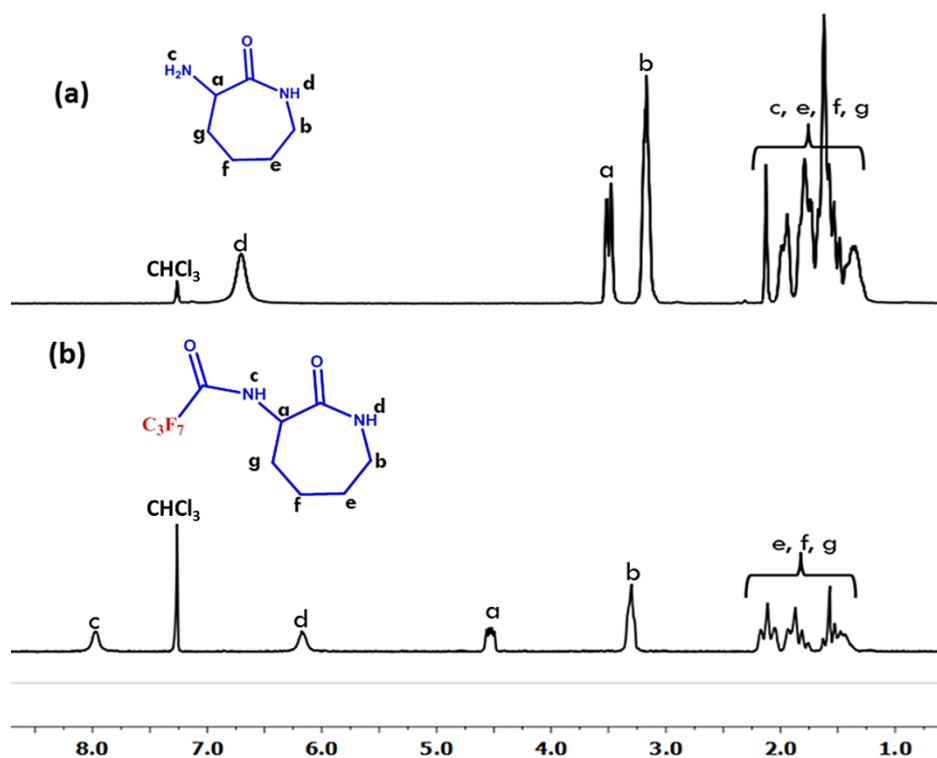
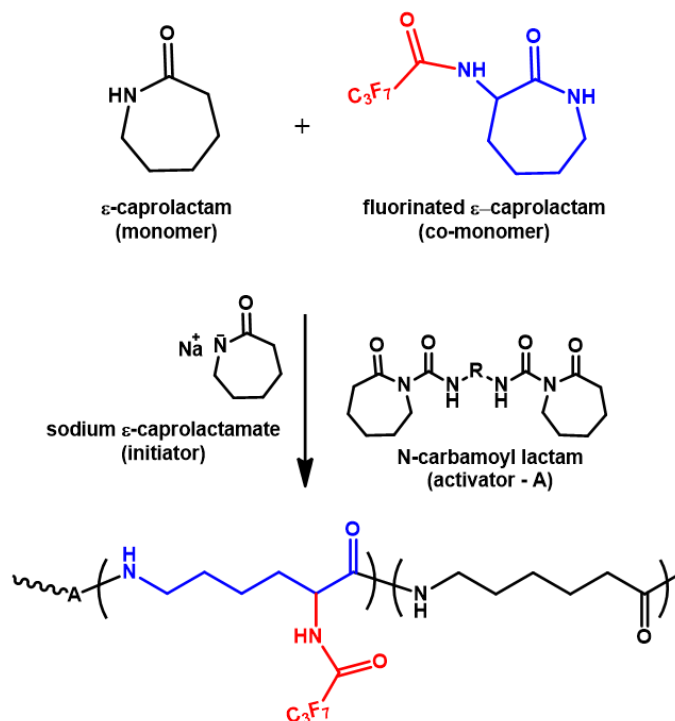


Figure II-1. ^1H NMR spectra of (a) α -amino- ϵ -caprolactam, (b) perfluorobutyryl-amido- ϵ -caprolactam in CDCl_3 .



Scheme II-4. Anionic ring-opening copolymerization of ϵ -caprolactam (CL) and perfluorobutyrylamido- ϵ -caprolactam.

A series of polymerization reactions was performed by using different molar ratio of C10 to C20 (Table II-1). Addition of 2 or 4 wt% of fluorinated compound to CL polymerization enables the polymerization and spawned a decrease of the rate as longer time (24 hours) are required to reach 63-67% of conversion (runs 2 and 3). A decrease of reactivity is clearly observed when it is compared to the usual PA6 synthesis under similar experimental conditions (run 1). Since yield is not completed, exact amount of introduced comonomer is probably lower than the theoretical one. In fact, determination of the exact amount of fluorinated units in the polymer chain by NMR was not possible because of the restricted solubility of resulting polymer in common organic solvent.

Table II-1. Synthesis of polyamide 6 and polyamide 6 bearing fluorinated groups at 140 °C in bulk.

Run	Activator ^a (C20, mol/L)	Initiator ^b (C10, mol/L)	Ratio ([C10] [C20])	CL ^c (mol/L)	CL _F ^d (mol %)	CL _F ^d (wt %)	Time	Conv ^e %
P1, PA6	0.02	0.153	7.65	7.38	-	-	15min	98
P2, 2%F-PA6	0.02	0.153	7.65	7.20	0.83	2	24h	67
P3, 4%F-PA6	0.02	0.153	7.65	7.02	1.68	4	24h	63
P4, 2%F-PA6	0.02	0.306	15.3	6.18	0.94	2	15min	90
P5, 4%F-PA6	0.02	0.306	15.3	6.01	1.90	4	24h	63

^a C20 = hexamethylene-1,6-dicarbonylcaprolactam in ϵ -caprolactam

^b C10 = sodium ϵ -caprolactamate in ϵ -caprolactam

^c CL = ϵ -caprolactam

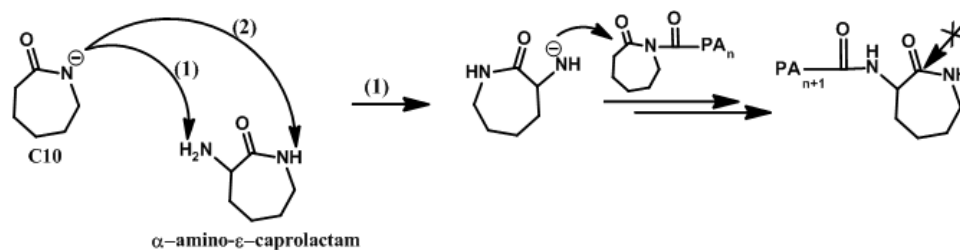
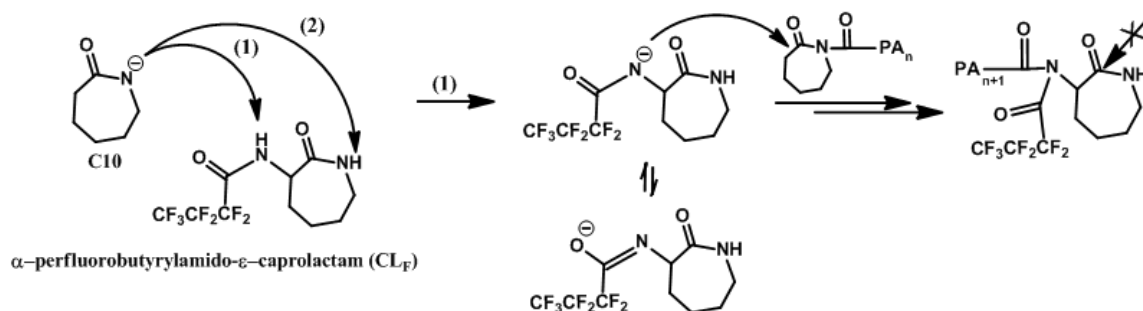
^d CL_F = fluorinated ϵ -caprolactam; theoretical values

^e determined gravimetrically.

As early mentioned, reactivity of anionic polymerization of CL is related to the many parameters such as lactam size and their substituents, the nature of the activator, the initial ratio of initiator and activator concentrations, the permittivity of the reaction medium, and the reaction temperature as well as the nature of the counter-ion²¹⁻²³.

To the best of our knowledge, copolymerization of α -amino- ϵ -caprolactam and CL was also carried out with the same copolymerization conditions of CL_F. However, this reaction could not end with any copolymerization. This result is probably related to the different acidities of the hydrogen atoms where one is located in α position of the lactam ring (primary amine) (pK_b > 36) and hydrogen in an amide group (pK_b = 27.1). The acidity difference of these hydrogens led to a competitive proton abstraction by C10, Scheme II-5-a.

Therefore, this competition of deprotonating and especially favoring for primary amine protons in α position may cause to the formation of two distinct amide anions. After deprotonating of primary amine of the α -amino- ϵ -caprolactam, obtained anion can attack active carbonyl side and deactivate ring-opening polymerization of these monomers or oligomers instead of ring-opening polymerization. There was the same risk in anionic polymerization of the fluorinated derivatives of α -amino- ϵ -caprolactam with different acidity of α position of the lactam ring (primary amine) and hydrogen in an amide group, Scheme II-5-b. However, a deprotonating from the same position would not get resonance with endocyclic carbonyl group of CL_F ring since one exocyclic carbonyl has strong electron withdrawing group fluorine, Scheme II-5(2). But, still this effect could consume more C10 than expected. Addition to, amide anions in α position would attack to active carbonyl side and deactivate ring-opening polymerization of these monomers or oligomers instead of ring-opening polymerization. The other possible side reaction is, as already mentioned (see chapter I of this manuscript, *side-reactions*), that the presence of amide N anions along the polymer chain may produce imide groups and lead to polymer branching in strongly basic medium²⁴. Similar effect can be a concern for this anionic polymerization because of the presence of the exocyclic amide N anion on CL_F . These possible side reactions shed light on lowering rate of polymerization therefore reducing the yield.

 (a) deprotonation of α -amino- ϵ -caprolactam

 (b) deprotonation of CL_F

Scheme II-5. Deprotonating possibilities of α -amino- ϵ -caprolactam (1) or CL_F (2) by C10.

2. Rate of polymerization

During the polymerization of ϵ -caprolactam, temperature profiles of AROP of homo- and copolymerization were monitored by calorimetric measurements because AROP of ϵ -caprolactam is an exothermic reaction^{25, 26} and this property allows monitoring the rate of monomer consumption, i.e.

$$R_p = - \frac{d[CPL]}{dt} = k_p \times f \times [Initiator] \times [Catalyst] \quad eq(1)$$

To overcome side reactions such as transamidation reactions and Claisen-type condensation^{27, 28}, we increased the C10 amount while adding of fluorinated comonomer to able to activate more (co)monomers. Decreased reaction efficiency can be explained by the structure of the novel fluorinated comonomer. The chemical structure has a remarkable influence on reactivity and affects chemical and physical properties of the resulting polymer.

Increasing the C10/C20 ratio, corresponding to an increase of the relative amount of the activated monomer in the medium, allowed to decrease the polymerization time down to 15 minutes and to obtain a high yield (90%) when 2 wt% of fluorinated co-monomer was added (P4, Table II-1). This enhanced reactivity was not observed anymore using higher amount of CL_F (P5, 4wt %). Monitoring the evolution of temperature versus time confirms fast copolymerization (P4) which shows a polymerization exotherm of 27 °C at 120 seconds (Figure II-2). Despite the doubled amount of activated monomer as compared to the one used in PA6 synthesis, the polymerization and crystallization rates occur more slowly. This exotherm used as a reference was found to be equal to 44 °C after 50 seconds. The flat evolution of temperature with time and limited conversion by using 4 wt% of fluorinated co-monomer (P5) indicates clearly a decreased reactivity of the overall polymerization process, and the introduction limit of fluorinated groups into PA6. This result is accounted for by the higher relative amount of the acyl- group of the comonomer, which is leading to some side reactions akin to the ones involving the acyl- groups as mentioned above.

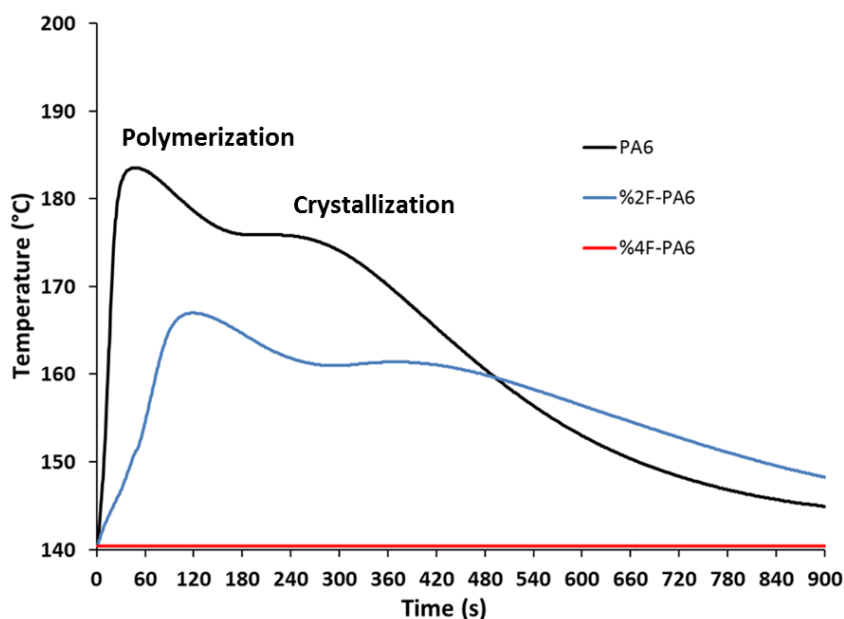


Figure II-2. Temperature/Time diagrams of P1 (PA6) black line; P4 (2%F-PA6) blue line; and P2 (2%F-PA6), P3 (4%F-PA6) and P5 (4%F-PA6) red line.

3. Polymer characterization by NMR and ATR-IR

Introduction of bulky pendant fluorine groups to the polymer chains increases the solubility of fluorinated polymers because of the replacement of symmetrical structures with unsymmetrical ones. Bulky units decrease interactions between polymer chains, breaking hydrogen bonds, and lead to less packing and crystallinity²⁹⁻³¹. The solubility of the fluorine-containing polyamides in various organic solvents at 2.0% (m/v) were tested overnight at 20 and 70 °C and presented in Table II-2. All the polymers could be readily dissolved in strong acids such as sulfuric acid and polar solvent hexafluoroisopropanol at room temperature and at 70 °C. On the other hand, they were not soluble in some common organic solvents such as *N,N*-dimethylformamide, tetrachloroethylene, methanol, and dimethyl sulfoxide. Obviously, their minor improved solubility in dichloromethane, *N,N*-dimethylformamide, methanol and chloroform are due to the fact that the bearing trifluoromethyl groups allow the solvent molecules to diffuse into the polymer chains. In another word, due to lower interactions between chains, the enthalpy contribution (ΔH) to the free enthalpy (ΔG) is not sufficient to counter balance the contribution of entropy (ΔS). The entropy contribution is then the dominant factor ($\Delta S > 0$), which brings about solubility of the polymer ($\Delta G < 0$).

Table II-2. Solubility^a of PA6 and fluorinated derivatives.

Polymer	Solvent						
	Water	HFIP	H ₂ SO ₄	CH ₂ Cl ₂	DMF	CH ₃ OH	CHCl ₃
P1, PA6	-	+	+	-	-	-	-
P2, 2%F-PA6	-	+	+	-	-	±	-
P3, 4%F-PA6	-	+	+	±	±	±	±
P4, 2%F-PA6	-	+	+	-	-	±	-
P5, 4%F-PA6	-	+	+	±	±	±	±

^aSymbols: +, soluble in 30 min; ±, partly soluble in 24 h; -, insoluble at 20 and 70 °C. HFIP hexafluoropropanol, H₂SO₄ sulfuric acid, CH₂Cl₂ dichloromethane, DMF *N,N*-dimethylformamide, CH₃OH methanol, CHCl₃ chloroform.

These new polyamides were characterized by ATR-FTIR spectroscopy (Figure II-3). PA6 shows characteristic absorption bands at 3300 cm⁻¹ attributed to the *N*-H band and also at 2931-2860 cm⁻¹ corresponding to the CH₂ symmetric and asymmetric stretching vibrations. The sharp peak at 1640 cm⁻¹ corresponds to the stretching vibration of the C=O group of the amide functionality and the peak around 1540 cm⁻¹ is attributed to combination of the bending vibration of the *N*-H bond and stretching vibration of the C-N bond of the amide group. By comparison with neat PA6, PA6 having fluorinated bulky groups showed absorption bands at 1234 cm⁻¹ and at 1160 cm⁻¹, pursuant to symmetric and asymmetric stretching vibrations of C-F band, respectively.

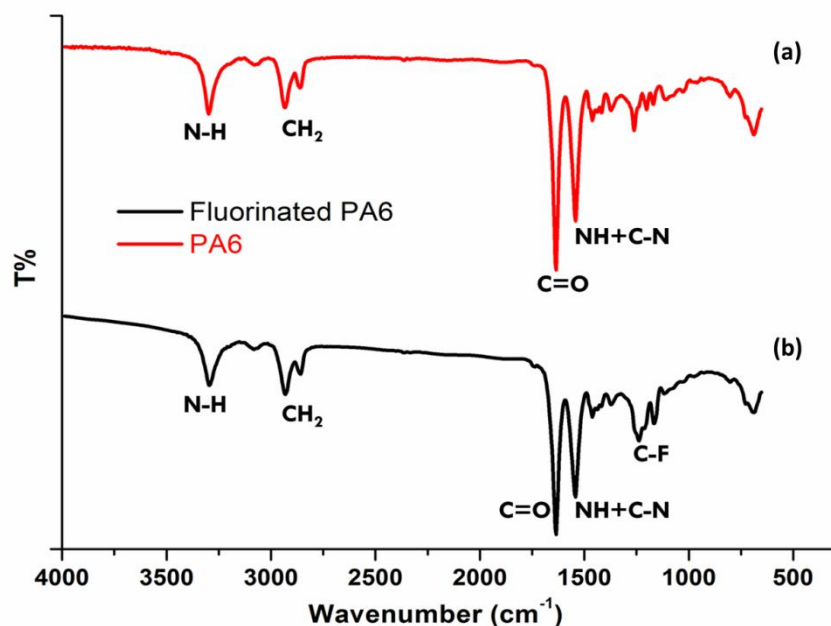


Figure II-3. ATR-FTIR spectrums of neat polyamide 6 (a) and polyamide 6 bearing fluorinated groups (b).

The structure of the novel polyamides bearing fluorinated groups were also confirmed by the ¹⁹F magic angle spinning (MAS) NMR spectra (Figure II-4). They exhibit characteristic signals assigned to the C₃F₇- group by the presence of the CF₃- group centered at -81 ppm and the CF₂- groups in the -120 to -130 ppm range, indicating the incorporation of fluorinated groups into the polymer. Addition to, integral ratios of CF₃- and CF₂- were matched with fluorine unit on the structure.

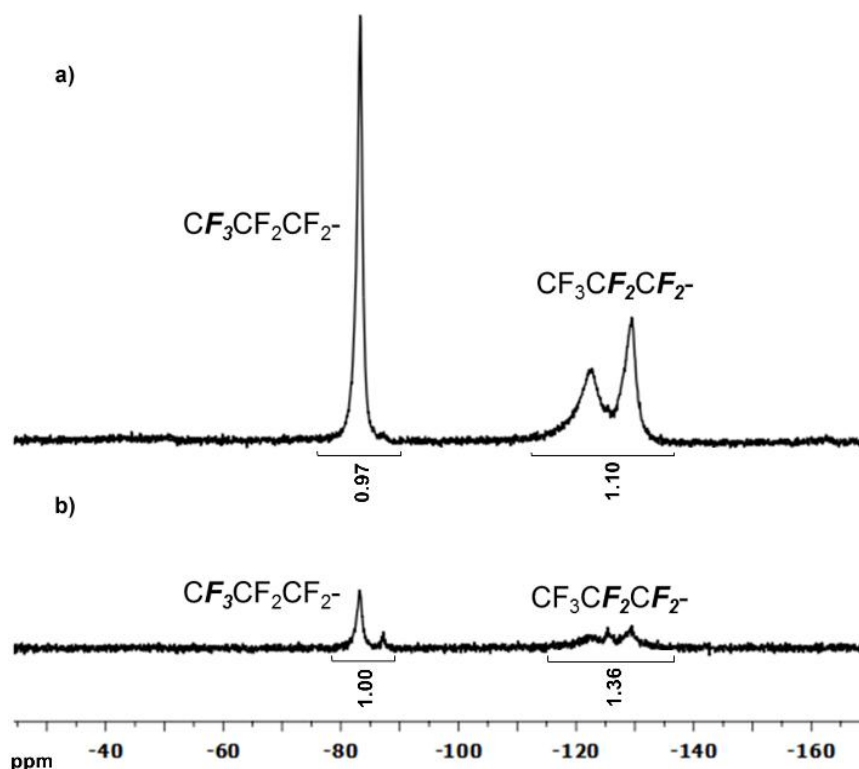


Figure II-4. ^{19}F MAS NMR spectrums of 4%F-PA6 (a) and 2%F-PA6 (b).

4. Thermal characteristics of modified polyamide 6 and investigation of degradation mechanism

Thermal behavior of neat PA6 and PA6-based copolymers having theoretically 2wt % and 4 wt% of perfluorobutyryl units was investigated by thermo gravimetric analysis (TGA) and differential scanning calorimetry (DSC).

The DSC second heating cycle curves of PA6 and PA6s bearing fluorine groups are shown in Figure II-5. DSC was used to determine the melting point³² and glass-transition temperature values (T_g s) of the samples obtained from the second heating scans with a heating rate of 10 °C/min under nitrogen, as shown in Figure II-5 (second heating scan) and in Table II-3. As it is known, T_g of PA6 is around 50-55 °C and it was confirmed (P1). PA6s bearing fluorine units (P2-P5) showed slightly increased T_g values to 57-58 °C. This slight T_g increasing is related to bulky fluorine groups on PA6 chains. The bulky fluorine groups can minimize the mobility of amorphous phase because of the blocked structure. Addition to, the bulky groups can also inhibit hydrogen bonding between polymer chains and increase free volume in the crystalline phase due to less packing and non-symmetric structures⁷. A

decreased polarizability due to fluorination brings about a decrease of interactions between chains (by induced dipolar interactions) with a potential impact on T_g . In contrast and more significantly, melting temperature and crystallinity by ΔH_m (2nd DSC runs) were decreased while increasing fluorine-containing units in PA6 (see, Figure II-S4-7).

Table II-3. Thermal properties of polyamide 6 and PA6s bearing fluorine from DSC and TGA.

Sample	DSC		DSC			TGA				
	1 st Scan		2 nd Scan							
	T_m (°C)	ΔH_m (j/g)	T_g^a (°C)	T_c (°C)	ΔH_c (j/g)	T_m (°C)	ΔH_m (j/g)	T_5 (°C) ^b	T_{10} (°C) ^c	T_d (°C) ^d
P1, PA6	213	92.0	53	171	60	216	70	290	300	308
P2, 2%F-PA6	209	97.0	52	165	47	204	47	272	297	363
P3, 4%F-PA6	206	96.2	58	160	52	198	51	304	338	365
P4, 2%F-PA6	215	93.4	57	177	67	215	70	330	355	390
P5, 4%F-PA6	216	106	57	171	60	210	67	322	346	386

^aFrom the second heating trace of DSC measurements conducted at a heating rate of 10 °C/min,

^bDecomposition temperature at a 5% weight loss,

^cDecomposition temperature at a 10% weight loss,

^dMaximum of the peak decomposition temperature.

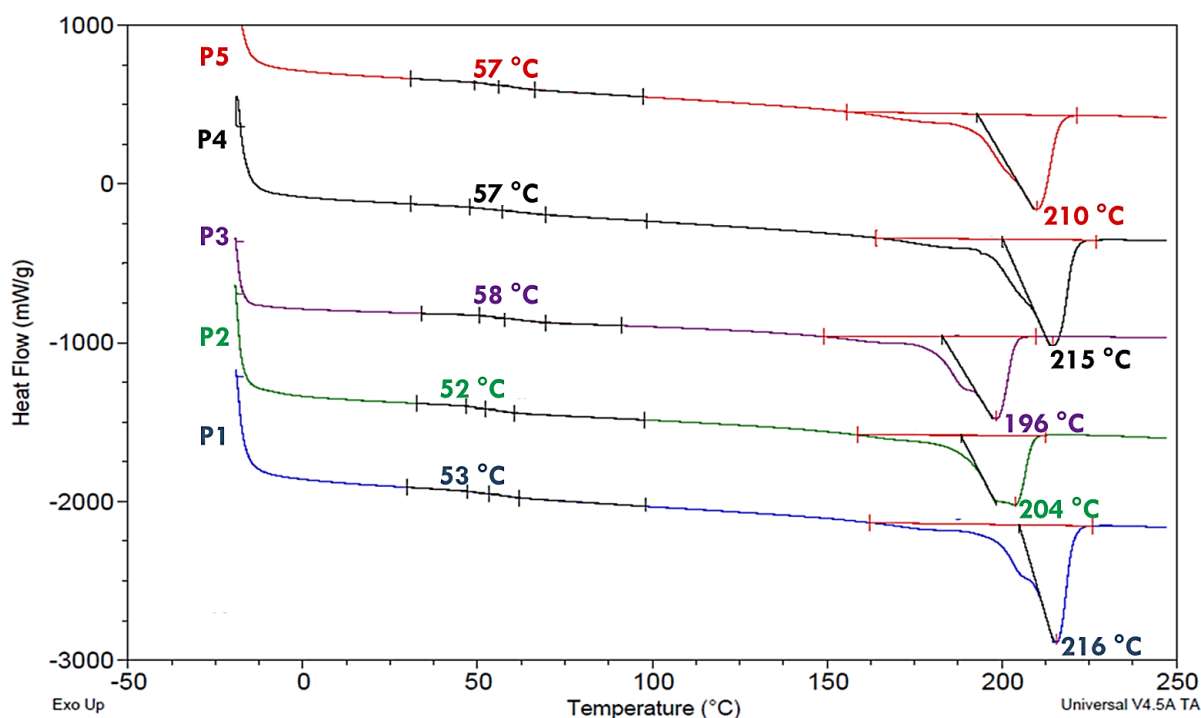


Figure II-5. DSC thermal curves of P1 (PA6), P2(2%F-PA6), P3(4%F-PA6), P4(2%F-PA6), and P5(4%F-PA6) in second heating cycle.

Thermal stability of polyamides was also investigated by TGA at a heating rate of 10 °C/min under nitrogen atmosphere. The thermograms of PA6 and modified PA6s are shown in Figure II-6 and the results are summarized in Table III-4. A remarkable increase of degradation temperatures of the fluorinated polymers was observed. TGA also confirmed that a major weight loss was observed at a temperature higher than 350 °C, at which the weight loss is observed as far as PA6 is concerned. Onset decomposition temperatures³¹ as well as weight loss temperatures of 10% (T_{10}) and 5% (T_5) were all determined from original curves and listed in Table III-4. The T_5 and T_{10} values of the neat PA6 (P1) and fluorinated PA6s (P2-5) increased from 294–303 °C to 330–360 °C, respectively. The data from thermal analysis showed that the resulting polymers have fairly high thermal stability.

In addition to, TGA of CL_F and PA6 artificial kind of mixture was taken (Figure II-6) to demonstrate that after polymerization and washing there are no more fluorinated monomer component (non-reacted) and its effect on thermal degradation by comparison with PA6 bearing fluorine units. As it can be seen from Figure II-7, the artificial mixture has two

degradation points first CL_F and following PA6 thermal degradation different from copolymerized systems (Figure II-6).

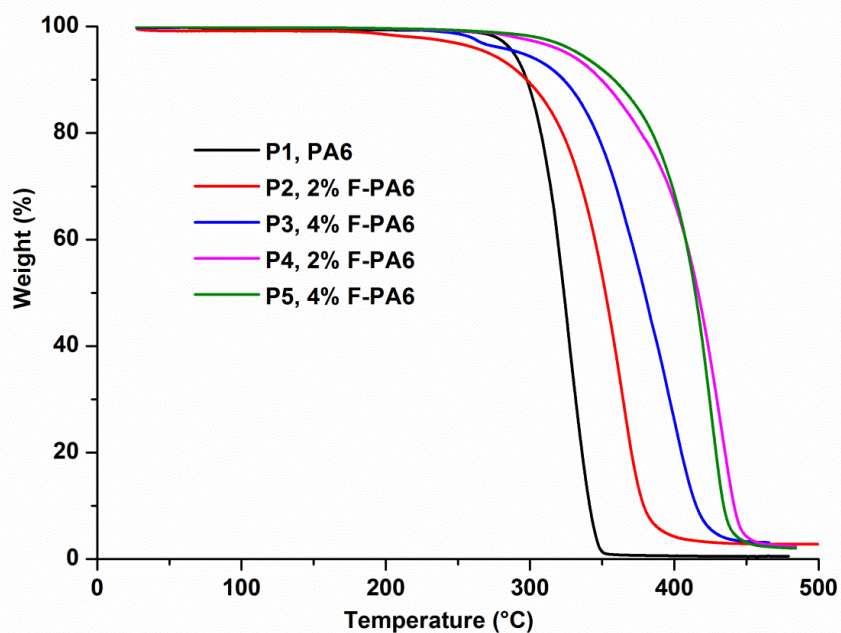


Figure II-6. TGA thermograms under a nitrogen atmosphere of P1 (PA6), P2 (2%F-PA6), P3 (4%F-PA6), P4 (2%F-PA6), and P5 (4%F-PA6).

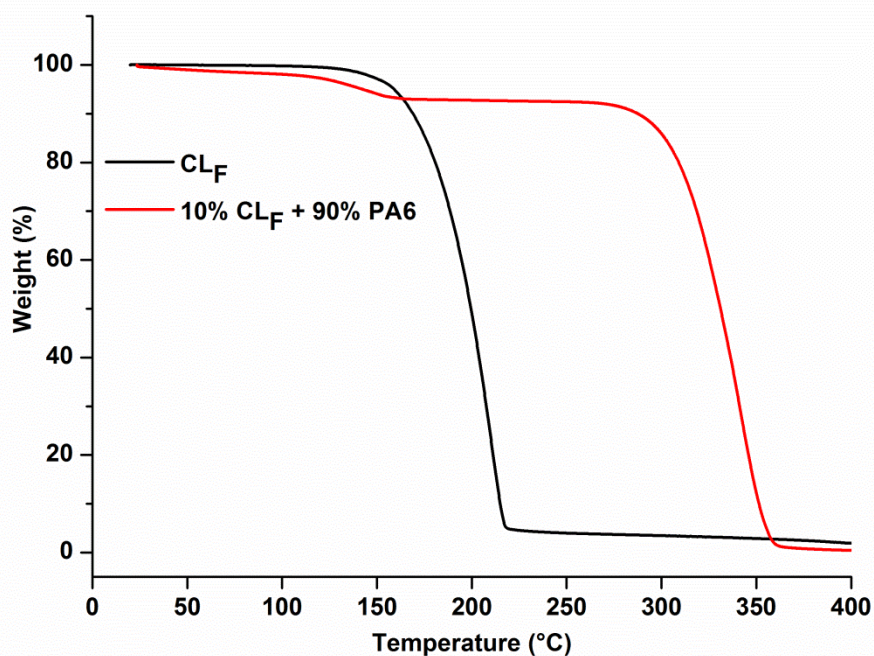
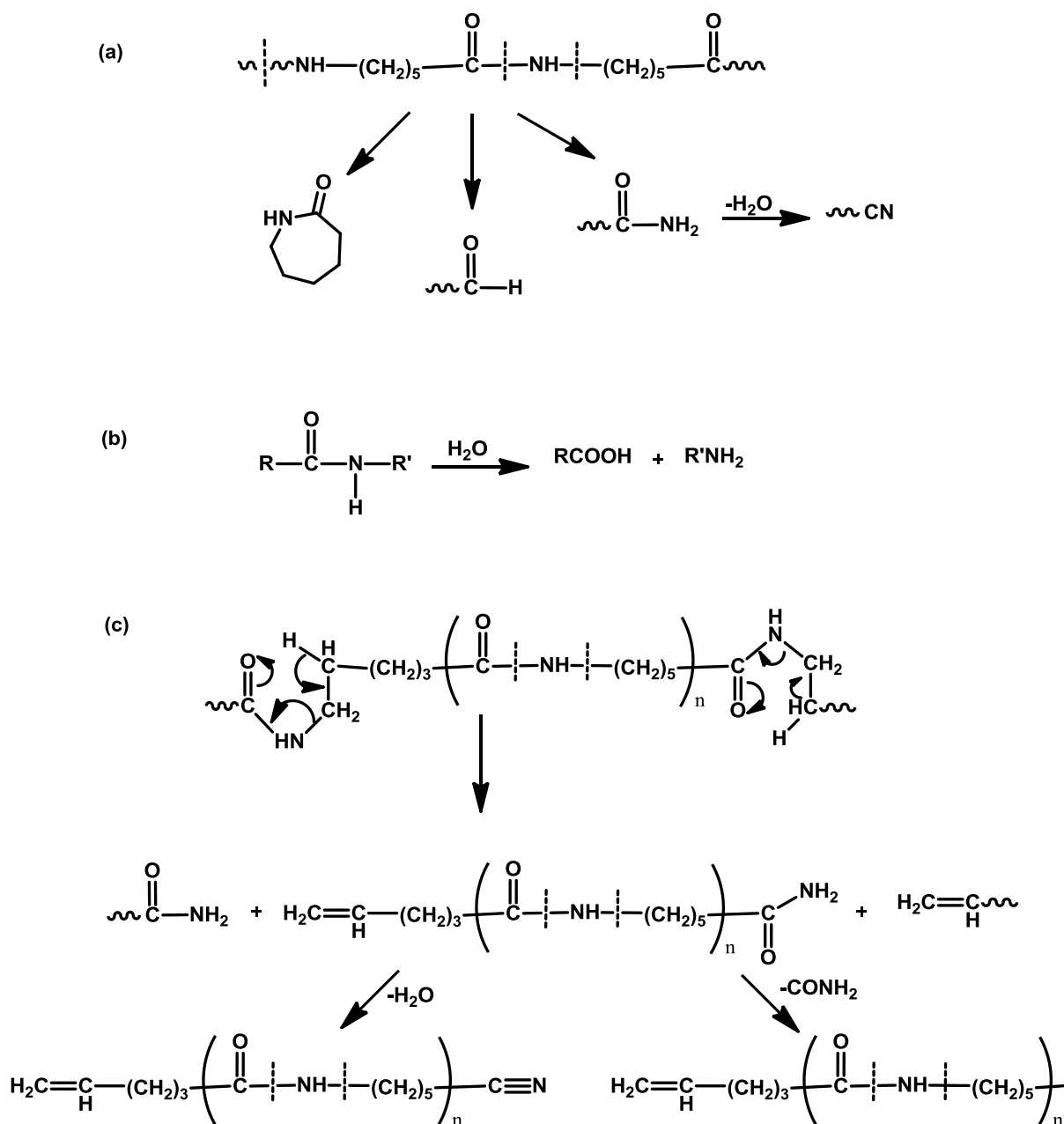


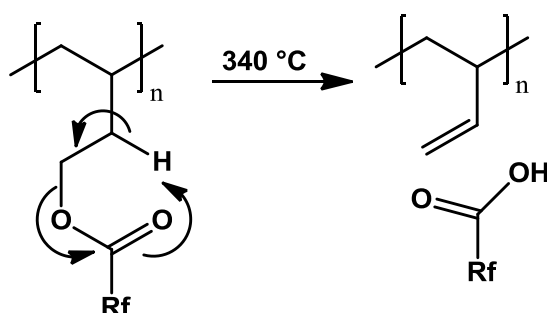
Figure II-7. TGA thermograms under a nitrogen atmosphere of CL_F and neat PA6 with CL_F (10 % fluorinated monomer).

Although the literature does not report any precise thermal degradation mechanism for aliphatic polyamide family (PA6, PA6.6, PA6.10, PA11, PA12), PA6 thermal degradation is mostly explained with three types of mechanisms. The mechanisms are homolytic scission (Scheme II-6a), hydrolysis (Scheme II-6b), and intramolecular hydrogen transfer (cis-elimination) (Scheme II-6c), were reviewed in detail by Levchik et al³³.



Scheme II-6. Thermal degradation mechanisms³³ of polyamide 6: a) homolytic scission, b) hydrolysis, c) intramolecular hydrogen transfer.

Thermal depolymerization of PA6 was studied extensively in different ways and explained mostly with producing cyclic lactam oligomers and scission of weak C-N bonds^{33, 34}. Thermal ester cleavage of pendant fluorinated group on other polymer chains was also shown to occur (Scheme II-7)³⁴. This can be explained by that the presence of an electron withdrawing fluorinated substituent could increase the electrophilicity of C=O and thus favors cleavage of pendant fluorinated group responsible for thermal degradation and release of low molar mass volatiles.



Scheme II-7. Proposed thermal cleavage of fluorinated side chains of polymer³⁴.

The measurement of derivative weight loss with temperature (Figure II-8) of all prepared polyamide samples indicates peaks or shoulders which can be related to different degradation mechanisms and associated to the mechanisms so far proposed. The improvement of the thermal stability of fluorine bearing PA6s is explained by minimizing the depolymerization process at 300-350 °C and shifting to higher degradation point than 400 °C due to the introduction of fluorine-containing units in the chains breaking the backbone regularity and/or affecting electronegativity effect of fluorine atoms. The bond scissions and formation of cyclic compounds occur at higher temperature and are probably accompanied by scission of amide linkage of perfluorobutyrylamido in PA6 (Scheme II-8), as described for ester linkages.

To conclude, we believe that the introduction of fluorinated units into PA6 slows down the depolymerization reaction due to the blocked structure formation, stemmed from presence of fluorine pendant units, during the thermal degradation.

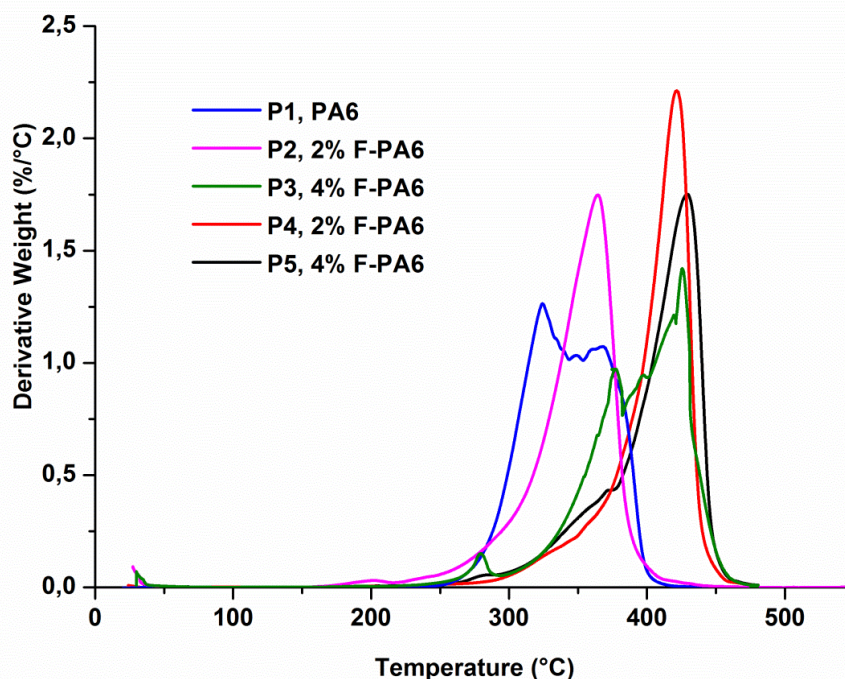
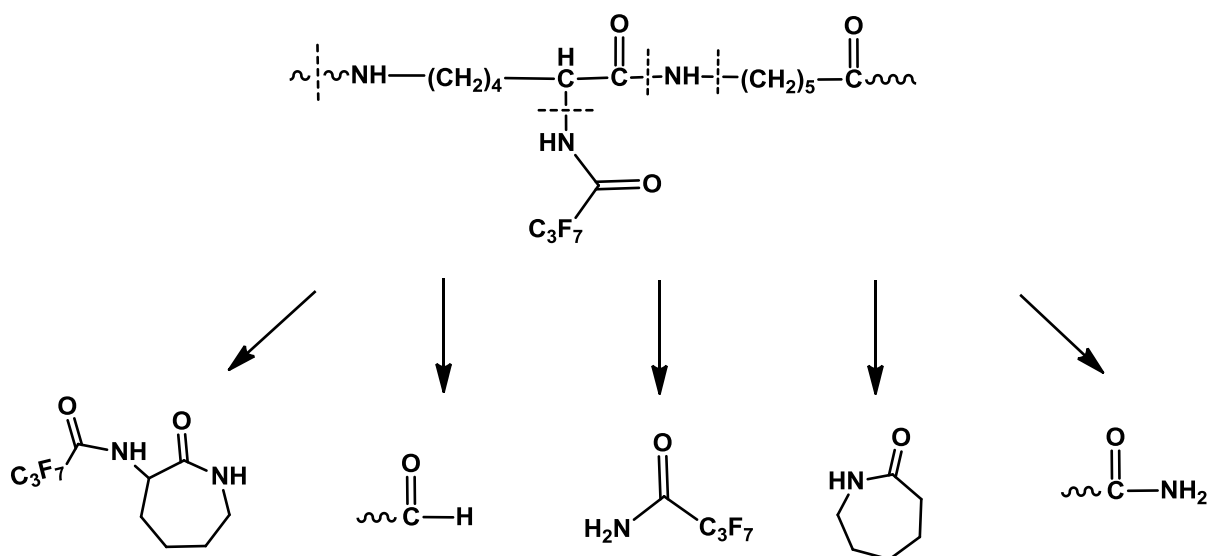


Figure II-8. Rate of weight loss of P1 (PA6), P2 (2%F-PA6), P3 (4%F-PA6), P4 (2%F-PA6), and P5 (4%F-PA6).



Scheme II-8. Proposed thermal degradation mechanism of polyamide 6 bearing fluorinated groups.

The dynamic mechanical behavior³⁵ of the resulting polymers bars (heat pressed), elastic (storage) modulus (E') and loss factor ($\tan \delta$) against temperature, are shown in Figure II-9 and Figure II-10. These figures clearly showed that an increased amount of fluorinated

groups on PA6 chains reduces E' before and after T_g . It can be related to decreasing of crystallinity due to restricted packing of PA6 chains. This effect can obviously be seen from reduced elastic modulus values in Figure II-9 which is reduced from 2.15×10^9 Pa (P1) to 2.80×10^8 Pa (P2), 2.72×10^8 Pa (P3), 2.51×10^8 Pa (P5), and 8.2×10^7 Pa (P4) (see, Figure II-S9-13). This exploration appears then delicate when increased C10 amount is added as T_m and ΔH_m do not vary much from neat PA6 (Table II-3). $\tan\delta$ curve is shifting to higher temperatures with increasing amount of bulky fluorine groups in PA6 chains compared to neat PA6. The maxima of $\tan\delta$ at 72 °C, 74 °C, 81 °C, 77 °C and 79 °C for P1, P2, P3, P4 and P5 (see, Figure II-S9-13), respectively. The shifting of $\tan\delta$ is related to the increasing amount of bulky fluorine content in line with less mobility of the amorphous phase.

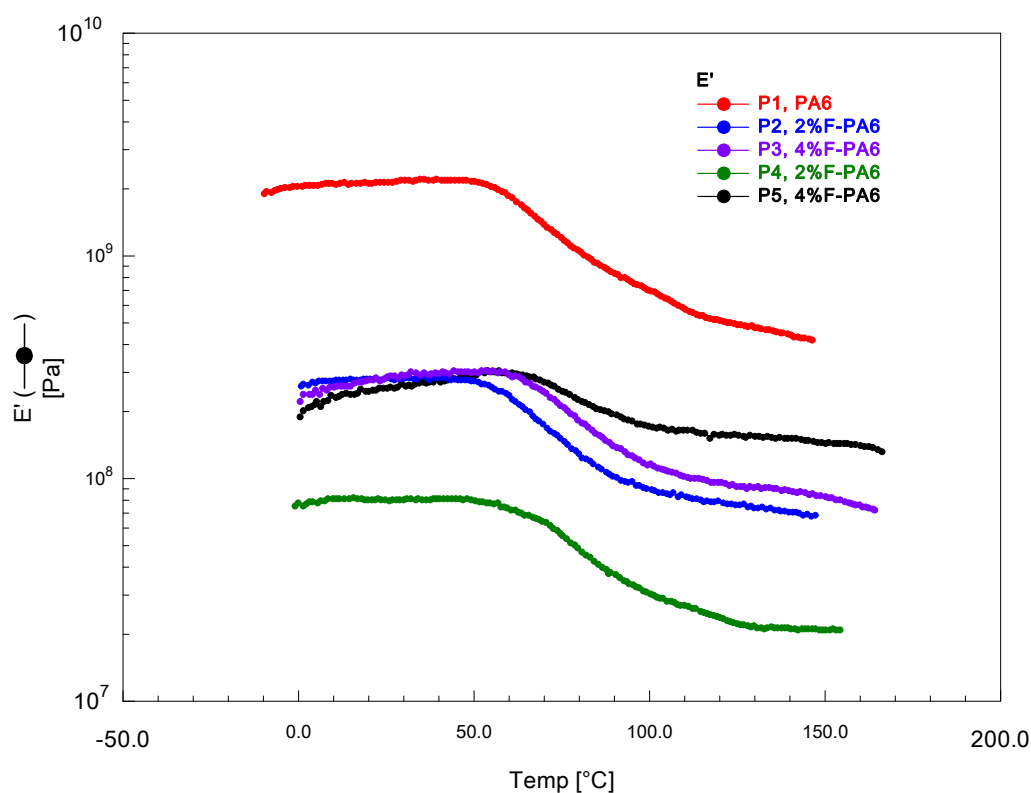


Figure II-9. Elastic modulus (E') of P1 (PA6), P2 (2%F-PA6), P3 (4%F-PA6), P4 (2%F-PA6), and P5 (4%F-PA6) by DMA.

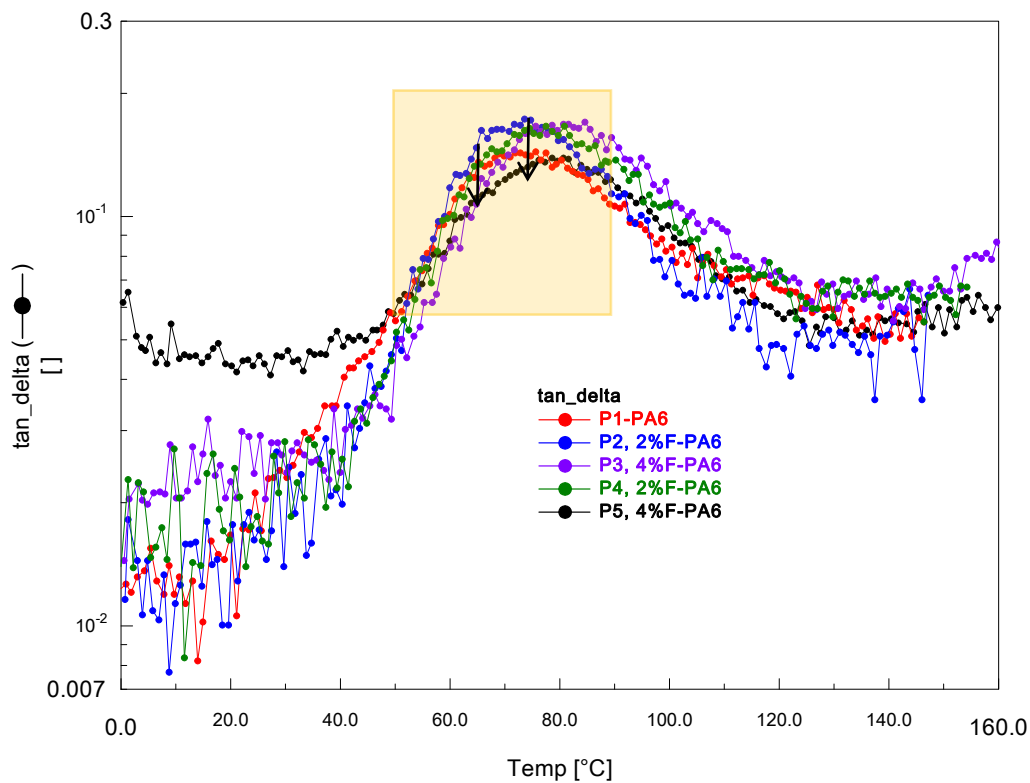


Figure II-10. Loss factors (Tan δ) of P1 (PA6), P2 (2%F-PA6), P3 (4%F-PA6), P4 (2%F-PA6), and P5 (4%F-PA6) by DMA.

5. Hydrophobicity and Water Uptake Determination

Wettability is one of the important properties of solid surface for both fundamental and practical aspects³⁶. It was also one of the main issues of this study. The wettability was determined by measuring the contact angle (CA) which is the most common way to measure the wettability of a surface of polymers. Evaluations of liquid–solid contact angles are commonly used to evaluate solid surface tension γ_s of polymers. CA measures the wettability of a solid surface by a liquid via the Owens- Wendt-Kaelble method^{37, 38} :

$$\gamma_L(1 + \cos \theta) = 2 \left[(\gamma_S^d \gamma_L^d)^{\frac{1}{2}} + (\gamma_S^p \gamma_L^p)^{\frac{1}{2}} \right] \quad eq(2)$$

where γ^d and γ^p represent the dispersion and the polar of surface tension, respectively, and θ is the contact angle. As there are two unknowns (γ_S^d, γ_S^p), it is essential to have at least two wetting liquids results of known γ_L^d and γ_L^p . We used three liquids (distilled water, ethylene

glycol and diiodomethane) and for each liquid three drops to different surface points were taken then averaged and summarized in Table II-4.

Table II-4. Static contact angles, surface energies and water uptakes of polyamide 6 and polyamide 6 bearing fluorinated groups.

Polymer	Contact Angle (°)			Surface Energy (γ) (mN/m)			Water uptake (%) ^b
	H ₂ O	CH ₂ I ₂	EG ^a	Polar	Dispersive	Total	
P1, PA6	61	30	34	10.60	38.84	49.47	10
P2, 2%F-PA6	70	36	36	6.94	38.75	45.70	14
P3, 4%F-PA6	74	39	37	5.59	38.52	44.11	16
P4, 2%F-PA6	70	35	39	6.74	38.63	45.37	13
P5, 4%F-PA6	74	38	38	5.58	38.60	44.18	16

^aEthylene glycol

^b Water uptake (%) = $100 \times (W - W_0) / W_0$; W: weight of polymer sample after standing in water at 80°C for 24h; W₀: weight of polymer sample after being dried in vacuum at 100 °C.

The sessile drop method was used to characterize the surface energy of the pure and modified PA6 films which were prepared by spin coating at room temperature. The contact angles were measured with distilled water, ethylene glycol and diiodomethane and the surface energy was calculated.

At first, the increase of water contact angle (WCA) from 61° to 70° (2wt% of added CL_F) and then 74° (4wt% of added CL_F) agree with the introduction of fluorine in PA6, Figure II-11.

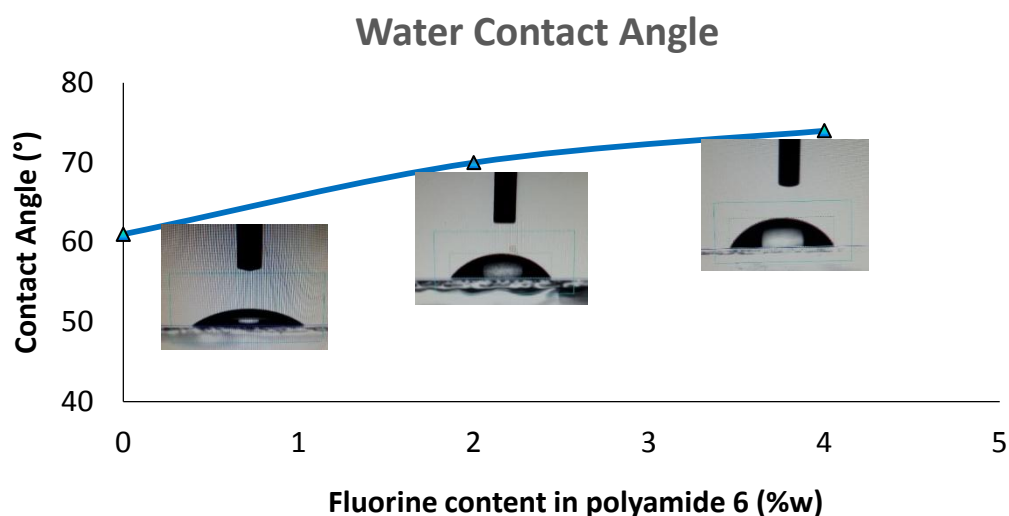


Figure II-11. Water contact angles of 2 and 4w% of fluorine pendant PA6s and PA6.

According to Owens- Wendt- Kaelble^{37, 38}, generally accepted to measure the interaction between liquid and solid surface, the higher the contact angle towards distilled water, the lower the surface energy. Despite the fact that exact values of fluorine content in the polymer might be lower than the theoretical ones due to non-complete conversions, the surface energy was shown to decrease significantly with the increase of fluorine content in agreement with a higher surface hydrophobicity of the material.

Fluorine pendant PA6s have higher water uptake compare to PA6, because of less regular structure of fluorine pendant polyamides. Many fluorinated aliphatic polymers⁶⁻⁸ are reported in the literature with higher water contact angle and higher water uptake because of the less regular structure. Any pendant groups on polyamide chain also lead to chain separation and to decreasing chain packing because of less hydrogen bond interactions between *N*-H and C=O, by increasing water accessibility. In our case, these fluorinated pendant groups are attached to the main chain by additional amide bonds which have also an influence on increased water uptake. Kinetic water uptake measurements of all polymer slices (P1-5), which were prepared by heat pressing and before dried overnight at 90 °C in an oven under vacuum, were completed in 13h at 80 °C (Figure II-12). The polymer slices thicknesses were 0.137, 0.121, 0.153, 0.125 and 0.124 cm for P1-P5, respectively. Due to the less packing of polymer chains, and in addition to that, at high temperature of 80 °C water vapors could penetrate faster over PA6s bearing bulky fluorine units than neat PA6. In first 30 min., P2 and P4 which are supposed to have the same amount of fluorine units showed

that P2 had a bit faster and higher water uptake than P4. Comparison between P3 and P5 displayed the same water uptake and water uptake kinetics. As a matter of fact, the higher water uptake, despite higher water contact angle, is not surprising outcome since increased amorphous character due to the pendant groups was shown in previous part of this chapter.

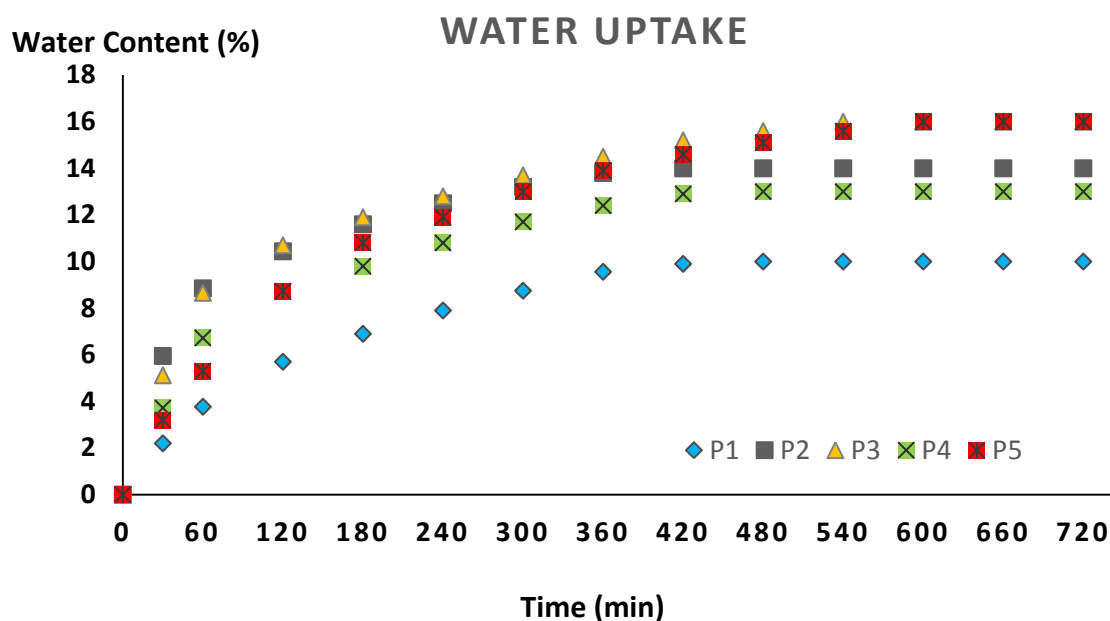


Figure II-6. Kinetic water uptake measurements of P1, PA6; P2, 2%F-PA6; P3, 4%F-PA6; P4, 2%F-PA6; and P5, 4%F-PA6 in 13h at 80 °C.

Conclusion

Polyamide 6 (PA6) bearing fluorinated groups were successfully prepared by a one-step anionic ring-opening polymerization of ϵ -caprolactam with its fluorinated derivative sourced from cyclic lysine. A short reaction time with high yield was obtained when 2 wt% of α -perfluorobutyrylamido- ϵ -caprolactam was added to ϵ -caprolactam in bulk at 140 °C. PA6 with higher fluorine content could also be synthesized, however, with lower rate of polymerizations and yields due to the competitive proton abstraction of exocyclic and amide protons of the α -perfluorobutyrylamido- ϵ -caprolactam. The striking point is the increased surface hydrophobicity as well as high thermal stability of these novel PA6 materials. Despite increasing surface hydrophobicity, water uptakes of polyamides bearing pendant fluorinated groups were increased. This can be related to less interaction between the polymer chains due to the pendant units. Besides, bulky fluorinated pendant groups on the polymer

backbone demonstrated higher thermal stability via rotational barriers by thermogravimetric analysis. Slightly increase in glass transition temperatures and loss factors were demonstrated, depending on less mobility of the amorphous phase, by differential scanning calorimetry and dynamic mechanical analysis, respectively.

Experimental and supporting informations

Materials. DL- α -amino- ϵ -caprolactam (BASF) was purified by solubilization in toluene and filtered to eliminate non-soluble impurities. After evaporation of toluene a white product was obtained. Perfluorobutyryl chloride (98%) and triethyl amine (>99.5%) were purchased from Sigma-Aldrich and used without further purification. ϵ -Caprolactam (CL) (BASF, 99 %) was recrystallized from dry cyclohexane prior to use. Brüggolen® C20 (17 % w/w of isocyanate in CL, *N, N'*-hexamethylenebis (2-oxo-1-azepanylcarboxamide) or hexamethylene-1, 6-dicarbamoylcaprolactam in CL, Brüggemann Chemical), Brüggolen® C10 (~18 % w/w of sodium ϵ -caprolactamate in CL, Brüggemann Chemical). Tetrahydrofuran, chloroform and diethylether were purchased from Sigma-Aldrich. 1, 1, 1, 3, 3, 3-Hexafluoro-2-propanol (HFIP) (Acros Organics, ≥ 99.7 %) was used without any further purification.

Measurements. ^1H NMR spectra of reactants were recorded by using a Bruker AC250 instrument at a proton frequency of 250 MHz at room temperature. ^{19}F solid state NMR spectra were recorded on a Bruker 400 Avance I 400 MHz spectrometer at room temperature. During experiments, magic angle spinning (MAS) rate was 30 kHz using a Bruker 2.5 mm HX probe. Number of co-added transients was 256 and recycle delay was 5s. Single-pulse experiment (90 degree pulse of duration) was 1.8 μs , FID acquisition time was 41 ms. Rate of polymerization was followed by temperature vs time monitoring using an ALMEMO2590 AHLBORN thermocouple. The Fourier Transform Infrared (FTIR) spectra were recorded using Nicolet Nexus with an Attenuated Total Reflectance (ATR) accessory by continuum microscope provided with an ATR Germanium (Ge) crystal. Differential scanning calorimetry (DSC) measurements of PA6 samples (~10 mg) were performed on a Perkin-Elmer Diamond DSC with a heating-cooling rate of 10 $^{\circ}\text{C}\cdot\text{min}^{-1}$ under nitrogen flow (10 $\text{mL}\cdot\text{min}^{-1}$) with aluminum pans. Results were obtained from the second run. Thermo gravimetric analysis (TGA) was performed on a Perkin-Elmer Diamond TA/TGA with a heating rate of 10 $^{\circ}\text{C}\cdot\text{min}^{-1}$ under nitrogen flow. Dynamic mechanical thermal measurements were performed in a single-cantilever bending mode on an MKII dynamic mechanical thermal analyzer with a flat sample (prepared by heat pressing) at a heating rate 5 $^{\circ}\text{C}\cdot\text{min}^{-1}$. The operating temperature range was -10 $^{\circ}\text{C}$ to 170 $^{\circ}\text{C}$, and the frequency was 1 Hz. The storage modulus (E'), loss modulus (E''), and loss factor ($\tan \delta$) for each sample were automatically

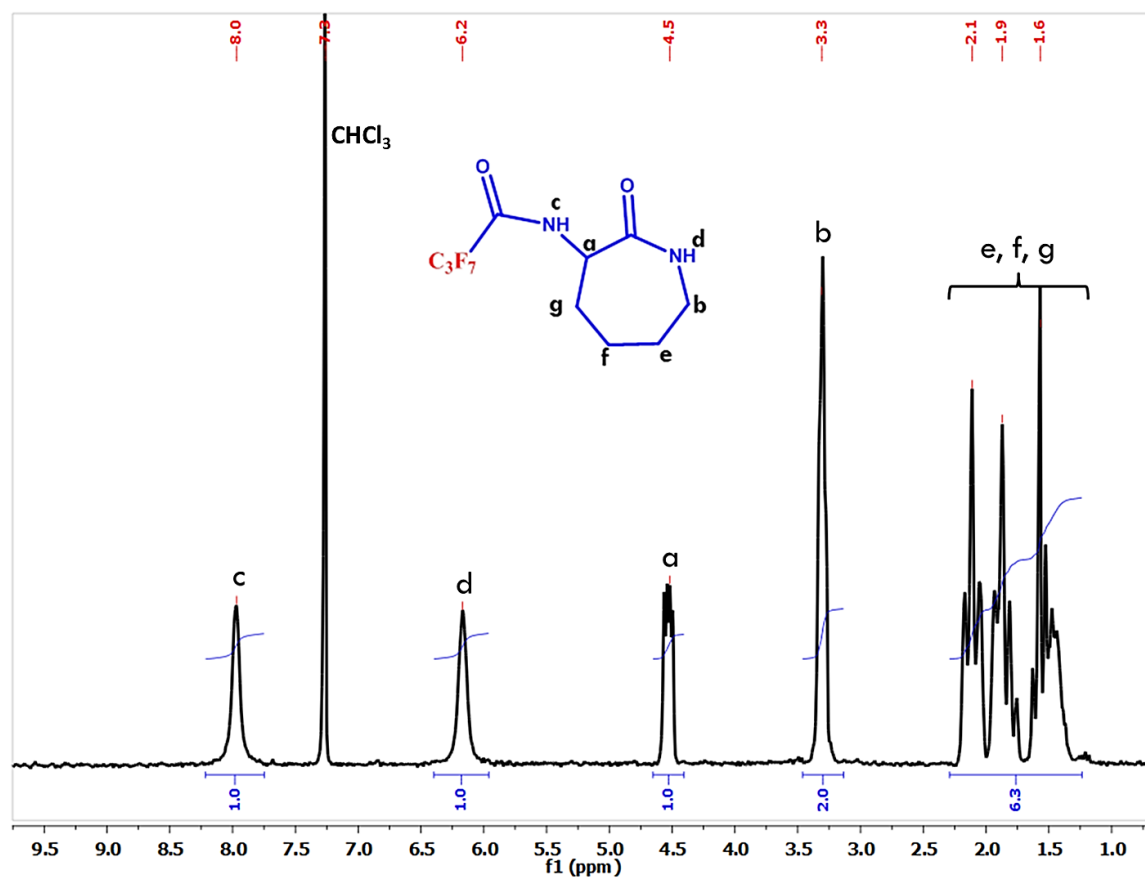
recorded by a computer throughout the test. For surface characterization, thin films of PA6 precursors were spin coated (Specialty Coating Systems, P67080 Spin Coater) on glass plates from 5% solutions in hexafluoroisopropanol at 2000 rpm for 5 min and then dried at 80 °C overnight under vacuum. The water, ethyleneglycol and diiodomethane contact angles were measured using the sessile drop method with a drop volume of 2, 2 and 1.5 μl , respectively, on a contact angle system by Krüss DSA 100 at 25 °C. More than four different positions were measured on a given sample and the average values were plotted. For water uptake measurements, all polymer slides were prepared by heat pressing. Their thicknesses were 0.137, 0.121, 0.153, 0.125 and 0.124 mm for P1-P5, respectively.

Synthesis of α -perfluorobutyrylamido- ϵ -caprolactam (CL_F). To the solution of α -amino- ϵ -caprolactam (1.28 g, 10 mmol) and triethylamine (5.05 g, 50 mmol) in 50 mL of tetrahydrofuran (THF) cooled in an ice bath, perfluorobutyryl chloride (2.32 g, 10 mmol) was added dropwise while purging the reaction flask with argon. After 15 min, the ice bath was removed and the reaction was allowed to proceed overnight at room temperature. The precipitate was removed by filtration, then THF was evaporated and the product was resolved in chloroform and washed with distilled water. The organic phase was separated, dried over anhydrous Na_2SO_4 , filtered, evaporated and recrystallized from diethylether. White solid was obtained (85% yield), m.p. 142 °C. ^1H NMR (CDCl_3) δ (ppm) = 8.0 (s, 1H), 6.2 (s, 1H), 4.5 (dd, 1H), 3.3 (m, 2H), 2.1–1.6 (m, 6H). ^{13}C NMR (CDCl_3) δ (ppm) = 173.8, 52.95, 42.13, 30.40, 28.68, 27.78. IR (cm^{-1}): 3370, 1714, 1678, 1554, 1350, 1250, 1150, 958, 840.

Synthesis of polyamide 6 (P1). Polyamide 6 was prepared in bulk by anionic ring-opening polymerization. ϵ -Caprolactam (8.35 g, 73.8 mmol) and sodium ϵ -caprolactamate (1.15 g, 1.53 mmol) were added in a glass reactor at 140 °C under nitrogen atmosphere (Figure II-S2). After hexamethylene-1,6-dicarbamoylcaprolactam (0.5 g, 0.21 mmol) was added to the molten mixture, the polymerization started. After reaction, the polymer obtained was crushed and refluxed in water and then dried in an oven overnight at 90 °C under vacuum before analysis. Conversion of the monomer was determined gravimetrically. ^1H NMR (HFIP/ CDCl_3) δ (ppm) = 6.0 (s, 1H), 3.1 (m, 2H), 2.0 (m, 2H), 1.25-1.75 (m, 6H). ^{13}C NMR (HFIP/ CDCl_3) δ (ppm) = 176.5, 50.55, 40.25, 36.20, 28.09, 25.81, 24.85.

Synthesis of polyamide 6 bearing fluorine moieties (P4). Polyamide 6 bearing fluorinated moieties were prepared by a one-step pathway by anionic ring opening polymerization. α -perfluorobutyrylamido- ϵ -caprolactam (0.2 g, 0.62 mmol), ϵ -caprolactam (7.0 g, 61.9 mmol) and sodium ϵ -caprolactamate (0.42 g, 3.063 mmol) were added to a glass reactor under nitrogen atmosphere and were molten at 140 °C with continuous stirring. Hexamethylene-1,6-dicarbamoylcaprolactam (0.5 g, 0.21 mmol) was then added to start the polymerization. After reaction, all polymers were crushed and refluxed in water first and then with dichloromethane. The polymers were dried in an oven overnight at 90 °C under vacuum before any analysis. Yields were determined gravimetrically.

Annexe: Supporting Information

Figure II-S1. $^1\text{H-NMR}$ of perfluorobutyramido- ϵ -caprolactam.

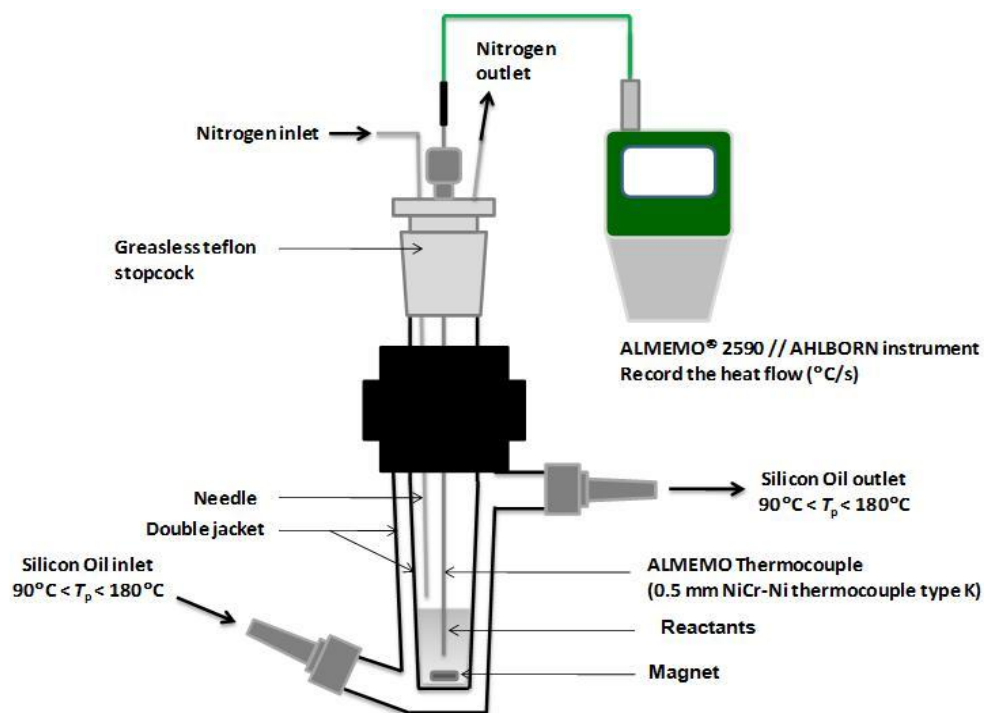


Figure II-S2. Anionic polymerization procedure: Reactor for the calorimetric measurements of monomer consumption during the polymerization.

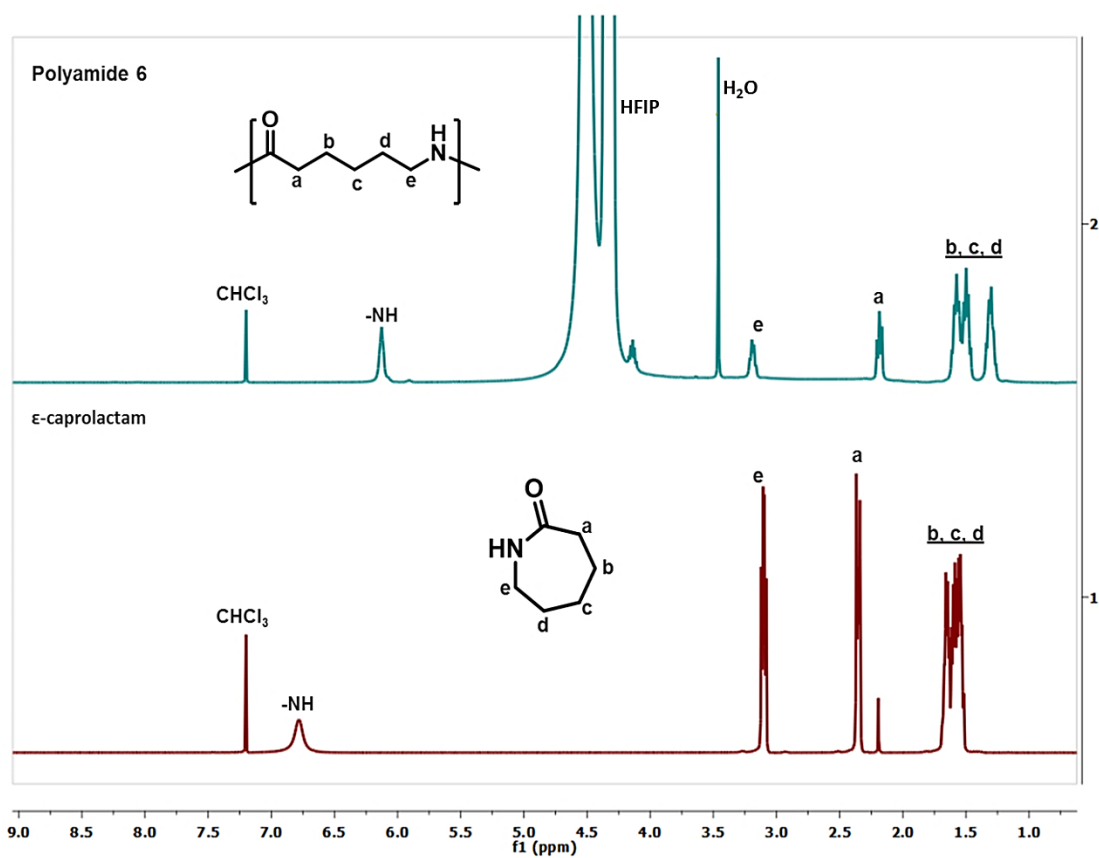


Figure II-S3. ¹H-NMR of polyamide 6 in HFIP-CDCl₃(2) and ε-caprolactam in CDCl₃(1).

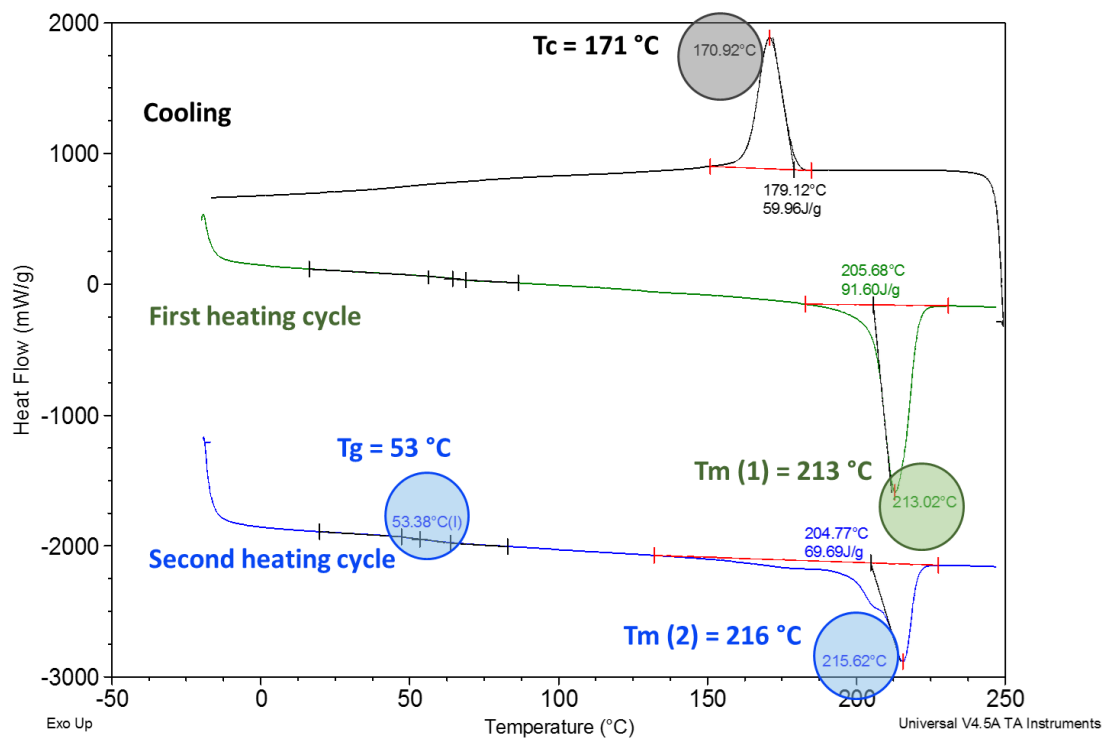


Figure II-S4. DSC curves of P1, PA6: first heating, cooling and second heating.

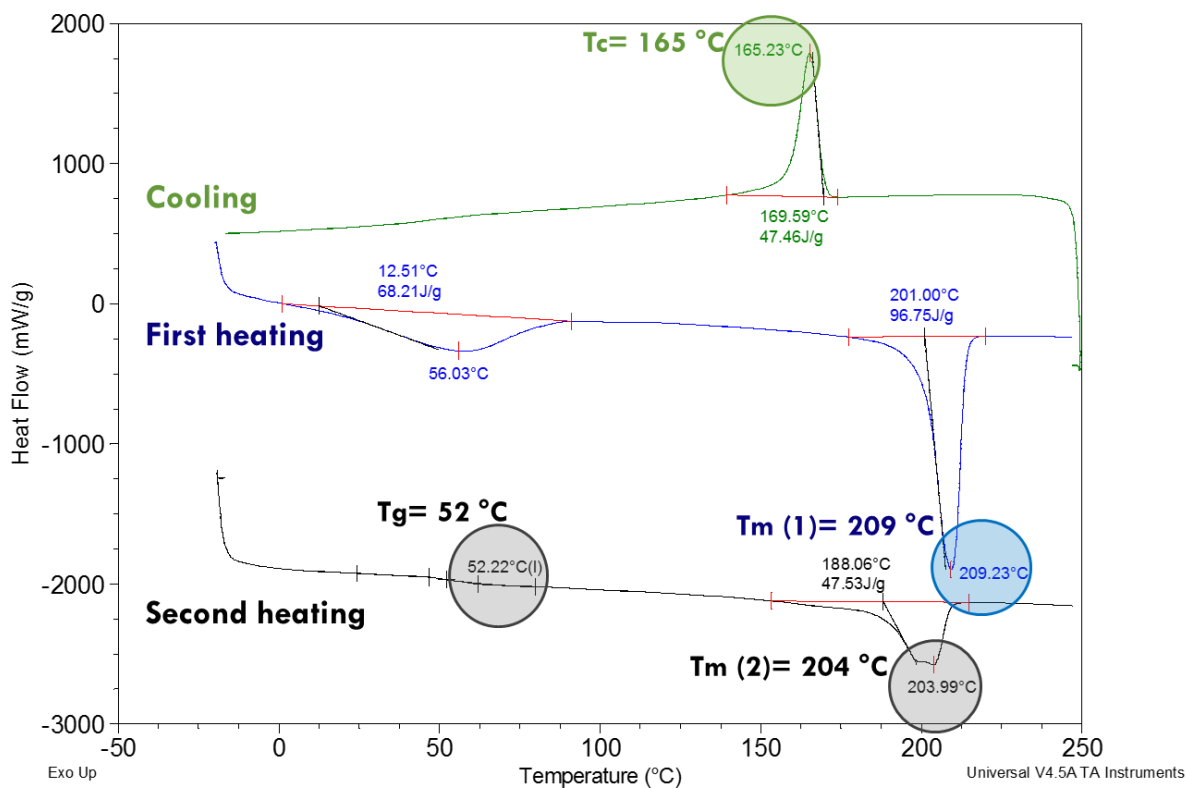


Figure II-S5. DSC thermal curves of P2, 2%F-PA6: first heating, cooling and second heating.

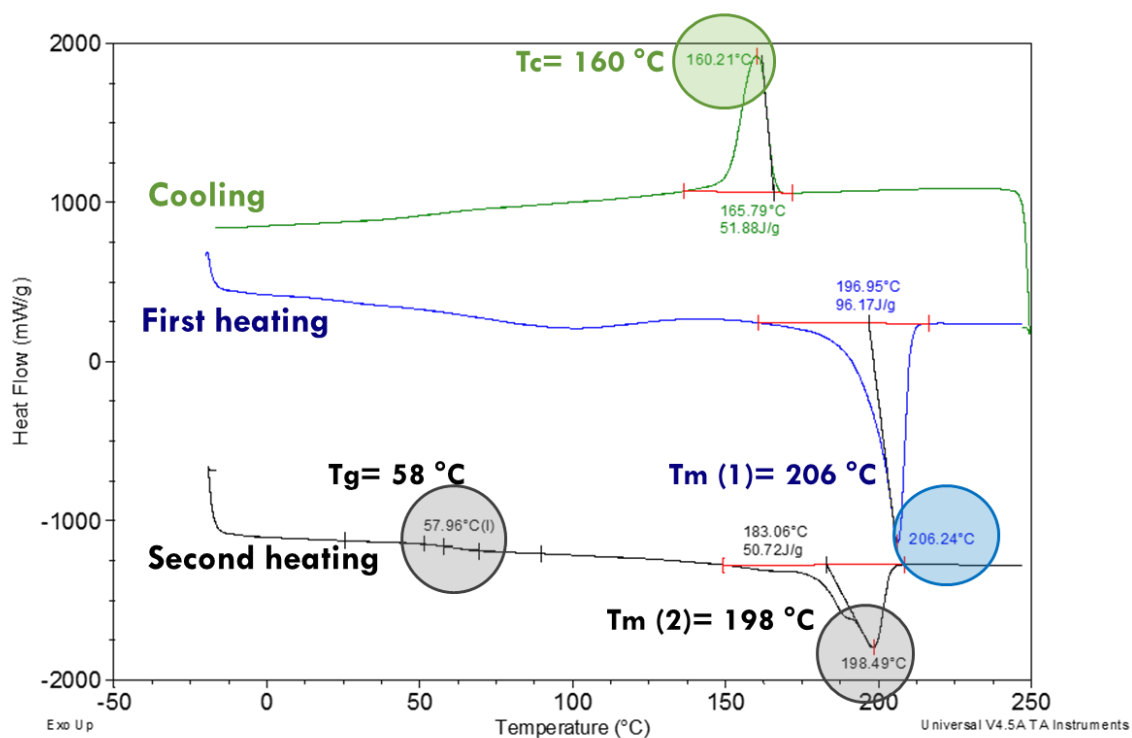


Figure II-S6. DSC thermal curves of P3, 4%F-PA6: first heating, cooling and second heating.

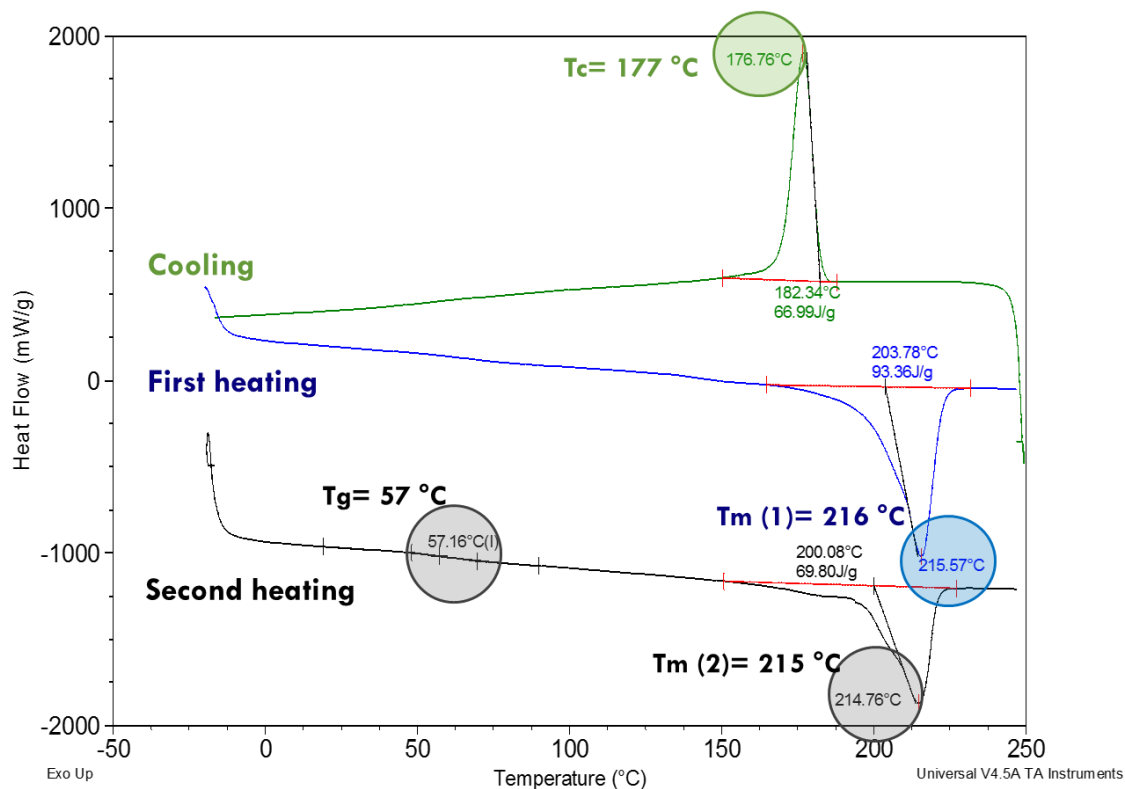


Figure II-S7. DSC thermal curves of P4, 2%F-PA6: first heating, cooling and second heating.

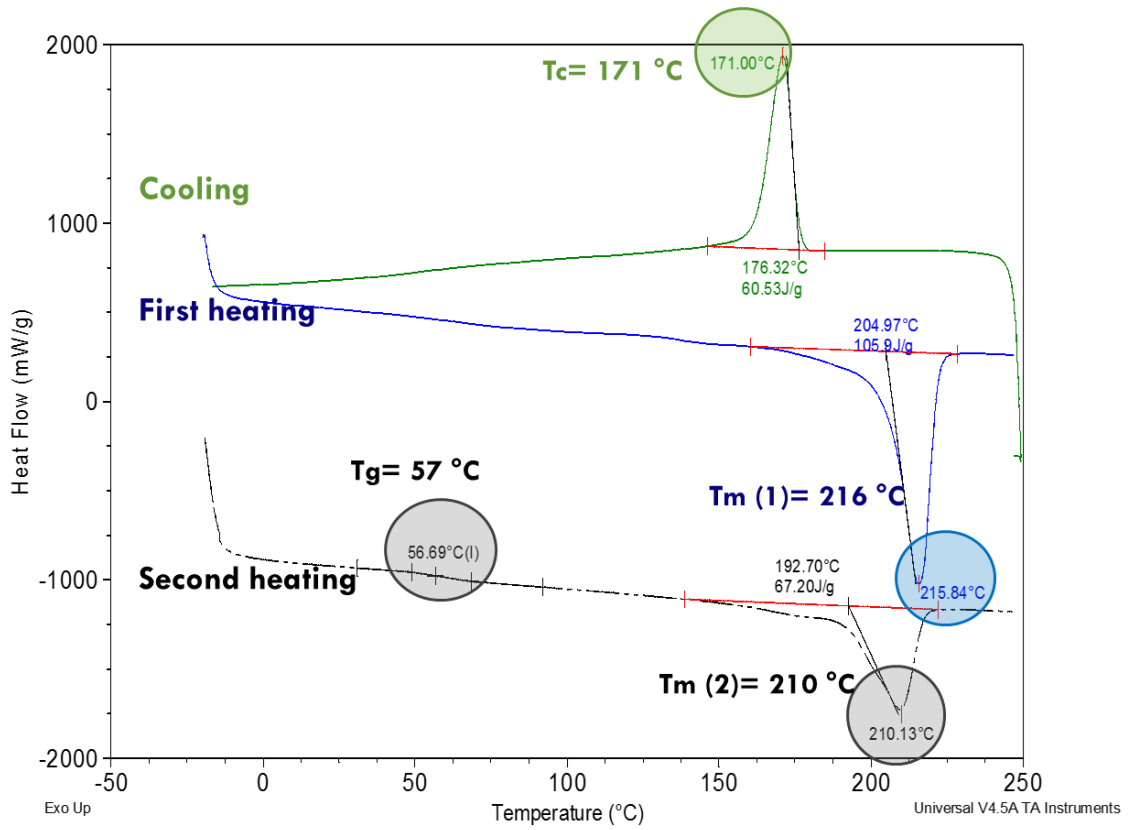


Figure II-S8. DSC thermal curves of P5 4%F-PA6 : first heating, cooling and second heating.

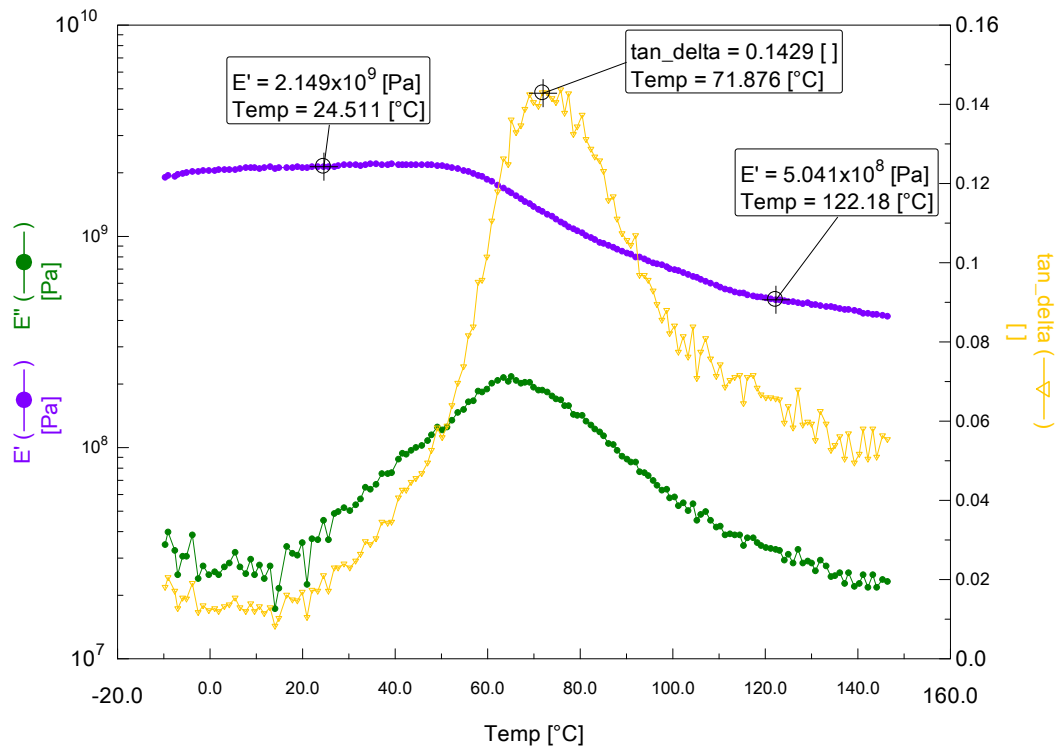


Figure II-S9. DMA analysis of P1, PA6.

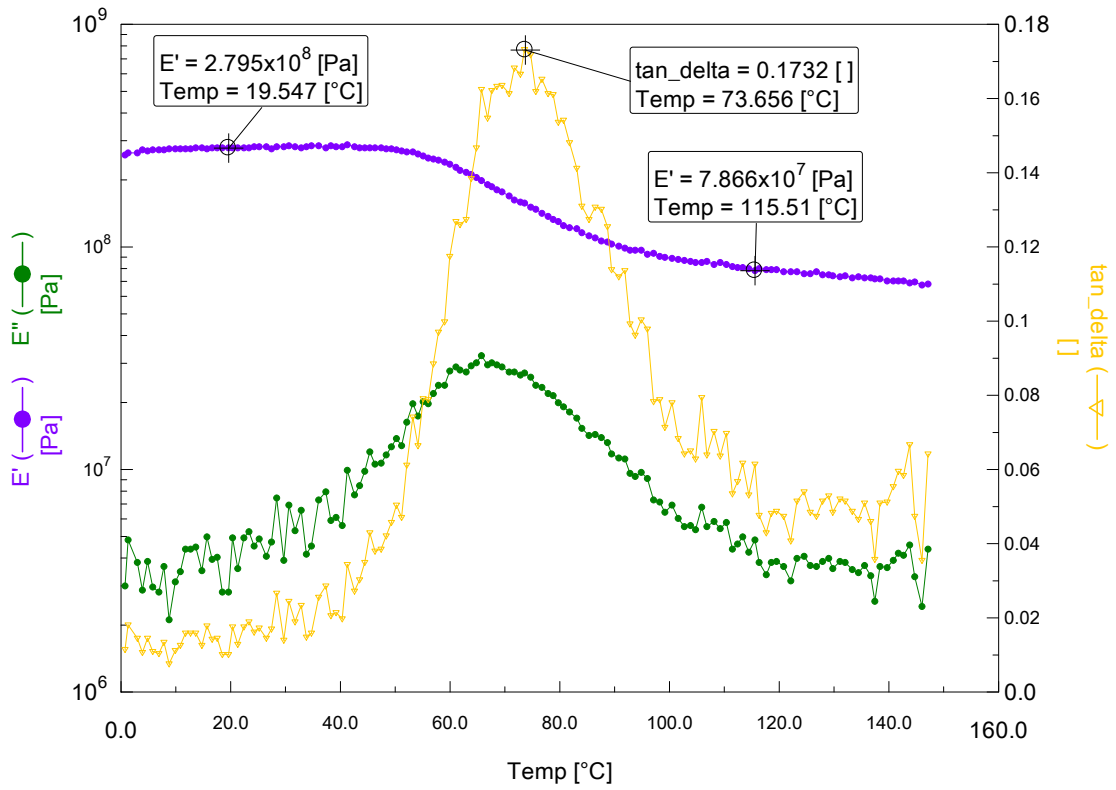


Figure II-S10. DMA analysis of P2, 2%F-PA6.

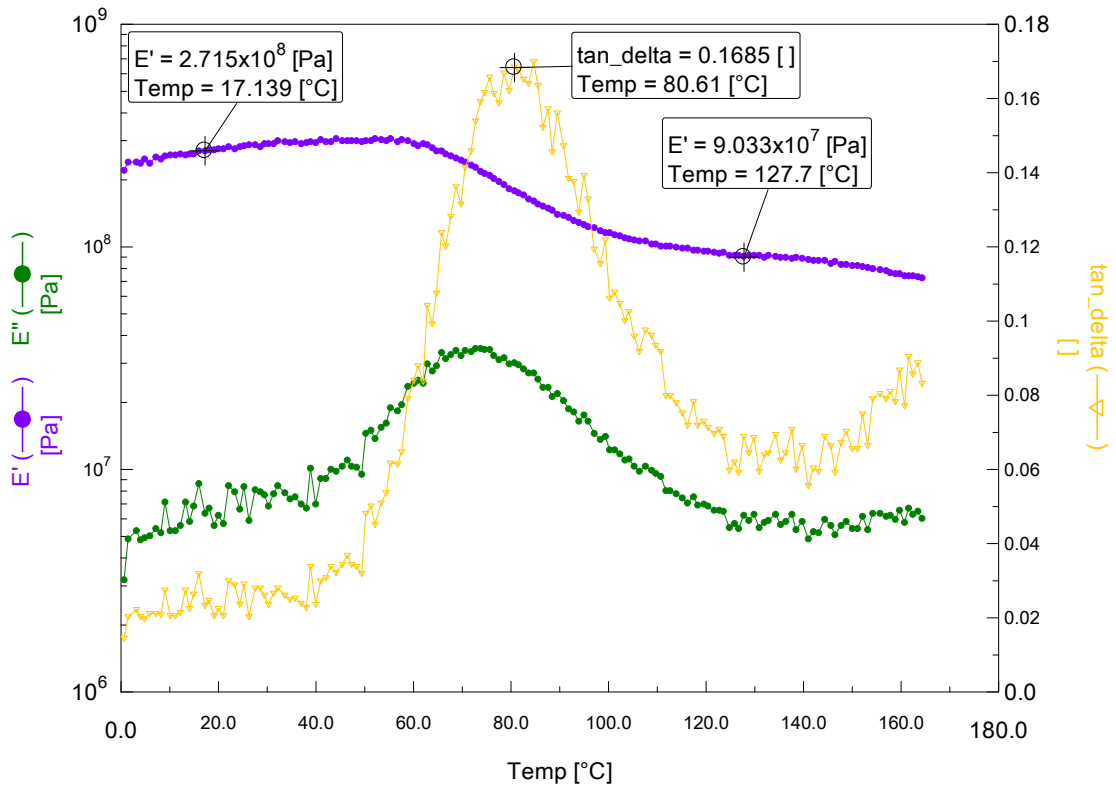


Figure II-S11. DMA analysis of P3, 4%F-PA6.

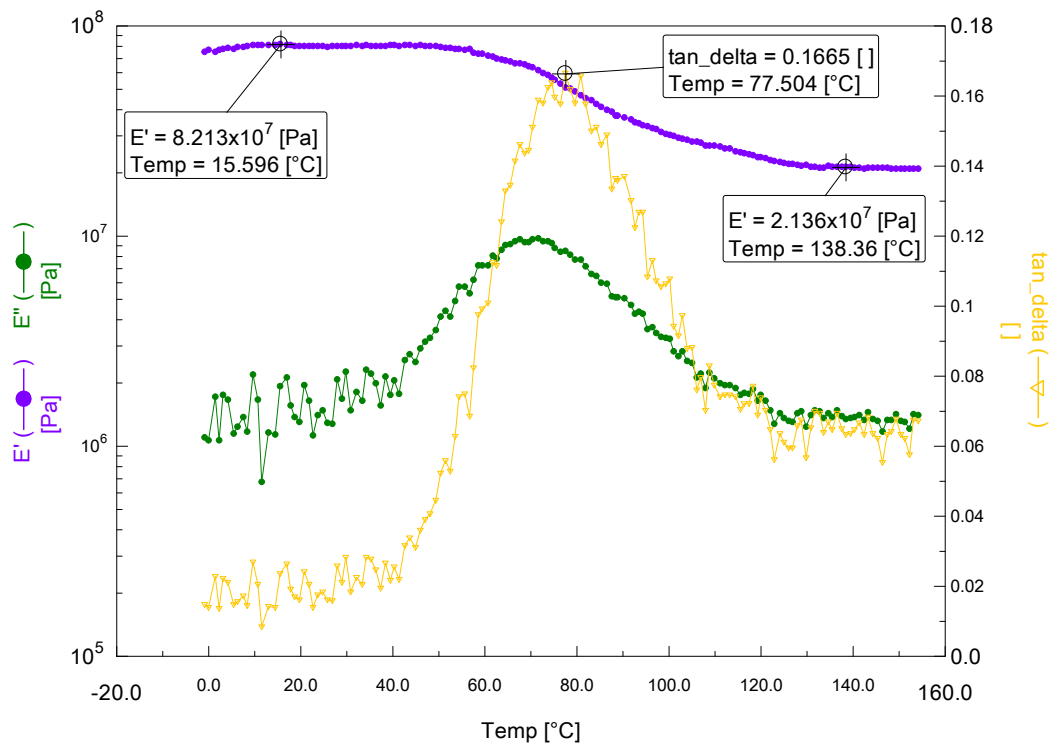


Figure II-S12. DMA analysis of P4, 2%F-PA6.

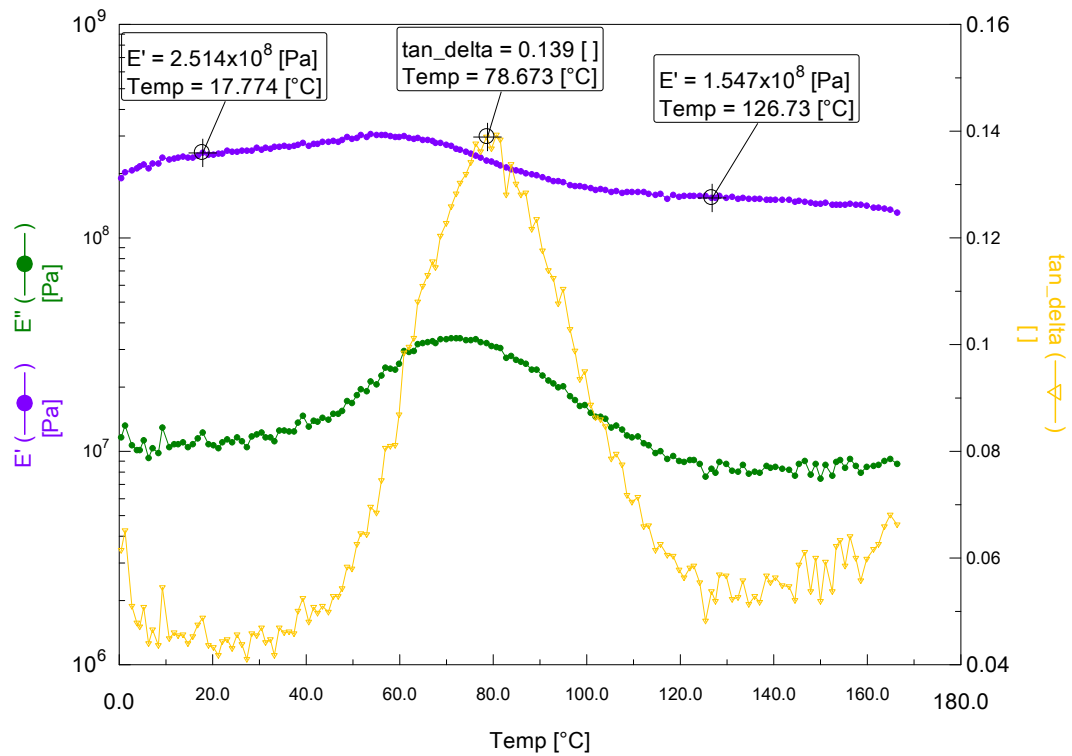


Figure II-S13. DMA analysis of P5, 4%F-PA6.

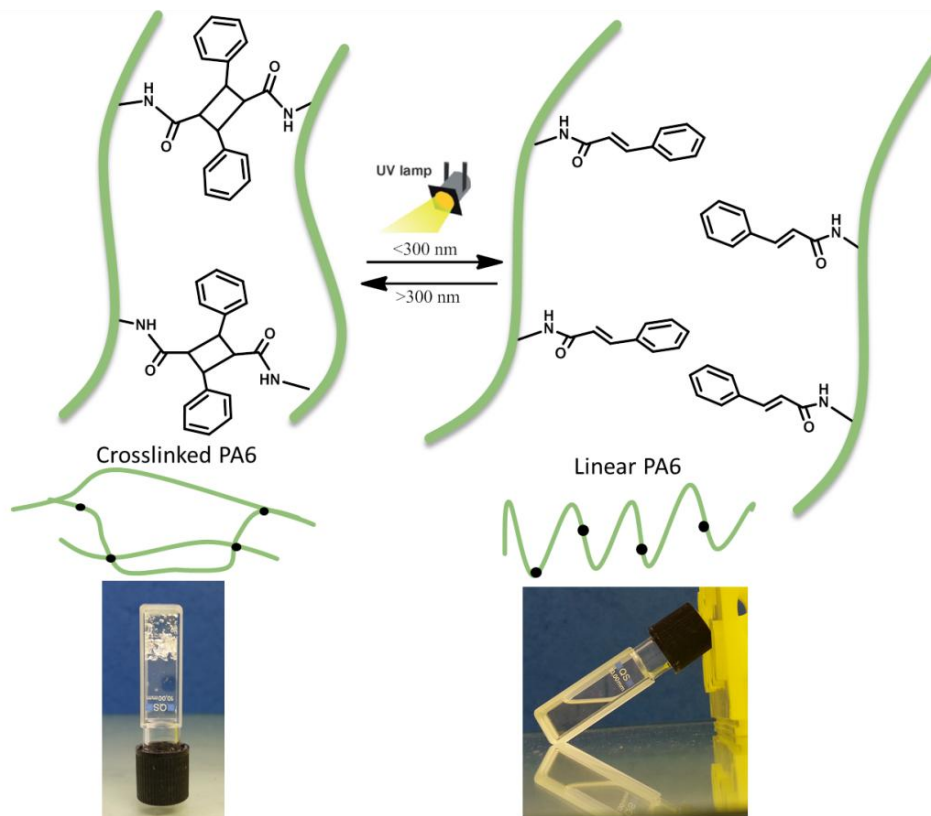
References

1. B. Ameduri, Boutevin, B., *Elsevier Science*, 2004, ISBN: 978-0-08-044388-1.
2. B. Ameduri, *Chemical Reviews*, 2009, **109**, 6632-6686.
3. F. Boschet and B. Ameduri, *Chemical Reviews*, 2014, **114**, 927-980.
4. Y. Y. Durmaz, E. L. Sahkulubey, Y. Yagci, E. Martinelli and G. Galli, *Journal of Polymer Science Part A: Polymer Chemistry*, 2012, **50**, 4911-4919.
5. D. Gan, A. Mueller and K. L. Wooley, *Journal of Polymer Science Part A: Polymer Chemistry*, 2003, **41**, 3531-3540.
6. B. S. Marks and G. C. Schweiker, *Journal of Polymer Science*, 1960, **43**, 229-239.
7. A. E. Mera and J. R. Griffith, *Journal of Fluorine Chemistry*, 1992, **59**, 81-89.
8. T. Kiyotsukuri, N. Tsutsumi, T. Sandan and M. Nagata, *Journal of Polymer Science Part A: Polymer Chemistry*, 1990, **28**, 315-322.
9. Y. Chujo, A. Hiraiwa, H. Kobayashi and Y. Yamashita, *Journal of Polymer Science Part A: Polymer Chemistry*, 1988, **26**, 2991-2996.
10. T. Kiyotsukuri, N. Tsutsumi, K. Okada, K. Asai and M. Nagata, *Journal of Polymer Science Part A: Polymer Chemistry*, 1988, **26**, 2225-2234.
11. X.-L. Liu, D. Wu, R. Sun, L.-M. Yu, J.-W. Jiang and S.-R. Sheng, *Journal of Fluorine Chemistry*, 2013, **154**, 16-22.
12. Y. Oishi, S. Harada, M.-A. Kamimoto and Y. Imai, *Journal of Polymer Science Part A: Polymer Chemistry*, 1989, **27**, 3393-3403.
13. E. Hamciuc, C. Hamciuc, I. Sava and M. Bruma, *European Polymer Journal*, 2001, **37**, 287-293.
14. Z. Ge, S. Yang, Z. Tao, J. Liu and L. Fan, *Polymer*, 2004, **45**, 3627-3635.
15. J. Stehlíček and T. Šebenda, *European Polymer Journal*, 1986, **22**, 5-11.
16. J. Stehlíček and J. Šebenda, *European Polymer Journal*, 1986, **22**, 769-773.
17. K. Hashimoto, *Progress in Polymer Science*, 2000, **25**, 1411-1462.
18. J. W. Frost, *US Patent* 2007, **US2007/014977**.
19. E. Tarkin-Tas, H. Tas and L. J. Mathias, *Macromolecular Symposia*, 2012, **313-314**, 79-89.
20. W. Pfefferle, B. Möckel, B. Bathe and A. Marx, in *Microbial Production of L-Amino Acids*, eds. R. Faurie, J. Thommel, B. Bathe, V. G. Debabov, S. Huebner, M. Ikeda, E. Kimura, A. Marx, B. Möckel, U. Mueller and W. Pfefferle, Springer Berlin Heidelberg, 2003, vol. 79, pp. 59-112.
21. J. Šebenda, in *Comprehensive Polymer Science*, ed. A. L. A. G. Eastmond, S. Russo, P. Sigwalt, Pergamon Press, Oxford, UK, 1989, vol. 3, p. 511.
22. B. Coutin and H. Sekiguchi, *Journal of Polymer Science: Polymer Chemistry Edition*, 1977, **15**, 2539-2541.
23. J. S. J. P Cefelin P., J. Šebenda, *J. Polym. Sci. C*, 1973, **42**, 79.
24. J. S. a. J. S. P. Cefelín, *Collect. Czech. Chem. Commun.*, 1974, **39**, 2212-2220.
25. K. Khodabakhshi, M. Gilbert, P. Dickens and R. Hague, *Advances in Polymer Technology*, 2010, **29**, 226-236.
26. G. C. Alfonso, G. Bonta, S. Russo and A. Traverso, *Die Makromolekulare Chemie*, 1981, **182**, 929-939.
27. P. Petrov, V. Gancheva, T. Philipova, R. Velichkova and R. Mateva, *Journal of Polymer Science Part A: Polymer Chemistry*, 2000, **38**, 4154-4164.

28. R. Mateva and P. Petrov, *European Polymer Journal*, 1999, **35**, 325-333.
29. J.-W. Jiang, X.-L. Pei, S.-R. Sheng, X.-Y. Wu, X.-L. Liu and C.-S. Song, *Polymer Bulletin*, 2011, **67**, 263-274.
30. D.-J. Liaw and F.-C. Chang, *Journal of Polymer Science Part A: Polymer Chemistry*, 2004, **42**, 5766-5774.
31. H. Behniafar and M. Sedaghatdoost, *Journal of Fluorine Chemistry*, 2011, **132**, 276-284.
32. H. Jia, A. Wildes and S. Titmuss, *Macromolecules*, 2011, **45**, 305-312.
33. S. V. Levchik, E. D. Weil and M. Lewin, *Polymer International*, 1999, **48**, 532-557.
34. H. Ohtani, T. Nagaya, Y. Sugimura and S. Tsuge, *Journal of Analytical and Applied Pyrolysis*, 1982, **4**, 117-131.
35. I. Goodman and R. N. Vachon, *European Polymer Journal*, 1984, **20**, 529-537.
36. Y.-L. Zhang, H. Xia, E. Kim and H.-B. Sun, *Soft Matter*, 2012, **8**, 11217-11231.
37. D. K. Owens and R. C. Wendt, *Journal of Applied Polymer Science*, 1969, **13**, 1741-1747.
38. D. H. Kaelble, *The Journal of Adhesion*, 1970, **2**, 66-81.

Chapter III

Synthesis of Reversible and Irreversible Crosslinked Polyamide 6



Reversible crosslinked polyamide 6

Keywords : Anionic ring-opening polymerization, ϵ -caprolactam, α -amino- ϵ -caprolactam, lysine, polyamide 6, crosslinking, crosslinked polyamide 6, photoresponsive groups, cinnamoyl pendant polymers, dimerization, reversible crosslinking.

Summary: In first part of this chapter, we focused on the controlled synthesis of polyamide 6 chemical networks by anionic ring-opening copolymerization of ϵ -caprolactam (CL) with synthesized bis- ϵ -caprolactam derived from α -amino- ϵ -caprolactam via using sodium ϵ -caprolactamate as an initiator and hexamethylene-1,6-dicarbamoylcaprolactam as di-functional activator in bulk at 140 °C. A urea-based bis-monomer and CL were first shown to copolymerize with a decreasing polymerization rate due to side reactions. On the contrary, quantitative copolymerization of CL with various amounts of bis-*N*(2-oxo-3-azepanyl)-1,6-hexamethylenediamide, an amide-based bis-monomer, leads to kinetics as fast as homopolymerization of CL. Crosslinked PA6 with network exhibiting elastic or viscoelastic behaviors, depending on the amount of crosslinker, were observed and characterized by swelling test in hexafluoroisopropanol, dynamic mechanical analysis and rheology measurements. Crystallinity and swelling were shown to decrease with increasing content of crosslinking agent.

On the other hand, photosensitive polymers are used for reversible crosslinking and have gained a strong attention in development of different polymeric systems for diverse applications. A particular attention is paid to polymers with cinnamoyl groups either in the backbone or in the pendent position because of their excellent photoreactivity and their crosslinking upon UV light irradiation or heating. Second part of this chapter aims at synthesizing a novel photo- and thermosensitive polyamide 6 by anionic ring-opening copolymerization of ϵ -caprolactam and α -cinnamoylamido- ϵ -caprolactam. The photochemical reversible crosslinking of solutions and thermal crosslinking of spin-coated films made up of these new cinnamoyl-functionalized polyamides was monitored by UV-visible spectroscopy. These novel aliphatic polyamide copolymers were characterized by magic angle spinning solid-state NMR and their thermal behaviors were studied by thermogravimetric analysis and differential scanning calorimetry. Thermal analysis showed that crosslinking imparts higher thermal stability and glass transition temperature to polyamide.

Chapter III

Synthesis of reversible and irreversible crosslinked polyamide 6

TABLE OF CONTENTS

Introduction	128
1. Synthesis of irreversible crosslinked polyamide 6	129
1.1. Synthesis of polyamide 6	130
1.2. Synthesis of bis-caprolactam from cyclic lysine.....	131
1.3. Synthesis of crosslinked polyamide 6	133
1.4. Characterization of crosslinked polyamide 6	136
2. Toward reversible crosslinked polyamide 6	141
2.1. Synthesis of α -cinnamoylamido- ϵ -caprolactam	143
2.2. Copolymerization and crosslinking	144
2.3. Reversibility: De-crosslinking and re-crosslinking.....	154
Conclusion	157
Experimental and supporting information.....	159
Annexe: Supporting Information	165
References.....	178

Introduction

Polyamides are versatile engineering thermoplastics that cover a wide range of relevant applications in industry. One of the most common polyamides is the poly(ϵ -caprolactam) (PA6) which is also known as Nylon-6, Ultramid®, Ertalon® 6, Nylatron® 6, Akulon® Ultraflow®, and Grilon®. The industrial production of PA6 involves either hydrolytic¹ or anionic²⁻⁴ ring-opening polymerization (AROP) of ϵ -caprolactam (CL). While the hydrolytic polymerization of CL is the most important way for commercial production of PA6, rapid anionic polymerization of molten CL is mainly used to develop Reactive Injection Molding (RIM) processes at relatively low temperature (i.e. at ~130 °C against 250 °C for the hydrolytic/acidolytic polymerization systems) for the fabrication of large and thin PA6 shapes within few minutes^{5,6}.

PA6 synthesized via ring-opening polymerization possess a hard semi-crystalline phase, melting endotherm in the range of 190-238 °C and excellent fatigue life, good abrasion resistance, low to moderate absorption of water (about 10%), excellent bend recovery rate and good resistance to most common solvents and weak acids⁷. High reaction rate combined with a relatively low cost and good mechanical performances makes it an attractive choice for producing structural auto body part such as fenders, doors panel and hoods^{8,9}. It is still desirable, in order to extend the range of applications for PA6 RIM materials, to have polyamides with functional groups in the polymer backbone which can tune the physico-chemical properties. In this regard, secondary reactions¹⁰ involved in non-isothermal anionic bulk polymerization of CL at high temperature ($T_p > 150$ °C) provide, from the formation of β -ketoamides (3-oxoamide^{11, 12} and *N*-acyl-3-oxyamides^{13, 14}) and *N*-alkyl diacylamines² structural units within the polymer backbone, a pathway from subsequent condensation reactions of the 3-oxoamides and its *N*-acylated derivatives can lead to stable uracil¹⁵ and ketone¹⁶ branching sites.

Applicability of PA6's engineered plastics with enhanced physico-chemical properties can be obtained by using functional caprolactams¹⁷⁻²⁴, which are capable to homopolymerize or copolymerize with CL via anionic or hydrolytic routes. Homopolymers of 5-azepane-2-one ethylene ketal (γ -ethylene ketal- ϵ -caprolactam) and its copolymers with ϵ -caprolactam was successfully synthesized by the AROP process using *N*-acetyl-caprolactam and NaH at 140

°C¹⁷. The deacetylation of the poly(γ -ethylene ketal- ϵ -caprolactam) quantitatively releases ketone groups, which can further be reduced yielding poly[imino(4-hydroxyl-1-oxohexane-1,6-diyl)]. Both, the racemic and optically active poly[imino(4-hydroxylmethylene-1-oxohexane-1,6-diyl)] was synthesized by anionic ring-opening polymerization of their corresponding tert-butoxymethylene- ϵ -caprolactam after the tert-butyl protective groups were removed by acidolysis in the presence of traces of HCl¹⁷. These PA6 bearing hydroxyl pendant group could provide a new pathway for further developments. Thin films of PA6 and its copolymers containing higher than 25 mole % of imino(1,4-oxohexane-1,6-diyl) monomer units sensitively responding to thermal (300 °C) or UV (40W/cm² mercury lamp) photo-crosslinking reactions have been reported¹⁷. Here the crosslinking was demonstrated by the insolubility of the resulting materials, usually solubilized in good organic solvents, and the higher glass transition temperatures of the materials with the increasing monomer feed ratio γ -ethylene ketalcaprolactam/ ϵ -caprolactam. Hyperbranched poly(ϵ -caprolactam), which can contain fractions of crosslinked PA6, were prepared by acidolyticring-opening polymerization of γ -aminoethyl- ϵ -caprolactam or γ -carboxyethyl- ϵ -caprolactam¹⁸. A melt shear viscosity of polyamide (i.e. material resistant to shear flow) e.g., poly(ϵ -caprolactam) containing benzy sulfonate alkali salts, was also successfully synthesized by hydrolytic ring-opening polymerization of γ -benzy sulfonate- ϵ -caprolactam¹⁹. The thermal polymerization of the β -carboxymethyl- ϵ -caprolactam gives poly[(2,2-dioxo-1,4-piperidinediyl)trimethylene] with higher crystalline melting endotherm of 280 °C than its counterpart PA6 which can show relevant applications at high temperature and in fire resistance or as reinforcement²⁰⁻²⁴.

Drawbacks of these all systems are multi-synthesis steps of monomer or/ and polymer with extended reaction times and often ending up with low yields.

In this chapter work, we have studied non-reversible and reversible crosslinked polyamide 6. First part is dedicated to non-reversible crosslinked polyamide 6 and second part highlights reversible crosslinked polyamide 6.

1. Synthesis of irreversible crosslinked polyamide 6

The controlled synthesis of PA6 chemical networks by anionic ring-opening copolymerization of CL with bis- ϵ -caprolactam, i.e. N -functionalized α -amino- ϵ -

caprolactambis-monomers), using sodium ϵ -caprolactamate (C10) as an initiator and hexamethylene-1,6-dicarbamoylcaprolactam (C20) as a di-functional fast activator was carried out in bulk at 140 °C.

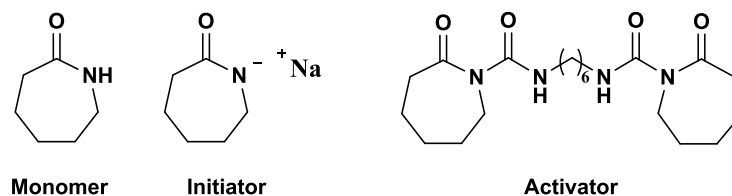
Crosslinked PA6 with network exhibiting elastic or viscoelastic behaviors, depending on the amount of crosslinker, were observed and characterized by swelling in hexafluoroisopropanol, dynamic mechanical analysis and rheology measurements. Crystallinity and swelling were shown to decrease with increasing the content of crosslinking agent (eq 1). In first part of this chapter, the production of controlled PA6 chemical networks by anionic bulk copolymerization of CL and *N*-functionalized α -amino- ϵ -caprolactambis-monomers at low feed ratio, i.e. up to 2.8 mol%, is discussed in terms of rate of polymerization, thermal and rheological properties for an eventual processability at moderate temperature.

$$Q_{\text{HFIP}} = \frac{V_f}{V_i} = 1 + \left(\frac{m_f}{m_i} - 1 \right) (\rho_{\text{PA6}} / \rho_{\text{HFIP}}) \quad \text{eq(1)}$$

1.1. Synthesis of polyamide 6

One important criterion in polyamide 6 (PA6) molding process is the eject (cycle) time. The molding temperature of the PA6 (i.e. 90 < T < 200 °C) is below the melting point of the PA6 (T_m = 200-220 °C). Thus, unlike the polyurethanes and epoxy materials, the maximum temperature increasing of PA6 ($\Delta H_p = 13.4 \text{ kJ.mol}^{-1}$)^{25, 26} within the mold is not critical as far as thermal degradation is not reached and formation of irregular structures within polymer backbone is expected. The maximum temperature affects mainly the crystallization rate which is a major factor in determining the optimum processing conditions, *i.e.* the required eject time.

The initial used polymerization system in a glass reactor contains ϵ -caprolactam (CL), sodium caprolactamate (C10) and difunctional hexamethylene-1,6-dicarbamoylcaprolactam (C20) as monomer, initiator and activator, respectively (Scheme III-1).

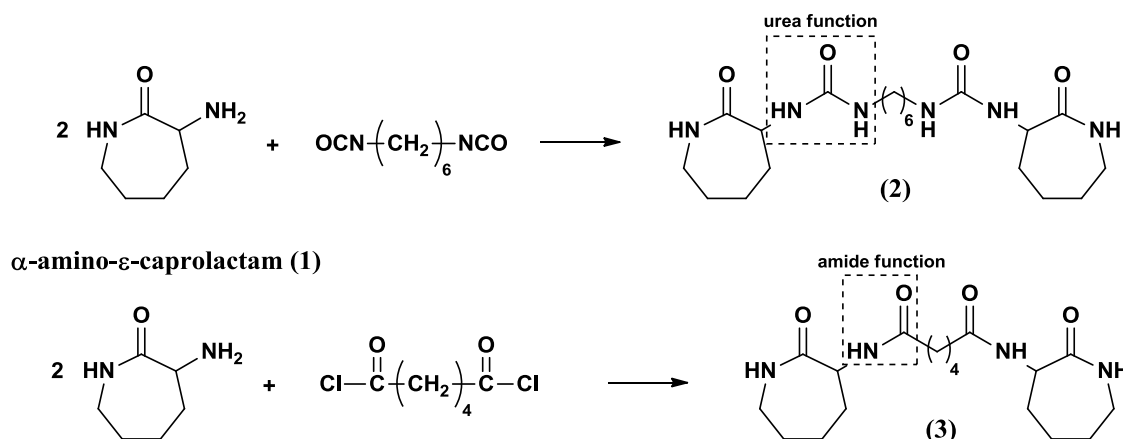


Scheme III-1. Monomer (ϵ -caprolactam), initiator (*i.e.* sodium caprolactamate), activator (*i.e.* hexamethylene-1,6-dicarbamoylcaprolactam).

Although the polymerization medium became very viscous within a few seconds, complete conversion was obtained in the range $120 \leq T \leq 180$ °C (targeted $\overline{DP}_n = ([CL]_0 + [(3)]_0) / [C20]_0 = 74$). Below 130 °C, the polymerization is slow with a premature crystallization. Above 130 °C, the exothermal temperature peak is a major factor for increasing crystallization time and thus the eject time if applied to the molding process.

1.2. Synthesis of bis-caprolactam from cyclic lysine

Copolymerization experiments of CL with the synthesized crosslinking agents from α -amino- ϵ -caprolactam (**1**), the *N*-functionalized α -amino- ϵ -caprolactam bis-monomers, 1,1'-hexamethylenebis(2-oxo-3-azepanylurea) (**2**) or bis-*N*(2-oxo-3-azepanyl)-1,6-tetramethylenediamide (**3**) (Scheme III-2) were carried out at 140 °C. Their synthesis was monitored by ^1H NMR in d_6 -DMSO.



Scheme III-2. Synthesis of *N*-functionalized α -amino- ϵ -caprolactam bis-monomers (1,1'-hexamethylenebis(2-oxo-3-azepanylurea) (**2**) or bis-*N*(2-oxo-3-azepanyl)-1,6-tetramethylenediamide) (**3**) used as co-monomers for ϵ -caprolactam polymerization.

Characteristic signals of urea functions in compound (**2**), obtained after reaction of the primary amine of α -amino- ϵ -caprolactam with an isocyanate function, are located at 6.15 and 6.35 ppm (Figure III-1). The protons of newly formed amide functions of (**3**), by reaction between α -amino- ϵ -caprolactam with a diacyl chloride, are visible in the spectrum at 7.78 ppm (Figure III-2). The obtained products, yields higher than 90%, were also identified by ^{13}C NMR (See, Figure III-S1 and Figure III-S2).

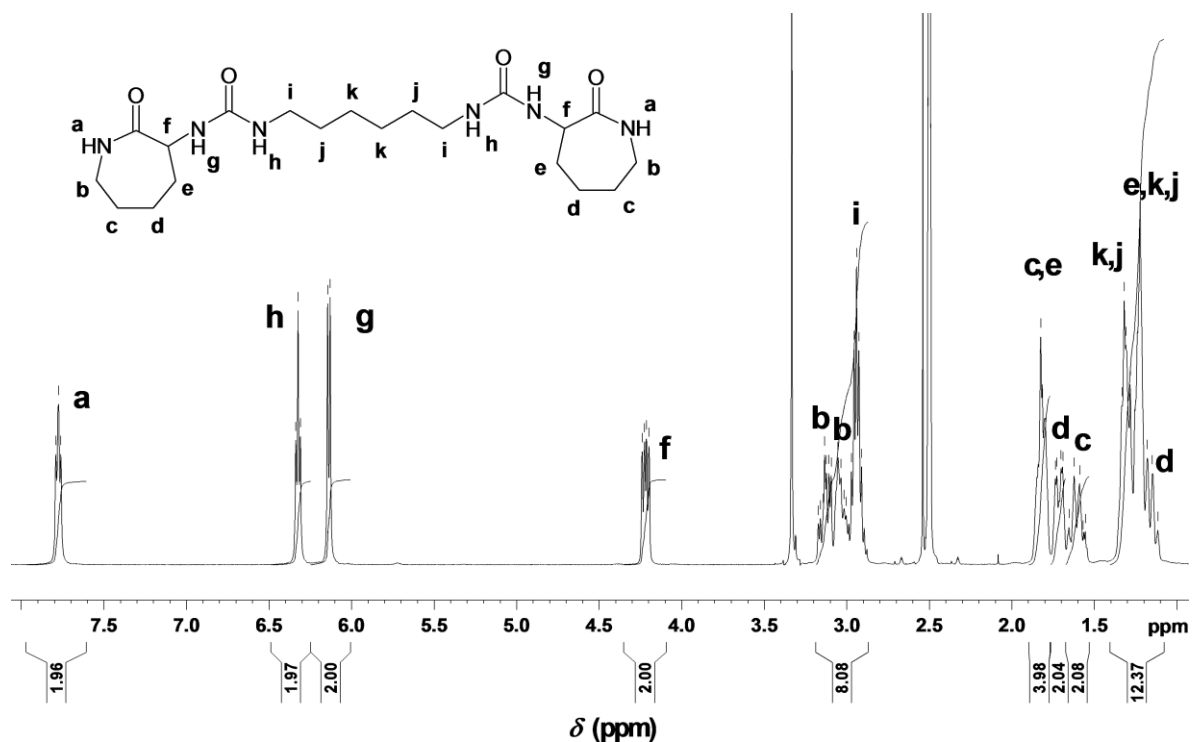


Figure III-1. ^1H NMR spectrum of 1,1'-hexamethylenebis(2-oxo-3-azepanylurea) (**2**) in $\text{d}_6\text{-DMSO}$.

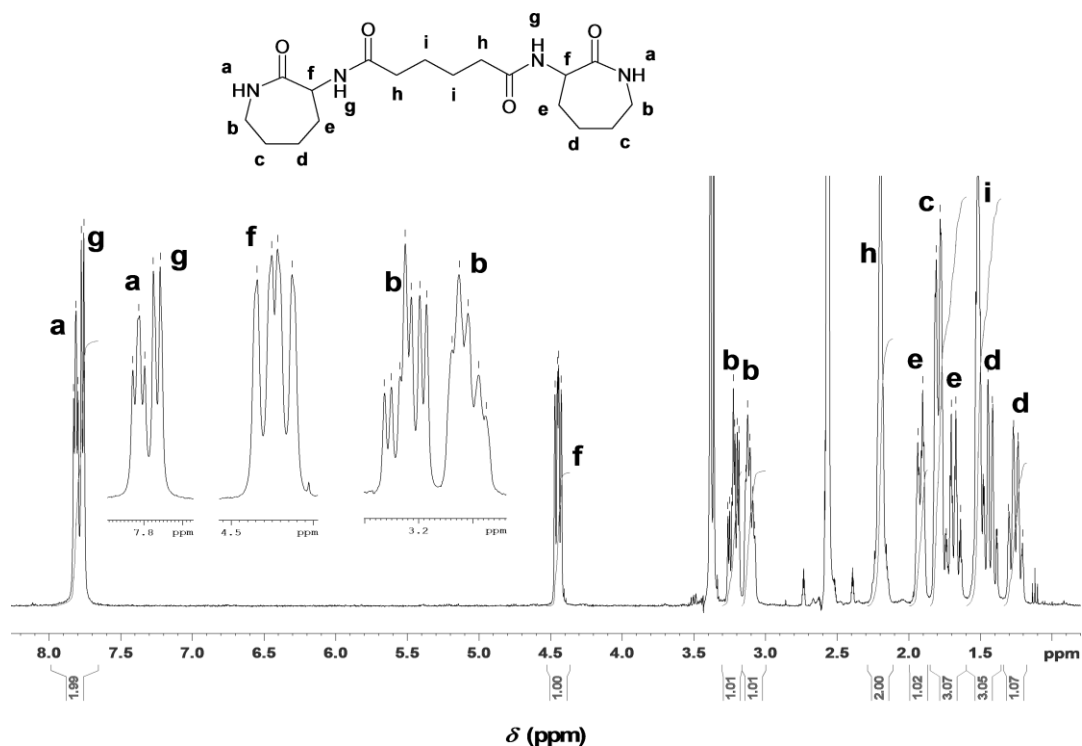


Figure III-2. ^1H NMR spectrum of bis-*N*(2-oxo-3-azepanyl)-1,6-tetramethylenediamide (**3**) in $\text{d}_6\text{-DMSO}$.

1.3. Synthesis of crosslinked polyamide 6

All copolymerization experiments carried out between CL and the co-monomers (**2**) and (**3**) yields are higher than 90% and mostly near 98-99% under standard conditions, the amount of initiator, i.e. sodium ϵ -caprolactamate, being a key parameter for getting a high value (Table III-1). Polymerization time is shown to be increased by the presence of the co-monomer (**2**) which possesses urea functions. The higher amount of sodium ϵ -caprolactamate enables an increase of the polymerization rate.

Table III-1. Anionic bulk copolymerization of ϵ -caprolactam with various crosslinking agents initiated by sodium ϵ -caprolactamate (C10) and activated by hexamethylene-1,6-dicarbamoylcaprolactam (C20) ($T_p = 140$ °C).

Sample	ϵ -caprolactam (mmol)	Crosslinker (mmol)	Activator (mmol)	Initiator (mmol)	t_p (ΔT_p) ^a s (°C)	t_c (ΔT_c) ^b s (°C)	Yield ^c %
PA6 0.1	56.5	-	0.85	1.18	51 (39)	206 (32)	99
PA6 2.1	55.5	2 (0.42)	0.85	1.18	105 (33)	229 (31)	97
PA6 2.2	55.5	2 (0.42)	0.85	2.04	85 (35)	216 (28)	99
PA6 3.1	55.0	3 (0.42)	0.85	1.18	47 (38)	181 (28)	99
PA6 3.3	54.3	3 (1.23)	0.85	1.18	58 (31)	225 (27)	99

^a The maximum exotherm (ΔT_p) during the polymerization and its relative time (t_p),

^b The maximum crystallization exotherm (ΔT_c) and its relative time t_c ,

^c Evaluation by gravimetric measurement.

Indeed, increasing the amount of crosslinker(**2**) without increasing the initiator one leads to copolymerization associated to a continuous decrease of the maximum exotherm (Figure III-3a). One can note the presence of two exotherms, the first one corresponding to the polymerization and the second one to the crystallization process. At a molar ratio (**2**)/C20/C10 equal to 0.753/1/1.4 (run PA6 2.5), the polymerization is much slower as shown by a longer polymerization time and a low maximum exotherm with $\Delta T_p = 10$ °C as compare to $\Delta T_p = 39$ °C for the reference (PA6 0.1). Increasing the amount of initiator (i.e. activated monomer) enables faster copolymerizations and crystallization, allowing an increase of the crosslinker amount (Figure III-3b).

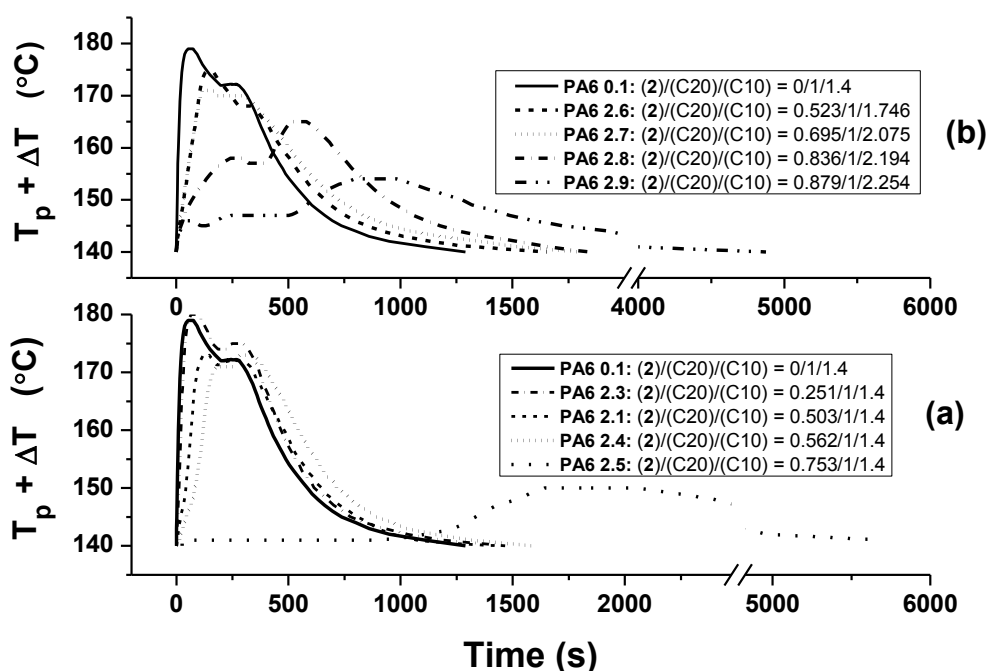


Figure III-3. Temperature change with time dependence ($T_p = 140\text{ }^\circ\text{C}$) for the polymerization of ϵ -caprolactam (PA6 0.1) and copolymerization of ϵ -caprolactam with 0.212 (PA6 2.3), 0.42 (PA6 2.1), 0.44 (PA6 2.6), 0.48 (PA6 2.4), 0.59 (PA6 2.6), 0.64 (PA6 2.5), 0.71 (PA6 2.8) and 0.74 (PA6 2.9) mmol of (2).

As shown in the literature, urea derivatives can be hydrolyzed at low or high pH yielding an isocyanate via an intermediate zwitterion²⁷. Urea functions present in co-monomer (2) are expected to react with sodium ϵ -caprolactamate. Using an urea-based model reactant free of lactam, e.g. 0.186 g (1.185/2 mmol) or 0.372 g (1.185 mmol) of 1,1'-hexamethylenebis(3-tert-butylurea) (Figure III-S3), the homopolymerization of CL (C20/(C10) = 0.845mmol/1.185 mmol) was totally inhibited. With increased C10 amount, e.g. 0.89 g (1.185 mmol) or 1.78 g (2.370 mmol), the polymerization of CL starts at once with polymerization rate almost identical than the one obtained without this model additive. The differences in polymerization activity between CL and CL/(2) system were overcome by using an excess of 2 n/n C10/(2). All materials prepared in presence of (2) or (3) were shown to crosslink as they are not anymore soluble and can swell in hexafluoroisopropanol (HFIP).

1.4. Characterization of crosslinked polyamide 6

Copolymerization between CL and various amounts of bis-monomer with amide function (**3**), free of urea functions, leads to fast kinetics similar to the homopolymerization reference (Figure III-4). It was possible to increase the amount of amide-based bis-monomer without increasing the C10 content. The increase of the feed molar ratio (**3**)/CL gradually decreases the crystallization exotherm (ΔT_c), with an expected increase of the crosslinking density.

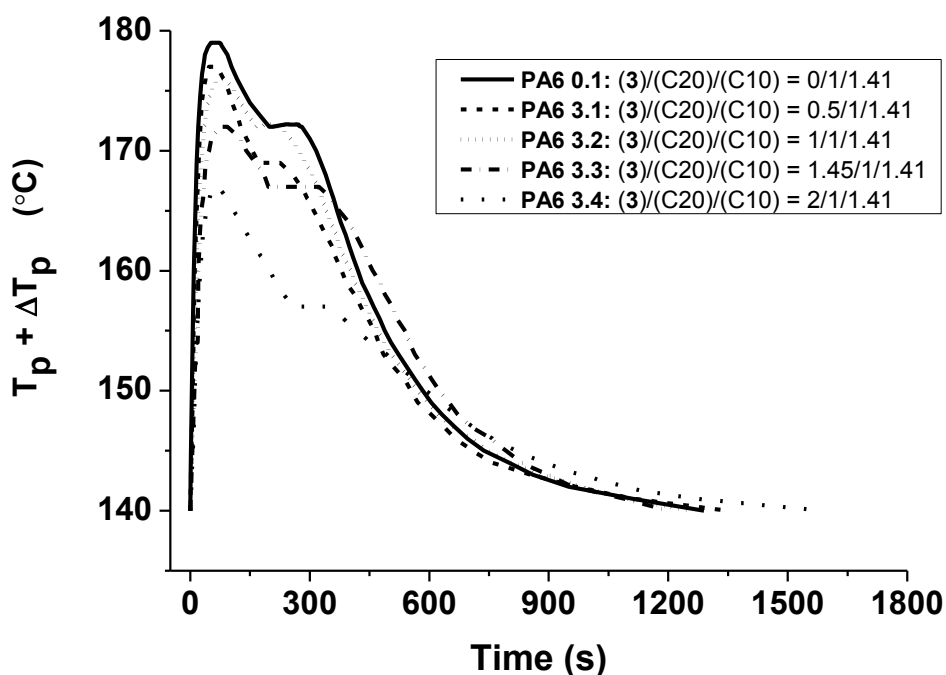


Figure III-4. Temperature change ($T_p + \Delta T$) with time dependences ($T_p = 140$ °C) for the polymerization of ϵ -caprolactam (PA6 0.1) and copolymerization of ϵ -caprolactam with 0.42 (PA6 3.1), 0.85 (PA6 3.2), 1.23 (PA6 3.3), and 1.7 (PA6 3.4) mmol of (**3**).

The collapsed and HFIP swollen forms of the crosslinked PA6 (sample 3.4) are shown in Figure III-5. Looking into more details by following DSC measurements (Figure III-S4-9), the increase of the amount of bis-monomer (**3**), from 0.90 mol% to 2.83 mol% ($F_{(3)}$ values, Table III-2), show a gradual decrease of the melting temperature down to 194 °C accompanied to a decrease of the crystallinity degree down to 12%. These values can also be compared to 216 °C and 37% respectively for the linear and reference PA6 0.1. In addition, the degree of swelling in HFIP (QHFIP) (eq 1) decreases from 53 to 27 which is in agreement with an

increase of the crosslinking density. These trends were also observed at higher polymerization degrees (PA6 3.8, PA6 3.9 and PA6 3.10 samples, Table III-2).

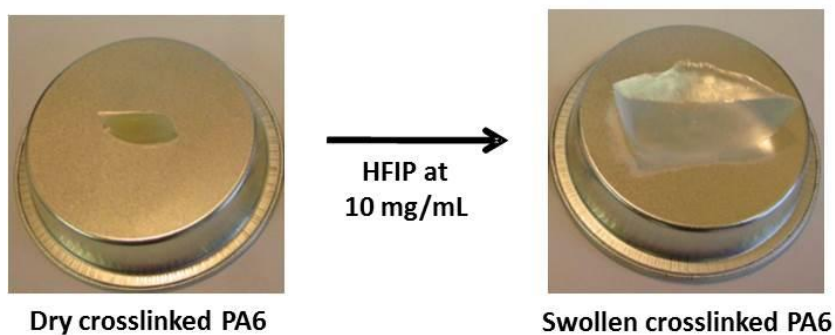


Figure III-5. Swelling test in hexafluoroisopropanol (HFIP) on sample PA6 3.4 at 25 °C obtained by the anionic bulk copolymerization of ϵ -caprolactam with the amide-based bis-monomer (**3**) at 140 °C.

Table III-2. Anionic bulk copolymerization of ϵ -caprolactam with various amount of amide-based crosslinking agent (**3**) ($n_{C10}=1.18$ mmol, $T_p = 140$ °C).

Sample	(3)/ C20 ^a	C20 mmol	([CL] ₀ +[(3)] ₀) /[C20] ₀	F _(3) (W _(3)) ^b mol% (wt%)	T _m (ΔH_m) ^c °C (J.g ⁻¹)	X ^d %	(G') _{$\omega=0.1$rad/s} (Pa)	Q _{HFIP} ^e
PA6 0.1	0	0.85	74	0(0)	216(70.8)	37	>10	N.A.
PA6 3.7	0.67	0.85	74	0.90(2.7)	209(60.7)	32	18 700	53
PA6 3.6	0.84	0.85	74	1.13(3.3)	198(45.4)	24	21 600	48
PA6 3.2	1	0.85	74	1.37(4.0)	195(37.9)	20	23 400	43
PA6 3.5	1.34	0.85	74	1.84(5.3)	194(32.0)	17	237 000	35
PA6 3.3	1.45	0.85	74	2.09(6.0)	195(30.1)	16	238 000	32
PA6 3.4	2	0.85	74	2.83(8.0)	194(22.2)	12	240 000	27
PA6 3.8	2.57	0.43	142	1.80(5.3)	198(39.2)	21	170 000	36
PA6 3.9	2.24	0.25	259	0.86(2.7)	203(44.9)	24	210 000	45
PA6 3.10	2	0.10	552	0.32(1.0)	213(56.0)	27	21 670	59

^a Molar ratio,^b F_(**3**) and W_(**3**) = [3]/([3]+[CL]) in mole and weight percent respectively,^c From the second heating scan of DSC, heat flowing rate 10 °C.min⁻¹,^d Crystallinity % ; $\Delta H^0=190$ J.g⁻¹,^e Degree of swelling in hexafluoroisopropanol (HFIP), eq (1).

The dynamic mechanical analysis results on PA6 3.5 sample showed a solid-like storage modulus (E') of 0.8 GPa for temperature below -50 °C and, for temperatures higher than T_m (200-220 °C), a persistent rubbery plateau of E' = 105 Pa (Figure III-6), close to the value measured by rheometry.

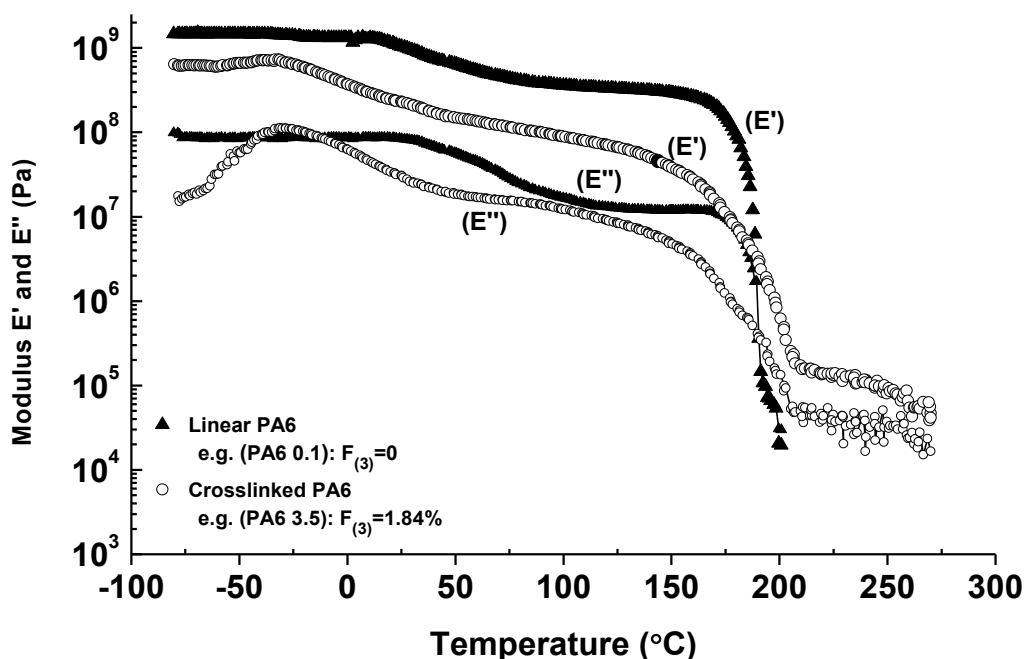


Figure III-6. Temperature dependences of storage E' and loss E'' moduli of PA6 synthesized by bulk anionic polymerization of ϵ -caprolactam (PA6 0.1) and copolymerization of ϵ -caprolactam with 1.84 mol% of amide-based bis-monomer (**3**) (PA6 3.5).

Indeed, under standard conditions ($([CL]_0 + [3]_0) / [C20]_0 = 74$), the melt rheology experiments at 250 °C showed that PA6 containing (**3**) at $F_{(3)} \geq 1.84$ and $(3)/\text{Activator (C20)} \geq 1.34$ can behave as a chemical network with a rubbery plateau unchanged at all angular frequencies screened (i.e. from 0.04 to 400 rad.s⁻¹) (Figure III-7). $G' > G''$ and G' values at $\omega = 0.1$ rad/s around 240 000 Pa indicate an elastic regime which agree with a PA6 chemical network (Table III-2, Figure III-8). At low crosslinker (**3**) feed ratio ($0.30 < F_{(3)} < 1.84$), a wide range of rheological properties in the viscoelastic regime is observed and expressed by storage modulus showing both minimum (i.e. onset of a melt shear viscosity behavior) and maximum around 25 000 Pa (Figure III-8). Below $F_{(3)} < 0.30$, a flow-like regime ($G'/G'' < 1$) is observed and confirmed by the solubilization of polymers in HFIP at 20°C. By carrying out the copolymerization experiments at $(3)/\text{Activator} \geq 2.24$, an elastic regime can be obtained at lower crosslinker feed ratio as long as $F_{(3)} \geq 0.86$ (runs 3.8, 3.9 and 3.10).

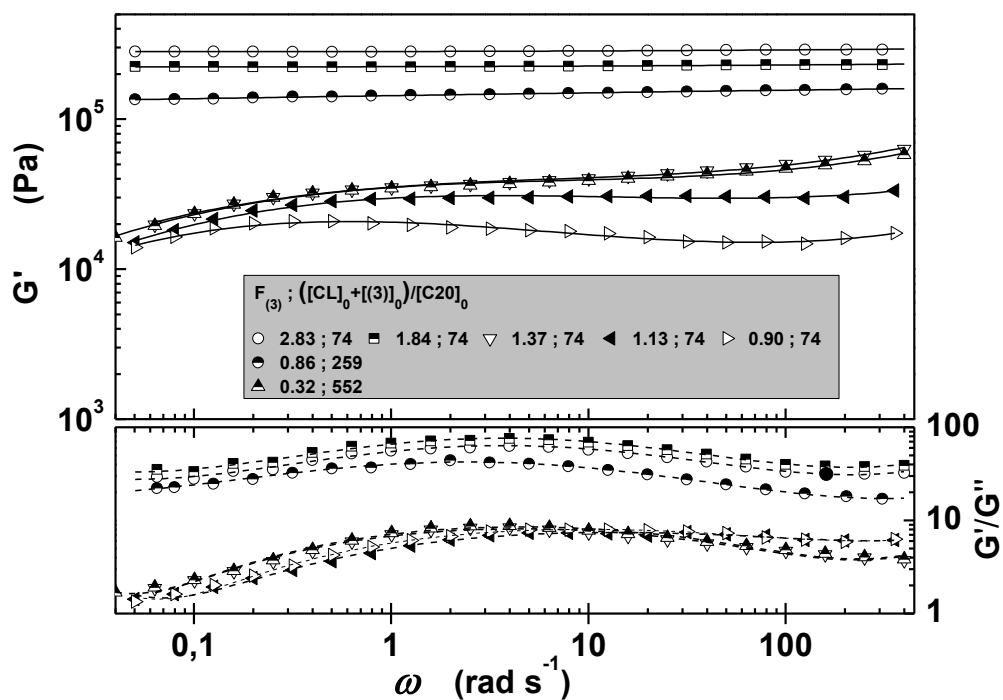


Figure III-7. Angular frequency dependences of the storage modulus G' and G'/G'' at 250 °C of PA6 synthesized by bulk anionic copolymerization of ϵ -caprolactam with various amount of amide-based bis-monomer (**3**) ($F_{(3)}$ in mol%).

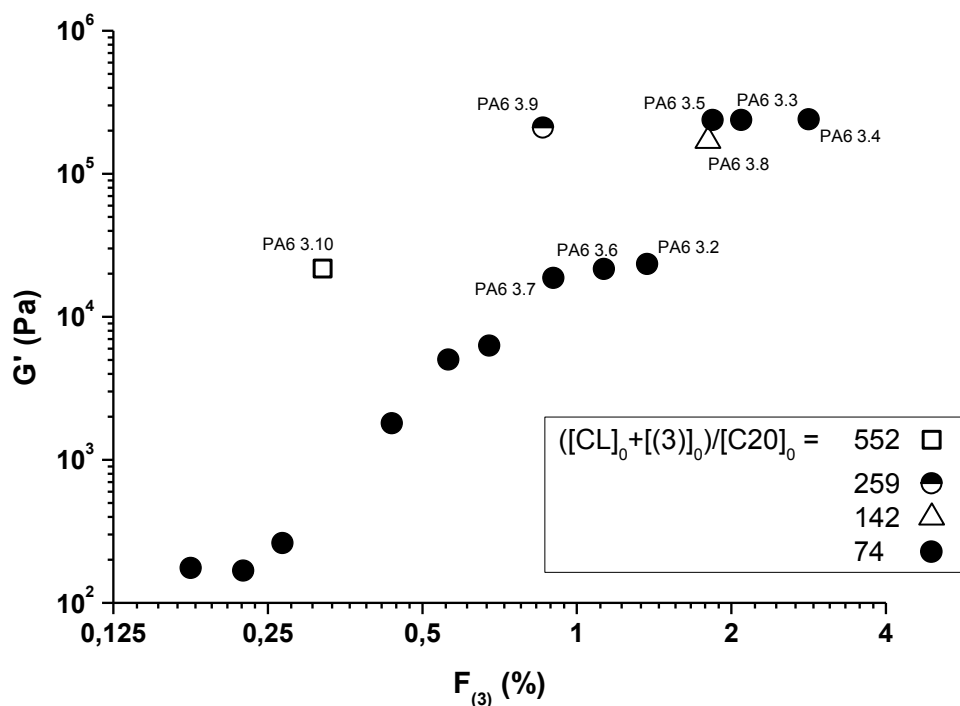


Figure III-8. Crosslinking agent (3) dependences of the storage modulus G' (at $\omega=0.1$ rad.s⁻¹) at 250 °C of synthesized PA6 by bulk anionic copolymerization of ϵ -caprolactam with various amount of activator (C20).

2. Toward reversible crosslinked polyamide 6

In recent decades, polymers containing photosensitive moieties proved a remarkable interest because of their potential use in a broad range of application fields such as photolithography^{28, 29}, photo-curable coatings³⁰ and photoresists³¹.

Cinnamoyl^{32, 33}, coumarin³⁴⁻³⁷, anthracene^{38, 39} and azobenzene^{40, 41} are the mostly used chromophore groups for photoresponsive systems by dimerization or isomerization reaction. Photoreversibility of these groups can be set in the main-chain or as pendant groups to enable controlling of some physical and chemical properties by crosslinking. Among photosensitive moieties, the photo-reactive cinnamoyl group dimerization, occurring through the [2+2] thermal or photochemical cycloaddition reaction⁴², was implemented for polymerization reactions and for crosslinking purposes⁴³. The so-obtained cyclobutane dimer combines thermal stability^{44, 45} and photosensitivity⁴⁶. The photochemical reversibility of the crosslinking was, for instance, nicely exploited for the synthesis of self-healing polymers⁴⁷.

⁴⁸and tunable shape-memory⁴⁹ materials. Recently, Oriol and coworkers studied on miktoarma star polymer bearing azobenzene photoresponsive units and reported the self-assembly properties of this novel polymer in water⁴⁰. Quite recently, Yagci and coworkers reported self-healing strategy for poly(propyl-ene oxide)s bearing coumarine-benzoxazine units based on light induced coumarine dimerization reactions³⁶.

On the other hand, thermoresponsive systems have gained great interest for the synthesis of reversible crosslinking polymers. The preparation of reversibly crosslinking polyurethane based on Diels-Alder reaction of furan and maleimide moieties⁵⁰ were studied by Du Prez and coworkers.

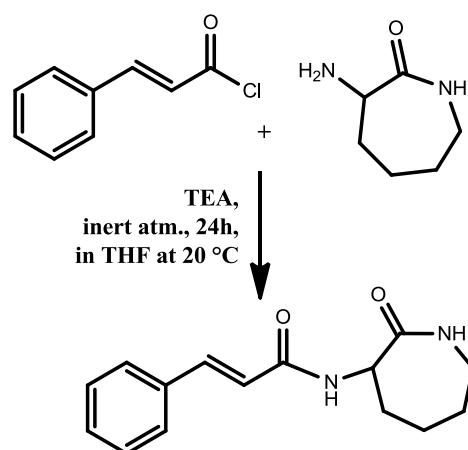
Experimental conditions as well as the nature of polymer chains have a significant influence on the efficiency of the dimerization reaction. Polymers bearing photosensitive groups show a higher photoreactivity in solution than in a solid-state coated film because the photosensitive groups are not in close vicinity enough in the solid state⁵¹. Besides, the efficiency of the dimerization reaction of pendant cinnamoyl groups decreases when the chain length increases owing to a lower mobility⁵².

The present part of this chapter III aimed to synthesize new reversible thermoplastic PA6 containing cinnamate units with better thermal properties due to the crosslinking. To the best of our knowledge, no investigation has been reported so far regarding the reversible crosslinking of PA6 bearing cinnamoyl photoreactive group. This chapter focuses on polymeric systems that exploit a photo-reversible dimerization reaction and a thermo-crosslinking of cinnamated PA6.

We synthesized novel PA6, which is both photo- and thermo-crosslinked, by anionic ring-opening polymerization (AROP) of ϵ -caprolactam and α -cinnamoylamido- ϵ -caprolactam as a novel comonomer in bulk. The photochemical and reversibility properties of the new polymers were studied in solution and as spin-coated films. After irradiation and/or heating of these samples, absorption changes were monitored by UV-visible spectroscopy. The new PA6 copolymers were characterized by magic angle spinning NMR and their thermal stability were studied by thermogravimetric analysis (TGA) and differential scanning calorimetry (DSC). The phase behaviors of novel crosslinked and neat PA6s have been investigated by dynamic mechanical analysis (DMA).

2.1. Synthesis of α -cinnamoylamido- ϵ -caprolactam

A successful synthesis of α -cinnamoylamido- ϵ -caprolactam (Cin-CL) monomer was achieved by a one-step amidation reaction (Scheme III-3) from α -amino- ϵ -caprolactam (ACL) which can be obtained from ring closure reaction of L-lysine (see chapter II, Scheme II-1). To the solution of α -amino- ϵ -caprolactam in tetrahydrofuran (THF), triethylamine (TEA) was added to deprotonate a primary amine and quench HCl which is produced by amidation reaction. After 1h activation by TEA, cinnamoyl chloride was added dropwise while purging the reaction flask with argon because in solution cinnamoyl chloride is sensitive to moisture and can easily exchange with $-\text{OH}$. This can lead to more difficult nucleophilic attack of activated α -amino- ϵ -caprolactam. After 24h reaction in an inert atmosphere and then purification steps, white solid product was obtained with 80% yield.



Scheme III-3. One-step amidation reaction of cinnamoyl chloride with α -amino- ϵ -caprolactam.

The structure of the α -cinnamoylamido- ϵ -caprolactam was confirmed by ^1H NMR analysis and Figure III-9a exhibits the typical proton signals attributed to ethylene groups of the α -aminocaprolactam structure between 1.25-2.30 ppm ($-\text{CH}_2$), primary amine at 2.10 ppm and amide proton (CO-NH-C) at 6.75 ppm. After reaction (Figure III-9b) endocyclic and exocyclic protons were observed at 6.10 and 7.10 ppm, respectively. Cinnamoyl aromatic protons appeared between 7.2 and 7.5 ppm. At the same time cinnamoyl alkene protons were shown at 6.5 ppm and 7.6 ppm. Indeed, integral ratios of i:h:c:b are 1:1:1:2 and support the synthesis and purification of the α -cinnamoylamido- ϵ -caprolactam (See, Figure III-S10).

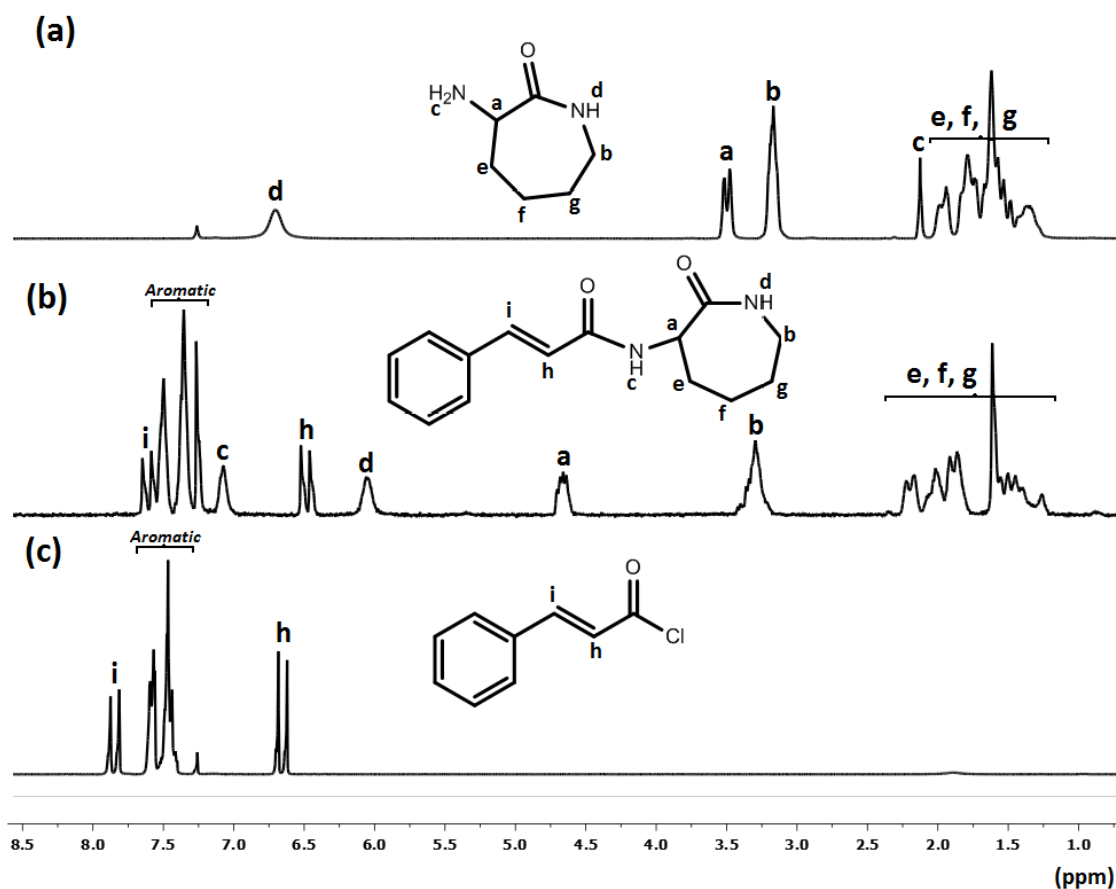


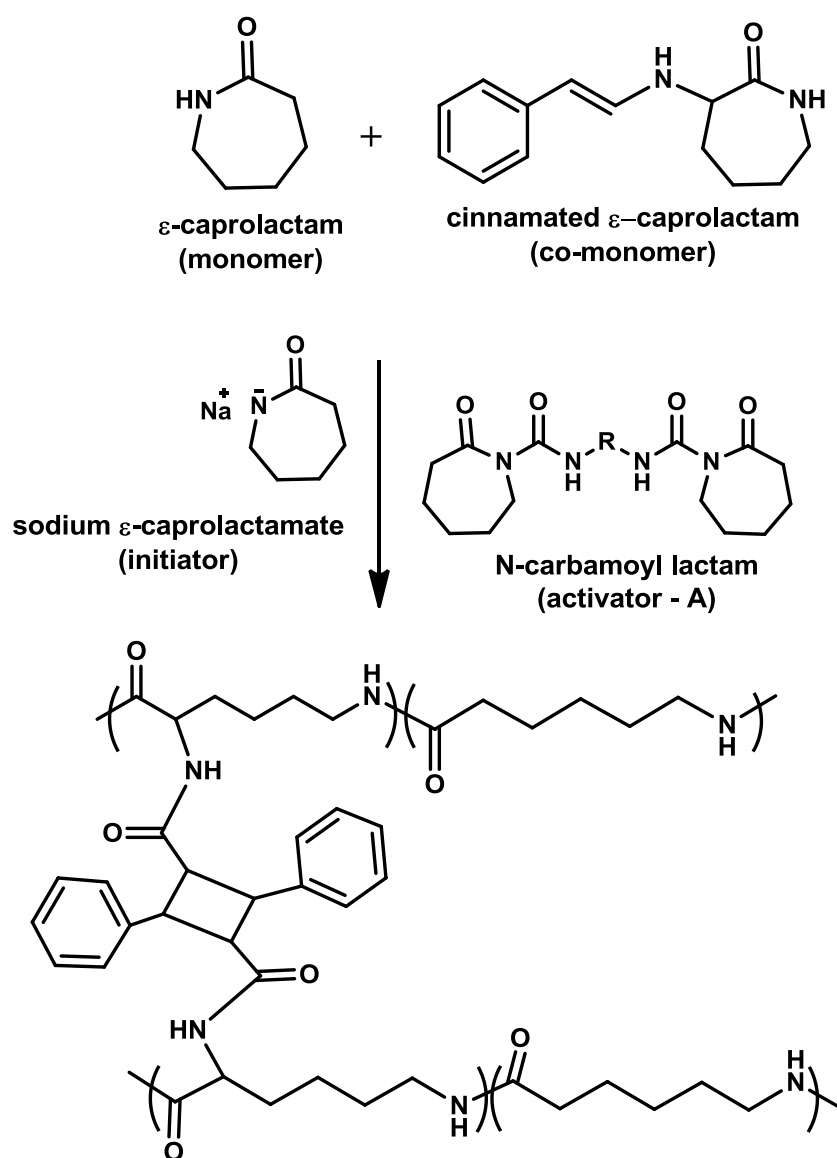
Figure III-9. ^1H NMR spectra of (a) α -amino- ϵ -caprolactam (ACL), (b) α -cinnamolyamido- ϵ -caprolactam and (c) cinnamoylchloride in CDCl_3 .

2.2. Copolymerization and crosslinking

First of all, neat PA6 was prepared by AROP in the specific reactor system (the same conditions with chapter II, Figure II-S2) which provides better inert atmosphere and easy way to measure rate of polymerization (temperature/time diagram). The polymerization was carried out in bulk at 140°C . ϵ -Caprolactam (CL, monomer) and sodiumcaprolactamate (C10, initiator) were added to a glass reactor at 140°C under nitrogen atmosphere to activate the monomer and were molten with continuous stirring after hexamethylene-1, 6-dicarbamoylcaprolactam (C20, activator) was added to mixture to start the polymerization. In 15 min., solidification completed and exothermy slows down, PA6 were taken from reactor and crushed then refluxed in water to remove unreacted reagents and then dried in an oven overnight at 90°C under vacuum before any analysis because moisture has plasticizing effect on PA6. Conversion of the monomer (98%) was determined

gravimetrically. During AROP of CL, crystallization and polymerization occur at about in the same time. The polymer starts to precipitate in the bulk mixture once it forms.

Syntheses of PA6 bearing different amount of cinnamoyl units were conducted exactly under the same polymerization conditions as the one of PA6 was carried out. Addition to that, Cin-CL comonomer was added to reaction tube in the same time with CL. Results are summarized in Table III-3 and the proposed reaction is depicted in Scheme III-4. After the polymerization step, all obtained copolymers were washed by refluxing first from water and then with dichloromethane (CH₂Cl₂) to remove unreacted Cin-CL comonomer and other reagents.



Scheme III-4. Anionic ring-opening copolymerization and thermal dimerization of ϵ -caprolactam and α -cinnamoylamido- ϵ -caprolactam.

Table III-3. Synthesis of polyamide 6 and polyamide 6 bearing pendant cinnamoyl groups at 140 °C in bulk and their solubility in HFIP.

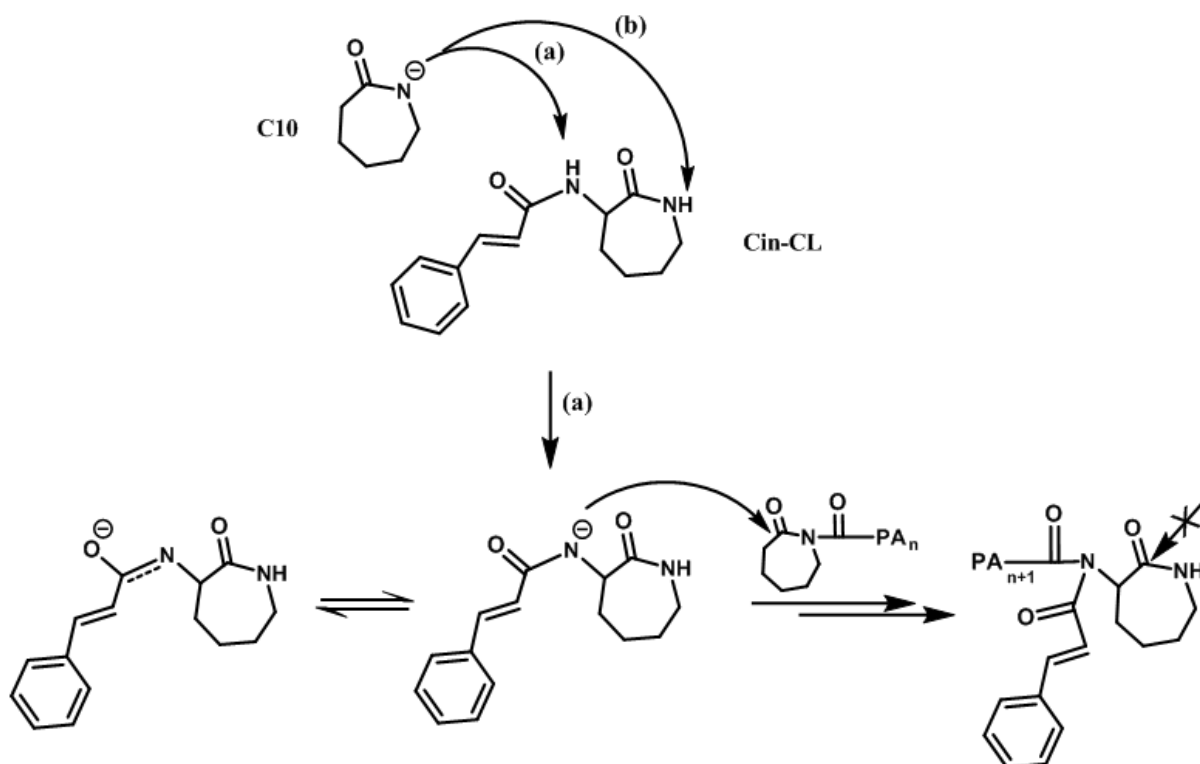
Run	C20, (mol/L)	C10, (mol/L)	[C10]/ [C20]	CL ^a (mmol)	Cin-CL ^b (mol %)	Cin-CL ^b (wt %)	t, min	Conv ^c %	Sol. ^d
1, PA6	0.02	0.153	7.65	73.8	-	-	15	98	S
2, 2%Cin-PA6	0.02	0.153	7.65	72.0	1.03	2	15	90	S
3, 6%Cin-PA6	0.02	0.153	7.65	68.4	3.20	6	30	60	NS
4, 10%Cin-PA6	0.02	0.153	7.65	65.0	5.48	10	24	60	NS

^a ϵ -caprolactam,^b α -cinnamoylamido- ϵ -caprolactam,^c Determined gravimetrically,^d Solubility in HFIP (hexafluoroisopropanol), S: Soluble, NS: Non-soluble.

Different molar ratios of α -cinnamoylamido- ϵ -caprolactam were used in each copolymerization with the same amount of activator and initiator at the same reaction temperature of 140 °C. As the relative amount of cinnamoyl unit was increased from 2% to 10%, the obtained polymers turned to gel formation in HFIP for 6 and 10% of Cin-PA6 (Run 3 and 4). Those polymers, which have higher quantity of cinnamate units, were thermally crosslinked because of the distance and mobility of dimerizable groups presented. It has already been shown that the dimerization reaction has a favorable encounter of the cinnamoyl groups in due to polymer chain mobility through heating and irradiation^{42, 51, 52}.

During the PA6 synthesis, an exothermic reaction^{53, 54}, crystallization and polymerization occur simultaneously (Figure III-10). This temperature/time data was followed by a thermocouple which is installed in the calorimeter to measure the reaction temperature. On the other hand, the copolymerization of CL with its derivative leads to a decrease of polymerization and crystallization exothermic temperatures (Run 2, Table III-3, and Figure III-10). The flat evolution of temperature with time and limited conversion were observed by using 10 wt% of the cinnamated monomer (Run 4, Table III-3). Figure III-10 indicates clearly a decreased reactivity of the overall polymerization process, and the introduction limit of cinnamated groups into PA6. The copolymerization of an increasing amount of α -

cinnamoylamido- ϵ -caprolactam slows down the rate of polymerization. The slowing down of the polymerization rate is an expected behavior, as early mentioned in Chapter II, as far as ring-opening polymerization of acyl derivative of CL is concerned. Here, there are also inevitable two side reactions. One is the competitive hydrogen abstraction, due to difference of hydrogen acidities, from the exocyclic and endocyclic amides by C10 (Scheme III-5). This effect can consume higher C10 amount than conventionally used for AROP of CL. The other side effect might be stemmed from occurrence of two different amides (endo- and exo-) by leading to imide groups and polymer branching. Therefore, these side reactions can affect activation of the monomer during ring-opening polymerization at the expense of kinetics. Addition to, occurring of the non-active chain-end group from deprotonation of exocyclic amide protons would limit to AROP.



Scheme III-5. Competitive proton abstractions from exo- and endocyclic amide protons.

Crosslinking of 2% Cin-PA6 did not occur during the AROP and after it was soluble in HFIP. It is mostly probable that a lower amount of the cinnamated monomer (2%) leading to a high distance between the chromophore groups and faster AROP than the dimerization reaction during the polymerization. On the other hand, 6% Cin-PA6 synthesis and crosslinking owing

to enough amount of cinnamated pendant unit (6%) were completed in a short polymerization time (15 min.). Only temperature/time diagrams of 2% and 6% of cinnamoyl pendant PA6 (Runs 2 and 3, Table III-3) were able to be observed and compared with PA6 in Figure III-10. On the other hand, 10%Cin-PA6 (Run 4, Table III-3) has a flat temperature/time diagram with a quite longer polymerization time (24h). After the copolymerization reaction, 6%Cin-PA6 and 10%Cin-PA6 were not soluble (gel formed) in hexafluoroisopropanol (HFIP) due to the crosslinking. The decelerating effect of the comonomer on the copolymerization process also reflects a lower monomer conversion compared to homopolymerization of CL (Table III-3). Since the copolymerization does not go to completion, the exact amount of comonomer incorporated inside the copolymer might be lower than the theoretically expected at full conversion. In fact, determination of the exact amount of cinnamated units in the polymer chain by NMR was not possible because of the non-solubility of the resulting polymer in any solvent.

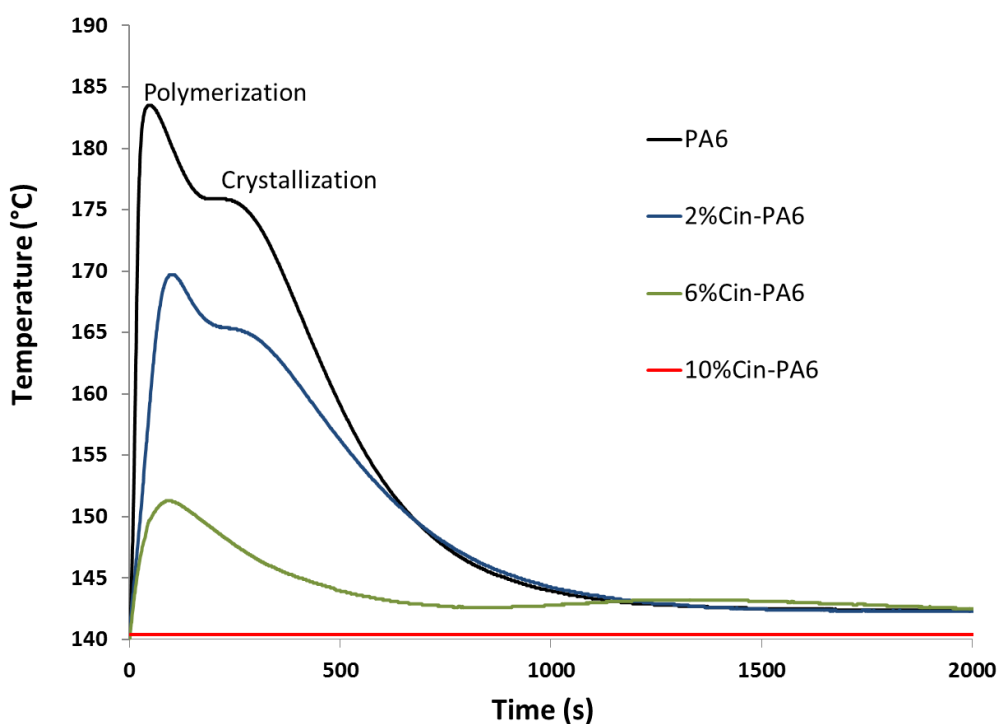


Figure III-10. Temperature-time diagrams of PA6, 2%Cin-PA6, 6%Cin-PA6 and 10%Cin-PA6.

The structure of PA6 with pendant cinnamoyl groups was confirmed via solid-state ^{13}C MAS NMR (Figure III-11) because of the poor solubility of PA6 in organic solvents except HFIP and also the insolubility of crosslinked PA6. To further explore and compare possible

influences of dimerized cinnamoyl units on polyamides, we prepared α -truxillic acid from cinnamic acid dimerization⁵⁵ by UV irradiation. As the dimerization proceeds during the copolymerization, the new carbon signals attributed to the aromatic carbons indicating the successful copolymerization. One signal in the carbonyl region and four different signals of aliphatic carbons of PA6 appeared and overlap the cyclobutane ring and its carbonyls. In addition to PA6 aliphatic carbon peaks, there is one more signal which may belong to overlapping cyclobutane ring carbons. As expected, the new chemical shift of aromatic carbon peaks appeared between 115 and 140 ppm, as shown in elsewhere⁵⁵. The solid-state chemical shifts of PA6 and PA6 with pendant cinnamoyl group were similar for aliphatic carbon and carbonyl groups. The dimerization-crosslinking (for more than 2% of α -cinnamoylamido- ϵ -caprolactam, Table III-3) proceeds during AROP of ϵ -caprolactam, was attributed to the cyclobutane ring formation.

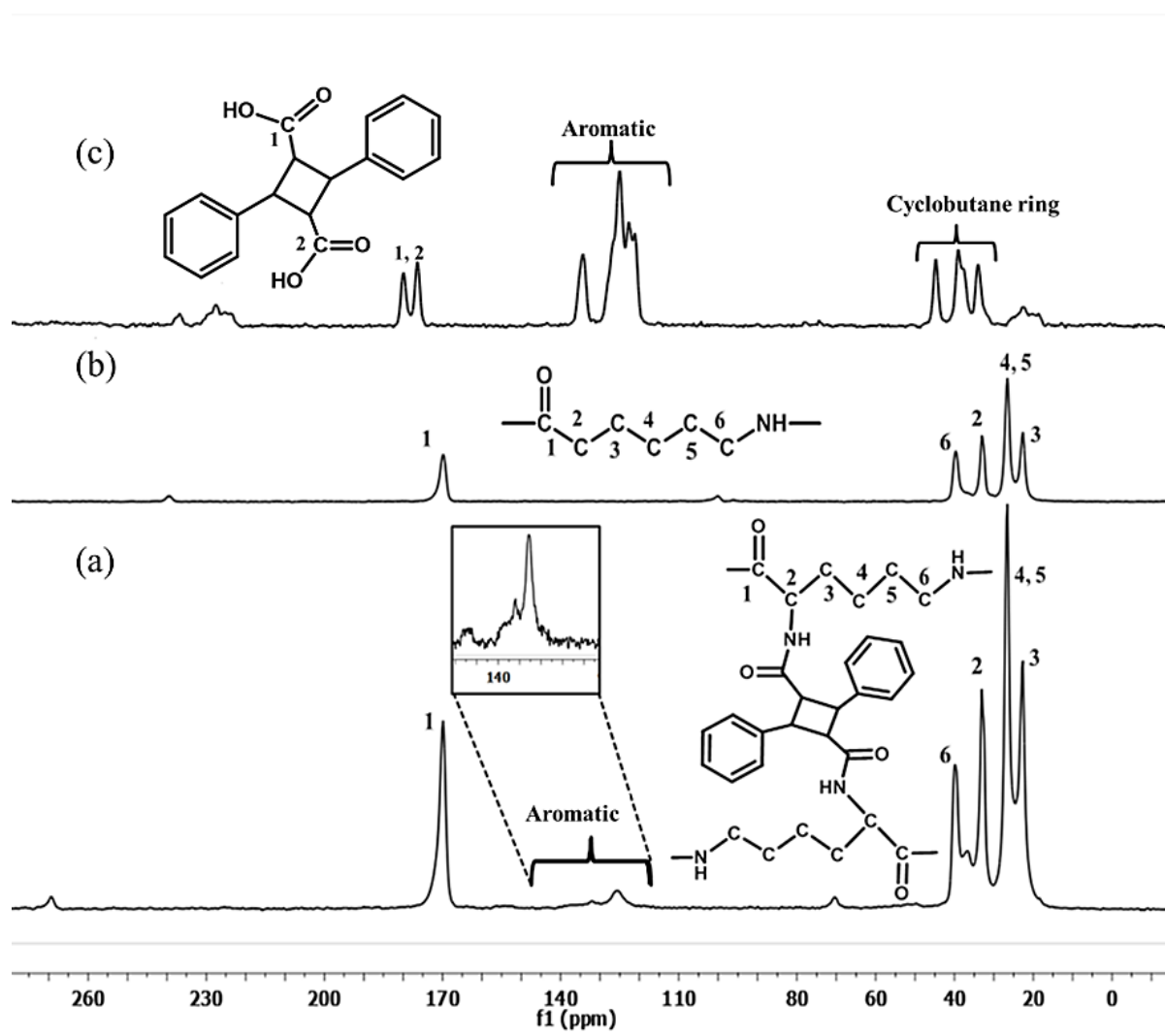


Figure III-11. ¹³C MAS NMR spectra of 10% Cin-PA6 (a), PA6 (b) and truxillic acid (c).

The peaks at 230 and 20 ppm (c); 240 and 100 ppm (b); 270 and 70 ppm (a) are spinning side-bands which are usually observed in solid-state NMR when the rate of the spinning of the tube at the magic angle is not fast enough. There is an averaging effect, which results in the splitting of one single peak in several peaks. The two peaks of each sample (a, b and c) are symmetric and look very similar but at different chemical shifts.

Thermal characterization of PA6 bearing cinnamoyl unit and the neat PA6 was investigated by differential scanning calorimetry (DSC). DSC measurements of PA6 copolymers having 2, 6 and 10 wt% of cinnamoyl units were performed in N₂ (Table III-4, Figure III-S11-Figure III-S14). The glass transition temperature (T_g) were reported from second heating scans because in first scans very broad transitions were detected. The copolymers of PA6 bearing cinnamoyl pendant groups demonstrated significant increase in T_g , compare to neat PA6 T_g of 53 °C, as much as the cinnamoyl amount increases with crosslinking. Melting points and melting enthalpies (ΔH_m) of the copolymers are lower compared to neat PA6. PA6 copolymers having rigid aromatic bulky groups, either crosslinked PA6 (10%*Cin*-PA6 and 6%*Cin*-PA6) or non-crosslinked (2%*Cin*-PA6), rise T_g due to inhibited close packing and reduced T_m and crystallinity. On the other hand, the single melting endotherms also confirm random copolymerization rather than block copolymerization.

Table III-4. Thermal properties PA6 and PA6s pendant cinnamoyl groups.

Sample	DSC 1 st Run		DSC 2 nd Run			TGA				
	T_m (°C)	ΔH_m (j/g)	T_g (°C)	T_c (°C)	ΔH_c (j/g)	T_m (°C)	ΔH_m (j/g)	T_5 (°C) ^a	T_{10} (°C) ^b	T_d (°C) ^c
PA6	213	92	53	171	60	216	70	290	300	308
2% <i>Cin</i> -PA6	213	82	59	170	56	214	60	307	321	330
6% <i>Cin</i> -PA6	210	87	62	152	48	204	47	308	336	346
10% <i>Cin</i> -PA6	210	89	61	152	42	201	44	361	390	407

^a Decomposition temperature at a 5% weight loss,

^b Decomposition temperature at a 10% weight loss,

^c Maximum of the peak decomposition temperature.

Thermal stability of the polyamides was investigated by thermogravimetric analysis (TGA) under nitrogen atmosphere. The TGA diagrams of PA6 and PA6 bearing cinnamoyl units are shown in Figure III-12 and the results are summarized in Table III-4. TGA curves also confirmed that thermal stabilities of the crosslinked (10%*Cin*-PA6 and 6%*Cin*-PA6) and non-crosslinked (2%*Cin*-PA6) polyamides are higher than neat PA6. For PA6, the initial decomposition temperatures of 5 and 10% weight losses (T_5 and T_{10}) at 290 and 300 °C. For 10%*Cin*-PA6, the initial decomposition temperatures of 5% and 10% weight losses are increased till 361 and 390 °C. Clearly, significant thermal stability improvement has been seen not only for crosslinked PA6 but also non-crosslinked aromatic bulky units bearing PA6. These properties make novel crosslinked PA6s attractive for high performance applications.

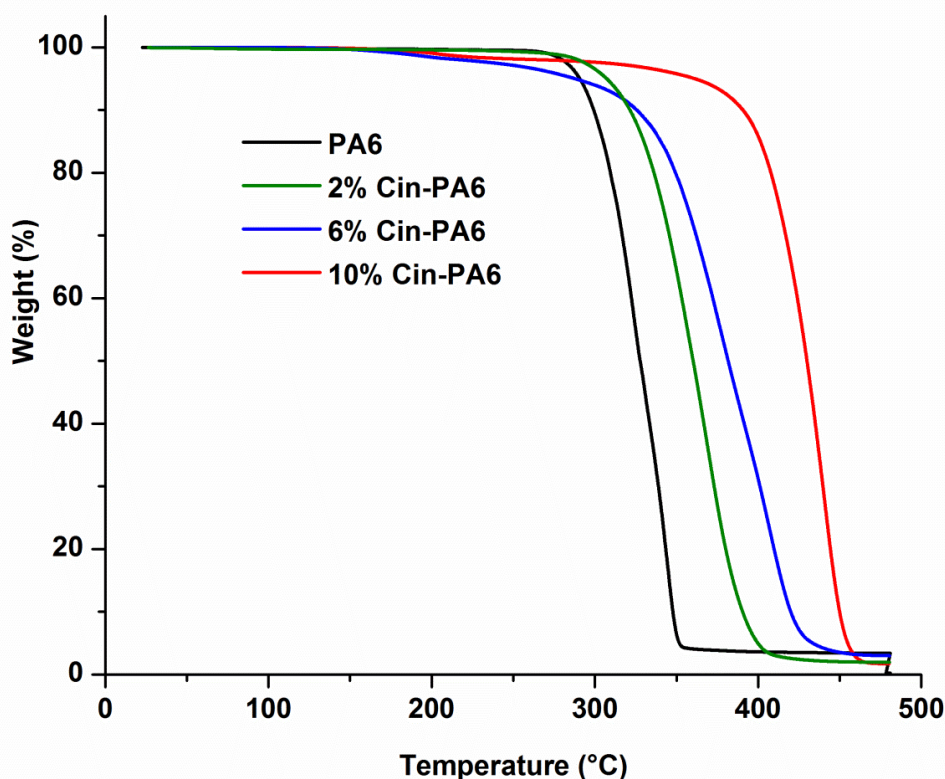


Figure III-12. TGA thermograms of PA6, 2%*Cin*-PA6, 6%*Cin*-PA6 and 10%*Cin*-PA6.

The thermal stability improvement of crosslinked or non-crosslinked PA6s bearing aromatic bulky groups is shown by shifting derivative weight losses to the higher temperatures. Purities of the obtained polymers can clearly be seen from single thermal degradation peaks (Figure III-13).

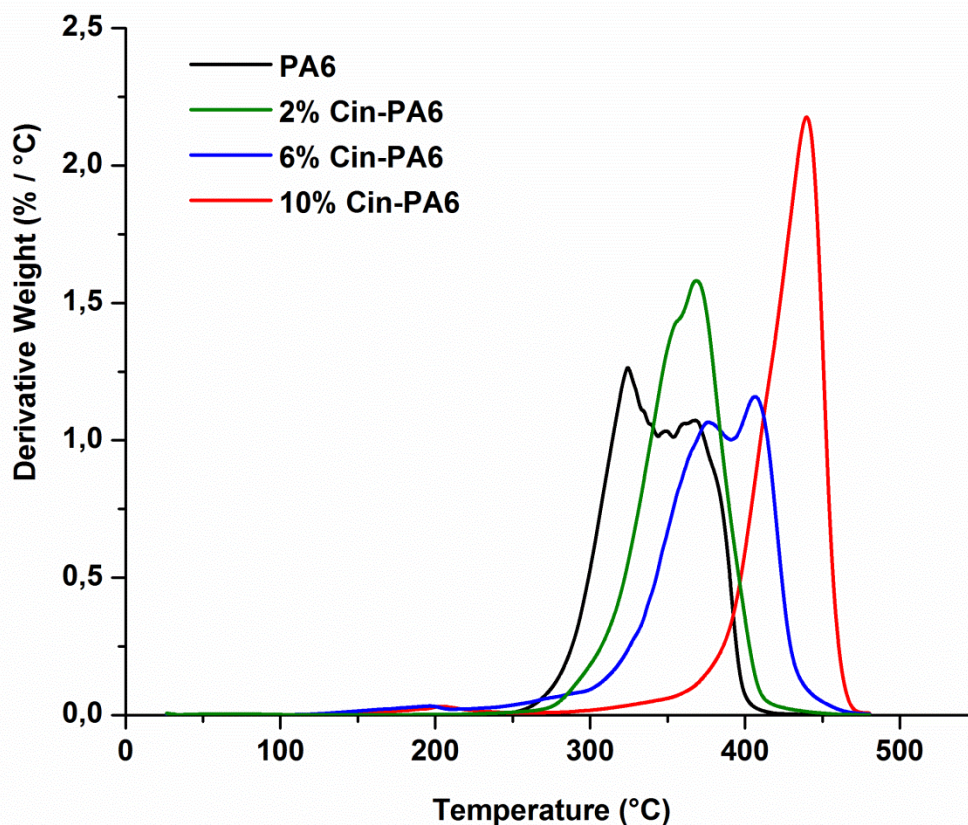


Figure III-13. Rates of weight loss of PA6, 2%Cin-PA6, 6%Cin-PA6 and 10%Cin-PA6.

Mechanical properties of crosslinked PA6 bearing cinnamoyl units were investigated by DMA. The elastic modulus (E') and loss factor ($\tan \delta$) are depicted against the temperature (Figures III-14 and 15). The decrease of E' down to $6-7 \cdot 10^8$ Pa agrees with reduced crystallinity which restricts the regular arrangement of PA6 chains. As can be seen in Figure III-15, $\tan \delta$ curve is shifting to higher temperatures with increasing the amount of cinnamoyl groups in PA6 chains compared to neat PA6. Actually, $\tan \delta$ shifting is related to more blocked amorphous phase due to pendant and bulky aromatic groups. Crosslinking of PA6 leads also to restriction of the polymer backbone mobility. The T_g was observed from the maxima of $\tan \delta$ at 72 °C, 74 °C, 78 °C and 84 °C for PA6, 2%Cin-PA6, 6%Cin-PA6 and 10%Cin-PA6, respectively.

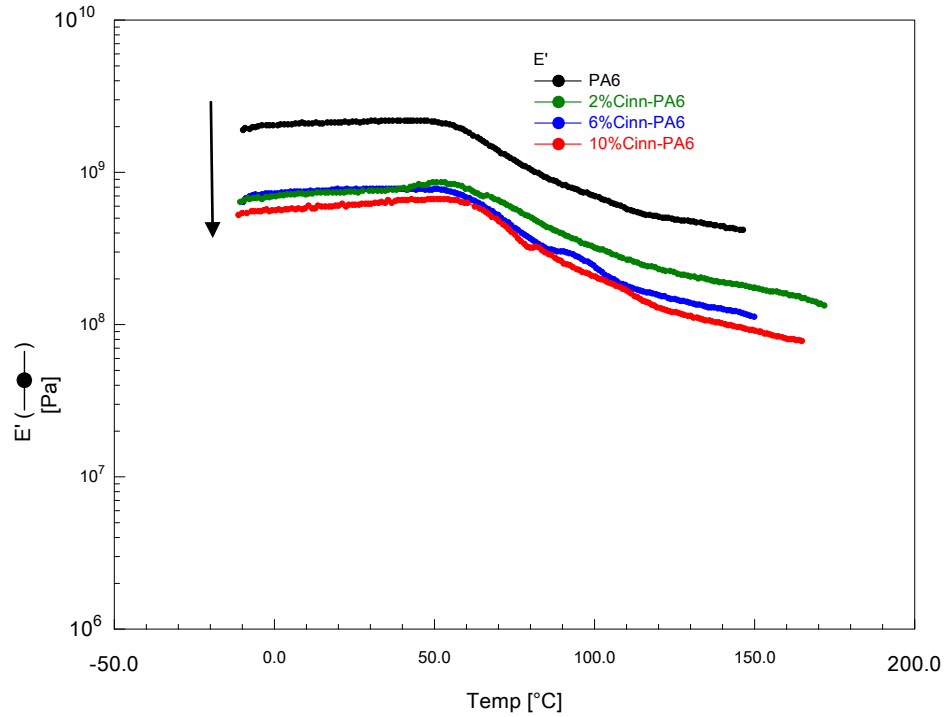


Figure III-14. Elastic moduli (E') of PA6, 2%Cin-PA6, 6%Cin-PA6 and 10%Cin-PA6 by DMA.

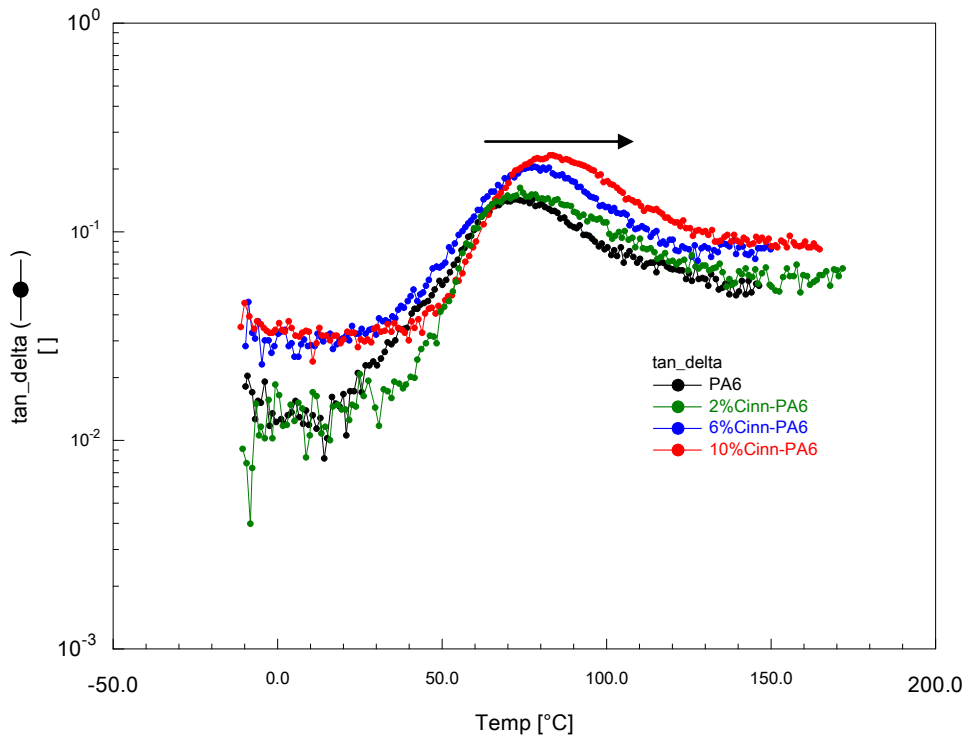
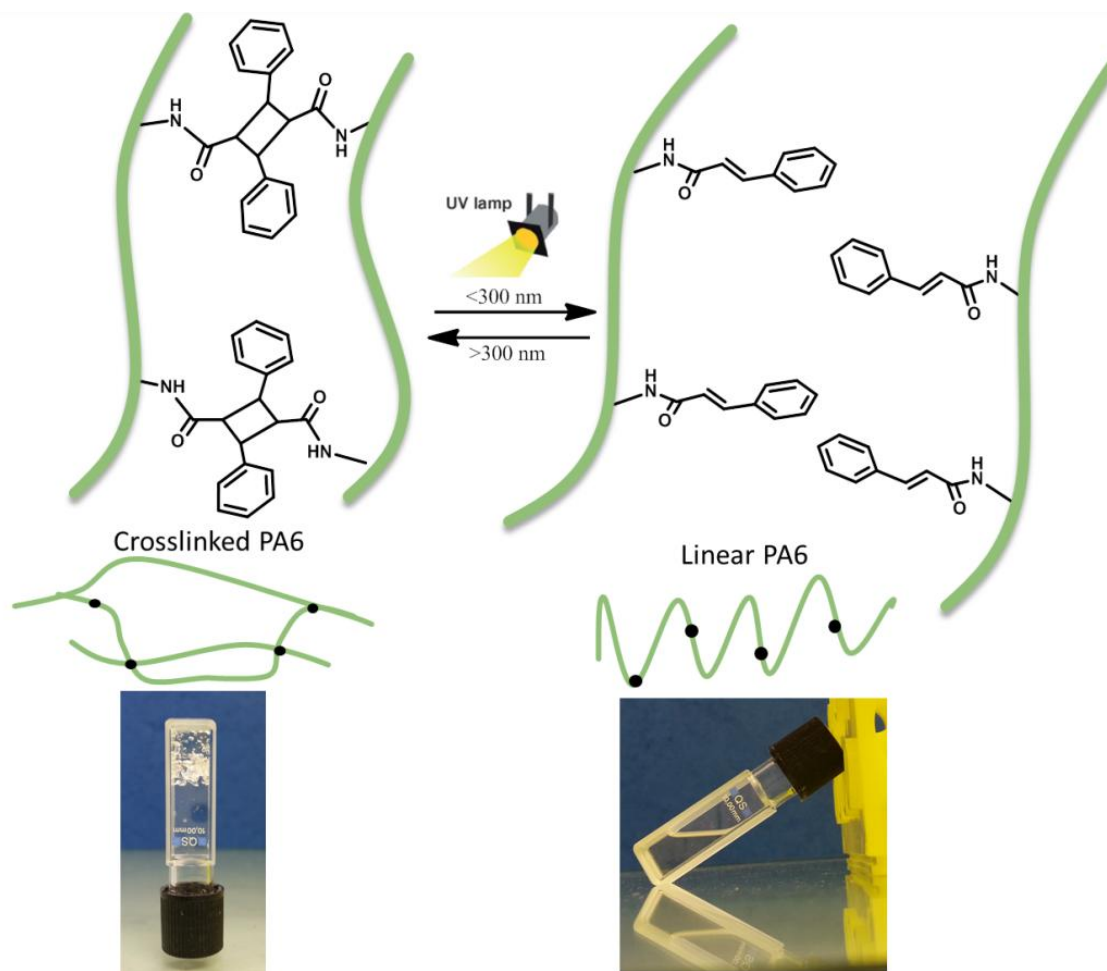


Figure III-15. Loss factors ($\tan \delta$) of PA6, 2%Cin-PA6, 6%Cin-PA6 and 10%Cin-PA6 by DMA.

2.3. Reversibility: De-crosslinking and re-crosslinking

Photochemistry of the 10% Cin-PA6 gel formed in HFIP was monitored by taking UV absorption spectra. After exposing the sample to 220-280 nm light irradiation for de-crosslinking (decomposition of the dimer), the gel in HFIP became a solution as represented in Scheme III-6.



Scheme III-6. From gel to solution form of $1.23 \times 10^{-4} \text{ mol L}^{-1}$ of PA6 bearing pendant cinnamoyl group in HFIP solution after irradiation at 254 nm for 6h.

The reversible photo- and thermo- dimerization and photocleavage reactions of the PA6 bearing cinnamoyl groups were monitored using UV absorbance spectroscopy. The results of the absorbance measurements as a function of irradiation time and wavelength are similar, Figure III-16 and 17, which showed the cleavage and dimerization of the cinnamoyl group. Polymers having cinnamoyl group are known to be insoluble⁴³ after photo-irradiation

between 325-380 nm and thermal treatment due to the [2+2] cycloaddition to form crosslinkages. As depicted in Figure III-16, the cinnamate residues reached to their highest absorption state in 6h irradiation. After decrosslinking, spectral changes of the spin-coated thin films upon UV irradiation at 325-380 nm and following heating at 140 °C for recrosslinking are shown in Figure III-17. Absorption spectra of spin-coated polymer film decreased gradually upon further irradiation with time. A more efficient decrease was also observed by heating at 140 °C for 1h after following the irradiation at 25 °C. Recrosslinking was also confirmed from the insolubility of the thin film after irradiation and heating at 140 °C. But there was a difference in terms of efficiencies of re-crosslinking by UV irradiation and heating. The reason of this difference in efficiency relies in the much higher mobility degree⁵⁶ of chains bearing pendant cinnamoyl units at high temperature during the thermal treatment compared to the lower temperature used during irradiation. It was already reported that, whenever photosensible groups are in close proximity in the condensed state compared to solution⁵¹, heating increases the mobility of chains and thus favors the diffusion of cinnamoyl units to each one another. Restricted solubility of cinnamoyl pendant PA6 allows only spin-coated film irradiation which is also required due topolar solvent effect of HFIP on dimerization. It is also noted for another systems⁵¹ that the UV spectrum of the recrosslinked content on the glass plate is broader than de-crosslinked samples in HFIP solutions. The percentages of reacted chromophore groups are related to the accessibility. Once the network starts to form, the encounter between two chromophores on different molecules is increasingly hindered⁵⁷.

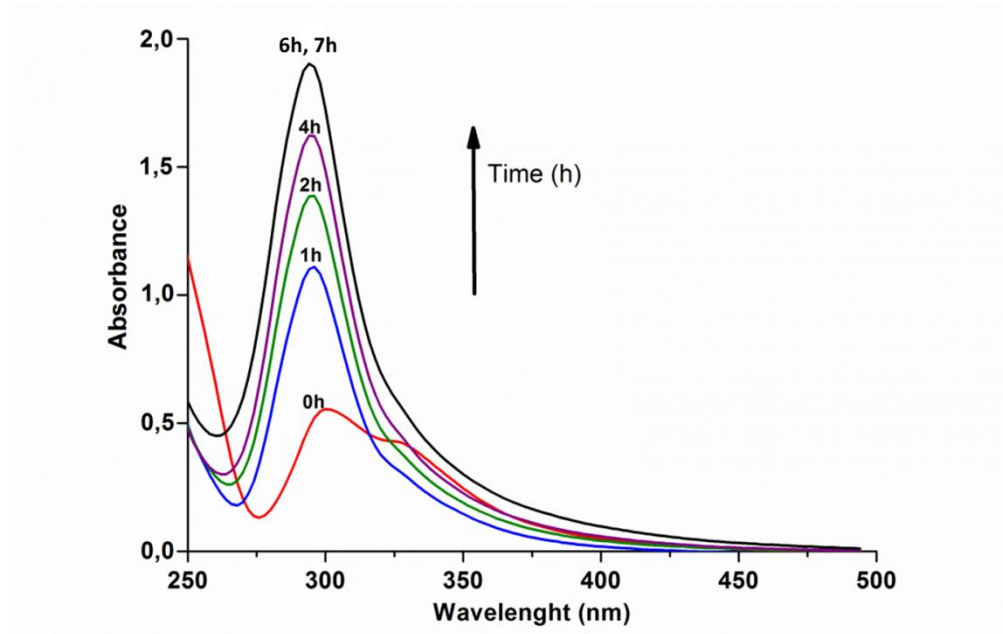


Figure III-16. UV absorption spectra of $1.23 \times 10^{-4} \text{ mol L}^{-1}$ of 10% Cin-PA6 bearing pendant cinnamoyl group in HFIP solution at irradiation times from 1h to 6h between 200-280 nm.

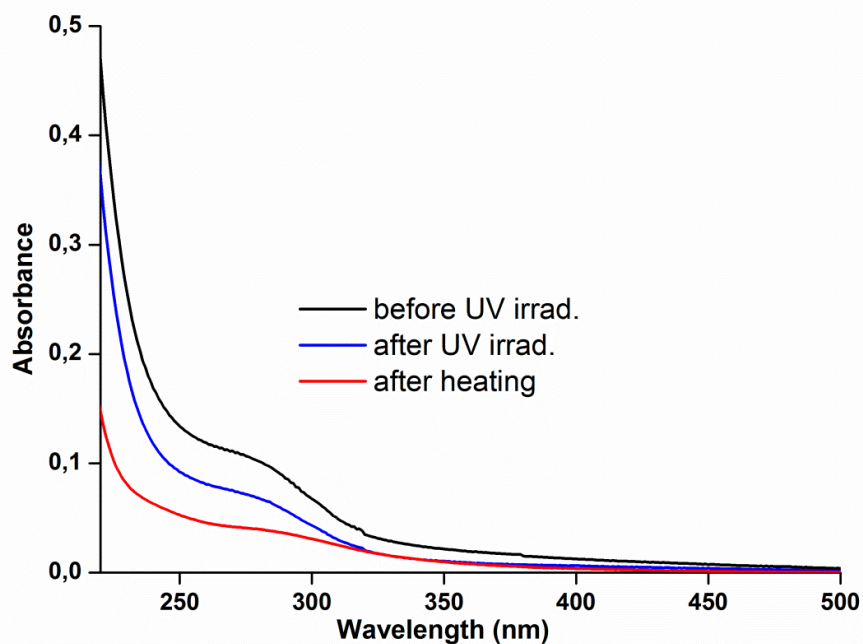


Figure III-17. UV absorption of 1% w/v spin-coated PA6 bearing pendant cinnamoyl group (10% Cin-PA6) before UV irradiation (black line), after UV irradiation 6h (blue line) between 325-380 nm and after heating at 140 °C for 60 min (red line).

Crosslinking rate of 10%*Cin*-PA6 was measured by following UV absorbance intensity of polymer film after UV irradiation and 1h heating at 140 °C, according to following expressioneq (2):

$$\text{Rate of crosslinking (\%)} = \frac{A_0 - A_T}{A_0} \times 100 \quad \text{eq (2)}$$

Where A_0 and A_t are absorption intensities of the C=C chromophore after irradiation or heating of times $t=0$ and $t= T$, respectively. The rate of crosslinking of cinnamated PA6 is 33% after 6h UV irradiation and 42% after 1h heating. The increased rate of crosslinking by heating is related to a higher mobility of the polymer chain at higher temperature (140 °C) than T_g (61 °C). After UV irradiation and heating of 10%*Cin*-PA6, the polymer became insoluble in HFIP due to the efficient crosslinking.

Conclusion

In first part of this chapter, as an attempt to limit the creep of polyamide 6 materials, a controlled crosslinking via the use of α -amino- ϵ -caprolactam-based bis-monomers in addition to ϵ -caprolactam polymerization was proposed. The presence of urea bonds was shown to limit the amount of bis-monomer introduced in order to reach high yields and fast kinetics due to side reactions. Using an amide-based bis- ϵ -caprolactam, i.e. bis-N(2-oxo-3-azepanyl)-1,6-tetramethylenediamide, synthesized from cyclic lysine and adipoyl chloride, the bulk copolymerization with CL at 140 °C was running similarly as the homopolymerization of the latter enabling its use in conventional Reaction Injection Molding or other processes. Chemically crosslinked polyamides 6 were obtained and different rheological behaviors from viscoelastic to elastic regimes were observed at 250 °C depending on the added amount of bis-monomer.

In second part of this chapter work, crosslinked polyamide 6 having thermo- and photosensitive cinnamoly group was investigated. Polymers with cinnamoyl groups either in the backbone or in the pendent position have drawn a particular attention because of their excellent photoreactivity and undergo crosslinking upon UV light irradiation or heating. The incorporation of cinnamoyl- into the polyamide 6 has also the potential for improving certain

polymer properties. We synthesized novel polyamide 6, which is both photo- and thermo-crosslinked, by anionic ring-opening polymerization of ϵ -caprolactam and its cinnamoyl derivative in bulk at 140 °C. The photochemical and reversibility properties of the new polymers were studied in solution and spin-coated films by UV-visible spectroscopy after irradiation and heating and monitored by the change in UV absorption. The novel polyamide 6 copolymer was characterized by magic angle spinning NMR and its thermal stability was studied by thermo gravimetric analysis and differential scanning calorimetry. Thermal analysis showed that crosslinked polyamide 6 has higher thermal stability and glass transition temperature than neat polyamide 6. Indeed, we present here for the first time reversible cinnamoylchromophore pendent polyamide 6 as a thermoplastic by photodimerization towards the generation of crosslinked non-soluble copolymers. This developed system can be attractive for self-healing and/or shape memory systems. For instance, such kind of thermo or photo- responsive system has a potential as novel material in the stimuli or environmentally responsive (smart) materials.

Experimental and supporting information

Materials. DL- α -amino- ϵ -caprolactam (BASF) was purified by solubilization in toluene and filtered to eliminate non-soluble impurities. After evaporation of toluene, a white product was obtained. Dichloromethane (DCM) (XilabReactifs, analytical grade), and dimethylsulfoxide (DMSO) (Sigma-Aldrich, $\geq 99.9\%$) were dried over calcium hydride and distilled before use. CL was recrystallized from dry cyclohexane prior to use. Ethanol (XilabReactifs, analytical grade), acetone (XilabReactifs, analytical grade), 1,1,1,3,3,3-hexafluoro-2-propanol (HFIP) (Acros Organics, $\geq 99.7\%$), and *tert*-butylamine (Sigma-Aldrich, 98%) were used without any further purification. Adipoyl chloride ($\geq 99\%$) and triethylamine ($\geq 99\%$) were purchased from Sigma-Aldrich then distilled right before use. Nitrogen was used to provide an inert atmosphere under which all reactions were carried out. Cinnamoyl chloride (98%) and triethylamine ($>99.5\%$) were purchased from Sigma-Aldrich and used without further purification.

Measurements. ^1H and ^{13}C NMR spectra were obtained from a Bruker AC 400 spectrometer. d_6 -DMSO (Cambridge Isotope Lab. Inc.) was used as the solvent with TMS and CDCl_3 used as internal reference. ^{13}C solid state NMR spectra were recorded on a Bruker 400 Avance I 400 MHz spectrometer at room temperature. During experiments, magic angle spinning²⁹ rate was 30 kHz using a Bruker 2.5 mm HX probe. Number of co-added transients was 256 and recycle delay was 5s. Single-pulse experiment were carried out and the 90 degree pulse of duration was 1.8 μs , FID acquisition time was 41 ms. Size exclusion chromatography (SEC) was performed on a Varian instrument equipped with a Varian ProStar 210 pump, Varian ProStar 355 differential refractometer as detector and three gel columns (supplied by Polymer Laboratories) used in series, PL HFIP gel guard column and two PL HFIP gel linear columns. HFIP, containing 0.05%w/w of potassium trifluoroacetate, was used as eluent at a flow rate of 1.0 $\text{mL}\cdot\text{min}^{-1}$ at 40 $^\circ\text{C}$ using CROCO-CIL[®]Thermostat HPLC columns heater. Data acquisition was performed using Polymer Laboratories Cirrus version 3.2 software. The measurements were carried out at 20 $^\circ\text{C}$ and the average molar masses (\overline{M}_n and \overline{M}_w) were derived from a calibration curve based on PMMA standards (0.580 to 1820 kDa). All HFIP sample solutions were passed through 0.45 μm PTFE membrane filter (supplied by CIL Cluzeau, France) prior to injection. The melt rheological properties were

determined using a TA Instrument AR2000 Rheometer with a conventional oven for temperature control. The measurements of PA6 samples were performed at 250 °C in the dynamic linear mode with 25-mm-aluminum-parallel-plate geometry (gap 1000 μm). The dynamic viscoelastic properties were investigated as function of angular frequency (ω) in the range 0.04-400 rad/s at a strain magnitude of 1%. A TA Instrument RSA3 was used to study dynamic mechanical properties of PA6 samples. The samples were analyzed under nitrogen atmosphere from -75 °C to 275 °C at a heating rate of 5 °C/min. The measurements were performed in tensile mode at a frequency of 1 Hz, an initial static force of 0.9 N, and strain sweep of 0.1 %. For surface crosslinking by heating and UV irradiation, thin films of PA6 precursors were spin coated (Specialty Coating Systems, P67080 Spin Coater) on glass plates from 1% solutions in hexafluoroisopropanol at 2000 rpm for 5 min and then dried at 25 °C overnight under vacuum. The UV irradiation of the spin coated films and solution were performed by UV lamp TQ 150: 150W between $\lambda = 200\text{-}280$ nm and 450HHL Halogen 325-380 nm 400W, consequently. UV absorbances of decrosslinked samples were followed by HITACHI U-3300 / 130-0614 model UV-Visible spectrophotometer.

Synthesis of 1,1'-hexamethylenebis(2-oxo-3-azepanylurea) (2). A 250 mL three-necked flask, equipped with a stirbar, is charged with 40 mL of freshly distilled anhydrous DMSO or DCM, 5g (39 mmol) of α -amino- ϵ -caprolactam (**1**) and 3.28 g (19.5 mmol) of hexamethylenediisocyanate. The solution was stirred at 40 °C for 19h under atmosphere of nitrogen. The insoluble product was recovered by filtration, and the crude product washed several times with acetone or ethanol. The final product was recovered from the crude material by removal of the solvent to constant weight. The final yield of the product is 92%. ^1H NMR in d_6 -DMSO: δ ppm = 7.77 (t, $-\text{CH}_2\text{NHCO}-$), 6.34 (t, $-\text{NHCONHCH}_2-$), 6.16 (d, $-\text{CO}(-\text{CH}_2)\text{CHNHCO}-$), 4.25 (m, $-\text{CO}(-\text{CH}_2)\text{CH}-\text{NH}-\text{CO}-$), 3.33 (m, $-\text{CHHNHCOCH}(-\text{CH}_2)\text{NH}-$), 3.03 (m, $-\text{CHHNHCOCH}(-\text{CH}_2)\text{NH}-$), 2.96 (d, $-\text{NHCONHCH}_2-$), 1.84 (m, $-\text{CHHCH}_2\text{CH}_2\text{CH}(\text{NH}-)\text{CO}-$), 1.74 (d, $-\text{CHHCH}(\text{NH}-)\text{CO}-$), 1.73 (d, $-\text{CHHCH}_2\text{CH}(\text{NH}-)\text{CO}-$), 1.56 (m, $-\text{CHHCH}_2\text{CH}_2\text{CH}(\text{NH}-)\text{CO}-$), 1.33 (m, $-\text{NHCONHCH}_2\text{CH}_2\text{CHH}-$), 1.31 (m, $-\text{NHCONHCH}_2\text{CHHCH}_2-$), 1.28 (m, $-\text{CHHCH}(\text{NH}-)\text{CO}-$), 1.22 (m, $-\text{NHCONHCH}_2\text{CH}_2\text{CHH}-$), 1.23 (m, $-\text{NHCONHCH}_2\text{CHHCH}_2-$) and 1.15 (d, $-\text{CHHCH}_2\text{CH}(\text{NH}-)\text{CO}-$). ^{13}C NMR in d_6 -DMSO: δ ppm = 175,20 (s, $-\text{NHCOCH}(\text{NH}-)\text{CH}_2-$), 156.96 (s, $-\text{NHCONH}-$), 51.91 (s, $-\text{CO}(-\text{CH}_2)\text{CHNHCO}-$), 40.72 (s, $-\text{CH}_2\text{NHCOCH}(-\text{CH}_2)\text{NH}-$), 38.96 (s, -

NHCONHCH₂-), 32.68 (s, -CH₂CH(NH-)CO-), 29.95 (d, -NHCONHCH₂CH₂-), 28.84 (s, -CH₂CH₂CH(NH-)CO-), 27.67 (s, -CH₂CH₂CH₂CH(NH-)CO-), 26.09 (s, -NHCONHCH₂CH₂CH₂-).

Synthesis of bis-*N*(2-oxo-3-azepanyl)-1,6-tetramethylenediamide (3). A 500-mL, three-necked flask, equipped with a magnetic stirbar, is charged with 100 mL of freshly distilled dry DCM, 12.8 g (100 mmol) of α -amino- ϵ -caprolactam (**1**) and 14 mL (100 mmol) of triethylamine. Then, a solution of 6.9 mL (47.6 mmol) of adipoyl chloride in 15 mL of DCM was added over 30 min via an addition funnel. The reaction mixture was stirred for 16h at 20°C. The insoluble product was recovered by filtration, and the crude product washed several times with ethanol or DCM to remove residue of triethyl ammonium chloride salt. The final product was recovered from the crude material by removal of the solvent to constant weight. The final yield of the product is 95%. ¹H NMR in d₆-DMSO: δ ppm = 7.83 (t, -CH₂NHCOCH(CH₂-)NH-), 7.79 (d, -COCH(CH₂-)NHCO-), 4.44 (m, -COCH(CH₂-)NHCO-), 3.23 (m, -CHHNHCOCH(CH₂-)NHCO-), 3.11 (m, -CHHNHCOCH(CH₂-)NHCO-), 2.2 (d, -CO(CH₂-)CHCOCH₂-), 1.92 (d, -COCH(CHH-)NHCO-), 1.8 (d, -CH₂CH₂NHCOCH(CH₂-)NHCO-), 1.68 (d, -COCH (CHH-)NHCO-), 1.51 (s, -COCH(CH₂-)NHCOCH₂CH₂-), 1.44 (m, -CHHCH₂CH(-CO)NHCO-), 1.23 (m, -CHHCH₂CH(-CO)NHCO-). ¹³C NMR in d₆-DMSO: δ ppm = 174.29 (s, -NHCOCH(NH-)CH₂-), 171.02 (s, -NHCOCH₂-), 51.18 (s, -NHCOCH(CH₂-)NHCO-), 40.59 (s, -CH₂NHCOCH(NH-)CH₂-), 34.85 (s, -NHCOCH₂-), 31.22 (s, -NHCOCH(CH₂-)NHCO-), 28.83 (s, -CH₂CH₂CH₂CH(CO-)NHCO-), 27.63 (s, -CH₂CH₂CH(NH-)CO-) and 24.85 (s, -NHCOCH₂CH₂-).

Synthesis of 1,1'-hexamethylenebis(3-*tert*-butylurea). In 40 mL dichloromethane, the synthesis of 1,1'-hexamethylene bis(3-*tert*-butylurea) by the reaction of 1.6 mL (10 mmol) of hexamethylenediisocyanate with 4.2 mL (40 mmol) of *t*-butylamine was identical to the preparation of (**2**). The white precipitate formed was filtered on fritted funnel, rinse with dichloromethane (3x50 mL) and recrystallized in ethanol at room temperature. The final product was recovered from the crude material by removal of the solvent under vacuum to constant weight. The final yield of the product is 73%. ¹H NMR (300 MHz, d₆-DMSO): δ ppm = 5.55 (s, (CH₃)₃C-HNCONH-CH₂-), 5.65 (s, (CH₃)₃C-HNCONH-CH₂-), 2.95 (t, (CH₃)₃C-HNCONH-CH₂-), 1.36 (p, -HNCONH-CH₂-CH₂-CH₂-CH₂-CH₂-CH₂-HNCONH-), 1.27 (p, (-HNCONH-CH₂-CH₂-CH₂-CH₂-CH₂-HNCONH-), 1.24 (s, -HNCONH-CH₂-CH₂-CH₂-CH₂-CH₂-CH₂-HNCONH-).

General procedure for the anionic homo- and copolymerization of CL-type monomer(s).

All polymerization reactions were carried out in bulk under dry nitrogen atmosphere in a 50 mL dry-clean glass tube reactor equipped with outer double jacket and sealed with a greaseless Teflon stopcock fitted with a 0.5 mm NiCr-Ni thermocouple type K (ALMEMO) to monitor calorimetrically the content of the reagent tube at temperatures ranging from 90 °C to 180 °C, using a Julabo heating oil circulator. In all experiments, the 50 mL glass tube reactor was flamed and cooled down under dry nitrogen atmosphere prior to introduction of monomer(s), initiator and activator (chapter II, FigureII-S2).

In typical experiments, 6.38 g of CL and 0.89 g (1.185 mmol) of initiator in CL (C10) were introduced into the reactor. The oil from the thermo-stated bath was continually passed through the outer double jacket. When the system was balanced to the temperature of polymerization, 0.417 g (0.845 mmol) of C20 (multiply by 0.17 (17%) = 0.0710 g of NCO functions or active chain ends = 1.690 = 2x0.845 mmol) was injected into molten initiator/monomer mixture for a total amount of polymerizing materials of $\sim 7.7 \pm 0.1$ g. After a proper interval, the polymerization was quenched by cooling the glass tube reactor into liquid nitrogen. The extraction of monomer and initiator residue was carried out in water heated under reflux for 48h. The polymer was dried in the oven at 110 °C by removal of the solvent to constant weight. The polymer yield was determined gravimetrically. As an example the results obtained with this run at 140 °C were as followed: $t = 19$ min, conversion = 99.7 %, $\overline{Mn}_{(SEC)} = 26\ 000\ \text{g}\cdot\text{mol}^{-1}$ and $D = 4$ (Sample PA6 0.1, **Table III-1**).

Representative synthetic procedure for the anionic copolymerization of CL with (2) at 140°C. This study was carried out as described above by adding the reagents as followed: CL, (2) and C10 were introduced into the reactor followed, when the system is balanced to 140 °C, by the addition of C20 for a total amount of polymerizing materials of ~ 7.5 -8 g. As an example (PA6 2.4): $[\text{CL}]_0 = 8.081\ \text{M}$, $[(2)]_0 = 55.3\ \text{mM}$, $[\text{C10}]_0 = 153.7\ \text{mM}$, $[\text{C20}]_0 = 109.6\ \text{mM}$, polymerization time = 26 min, conversion = 94.8%, $Q_{\text{HFIP}} = 58$ (swelling in HFIP).

Representative synthetic procedure for the anionic copolymerization of CL with (3) at 140 °C. This study was carried out as described above by adding the reagents as followed: CL, (3) and C10 were introduced into the reactor followed, when the system is balanced to

140°C, by the addition of C20 for a total amount of polymerizing materials of ~ 7.5-8 g. As an example (PA6 3.8): $[CL]_0 = 8.01 \text{ M}$, $[(\mathbf{3})]_0 = 147.2 \text{ mM}$, $[C10]_0 = 158.9 \text{ mM}$, $[C20]_0 = 57.3 \text{ mM}$, polymerization time = 30 min, conversion = 99.7%, $Q_{\text{HFIP}} = 36$ (swelling in HFIP), $(G')_{\omega=0.1 \text{ rad/s}} = 1.710^5 \text{ Pa}$ ($(G'/G'')_{\omega=0.1 \text{ rad/s}} = 27$).

Swelling test of crosslinked PA6 in HFIP at 20 °C. The state of swelling of the crosslinked PA6 was characterized by the degree of swelling at the equilibrium Q_{HFIP} . Q_{HFIP} is defined as the ratio between the final (swollen) volume V_f in HFIP and the initial (collapsed) volume V_i and may equally be given, according to the eq. (1), as the ratio between the weight fractions of the network in the initial and final gel, m_i and m_f , respectively; where ρ_{HFIP} (=1.45 g/mL) and ρ_{PA6} (1.14 g/mL) are the density of the solvent and the linear PA6 obtained by anionic polymerization, respectively.

Synthesis of α -cinnamoylamido- ϵ -caprolactam. To the solution of cinnamoyl chloride (5.2 g, 30mmol) and triethylamine (5.05 g, 50 mmol) in 50 mL of tetrahydrofuran (THF) cooled in an ice bath α -amino caprolactam (4 g, 30 mmol) was added dropwise while purging the reaction flask with argon. After 15 min, the ice bath was removed and the reaction was allowed to proceed overnight at room temperature. The precipitate was removed by filtration, then THF was evaporated and the product was resolved in chloroform. The solution was transferred to an extraction funnel and washed with dilute HCl (aq) (1×50 mL), distilled water (1×50 mL), and brine solution (1×50 mL), respectively. The organic phase was separated, dried over anhydrous Na_2SO_4 , filtered and evaporated. The product was further purified by recrystallization with diethyl ether to give a white powder (80% yield). $^1\text{H NMR}$ (CDCl_3) δ (ppm) = 7.26-7.49 (m, 5H), 7.64 (d, 1H), 7.07 (s, 1H), 6.5 (d, 1H), 4.6 (m, 1H), 3.3 (m, 2H), 2.3-1.2 (m, 6H).

Synthesis of polyamide 6. Polyamide 6 was prepared in bulk by anionic ring-opening polymerization. ϵ -Caprolactam (8.35 g, 73.8 mmol) and C10 (1.15 g, 8.5 mmol) were added in a glass reactor at 140 °C under nitrogen atmosphere. After C20 (0.5 g, 1.26 mmol) was added to the molten mixture, the polymerization started with solidification. After reaction, the polymer obtained was crushed and refluxed in water and then dried in an oven overnight at

90°C under vacuum before analysis. Conversion of the monomer was determined gravimetrically (**Table III-3**).

Synthesis of polyamide 6 bearing cinnamoyl groups. Polyamide 6 pendant cinnamoyl group was prepared by a one-step pathway by anionic ring-opening polymerization. α -cinnamoylamido- ϵ -caprolactam (0.2 g, 0.77 mmol), ϵ -caprolactam (8.15 g, 72 mmol) and C10 (1.15 g, 8.5 mmol) were added to a glass reactor under nitrogen atmosphere and were molten at 140 °C with continuous stirring after C20 (0.5 g, 1.26 mmol) was added to the mixture to start the polymerization. After reaction, all polymers were refluxed in water first and followed by washing with dichloromethane. The polymers were dried in an oven overnight at 90 °C under vacuum before any analysis. Conversions of the monomers were determined gravimetrically.

Synthesis of truxillic Acid⁵⁸. Trans-cinnamic acid (Aldrich, 99%) was recrystallized from acetone (Aldrich) to obtain the α -polymorph. The crystals (2 g, 13.5 mmol) were put in a reactor and distributed in 8 ml of heptane. The powder sample in solid state was exposed to 325-380 nm irradiation using a light source which is a 450HHL Halogen 400W for 24 h to obtain truxillic acid. It was confirmed by solid state ¹³C NMR.

Decrosslinking of polyamide 6. The 1.2×10^{-4} mol.L⁻¹ gel-solution of cinnamoyl-containing crosslinked polyamide 6 (%10Cin-PA6) in HFIP was prepared before irradiation. To induce the decrosslinking reaction, the sample was irradiated with a UV lamp TQ 150: 150W $\lambda = 200$ -280 nm at 25 °C for 7h and the distance between the sample and the light source was 4 cm. Absorbance increasing of cinnamoyl unit was followed by UV-absorbance.

Recrosslinking of polyamide 6. After 7h de-crosslinking of cinnamoyl pendent polyamide 6 solution (10%Cin-PA6), solvent was evaporated and 1% w/v of HFIP solutions of cinnamoyl-containing de-crosslinked polyamide 6 was prepared and spin-coated on quartz plate. Irradiations under re-crosslinking conditions were carried out placing the samples at 10 cm from the light source which is a 450HHL Halogen 325-380nm 400W. Following 7h irradiation, recrosslinking was completed with 1h heating at 140 °C. Absorbance decreasing of cinnamoyl unit was followed by UV-absorbance. The coated sample was not soluble in HFIP after re-crosslinking.

Annexe: Supporting Information

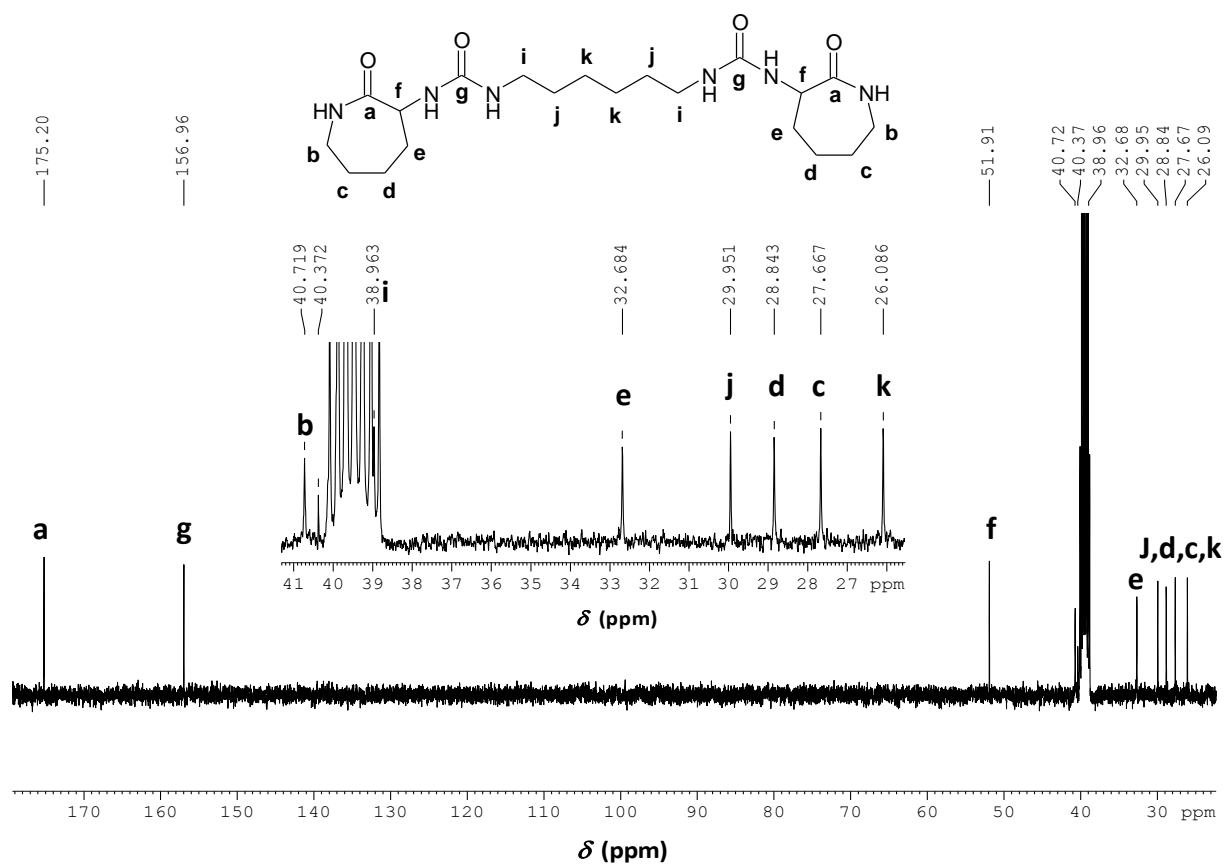


Figure III-S1. ^{13}C NMR (75 MHz, $\text{d}_6\text{-DMSO}$) spectrum of 1,1'-hexamethylenebis(2-oxo-3-azepanylurea)(2).

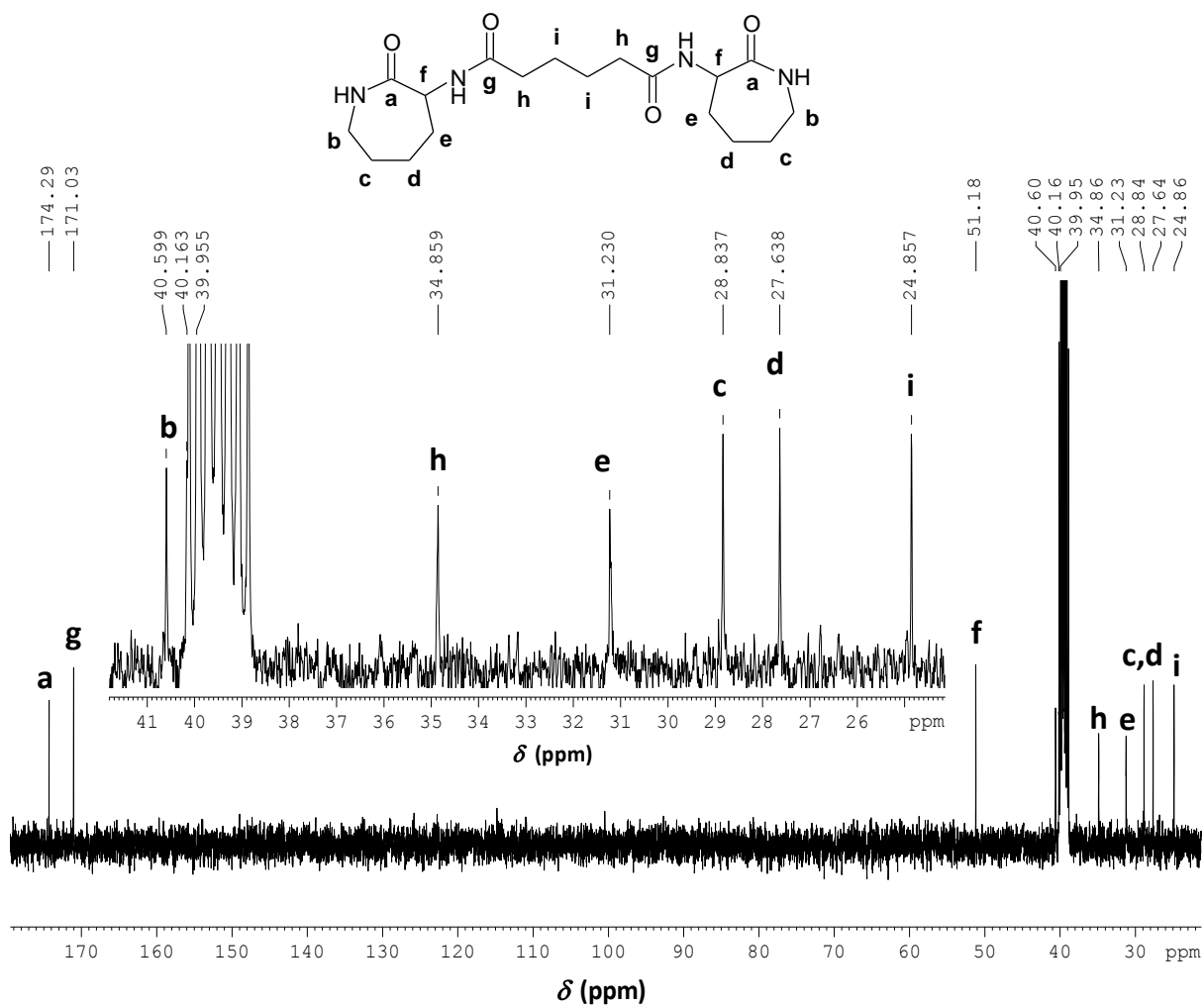


Figure III-S2. ^{13}C NMR (75 MHz, $\text{d}_6\text{-DMSO}$) spectrum of bis-*N*(2-oxo-3-azepanyl)-1,6-tetramethylenediamide(3).

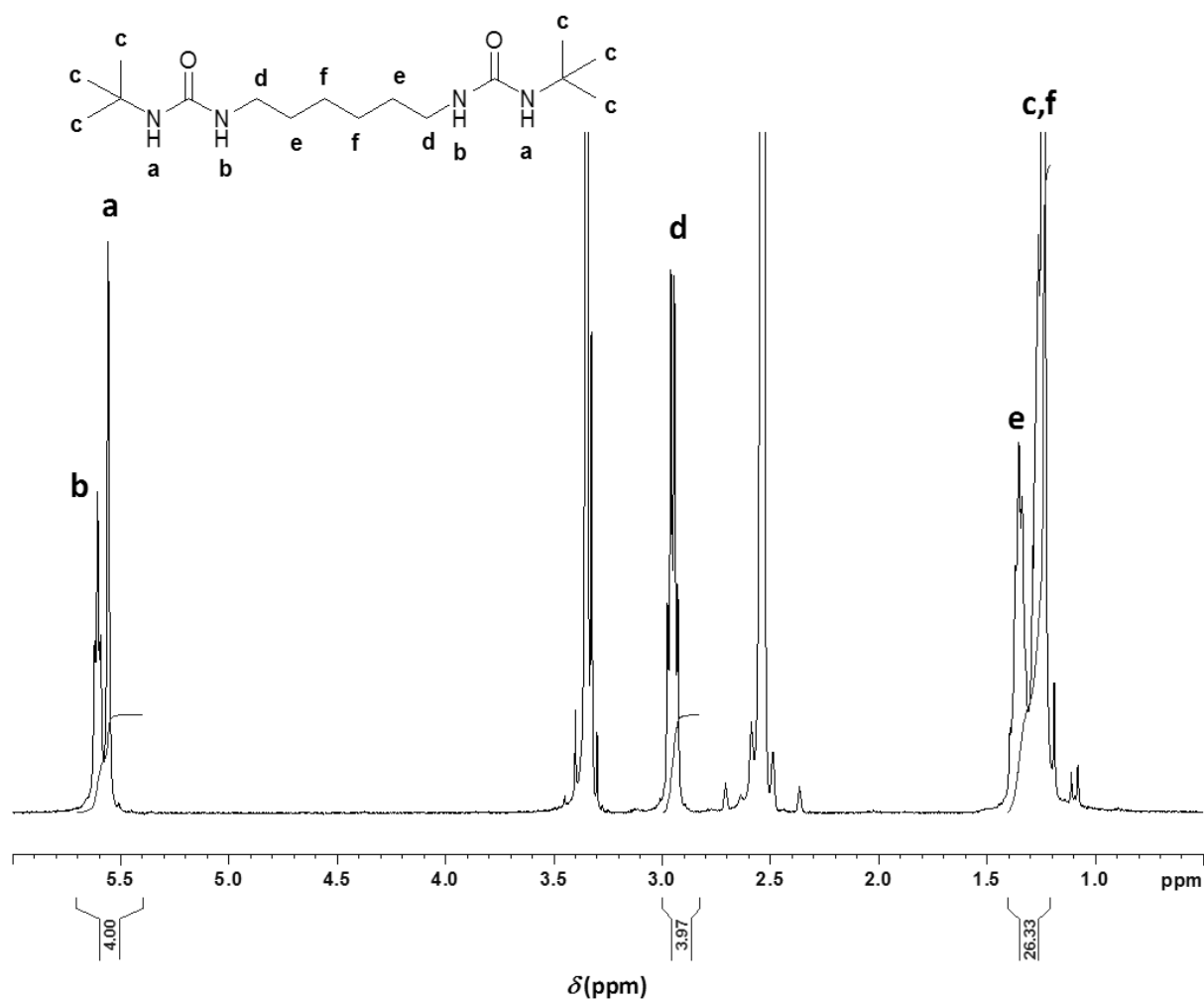


Figure III-S3. ¹H NMR (300 MHz, d₆-DMSO) spectrum of 1,1'-hexamethylenebis(3-tert-butylurea). For additional experimental information see experimental conditions.

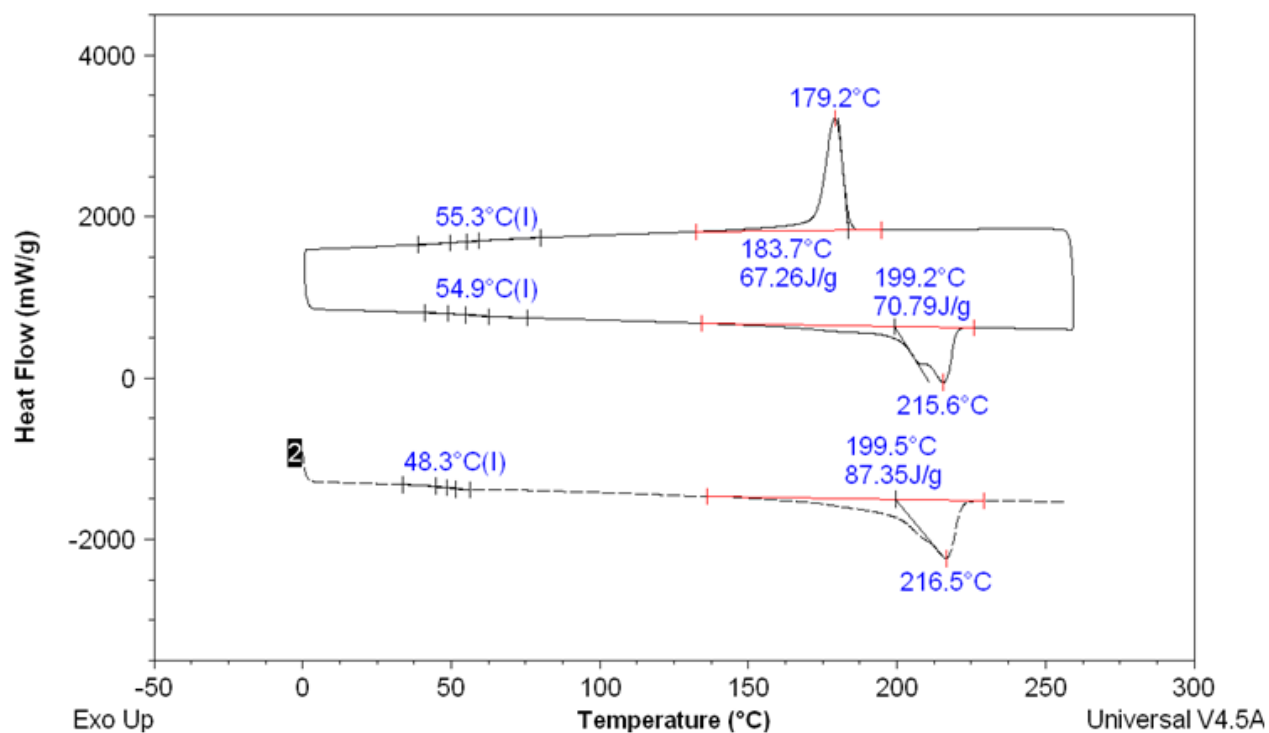


Figure III-S4. DSC thermogram (---) first and (—) heating cycle of a PA6 (**sample PA6 0.1, Table III-2**) obtained by anionic bulk homopolymerization of 62.53 mmol of ϵ -caprolactame (CL) (*i.e.* for a targeted DP of 74) initiated by 0.85 mmol of *N,N'*-hexamethylenebis(2-oxo-1-azepanylcarboxamide (C20) in the presence of 1.185 mmol of sodium ϵ -caprolactamate (C10) at $T_p = 140^\circ\text{C}$. Polymerization yield = +99.7%. The polymerization was carried out according to the general procedure for the anionic homo- and copolymerization of CL-type monomer(s).

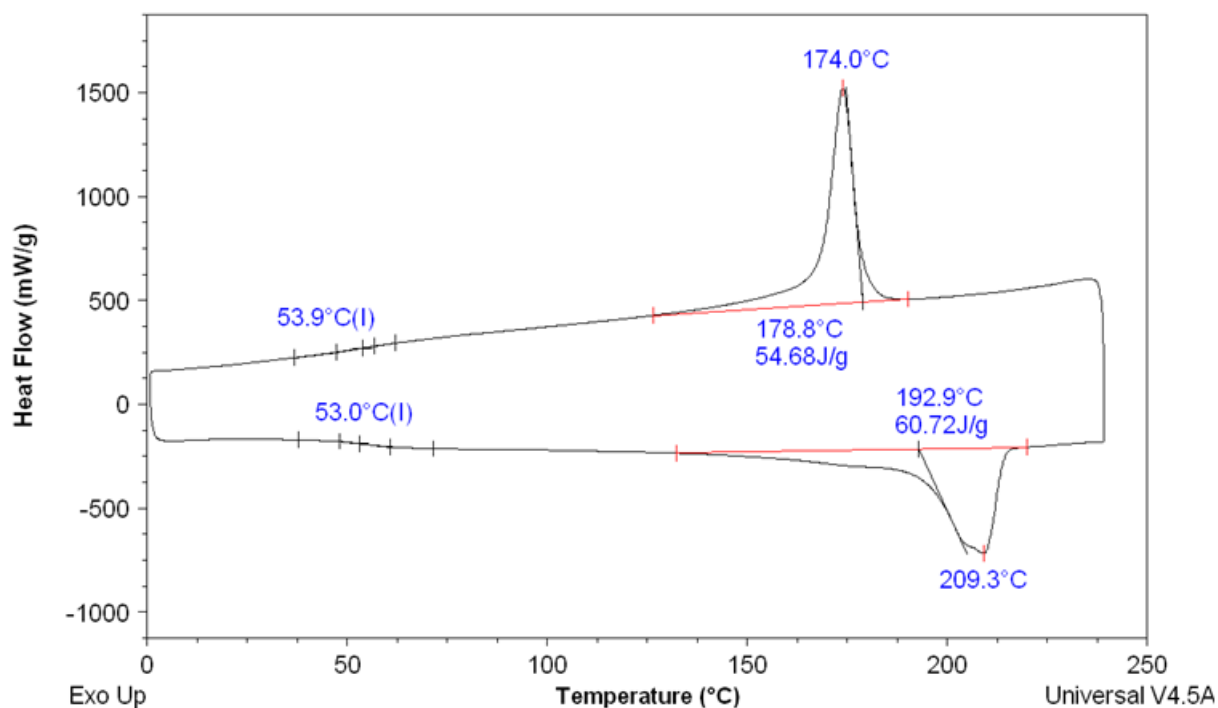


Figure III-S5. DSC thermogram first cooling and second heating runs ($10\text{ }^{\circ}\text{C}\cdot\text{min}^{-1}$) of a cross-linked PA6 (**sample PA6 3.7**, **Table III-2**) obtained by anionic bulk copolymerization of 61.96 mmol of ϵ -caprolactame (CL) with 0.566mmol of bis-*N*(2-oxo-3-azepanyl)-1,6-tetramethylenediamide (**3**) at $F_{(3)} = 0.9\%$ (*i.e.* for a targeted DP of 74) initiated by 0.845 mmol of *N,N'*-hexamethylenebis(2-oxo-1-azepanylcarboxamide (C20) in the presence of 1.185 mmol of sodium ϵ -caprolactamate (C10) at $T_p = 140\text{ }^{\circ}\text{C}$. Polymerization yield = 99.5%. The polymerization was carried out according to representative synthetic procedure for the anionic copolymerization of CL with (**3**).

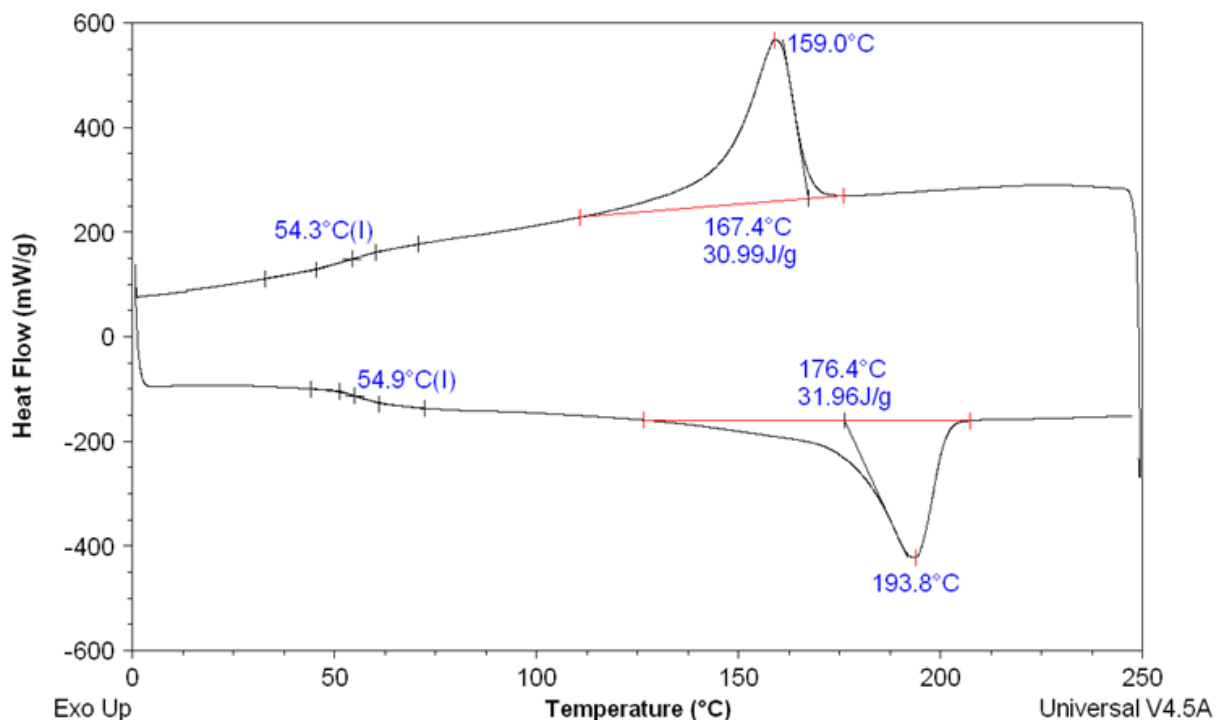


Figure III-S6: DSC thermogram first cooling and second heating runs ($10\text{ }^{\circ}\text{C}\cdot\text{min}^{-1}$) of a cross-linked PA6 (**sample PA6 3.5, Table III-2**) obtained by anionic bulk copolymerization of 61.4 mmol of ϵ -caprolactame (CL) with 1.132 mmol of bis-*N*(2-oxo-3-azepanyl)-1,6-tetramethylenediamide (**3**) at $F_{(3)} = 1.84\%$ (*i.e.* for a targeted DP of 74) initiated by 0.845 mmol of *N,N'*-hexamethylenebis(2-oxo-1-azepanylcarboxamide (C20) in the presence of 1.185 mmol of sodium ϵ -caprolactamate (C10) at $T_p = 140\text{ }^{\circ}\text{C}$. Polymerization yield = 98.4%. The polymerization was carried out according to the representative synthetic procedure for the anionic copolymerization of CL with (**3**).

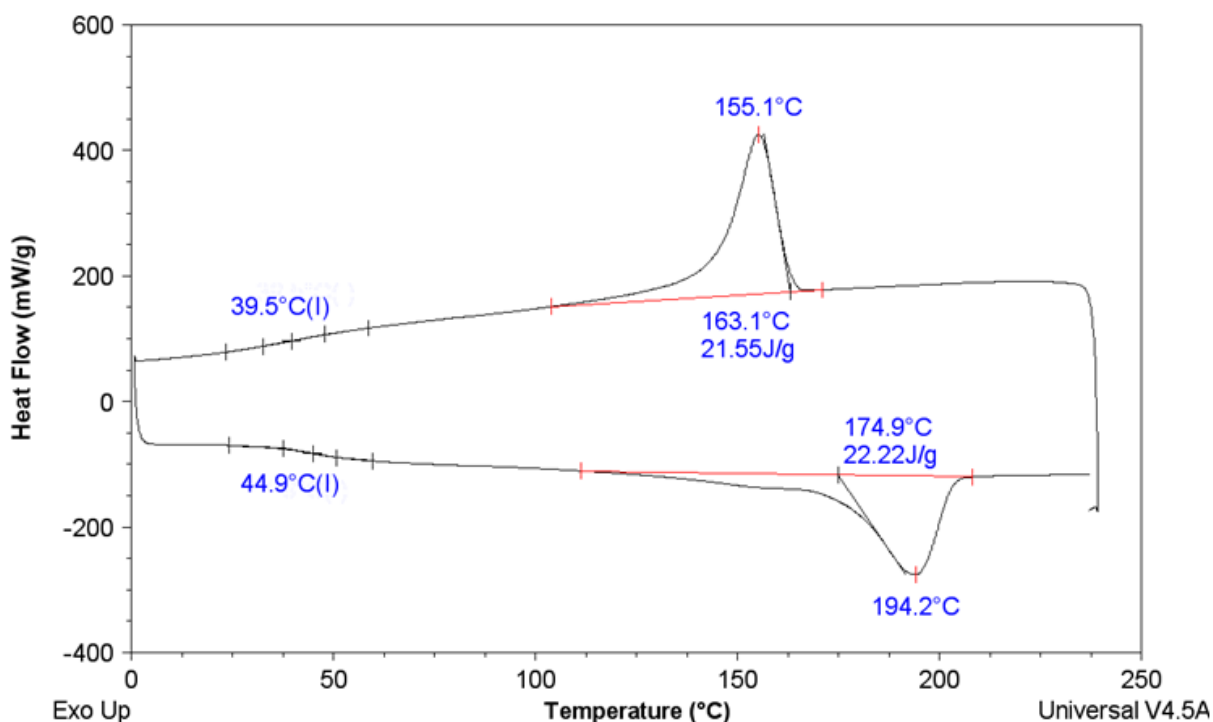


Figure III-S7: DSC thermogram first cooling and second heating runs ($10\text{ }^{\circ}\text{C}\cdot\text{min}^{-1}$) of a cross-linked PA6 (sample R3.3) obtained by anionic bulk copolymerization of 60.84 mmol of ϵ -caprolactame (CL) with 1.690 mmol of bis-*N*(2-oxo-3-azepanyl)-1,6-tetramethylenediamide (**3**) at $F_{(3)} = 2.83\%$ (*i.e.* for a targeted DP of 74) initiated by 0.845 mmol of *N,N'*-hexamethylenebis(2-oxo-1-azepanylcarboxamide (C20) in the presence of 1.185 mmol of sodium ϵ -caprolactamate (C10) at $T_p = 140\text{ }^{\circ}\text{C}$. Polymerization yield = 98.5%. The polymerization was carried out according to the representative synthetic procedure for the anionic copolymerization of CL with (**3**).

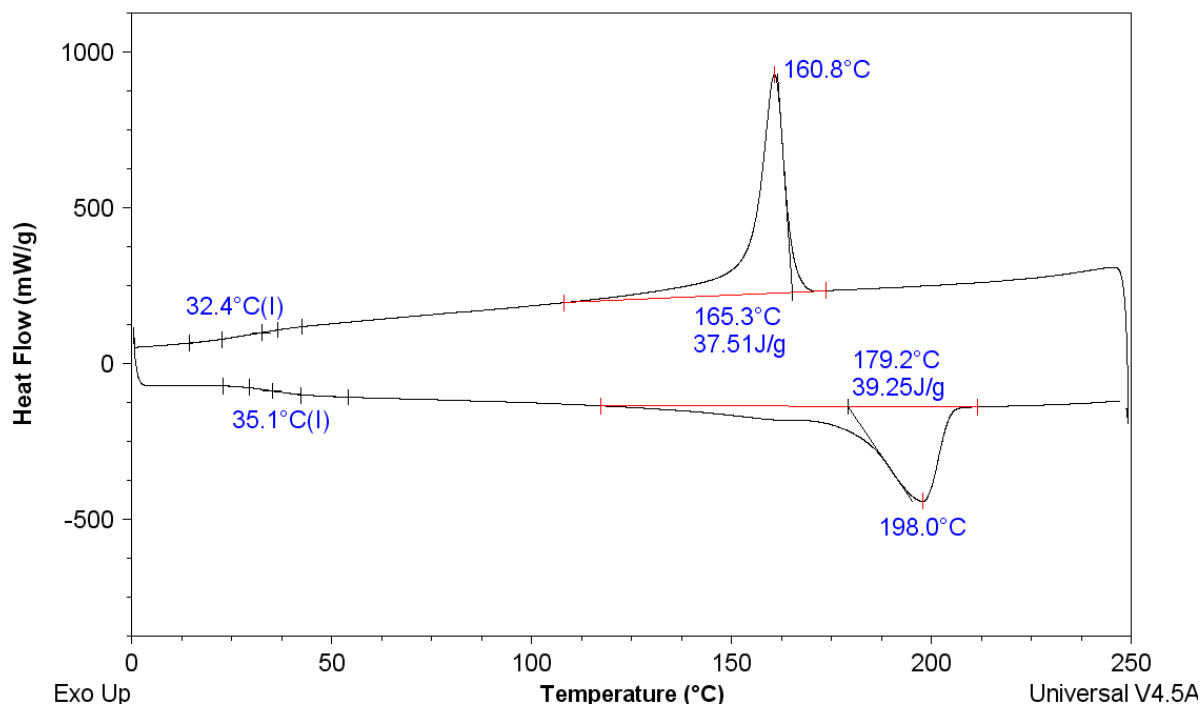


Figure III-S8: DSC thermogram first cooling and second heating runs ($10\text{ }^{\circ}\text{C}\cdot\text{min}^{-1}$) of a cross-linked PA6 (**sample PA6 3.8**, **Table III-2**) obtained by anionic bulk copolymerization of 60.62 mmol of ϵ -caprolactame (CL) with 1.145 mmol of bis-*N*(2-oxo-3-azepanyl)-1,6-tetramethylenediamide (**3**) at $F_{(3)} = 1.8\%$ (*i.e.* for a targeted DP of 145) initiated by 0.426 mmol of *N,N'*-hexamethylenebis(2-oxo-1-azepanylcarboxamide (C20) in the presence of 1.185 mmol of sodium ϵ -caprolactamate C10 at $T_p = 140\text{ }^{\circ}\text{C}$. Polymerization yield = +99.7%. The polymerization was carried out according to the representative synthetic procedure for the anionic copolymerization of CL with (**3**).

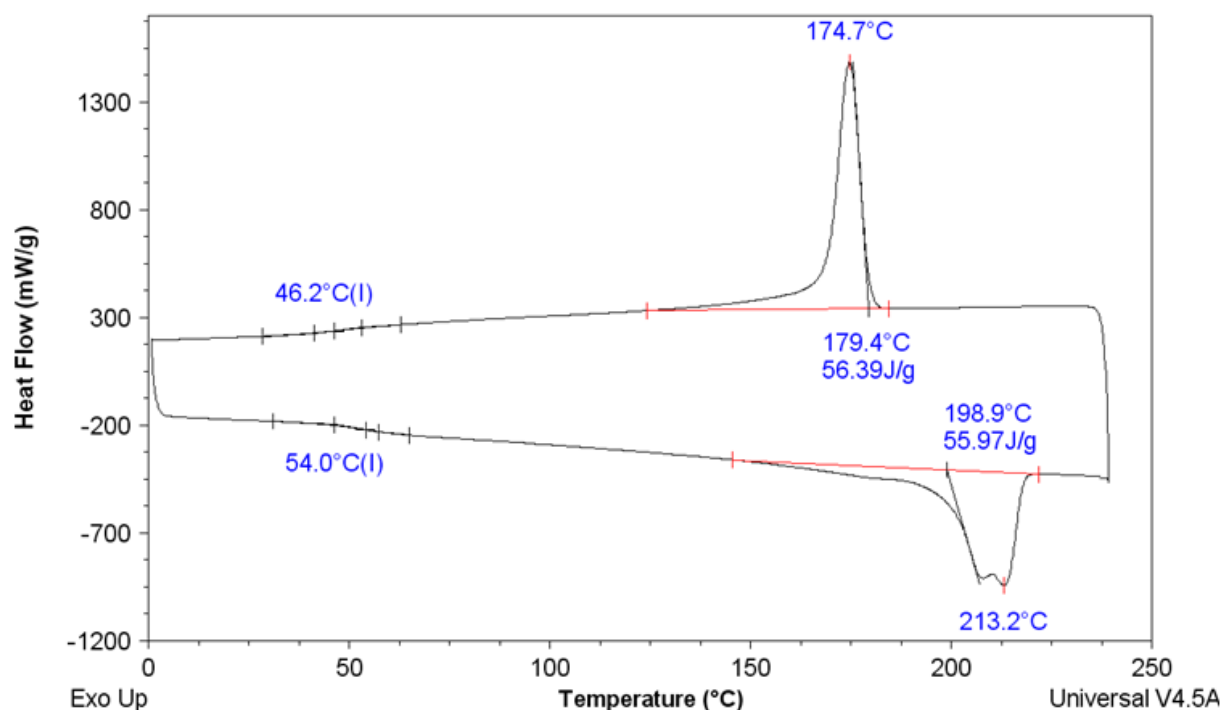


Figure III-S9: DSC thermogram (---) first and (—) heating cycle of a cross-linked PA6 (**sample PA6 3.10, Table III-2**) obtained by anionic bulk copolymerization of 57.75 mmol of ϵ -caprolactame (CL) with 0.210 mmol of bis-*N*(2-oxo-3-azepanyl)-1,6-tetramethylenediamide (**3**) at $F_{(3)} = 0.32\%$ (*i.e.* for a targeted DP of 552) initiated by 0.105 mmol of *N,N'*-hexamethylenebis(2-oxo-1-azepanylcarboxamide (C20) in the presence of 1.185 mmol of sodium ϵ -caprolactamate (C10) at $T_p = 140$ °C. Polymerization yield = 99.2%. The polymerization was carried out according to the representative synthetic procedure for the anionic copolymerization of CL with (**3**).

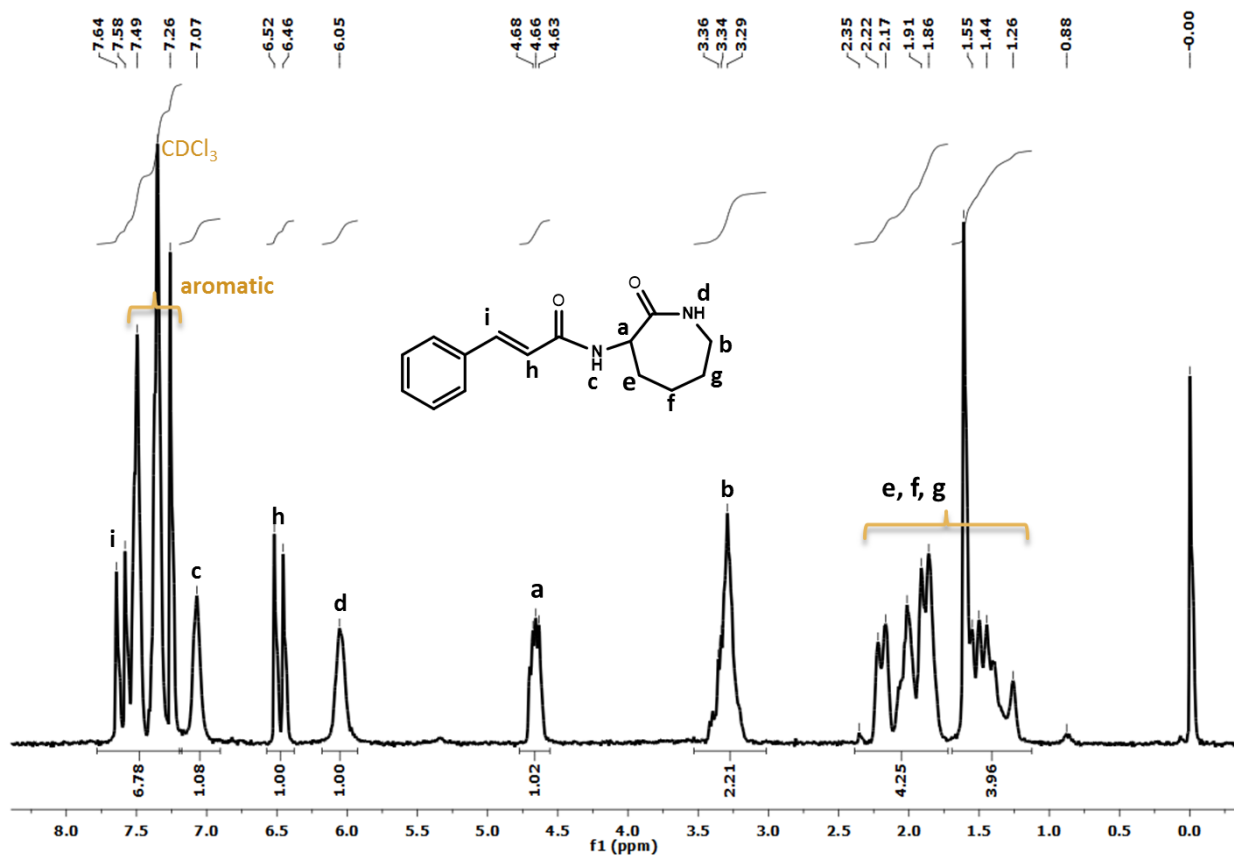


Figure III-S10. ^1H NMR of α -cinnamoylamido- ϵ -caprolactam in CDCl_3 .

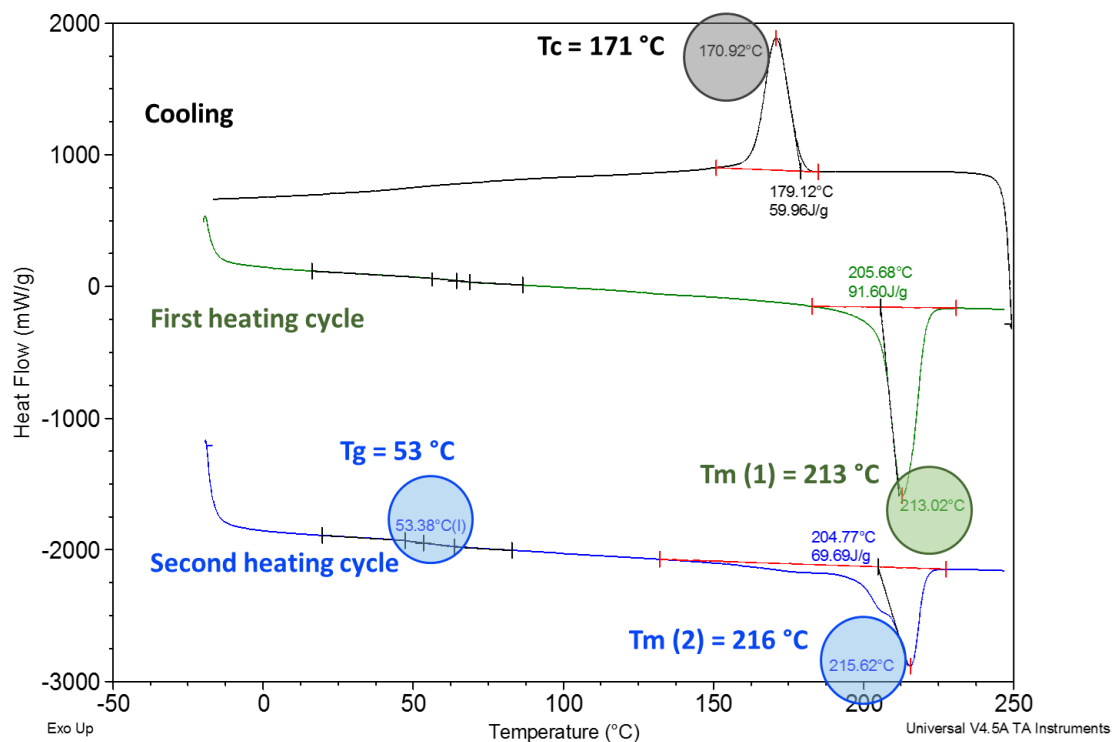


Figure III-S11. DSC thermogram of PA6.

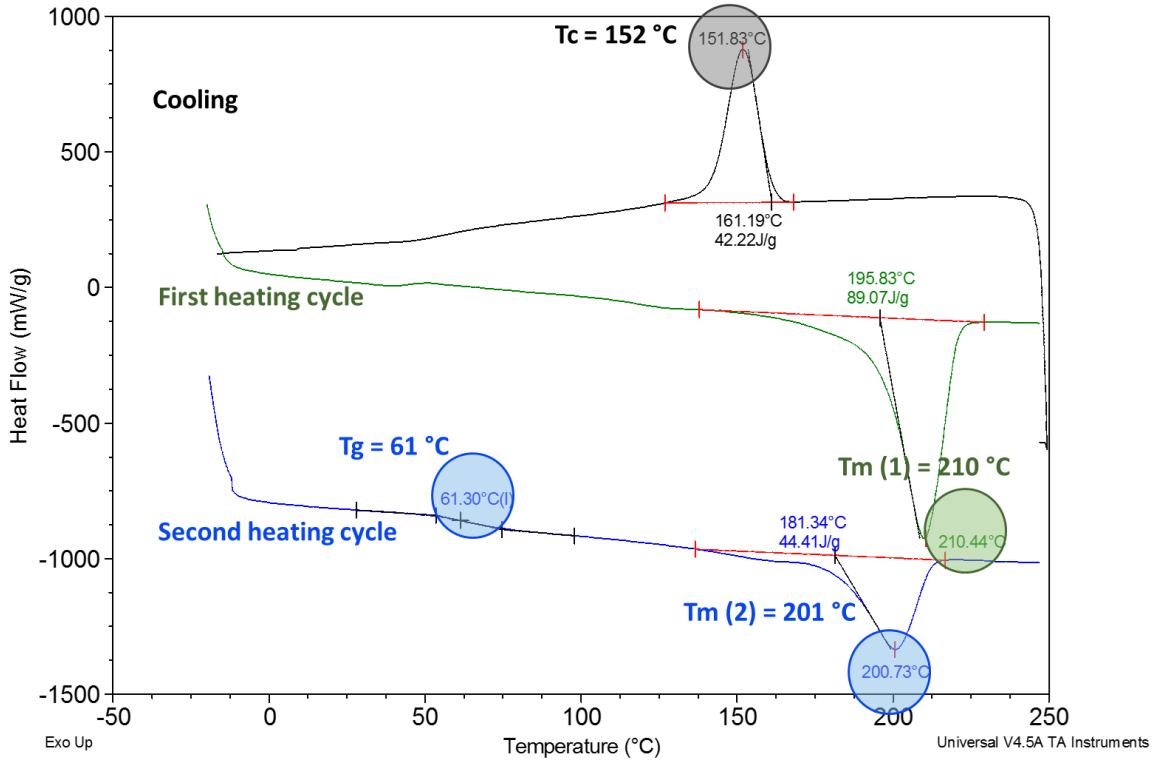


Figure III-S12. DSC thermogram of 10% Cin-PA6.

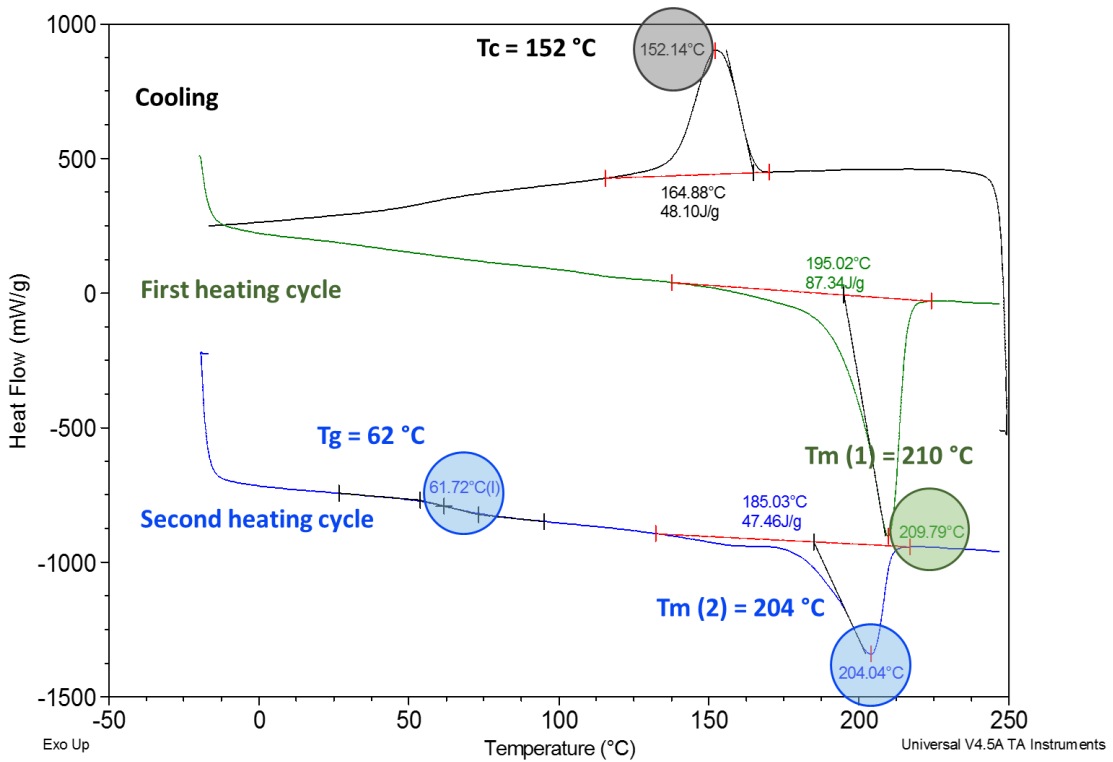


Figure III-S13. DSC thermogram 6% Cin-PA6.

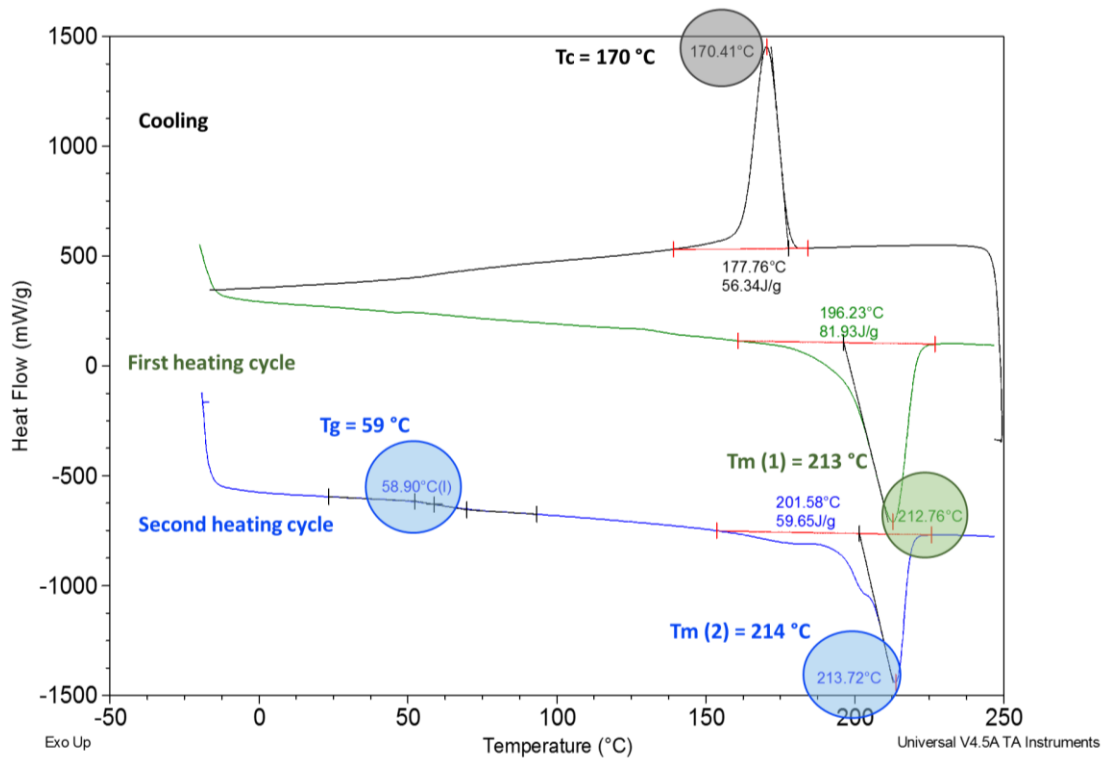


Figure III-S14. DSC thermogram 2%Cin-PA6.

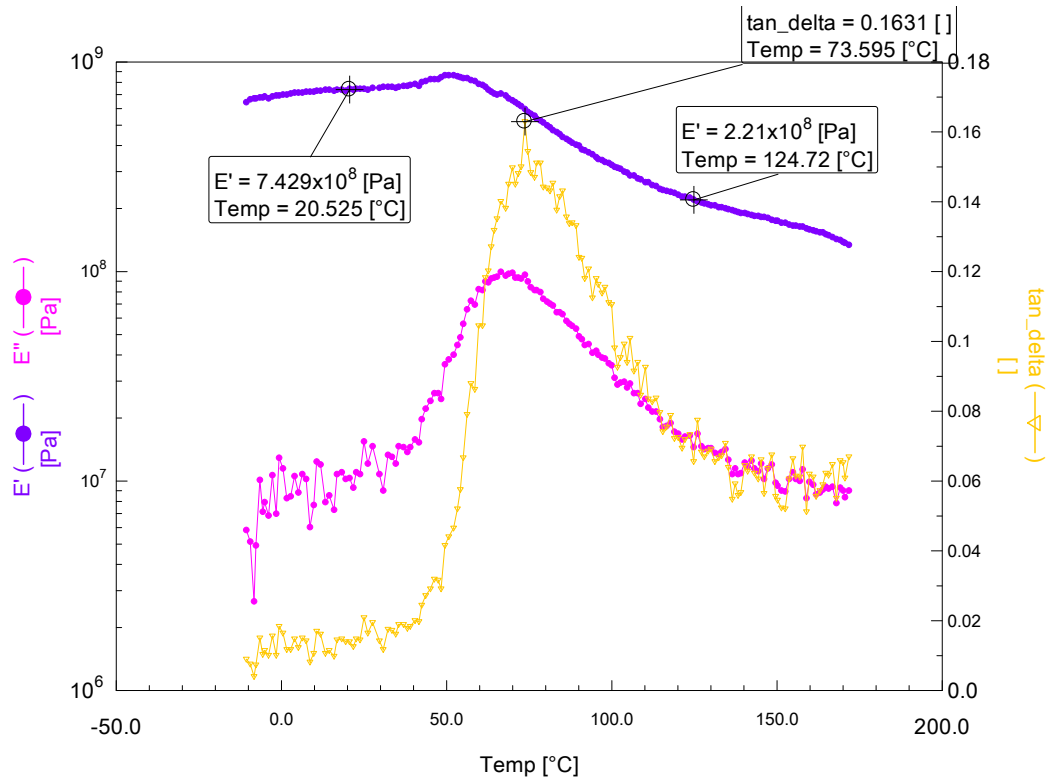


Figure III-S15. DMA thermogram 2%Cin-PA6.

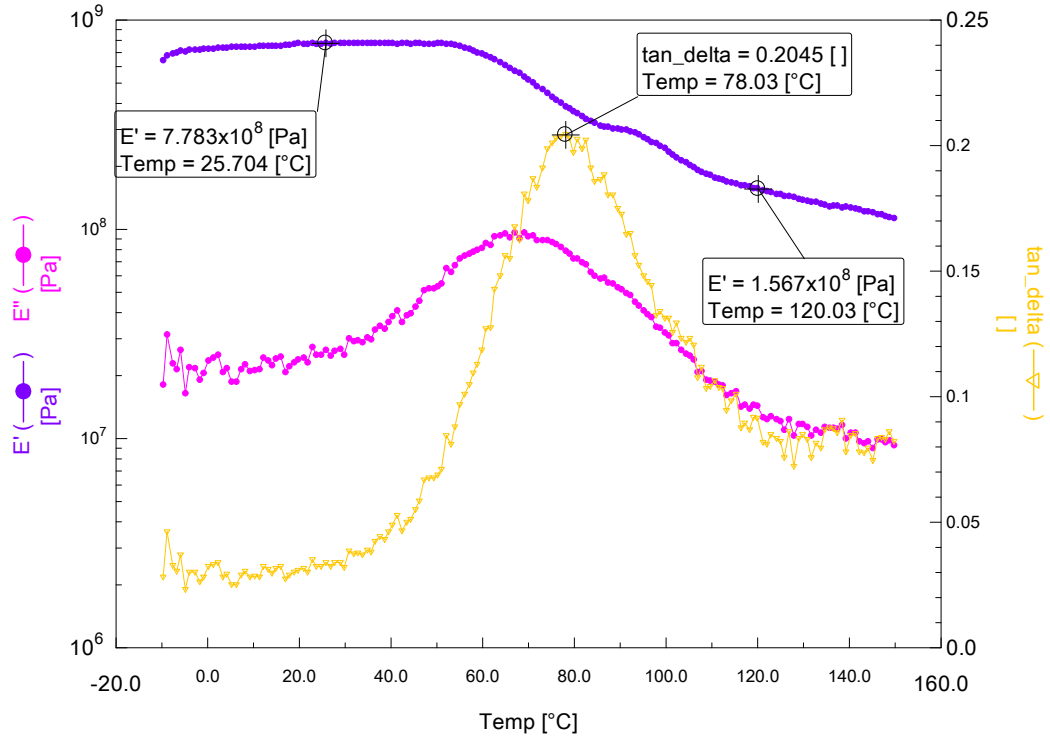


Figure III-S16. DMA thermogram 6% Cin-PA6.

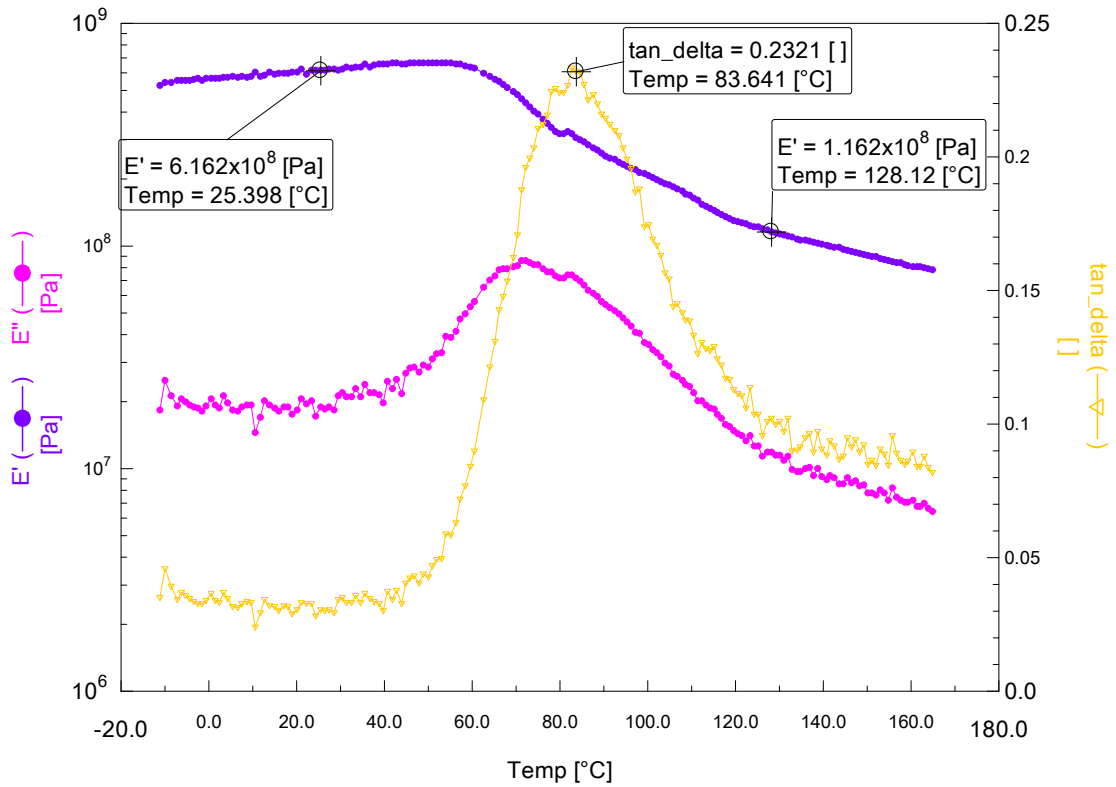


Figure III-S17. DMA thermogram 10% Cin-PA6.

References

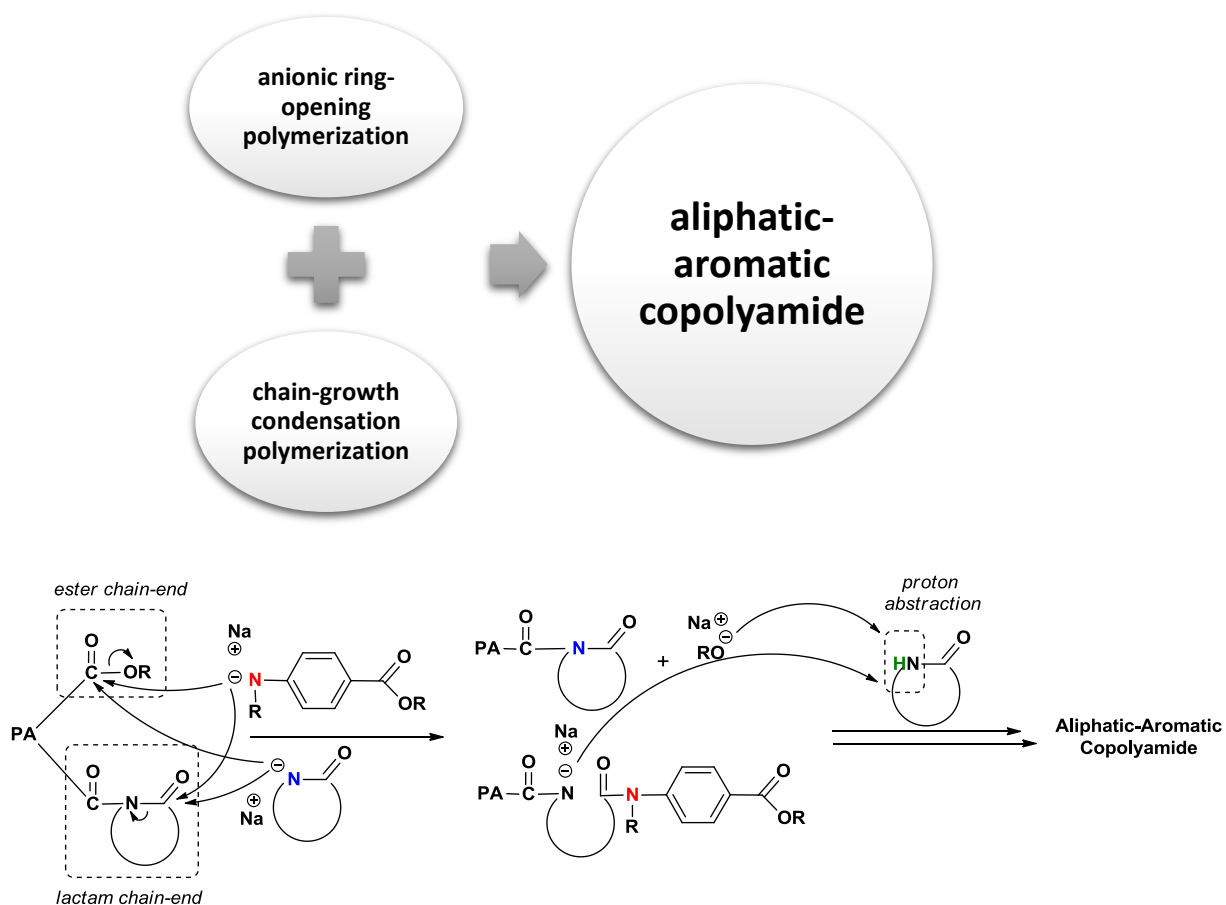
1. W. E. Hanford and R. M. Joyce, *Journal of Polymer Science*, 1948, **3**, 167-172.
2. J. Šebenda, in *Comprehensive Chemical Kinetics*, ed. T. Bamford C. H., C. F. H., Elsevier, Amsterdam, 1976, vol. 15, pp. 401-435.
3. J. A. N. Šebenda, *Journal of Macromolecular Science: Part A - Chemistry*, 1972, **6**, 1145-1199.
4. J. Roda, in *Handbook of Ring-Opening Polymerization*, ed. P. Dubois, Coulembier, O. Raquez, J. M., Wiley-VCH Verlag GmbH & Co. KGaA, Weinheim, 2009, pp. 165-192.
5. M. Kohan, in *Nylon Plastic Handbook*, ed. M. I. Kohan, Heuer New York, 1995, p. 631.
6. G. C. C. Alfonso, C.; Razore, S., in *Polymer Chemistry and Engineering*, ed. Kresta J. E., American Chemical Society Symposium Series, Washington D. C., 1985, vol. 270, pp. 163-179.
7. C. C. G. Alfonso, S. Razore, S. Russo, in *ACS Symposium Series, No. 270*, ed. K. J., American Chemical Society, Washington, DC,, 1985, p. 163.
8. R. S. Kubiak, *Plast. Eng.*, 1980, **36**, 55-61.
9. P. D. J. Coates, A. F. , *Plast. Rubber Proc. App.*, 1981, **1**, 223-238.
10. J. Šebenda, in *Comprehensive polymer Science*, ed. G. C. Eastmond, Ledwith, A., Russo, S., Sigwalt, P., Pergamon Press, London, 1989, vol. 3.
11. J. Stehlíček, B. Valter and J. Šebenda, *Die Makromolekulare Chemie*, 1986, **187**, 513-524.
12. J. Stehlíček and T. Šebenda, *European Polymer Journal*, 1986, **22**, 5-11.
13. C. Stehliceck J., P., Šebenda J., *Nuova Chimica*, 1973, **49**, 77-80.
14. J. Stehlíček, P. Čefelín and J. Šebenda, *Journal of Polymer Science: Polymer Symposia*, 1973, **42**, 89-94.
15. Š. J. Bukač Z., *Collect. Czech. Chem. Commun.* , 1967, **32**, 3537-3545.
16. T. J. Bukač Z., Šebenda J., *Collect. Czech. Chem. Commun.*, 1969, **34**, 2057-2064.
17. E. Tarkin-Tas and L. J. Mathias, *Macromolecules*, 2009, **43**, 968-974.
18. L. Chikh, X. Arnaud, C. Guillermain, M. Tessier and A. Fradet, *Macromolecular Symposia*, 2003, **199**, 209-222.
19. A. J. Nijenhuis, WO02/44246A1, 2002.
20. H. K. Reimschuessel, *Macromol. Synth.*, 1982, **8**, 37.
21. K. Reimschuessel Herbert, *USPatent*, US3542744, 1970.
22. K. Reimschuessel Herbert, *USPatent*, US3422093, 1969.
23. K. Reimschuessel Herbert, in *Addition and Condensation Polymerization Processes*, AMERICAN CHEMICAL SOCIETY, 1969, vol. 91, pp. 717-733.
24. H. K. R.-G. Reimschuessel, Luis; Sibilia, John P., *Journal of Polymer Science, Polymer Physics Edition* 1968, **6**, 559-574
25. J. Karger-Kocsis and L. Kiss, *Die Makromolekulare Chemie*, 1979, **180**, 1593-1597.
26. H. K. Reimschuessel, *Journal of Polymer Science: Macromolecular Reviews*, 1977, **12**, 65-139.
27. S. Salvestrini, P. Di Cerbo and S. Capasso, *Journal of the Chemical Society, Perkin Transactions 2*, 2002, 1889-1893.
28. L. Feng, J. Romulus, M. Li, R. Sha, J. Royer, K.-T. Wu, Q. Xu, N. C. Seeman, M. Weck and P. Chaikin, *Nat Mater*, 2013, **12**, 747-753.

29. E. Reichmanis, O. Nalamasu, F. M. Houlihan and A. E. Novembre, *Polymer International*, 1999, **48**, 1053-1059.
30. J. Jang, S. Nam, J. Hwang, J.-J. Park, J. Im, C. E. Park and J. M. Kim, *Journal of Materials Chemistry*, 2012, **22**, 1054-1060.
31. D.-J. Liaw, K.-L. Wang, Y.-C. Huang, K.-R. Lee, J.-Y. Lai and C.-S. Ha, *Progress in Polymer Science*, 2012, **37**, 907-974.
32. D. Shi, M. Matsusaki and M. Akashi, *Bioconjugate Chemistry*, 2009, **20**, 1917-1923.
33. M. Sandholzer, S. Bichler, F. Stelzer and C. Slugovc, *Journal of Polymer Science Part A: Polymer Chemistry*, 2008, **46**, 2402-2413.
34. J. He, X. Tong and Y. Zhao, *Macromolecules*, 2009, **42**, 4845-4852.
35. M. V. Biyani, C. Weder and E. J. Foster, *Polymer Chemistry*, 2014.
36. B. Kiskan and Y. Yagci, *Journal of Polymer Science Part A: Polymer Chemistry*, 2014, **52**, 2911-2918.
37. M. V. Biyani, C. Weder and E. J. Foster, *Polymer Chemistry*, 2014, **5**, 5501-5508.
38. Y. Zheng, M. Micic, S. V. Mello, M. Mabrouki, F. M. Andreopoulos, V. Konka, S. M. Pham and R. M. Leblanc, *Macromolecules*, 2002, **35**, 5228-5234.
39. Y. Sako and Y. Takaguchi, *Organic & Biomolecular Chemistry*, 2008, **6**, 3843-3847.
40. E. Blasco, B. V. K. J. Schmidt, C. Barner-Kowollik, M. Piñol and L. Oriol, *Macromolecules*, 2014, **47**, 3693-3700.
41. Q. Zhang, P. Schattling, P. Theato and R. Hoogenboom, *European Polymer Journal*. doi:10.1016/j.eurpolymj.2014.06.029, in press
42. S.-J. Sung, K.-Y. Cho, J.-H. Yoo, W. S. Kim, H.-S. Chang, I. Cho and J.-K. Park, *Chemical Physics Letters*, 2004, **394**, 238-243.
43. S. W. Lee, S. I. Kim, B. Lee, W. Choi, B. Chae, S. B. Kim and M. Ree, *Macromolecules*, 2003, **36**, 6527-6536.
44. J. Zhu, L.-P. Wu, Y.-Y. Zhang, X. Jin, S.-J. He, K.-Y. Shi, X. Guo, Z.-J. Du and B.-L. Zhang, *Journal of Applied Polymer Science*, 2006, **102**, 4565-4572.
45. N. Kawatsuki, H. Takatsuka, T. Yamamoto and O. Sangen, *Macromolecular Rapid Communications*, 1996, **17**, 703-712.
46. X. Coqueret, *Macromolecular Chemistry and Physics*, 1999, **200**, 1567-1579.
47. C.-M. Chung, Y.-S. Roh, S.-Y. Cho and J.-G. Kim, *Chemistry of Materials*, 2004, **16**, 3982-3984.
48. P. Froimowicz, D. Klinger and K. Landfester, *Chemistry – A European Journal*, 2011, **17**, 12465-12475.
49. A. Garle, S. Kong, U. Ojha and B. M. Budhlall, *ACS Applied Materials & Interfaces*, 2012, **4**, 645-657.
50. G. Rivero, L.-T. T. Nguyen, X. K. D. Hillewaere and F. E. Du Prez, *Macromolecules*, 2014, **47**, 2010-2018.
51. H. J. Ommer and H. Ritter, *Macromolecular Chemistry and Physics*, 1996, **197**, 797-809.
52. S.-J. Sung, D.-H. Kim, M. Kim and K. Cho, *Macromol. Res.*, 2010, **18**, 614-617.
53. K. Khodabakhshi, M. Gilbert, P. Dickens and R. Hague, *Advances in Polymer Technology*, 2010, **29**, 226-236.
54. G. C. Alfonso, G. Bonta, S. Russo and A. Traverso, *Die Makromolekulare Chemie*, 1981, **182**, 929-939.

55. M. Khan, G. Brunklaus, V. Enkelmann and H.-W. Spiess, *Journal of the American Chemical Society*, 2008, **130**, 1741-1748.
56. Y. Nakayama and T. Matsuda, *Journal of Polymer Science Part A: Polymer Chemistry*, 1992, **30**, 2451-2457.
57. P. Froimowicz, M. N. Belgacem, A. Gandini and M. C. Strumia, *European Polymer Journal*, 2008, **44**, 4092-4097.
58. I. Abdelmoty, V. Buchholz, L. Di, C. Guo, K. Kowitz, V. Enkelmann, G. Wegner and B. M. Foxman, *Crystal Growth & Design*, 2005, **5**, 2210-2217.

Chapter IV

Synthesis of Aliphatic-Aromatic Copolyamides by Combination of Anionic Ring Opening Polymerization and Chain-Growth Condensation Polymerization



Keywords : Chain-growth condensation polymerization, anionic ring-opening polymerization, copolymerization, ϵ -caprolactam, aromatic polyamide, polyamide synthesis.

Summary: In this chapter, combination of anionic ring opening polymerization (AROP) and chain-growth condensation polymerization (CGCP) for the synthesis of aliphatic-aromatic copolyamides was studied in a one-step reaction.

The CGCP of ethyl 4-butylaminobenzoate was carried out to tune polymerization conditions according to anionic ring-opening polymerization (AROP) of ϵ -caprolactam (CL) parameters.

In the meantime, the AROP of CL was conducted with different deprotonating agents, i.e. sodium or potassium alkoxides (t-BuOK, EtONa, MeONa) which are conventionally used in CGCP, was able to act as activator in AROP of CL. NO_2^- and CH_3^- derivatives, which is used mostly as an initiator in CGCP, were examined in AROP of CL.

In high quantity of aromatic units, for 50 and 30% of aramid units, aliphatic-aromatic copolyamides was synthesized and thermal and mechanical properties were investigated.

Chapter IV

Synthesis of Aliphatic-Aromatic Copolyamides by Combination of Anionic Ring Opening Polymerization and Chain-Growth Condensation Polymerization

TABLE OF CONTENTS

Introduction	186
1. Tuning the conditions for aliphatic-aromatic copolyamide synthesis	187
1.1. Effect of reaction temperature on chain growth condensation polymers	189
1.2. Effect of the activator on polymerization of ϵ-caprolactam.....	193
1.3. Effect of the initiator on polymerization of ϵ-caprolactam	195
2. Synthesis of aliphatic-aromatic copolyamide.....	197
3. Thermo-mechanical properties of polyamide 6 containing aromatic units	204
Conclusion	209
Experimental and supporting information.....	211
Annexe: Supporting Information	214
References.....	220

Introduction

As early mentioned, polyamides are widely used engineering thermoplastics in a broad range of application areas¹⁻⁶ because they have good mechanical properties such as tensile, flexural, and compressive strengths as well as resistance to abrasion and chemicals⁷.

Step growth condensation polymerization was the main route to synthesize aromatic polyamides⁸⁻¹⁷ until chain-growth condensation polymerization was developed by Yokozawa et al.^{18, 19, 20, 21}. They reported a new concept of living chain-growth condensation polymerization (CGCP), which can control molar mass (\overline{Mn}) and dispersity (\mathcal{D}) of aromatic polyamides²² (see chapter I of this manuscript, sections 2.2, 2.2.1., 2.2.3.).

Aramids are high-performance polymers and one of the toughest organic produced materials owing to their excellent thermal and mechanical properties. However, they are insoluble in many organic solvents due to π - π stacking of aromatic structures and intermolecular hydrogen bonding of amide linkages, which create good intermolecular packing and increase the crystallinity²³. High glass transition temperatures of aramids, above their decomposition temperatures, cause their thermal degradation before reaching the glass transition temperature which is an issue for processing by conventional melt- injection or compression molding. Solubility of conventional aramids can be improved by addition of flexible ether linkages, bulky structures, trifluoromethyl groups, linear aliphatic contents or non-linear rigid units.

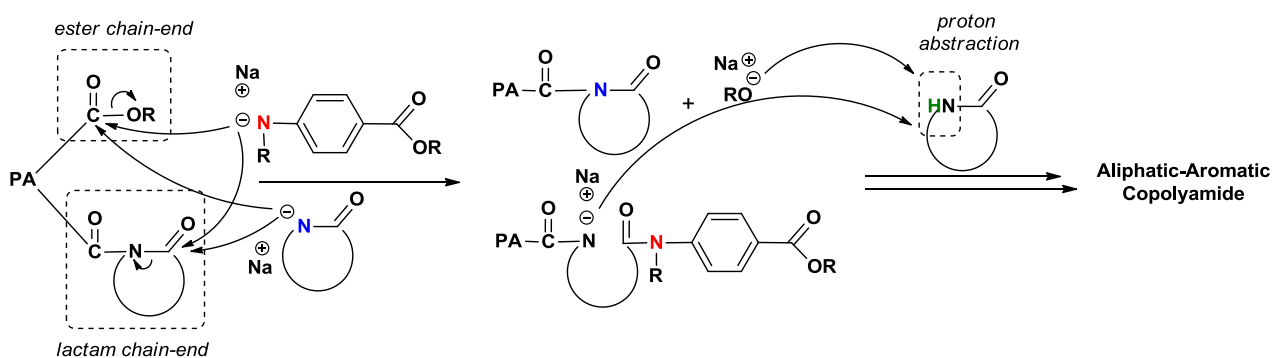
Polyamide 6 (PA6), which belongs to the class of aliphatic polyamides, is mainly synthesized by anionic ring-opening polymerization (AROP). PA6 has relatively less rigidity, much lower glass transition temperature and thermal stability than aramids. Addition of aramid polymers into the PA6 is known to change PA6 properties such as decreasing crystallinity and moisture absorption, depending on the amount of aramid units introduced²⁴.

In this chapter, the strategy is to find experimental conditions to combine CGCP and AROP for the synthesis of aliphatic-aromatic copolyamides. More generally, this approach is intended to demonstrate the possibility of merging of two chemistries and the synthesis of new materials based on PA6. Herein, PA6 copolymers with improved thermo mechanical properties were synthesized in a one-step reaction from *N*-alkyl aminobenzoate and ϵ -

caprolactam by CGCP and AROP combination. Molecular and physical characteristics of copolymers with various compositions are studied.

1. Tuning the conditions for aliphatic-aromatic copolyamide synthesis

The proposed method was optimized by varying major parameters including temperature (1), initiator type (2) and activator type on AROP of CL (3). Objectives of model reactions are depicted in Scheme IV-1. Our expectation is obtaining copolyamides through the nucleophilic attack of both activated (co)monomers and proton abstractions from non-activated monomers. Activated aromatic monomers and sodium ϵ -caprolactamate (C10) are intended to react both with ester and lactam chain ends.



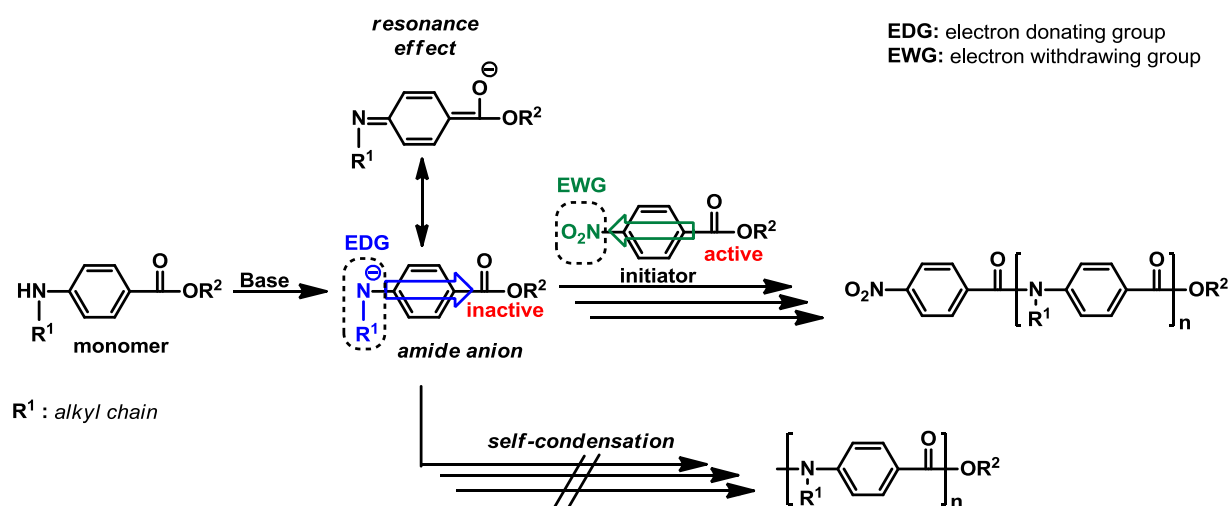
Scheme IV-1. Strategy for the synthesis of aliphatic-aromatic copolyamide.

Since “initiator” of CGCP and “activator” of AROP have the same role on each polymerization systems and homogenization of the both chemistries constitutes an importance for this study, “initiator” of CGCP is called as an “activator” in following experiments.

The combination of AROP and CGCP was examined by using different types of initiators and activators in an experimental condition which is in agreement with the industrial producing of PA6. Model reactions were proposed to demonstrate the feasibility or limitations of some reactions.

Scheme IV-2 illustrates conventional CGCP principles in a system. In CGCP, deprotonation of the monomer by strong base creates amide anions. The amide anion is an electron donating group (EDG) of the monomer which is deactivating its ester carbonyl group via resonance effect and suppressing the self-condensation. The benzamide bearing an alkyl

group is preferred since it increases the electronegativity of the amide anion and this deactivates the ester carbonyl group via resonance effect²². Thus, monomers bearing alkyl groups are used to prevent self-condensation (Scheme IV-2). Moreover, monomers having a long alkyl group eliminates the early precipitation more than shorter ones by increasing the solubility of resulting aromatic polyamides during the polymerization. Besides, the initiator also plays an important role on CGCP for controlled condensation polymers by preventing self-condensation. Since the initiator has an electron withdrawing group (EWG), rather than EDG of the monomer, the EWG (-NO₂) can activate ester carbonyl group. Therefore, the monomers prefer to react first with the activated ester carbonyl group of the initiator instead of each other (see chapter I of this manuscript, section 2.2.1.1.). Then, the polymerization continues by addition of monomers to the activated chain-end of the initiator.



Scheme IV-2. Synthesis of aromatic polyamide by chain growth polycondensation.

In a preliminary work, exploring of suitable activators, initiators and reaction temperatures for adapting CGCP to AROP were reported in order to combine both processes for synthesizing the targeted aliphatic/aromatic copolymers.

1.1. Effect of reaction temperature on chain growth condensation polymers

The synthesis of copolymer via hybrid copolymerization mechanism is strongly dependent to implementation at the same conditions.

As it is known, AROP of CL in bulk are conducted at 140 °C while CGCP of ethyl 4-butylaminobenzoate in solution can be succeeded at maximum 25 °C. Polymerization of CL in bulk can be carried out at 100 °C, which is the minimum polymerization temperature, since CL monomer has a melting point of 80 °C. However, the resulting polymers are obtained with lower conversion and it requires longer reaction time because of the less active monomers in anionic polymerization media. Moreover, the decreasing of the AROP temperature below 130 °C increases crystallization rate significantly which results in low conversion due to entrapment of monomer in the crystals. On the other hand, increasing the temperature higher than 170 °C is not also favorable for AROP of CL due to the branching side reaction which is reducing the crystallization degree²⁵ therefore decreasing the material stiffness. Thus, in bulk polymerization, a suitable temperature range of AROP of CL is 130-170 °C. On the other hand, conducting of CL polymerization in solution is not preferable because of slow rate of polymerization with limited conversion and economic concerns for industrial producing.

Considering this reaction temperature limitation of AROP, we focused on the evaluation of the CGCP temperature, since there are no detailed studies on this part. However, CGCP of ethyl 4-octylaminobenzoate was reported²² at quite low reaction temperatures such as -78 °C, -50 °C, -20 °C, 0 °C or 25 °C. After a series of polymerizations, close molar masses to the theoretical ones were observed²² at increased polymerization temperatures at least at 0 °C and room temperature. Nevertheless, CGCP at room temperature ends with higher \bar{D} (1.22) than at 0 °C \bar{D} (1.05). Therefore, a moderate temperature for CGCP is 0 °C. At low reaction temperatures (< 0 °C), the slow rate of the proton abstraction from the monomer can give a small amount of the deprotonated monomer, which caused to the dimerization between the deprotonated and non-deprotonated species. These dimers can act as an initiator and lead to self-initiated chain-growth condensation polymerization²⁶.

Herein, we report elevated polymerization temperatures for ethyl 4-butylaminobenzoate having shorter alkyl chain than the reported study in the literature²⁶. Several CGCP of ethyl

4-butylaminobenzoate were carried out in THF at elevated temperatures for 24h in the presence of the lithium bis(trimethylsilyl)amide(LiHMDS) as a base and phenyl 4-nitrobenzoate as an initiator, Table IV-1. Efficiency of the CGCP at these conditions was checked. When CGCP of ethyl 4-butylaminobenzoate was carried out at 0 °C (Run 1), it gained a lower molar mass than the theoretical one due to the lack of solubility of the resulting polymer which had a butyl pendant group. Considering this lowering of molar mass due to the solubility, controlling of following experiments at higher temperatures were expected before their precipitations.

TableIV-1. Synthesis of aromatic polyamide by chain-growth polycondensation in THF at different temperatures.

Run	Leaving Group	Initiator	Temp. (°C)	time (h)	$M_{n, \text{theo}}$ (g/mol)	$M_{n, \text{SEC}}^{\text{a}}$ (g/mol)	Conv. ^b (%)	\bar{D}^{a}
1	EtO-	Phenyl 4-nitrobenzoate	0	24	10000	2500	79	1.27
2	EtO-	Phenyl 4-nitrobenzoate	25	24	10000	2300	84	1.31
3	EtO-	Phenyl 4-nitrobenzoate	50	24	10000	1220	85	1.29
4	EtO-	Phenyl 4-nitrobenzoate	100	24	10000	1380	88	1.12

n (monomer, ethyl 4-butylaminobenzoate) = 2.25mmol,

n (initiator) = 0.04mmol,

n (base, LiHMDS) = 2.25 mmol,

^aDetermined by SEC in THF using PS Standarts.

^b Conversion was calculated by ¹H NMR in CDCl₃.

Polymers bearing octyl groups, as an alternative for butyl group, can be carried out with controlled molar masses²². But the monomer bearing an octyl pendant group is not readily available, which makes them undesirable reagents for the industrial processes, therefore it is not preferred for the following studies here.

In CGCP experiments, either LiHMDS (pKa = 36) or sodium bis(trimethylsilyl)amide (NaHMDS) (pKa = 26) are conventional bases. Investigations were first started with LiHMDS, but for following experiments LiHMDS is replaced with NaHMDS since there is a respective

price differences. Na metal is 5-6 times cheaper than Li metal because Na metal is more abundant than Li on earth.

In order to moderate the reaction temperature for AROP conditions, the reaction temperature was also increased to 25 °C, 50 °C and 100 °C. As the polymerization temperature increased from 0 °C to 25 °C, 50 °C and 100 °C, all results showed low molar masses with high conversions at increased polymerization temperatures (Table IV-1).

The resulting polymers were washed to remove residual monomers and other reagents and then characterized by ^1H NMR. Figure IV-1 illustrates the resulting polymer before and after washing and comparison with the ethyl 4-butylaminobenzoate monomer (Figure IV-S1). After polymerization, the $-\text{CH}_2$ (**d**) peak of the butyl pendant groups was shifted from 3.11 ppm to 3.76 ppm. The intensity of $-\text{CH}_2$ (**d**) at 3.11 ppm sourced from the monomer was decreased since it was consumed during the polymerization and after washing of the polymer this peak was disappeared completely. While aromatic protons of the polymer chain were revealed at 6.97 ppm and 6.70 ppm, chain end aromatic protons appeared at 7.79 ppm and 6.45 ppm. $-\text{CH}_2$ protons (a, b, c, a', b', c') of the pendant butyl groups appeared in the aliphatic region between 0.77 ppm and 1.55 ppm.

Conversions were calculated from ^1H NMR spectra of the polymers, before and after washing, based on distinguishable alkyl protons of residual monomers and resulting polymers, Figure IV-1. $-\text{CH}_2$ (**d**) signals of pendant butyl groups of the residual monomers appear at 3.11 ppm (**d''**) and polymerized units shift to 3.76 ppm (**d'**) as monomers are consumed in the production of polymers.

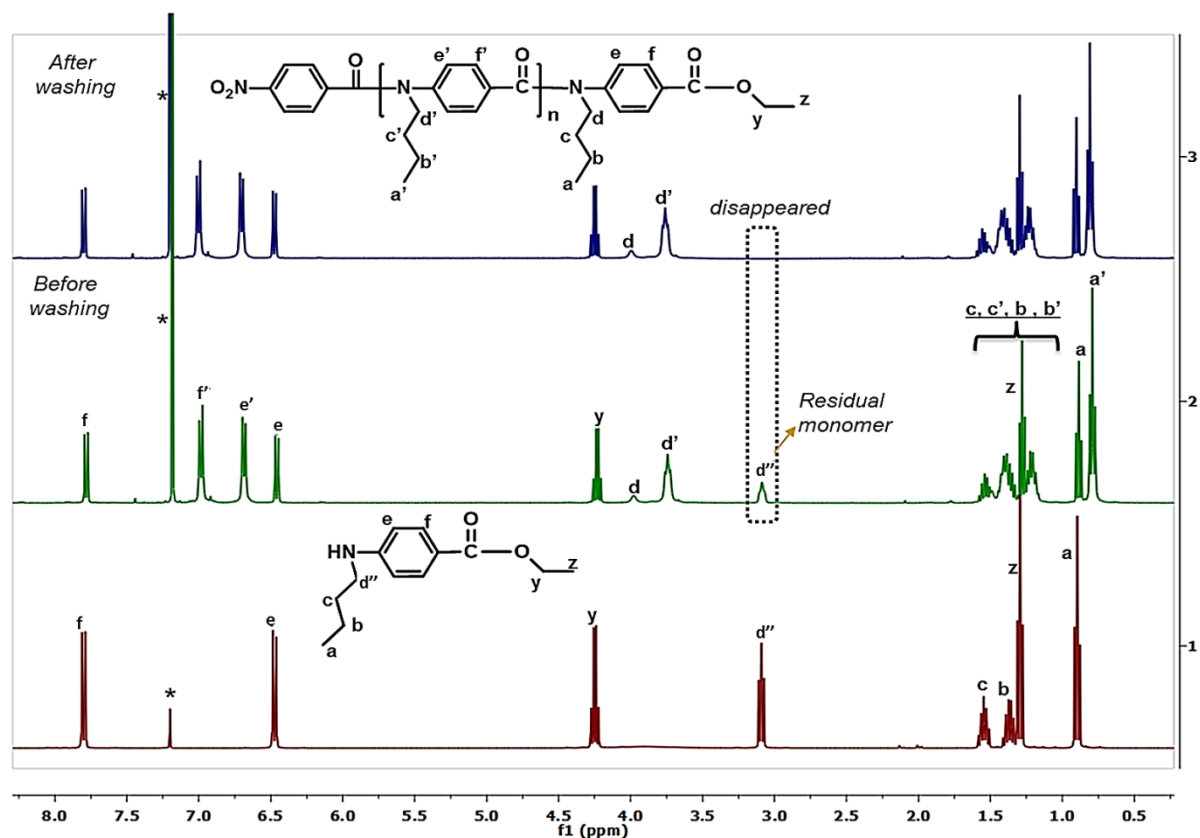


Figure IV-1. $^1\text{H-NMR}$ spectra of ethyl 4-butylamino benzoate (1), poly (4-butylaminobenzoate) before (2) and after washing (3). Peaks with asterisk were originated from solvent, CHCl_3 .

A comparison of the respective monomer and polymer signals allows the monomer conversion to be accurately determined for all polymers obtained at different temperatures ($0\text{ }^\circ\text{C}$, $25\text{ }^\circ\text{C}$, $50\text{ }^\circ\text{C}$ and $100\text{ }^\circ\text{C}$), in Figure IV-S2, Figure IV-S3, Figure IV-S4, Figure IV-S5. While molar masses were 2500 , 2300 , 1220 and $1380\text{ g}\cdot\text{mol}^{-1}$, conversions were increased from 79% , 84% , 85% to 88% , respectively. This lowering can be related to the loss of control of CGCP at high temperatures by too fast activating the polymerization compared to the conventional systems at lower temperatures ($0\text{ }^\circ\text{C}$ or $25\text{ }^\circ\text{C}$). In parallel to the increase of conversion and the decrease of molar masses, \mathcal{D} values were slightly increased except for the run 4. Aromatic polymers obtained at $100\text{ }^\circ\text{C}$ (run 4) showed slightly lower values since solubility limitations of the resulting polymer in THF might prevent from observing all polymers in size exclusion chromatography (SEC) analysis. One can note that polymerization

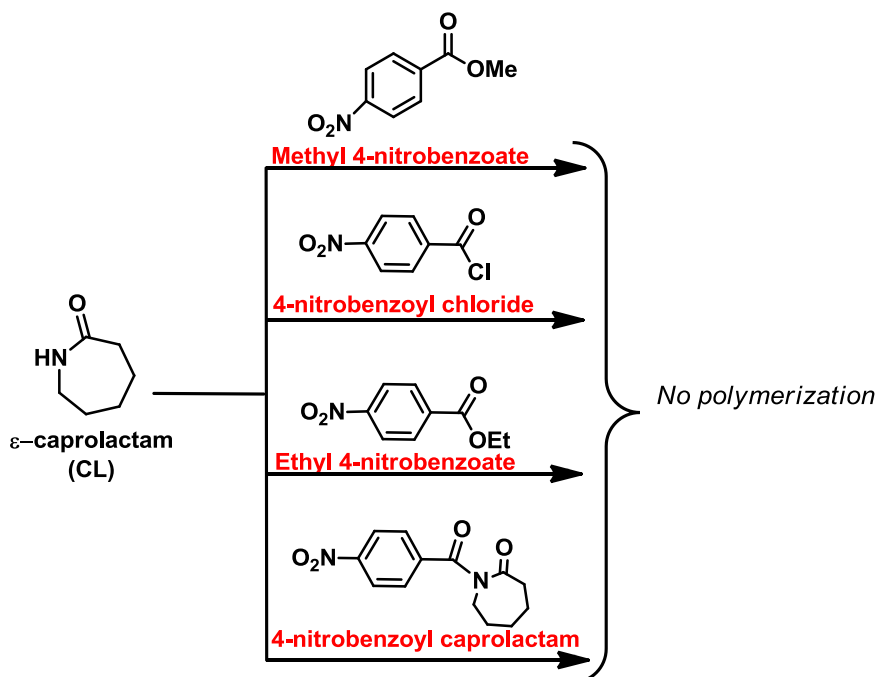
still occurs at 100 °C but with the limitation of early precipitation and probably some self-condensations.

1.2. Effect of the activator on polymerization of ϵ -caprolactam

To demonstrate the nucleophilic reactivity of sodium ϵ -caprolactamate (C10), the bulk AROP of CL with several activators having different leaving groups were carried out and their efficiency was compared with conventional CL polymerization through C20.

As it is mentioned in the literature review, ethyl 4-toluate, ethyl 4-nitrobenzoate, 4-nitrobenzoylchloride are known as efficient CGCP initiators with different substituents in para position such as nitro- ($-NO_2$) and methyl ($-CH_3$) group²². Owing to the electron withdrawing effect of the nitro- group, the initiator has a more reactive ester carbonyl group than monomers. On the other side, the initiator with a methyl substituent group has a more reactive ester carbonyl group than monomers where the amide anion strongly deactivated the ester carbonyl²².

In the prospect of the combination of CGCP and AROP, initiators of CGCP were investigated as AROP activators instead of C20. In first trials methyl 4-nitro benzoate, ethyl 4-nitrobenzoate and 4-nitrobenzoyl chloride were examined which have methyl-, ethyl- and chloride- leaving groups, respectively (Scheme IV-3).



Scheme IV-3. Possible activators for anionic ring-opening polymerization of ϵ -caprolactam.

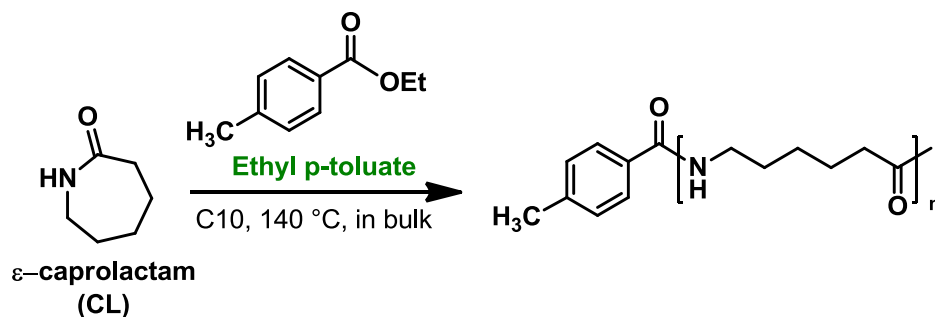
However, these groups could not activate the CL polymerization (Table IV-2). Following these experiments, 4-nitrobenzoyl caprolactam was synthesized and then used in CL polymerization. Unfortunately, this activator was also not efficient for the PA6 synthesis. Then, experimental conditions were shifted to an activator which has a substituted group (CH_3 -) different than $-\text{NO}_2$.

Table IV-2. Effect of the activator on polymerization of ϵ -caprolactam (CL) at 140 °C in bulk.

Run	Activator ^a	Initiator (C10, mmol)	Monomer (CL, mmol)	Conversion ^b (%)
1	C20	1.7	73.8	98
2	Methyl 4-nitrobenzoate	1.7	73.8	-
3	Ethyl 4-nitrobenzoate	1.7	73.8	-
4	4-nitrobenzoyl chloride	1.7	73.8	-
5	4-nitrobenzoyl caprolactam	1.7	73.8	-
6	Ethyl p-toluate	1.7	73.8	81

^a Activator = 1.3mmol, ^b Determined gravimetrically.

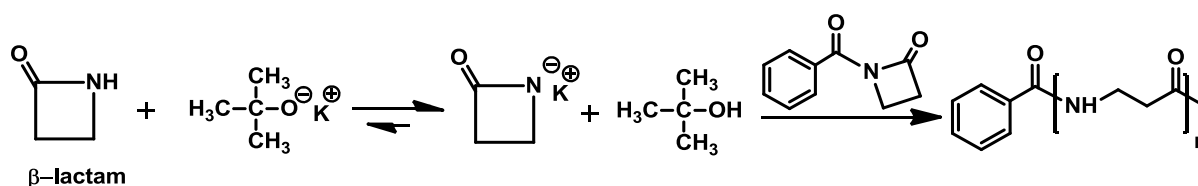
Activation of the CL polymerization by ethyl 4-toluate sheds light on the reason of the unsuccessful trials with activators bearing the $-\text{NO}_2$ substituent group, Scheme IV-4. This can be eventually explained by the reduction of the nitro pendant group ($-\text{NO}_2$), located on the initiator, to primary amine (NH_2 -) in the presence of alkoxy groups (sodium methoxide, ethoxide and propoxide) during the reaction²⁷. The advantage of the ethyl p-toluate relies on the presence of the methyl (CH_3 -) which is providing AROP with 81% yield. As a conclusion, sodium ϵ -caprolactamate can react with aromatic esters side chains.



Scheme IV-4. Ethyl p-toluate as an activator for anionic ring-opening polymerization of ϵ -caprolactam in bulk.

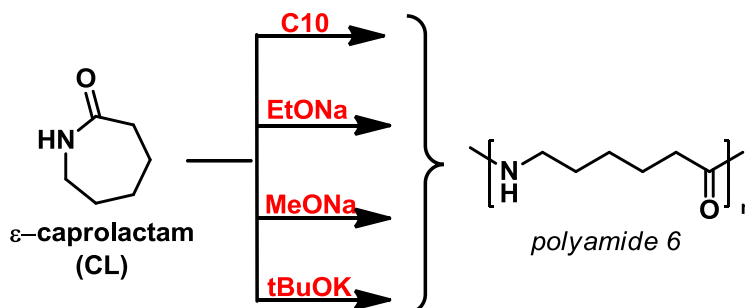
1.3. Effect of the initiator on polymerization of ϵ -caprolactam

For the AROP of CL, the lactamate anion (called as an initiator) is formed by the proton transfer from CL to strong basic catalysts such as alkali metals, alkaline metal hydrides and alkoxides²⁸⁻³⁰. Indeed, metal alkoxides are known to initiate the polymerization of some lactams. As it is depicted in Scheme IV-5, β -lactam living polymerization could proceed by using potassium t-butoxide³¹.



Scheme IV-5. Potassium t-butoxide catalyzed polymerization of β -lactam.

In the proposed novel polymerization system, it was obvious that there is an inevitable effect of CGCP leaving groups (LGs) on AROP as an initiator. These LGs were supposed to be active as much as C10. This property was examined by AROP of CL with EtONa, MeONa or tBuOK as an initiator and compared with C10, Scheme IV-6. We preferred to continue either with sodium (Na) or potassium (K) alkoxides, by taking into account of BASF concerns, since there is a respective price differences with Li.



Scheme IV-6. Initiators for anionic ring-opening polymerization of ϵ -caprolactam.

The experiments are summarized in Table IV-3, these results highlight the efficient deprotonation of the CL by MeONa, EtONa and tBuOK as all polymerizations achieved 98% conversion in a short reaction time of 20 min.

Table IV-3. Initiator effect on polymerization reactivity of ϵ -caprolactam in bulk at 140 °C.

Activator	Initiator	Monomer	Conversion ^a (%)	Time (min)	Slope (°C/s)
C20	C10	CL	98	20	1.89
C20	EtONa	CL	98	20	1.82
C20	MeONa	CL	98	20	2.33
C20	tBuOK	CL	98	20	3.54

n (monomer, CL) = 73.8 mmol. n (activator, C20) = 1.3 mmol. n (initiator) = 1.7 mmol.

^aDetermined gravimetrically.

These reactions were followed by the thermo-time diagram where a temperature probe was installed in the calorimeter to measure the reaction temperature, Figure IV-2. Since CL polymerization is exothermic, it was easy to follow these experiments by monitoring the exotherm-time rate plots, Figure IV-2. As explained in previous chapters, the first part of the reaction with increasing of the temperature belongs to the polymerization and the second one is showing the crystallization, Figure IV-2a. It is noted that, for tBuOK, the slope of the curve (Figure IV-2b) is significantly increased earlier than for C10, MeONa or the EtONa in reaction.

In reaction medium of tBuOK, potassium ϵ -caprolactamate is formed while other species form sodium ϵ -caprolactamate (C10). The potassium cations have a lower charge density than sodium cations. The delocalized electrons are less strongly attached to the metal cations in the potassium. Therefore, metallic bonding of potassium is weaker than metallic bonding of sodium. Thus, less energy is required to disrupt the metallic lattice in potassium which also makes them more reactive in AROP of CL. On the other hand, tBuO⁻ is also a good leaving group but is too reactive compare to EtO⁻ for CGCP. Therefore, it can easily lead to self-condensation side-reaction in CGCP.

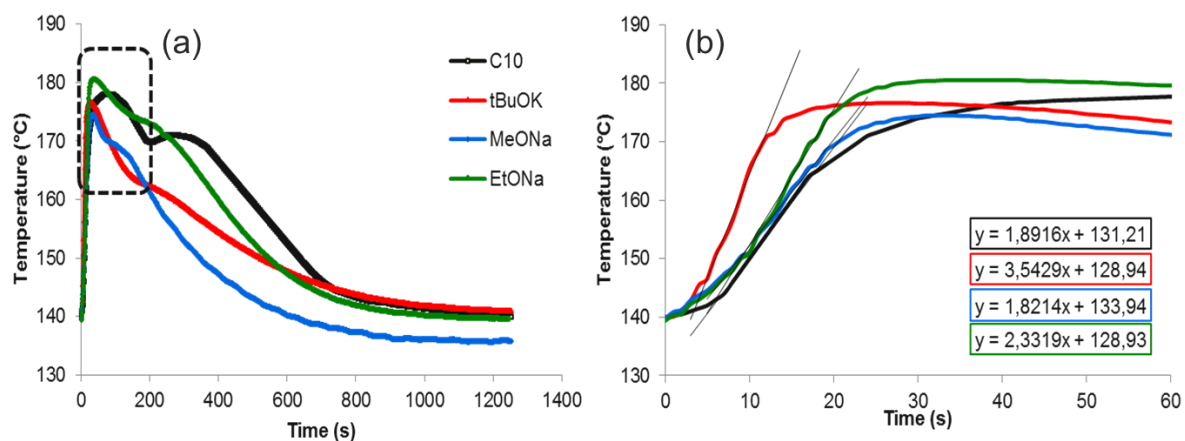


Figure IV-2. Polymerization exotherm-time plots of PA6 with C10, tBuOK, MeONa and EtONa.

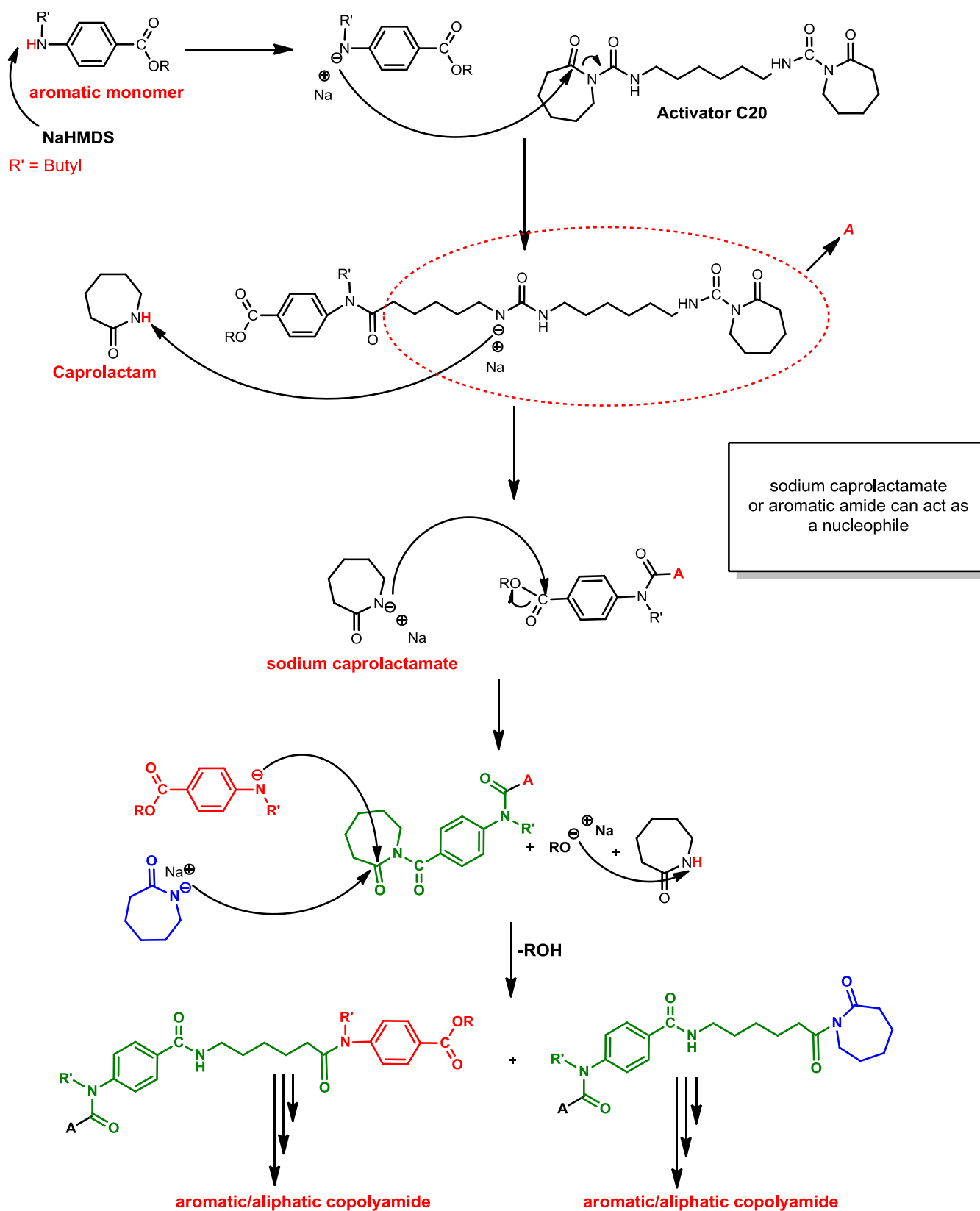
In the following part, the copolymerization of CL was conducted with ethyl 4-butylaminobenzoate. Because ethyl 4-butylaminobenzoate, having less reactive EtO- leaving group than tBuO-, gives more controllable condensation polymers. EtO- is the active group not only as a leaving group in CGCP but also as an initiator in AROP, as demonstrated above.

2. Synthesis of aliphatic-aromatic copolyamide

Copolyamides with different percentages of aromatic/aliphatic units were synthesized in bulk by combination of AROP and CGCP in one-step. The proposed copolymerization mechanism is depicted in Scheme IV-7. Nucleophilic attack to the activator (C20) can either be achieved by sodium ϵ -caprolactamate (C10) or aromatic amide. The propagation of anionic polymerization requires two reactive species: (1) the lactamate anion which was supplied from leaving group of CGCP or C10 and (2) the *N*-acyl lactam end group. In view of the fact that the monomer is activated by C10 and the alkoxide leaving group of CGCP, the level of basicity is maintained in the polymerization mixture. The anionic catalyst (alkoxide leaving group of CGCP) can react with the lactam monomer to form the active species and then it becomes an alcohol by deprotonating CL. As described in homopolymerization, the amide anion on the aromatic activated monomer is expected to deactivate the ester carbonyl site through the resonance effect which results in the inhibition of the self-condensation of the monomer. This allows the selective reaction between the initiator and the propagating end. Experimental trials carried out in this work are listed in Table IV-4. As

already known, CL could polymerize in 15 min with 98% yield (Run 1), meanwhile the copolymerization reactions (runs 2, 3 and 4) could also work but with lower yields and longer reaction times (24h). Scheme IV-7 shows the synthesis of copolymers: the benzamide comonomers were first deprotonated by a strong base, 1.02 equivalents of NaHMDS, in 24h. In another reactor, the CL monomer and C10 were mixed for a few minutes. Then, these two activated monomers were mixed in a polymerization reactor. Once C20 was added, the copolymerization took place (Table IV-4).

Synthesis of aliphatic-aromatic polyamide



Scheme IV-7. Proposed copolymerization mechanism of aromatic-aliphatic polyamide.

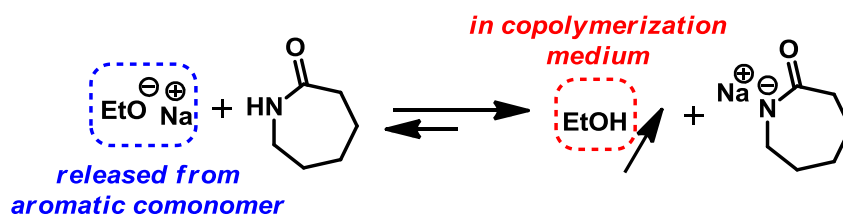
Table IV-4. Synthesis of polyamide 6 and aliphatic/aromatic copolymers at 140°C in bulk.

Run	C20, mmol	C10, mmol	CL ^a mmol	NaHMDS ^b , mmol	Ar ^c , mmol	CL ^a , wt %	Ar ^c , wt %	Time	Conv ^d %
PA6	1.30	1.70	73.8	-	-	100	-	15min	98
30%Ar-PA6	0.33	0.44	10.1	2.30	2.26	70	30	24h	70
50%Ar-PA6	0.33	0.44	4.52	2.30	2.26	50	50	24h	60

^a ϵ -caprolactam,^b 1M, in THF,^c Ethyl 4-butylaminobenzoate,^d Determined gravimetrically.

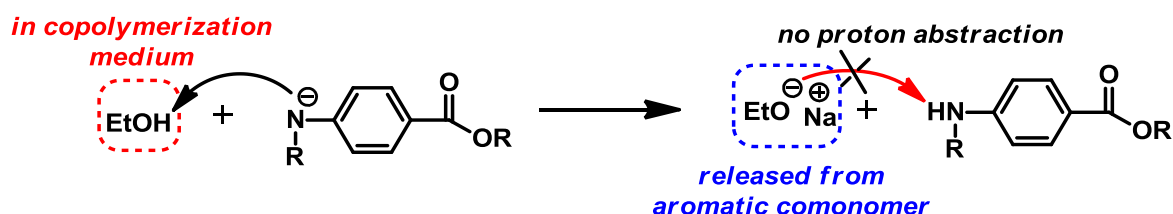
The copolymerization of ethyl 4-butylaminobenzoate and CL could be obtained via a one-step reaction from commercially available reagents for 30% and 50% of aromatic units in polyamides. After copolymerization, THF was used as a washing solvent. Unreacted CL, benzamide monomers and all reagents are soluble in THF and they could be removed by refluxing for 24h. But the copolymerization yield was lowering with an increasing amount of the aromatic comonomer in the polymerization medium. For 30%Ar-PA6 and 50%Ar-PA6 copolyamides, yields were 70 and 60%, respectively. Compare to neat PA6, copolymerization needs a longer reaction time and has a lower yield by lowering the reaction reactivity.

This lowering of the yield might be explained by high concentration of ROH (ethanol) in reaction medium which is released from the aromatic comonomer, once it reacts with sodium ϵ -caprolactamate (C10), which reduces the active aromatic comonomer amount. During the CGCP, the released EtONa (pKa = 16) groups has no efficiency to abstract a proton from the aromatic amides since they have no high basicity like NaHMDS (pKa = 26) or LiHMDS (pKa = 36). Once the activated aromatic comonomer solution is added to the CL polymerization reactor, according to the proposed reaction mechanism (Scheme IV-7), every single merging of C10 and aromatic ester carbonyl releases an ethoxide group to the reaction medium. As it is provided that ethoxide has the ability to abstract proton from CL and activates the AROP by affording ethanol in the reaction the medium, Scheme IV-8. One might think that occurring of ethanol is not so effective at a 140 °C reaction temperature since ethanol is supposed to be evaporated at that temperature but it can be trapped and can then play a role in this mechanism. Even small amount of ethanol can be in equilibrium with activated aromatic amide or sodium ϵ -caprolactamate (C10) which can quench the polymerization process of aromatic part.



Scheme IV-8. Proton abstraction from ϵ -caprolactam by sodium ethoxide.

According to this principle, the activated aromatic amide, which has not reacted with CL or the chain-end, can also abstract a proton from ethanol, Scheme IV-9. Activated aromatic amide has a higher basicity than the ethoxide since sodiummethoxide cannot deprotonate ethyl 4-butylaminobenzoate during the CGCP.



Scheme IV-9. Proton abstraction from ethanol by aromatic amide.

While the copolymerization reaction, every single merging between aromatic comonomer and C10 is releasing an alkoxy (ethoxide) group which becomes an alcohol since it can abstract a proton from CL. These alcohols can create equilibrium with CL which favors to consuming CL amount. Another reason of the reduced yield can be the presence of comonomers or oligomers in melted CL by hindering the movement of C10 to attack the growing chain. In the literature, this effect was also explained by the presence of cyclic oligomers in the anionic polymerization of CL³². Therefore, these effects are lowering the resulting copolymer yield. Indeed, the soluble part in THF is not only made up of (co)monomers and reagents. This soluble part may also contain random copolymers but with lower molar masses, which are soluble in THF.

¹H NMR technique was used to characterize the structure and the composition of the copolymers in CDCl₃/HFIP, Figure IV-3. Synthesized 30%Ar-PA6 was confirmed by ¹H NMR in HFIP/CDCl₃ and compared with starting monomers, ethyl 4-butylaminobenzoate (Figure IV-S1) and CL (Figure IV-S6), in Figure IV-3. After polymerization, the -NH peaks of CL is shifted

to 5.98 ppm from 6.78 ppm. $-\text{CH}_2$ (a and b) of butyl pendant group of the aromatic comonomer is shifted to 0.88 from 0.95 (a) and to 1.18 ppm from 1.60 ppm.

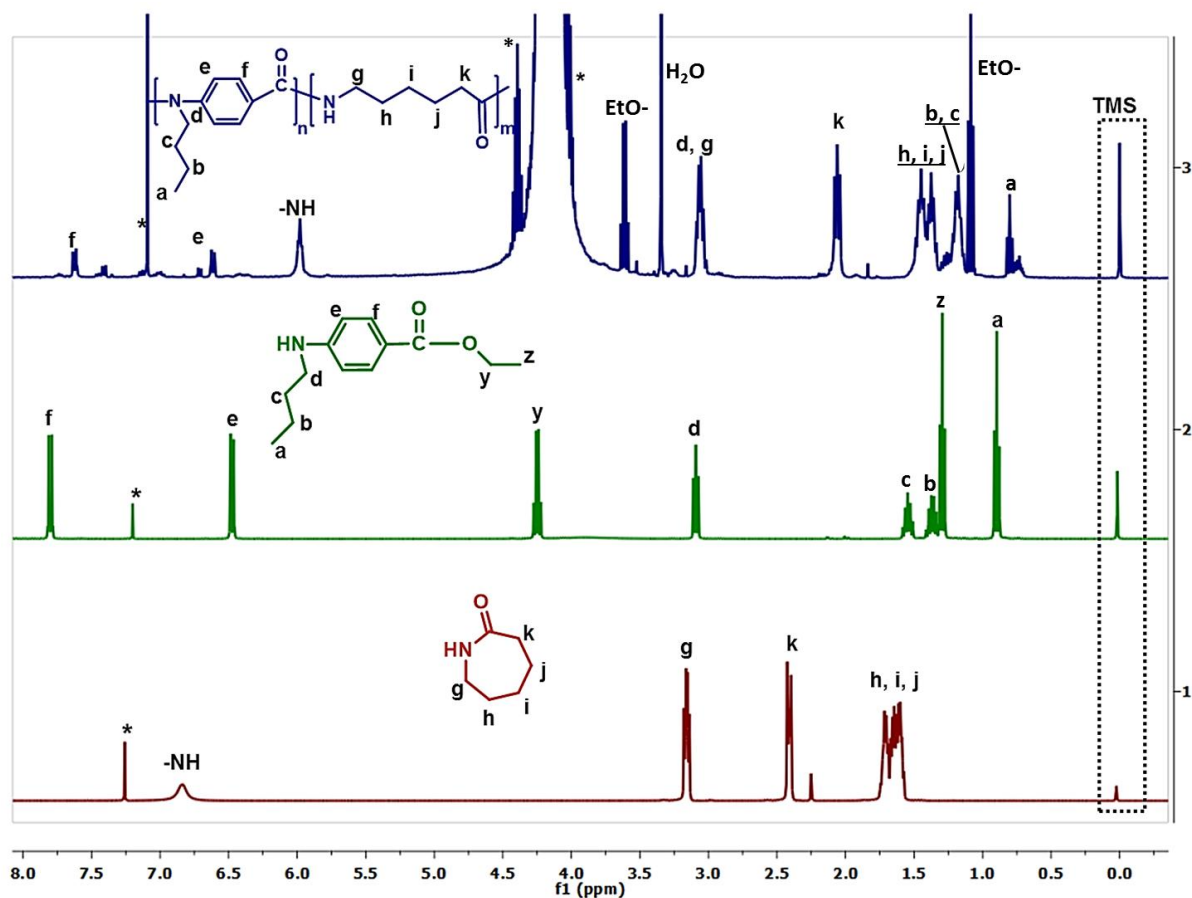


Figure IV-3. ^1H NMR spectrum in $\text{CDCl}_3/\text{HFIP}$ of, from top to bottom: 30%Ar-PA6, ethyl 4-butylbenzamide and ϵ -caprolactam. Peaks with asterisk were originated from solvents (CHCl_3 and HFIP).

^1H NMR integral results are provided to further confirm the above statement, Figure IV-4. Characteristic proton peaks of CL repeating units appeared at δ (ppm) 5.98 (**NH**), 2.06 (**$\text{CH}_2\text{-C=O}$**), 3.07 (**NHCH_2**), 1.45, 1.38 and 1.18 (**CH_2**). As shown in Figure IV-3, 30%Ar-PA6 exhibits the aromatic repeating units of ethyl 4-butylaminobenzoate. Aromatic ring peaks appeared at 7.64 and 6.49 ppm and butyl pendant groups were seen at 3.07 ppm (**$\text{CH}_2\text{N-}$**), 1.18 and 1.10 ppm (**$-\text{CH}_2\text{CH}_2-$**) and 0.80 ppm (**CH_3-**). Molar fraction of CL on 30%Ar-PA6 could be calculated from integrated intensity ratio of the 3.03 at 2.06 ppm ($I_{2.06}$) (**$\text{CH}_2\text{-CO}$**) to the 1.00 at 0.88 ppm ($I_{0.80}$) including alkyl (**CH_3-**) protons.

$$m (\%) \rightarrow = \frac{\frac{I_{2.06}}{2}}{\frac{I_{2.06}}{2} + \frac{I_{0.8}}{3}} \times 100 \quad (1)$$

Note that “ I ” in Eq. (1) can be substituted by $I_{2.06}$ (the integrated intensity of the $\text{CH}_2\text{-CO}$ peak at 2.06ppm), and also by $I_{0.80}$ (CH_3 -at 0.80 ppm). The $m\%$ value calculated from this ratio showed 82% of aliphatic repeating units and 18% of aromatic ones. Another ratio was between $-\text{NH}$ and CH_3 - (a) protons. The calculated average values were almost the same, 81% aliphatic and 19% aromatic contents in the copolymer.

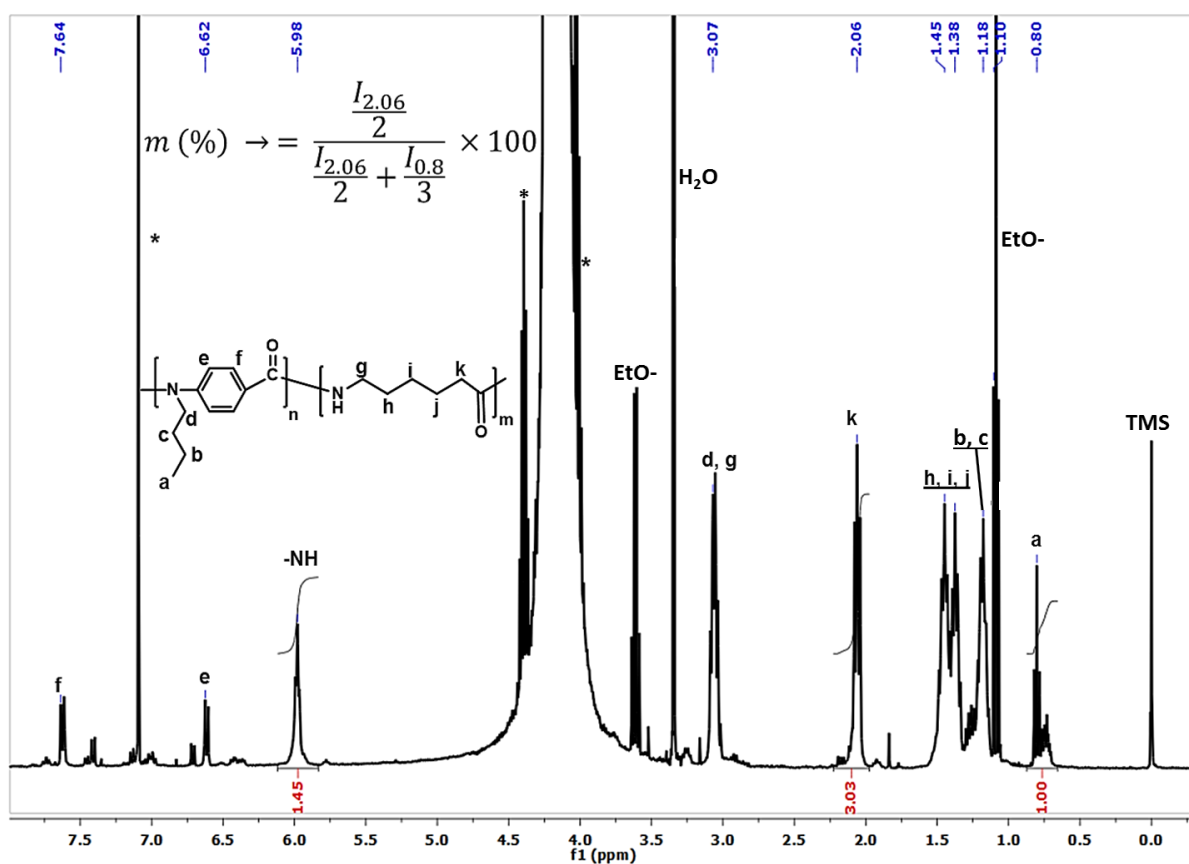


Figure IV-4. ^1H NMR spectrum of 30% Ar-PA6 in $\text{CDCl}_3/\text{HFIP}$. Peaks with asterisk were originated from solvents (CHCl_3 and HFIP).

The peaks at 1.10 and 3.62 ppm belongs to $-\text{CH}_3$ and $-\text{CH}_2$ protons of residual EtO- respectively which is leaving group of aromatic components in copolymerization and trapped in polymers.

The same calculation was used for 50%Ar-PA6 copolyamides, Figure IV-S7. In addition to these ratios, molar fraction of CL on 50%Ar-PA6, Table IV-4, could be calculated from integrated intensity ratio of the 1.72 at 2.07 ppm ($I_{2.07}$) ($\text{CH}_2\text{-CO}$) to the 1.00 and 0.81 ppm ($I_{0.08}$) including alkyl ($\text{CH}_3\text{-}$) protons. The m% value calculated from this ratio showed 28% of aromatic repeating units and 72% of aliphatic (Figure IV-S7). In addition to this ratio, aliphatic/aromatic percentages in the copolymer were also calculated from -NH and $\text{CH}_3\text{-}$. 76% of aliphatic and 24% of aromatic contents were detected.

They are lower than those expected from feed compositions in Table IV-4, indicating the combined copolymerization of benzamide and CL resulted in a copolymer, due to non-complete conversion and/or also different reactivity of comonomers. In two examples, the predominance of aliphatic units was observed. It is a logical outcome since the activated aromatic amide can be consumed by ethanol in the reaction medium.

3. Thermo-mechanical properties of polyamide 6 containing aromatic units

In the present study, DSC analyses (Table IV-5) revealed the semi-crystalline character of PA6 and the increasing amorphous character of PA6-co-Ar. Increasing aromatic content in the copolymer decreased ΔH_m (Table IV-5). The glass transition temperature corresponding to PA6 was increased for PA6-co-Ar polyamides from 53 °C to 68 °C (Figure IV-S8 and Figure IV-S9). As aromatic homopolymers are not present after purifying the copolymers according to NMR results, these results indicate the aromatic groups are incorporated into the PA6 main chains. Moreover, the single T_g indicates that there is only one relatively homogeneous structure in the final product, i.e., 30 and 50% Ar-PA6s (Figure IV-S8 and Figure IV-S9). 30%Ar-PA6 copolymers prepared with 30 mol % of aromatic units has only one melting endotherm, which is clearly showing that the resulting copolymer has a random structure rather than a block structure. 50%Ar-PA6 copolymers obtained from a 50-50% of aromatic/aliphatic ratio have no melting point and are amorphous. The butyl alkyl units on aromatic groups of the copolymers decrease the crystallinity by hindering the molecular packing and intermolecular hydrogen bonding between the polymer chains (Table IV-5).

Huang et al.³³ reported that the glass transition temperatures of polybenzamides before and after removing the octylbenzamide groups. For polybenzamides, the T_g value shifted

from 45 to 62 °C after removal of the octyloxybenzyl alkyl groups. This result is clearly showing a strong intermolecular hydrogen bonding effect which is increasing the crystallinity of polymer as hydrogen bonding in the polymer increases (see chapter I of this manuscript, section 2.3.2.).

Table IV-5. DSC and TGA analyses of PA6, 30%Ar-PA6 and 50%Ar-PA6 under N₂.

Sample	DSC					TGA		
	<i>T_g</i> (°C)	<i>T_c</i> (°C)	ΔH_c (J/g)	<i>T_m</i> (°C)	ΔH_m (J/g)	<i>T₅</i> (°C) ^a	<i>T₁₀</i> (°C) ^b	<i>T_d</i> (°C) ^c
PA6	53	171	60	216	70	290	300	308
30%Ar-PA6	65	137	19	195	23	293	314	317
50%Ar-PA6	68	-	-	-	-	302	325	323

^a Decomposition temperature at a 5% weight loss,

^b Decomposition temperature at a 10% weight loss,

^c Maximum of the peak decomposition temperature.

The incorporation of aromatic groups into PA6 also shows heat capacity changes which is assigned to the crystalline melting of PA6. *T_m* of 30%Ar-PA6 is shifted to a lower temperature (Figure IV-S8). This result can be related to the good dispersion of aromatic repeating units in the PA6 matrix along with the disordering of the system³⁴ and decrease of the crystallinity of PA6. This effect becomes clearer with the disappearance of melting point at a higher aromatic content (50%Ar-PA6) which bears witness of the formation of amorphous copolymers. This decrease and disappearance of the melting endotherms with increasing the aromatic content is related to the disordering effect of the butyl units of aromatic groups on the hydrogen bonding of PA6.

The TGA analysis in a nitrogen atmosphere is used to measure the thermal degradation behavior of the copolymers. Typical TGA thermograms of PA6 and aliphatic/aromatic copolyamides are shown in Figure IV-5. It illustrates that the higher the content in aromatic groups is, the more thermally stable the copolymers are. Thermal degradations of 30%Ar-PA6 and 50%Ar-PA6 shifted to higher temperatures than the neat PA6 degradation.

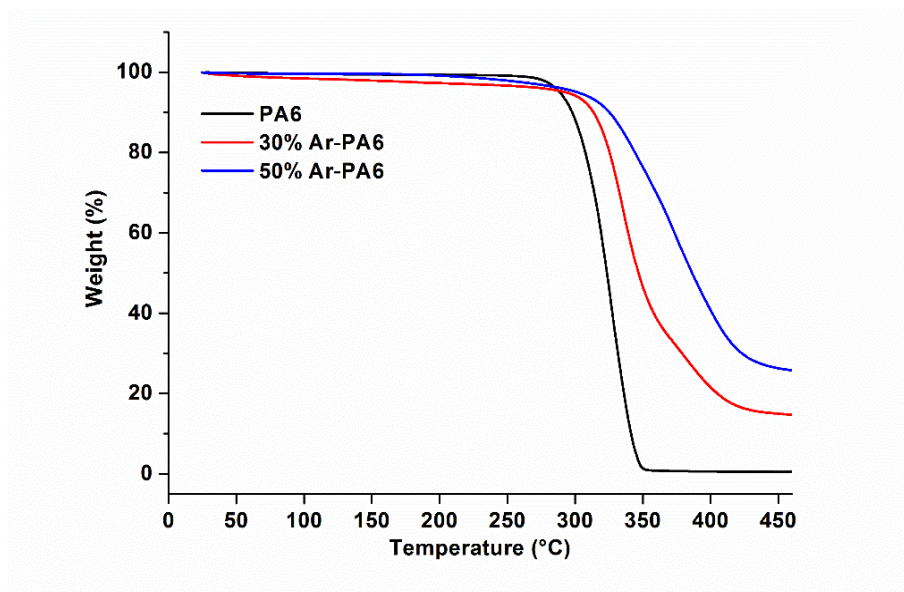


Figure IV-5. TGA thermograms of PA6, 30% Ar-PA6 and 50% Ar-PA6.

During the PA6 thermal degradation, two weight loss regions, 300-350 and 380-400 °C, were observed (Figure IV-6). These two degradations probably belong to the different thermal degradations of PA6, as early explained (see chapter II of this manuscript, section 4.). For the 30%Ar-PA6 copolymer, the first/major region shows the PA6 degradation and the second shifted region at higher temperature is related to the incorporation of aromatic units into PA6. 50%Ar-PA6 copolymer thermal degradation takes place at quite higher temperatures than neat PA6 and 30%Ar-PA6. This slight improvement in degradation temperatures is obviously related to the higher amount of aromatic units in PA6 chains. Thermal degradations of the copolyamides were not completed to 100% like PA6 when heated till 450 °C due to higher thermal degradation of the aromatic units. Some aromatic sequences are then expected in the random copolymer.

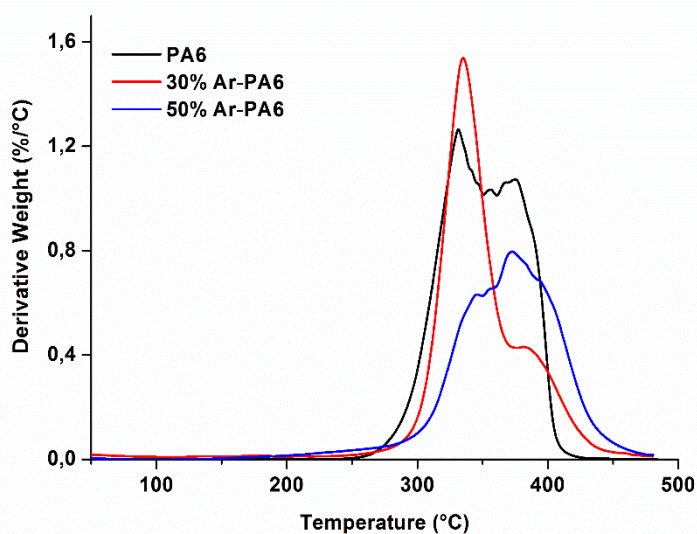


Figure IV-6. Rate of weight losses of PA6, 30%Ar-PA6 and 50%Ar-PA6.

As it is well known, wholly rigid aromatic polyamides exhibited higher glass transition temperature than aliphatic-aromatic copolyamides and homo aliphatic polyamides (PA6). But these aromatic polyamides drawbacks are their high melting point reducing the processability and decomposing before their melting point which is too high. Physical properties and thermal stabilities of wholly aromatic polyamides are known to be superior to those of PA6. Yokozawa and coworkers³⁵ reported the thermal properties of hyperbranched and linear aromatic homopolyamides, depending on the molar mass, *N*-alkyl pendant group and terminal alkyl ester group, by following T_g and T_{10} values from DSC and TGA analyses. The T_{10} of hyperbranched aromatic polyamide (HBAP) bearing *N*-alkyl groups were reported³⁵ at about 360-400 °C. They also studied the alkyl chain length effect on the T_g of well-defined hyperbranched aromatic polyamides. The HBAP bearing *N*-octyl groups has a T_g around 30 °C which is lower than the T_g of HBAP bearing ethyl group (110 °C). On the other hand, T_g values of HBAP with long *N*-alkyl groups is not affected by the polymer structure since the T_g values of *N*-octyl HBPA and *N*-octyl poly(*m*-benzamide) are reported to be similar³⁵.

The storage modulus (E') plots of the different systems, neat PA6, 30%Ar-PA6 and 50%Ar-PA6, were measured by DMA (Figure IV-S10 and Figure IV-S11) and are shown in Figure IV-7. The storage modulus E' of all polymers are close to each other. Particularly, the modulus around 140°C is lowering in parallel to their decreasing crystallinity along with a higher amount of aromatic units in the system. Normally, an increase of rigidity is expected to

slightly increase the storage modulus but, in this particular case, the interactions between the chains by hydrogen bonding are inhibited by the butyl pendant groups on aromatic repeating units (having alkyl group instead of proton).

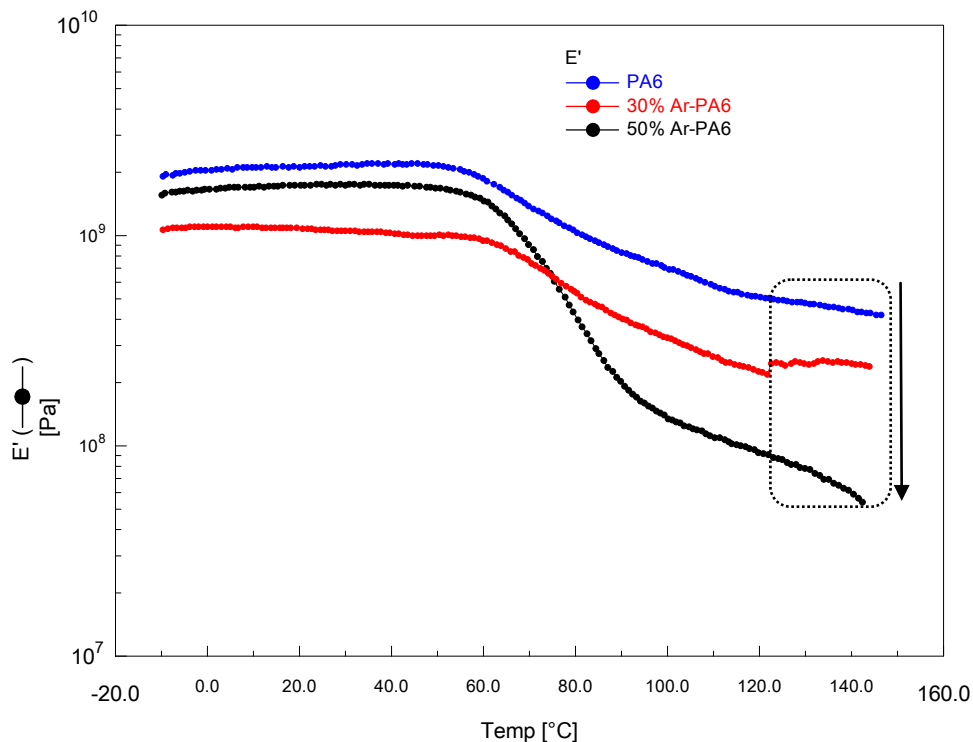


Figure IV-7. Elastic modulus (E') of PA6, 30% Ar-PA6 and 50% Ar-PA6 by DMA.

The plot of loss factor ($\tan\delta$) of the neat PA6, 30%Ar-PA6 and 50%Ar-PA6 were measured by DMA, Figure IV-8. Despite the presence of the butyl pendant group, the mechanical α -relaxation temperatures ($T\alpha$), determined at the maximum $\tan\delta$ value for the random copolyamides, are close to each other and higher than neat PA6. This is in agreement with increasing of Tg results from DSC measurements. Indeed, the $T\alpha$ is obtained at 72 °C to 79 and 81 °C for the PA6, 30%Ar-PA6 and 50%Ar-PA6, respectively. The incorporation of aromatic units into the PA6 by this new methodology improves clearly Tg and $\tan\delta$ of PA6.

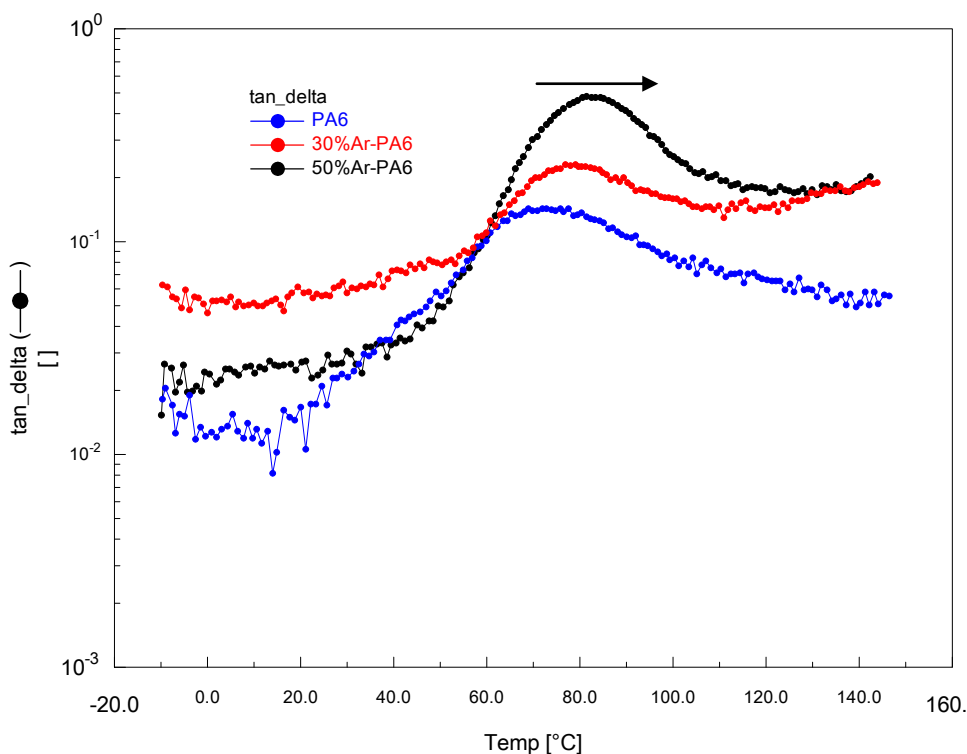


Figure IV-8. Loss factor (Tan δ) of PA6, 30%Ar-PA6 and 50%Ar-PA6 by DMA.

Conclusion

In this chapter, combination of anionic ring-opening polymerization (AROP) and chain-growth condensation polymerization (CGCP) was shown to proceed in a one-step reaction for the synthesis of aliphatic-aromatic copolyamides.

The chain growth condensation polymerization of ethyl 4-butylaminobenzoate was carried out in solution to demonstrate the efficiency of this reaction at elevated temperatures despite early precipitation of the aromatic polyamide due to the solubility loss with increasing molar masses. Self-condensation may occur in these conditions.

Meanwhile, the AROP of ϵ -caprolactam was conducted with different deprotonating agents, i.e. sodium or potassium alkoxides (t-BuOK, EtONa and MeONa) which can be formed by the nucleophilic attack of the ester groups of the aromatic monomers. Ethyl p-toluate, conventionally used in chain-growth condensation polymerization, was able to act as an activator in AROP of CL. NO₂⁻ derivatives, which is used mostly as an initiator in CGCP, caused side reactions by preventing the AROP of CL.

Aliphatic-aromatic polyamides were synthesized for 30 and 50 molar % of aromatic units. Regarding molecular and thermal characterizations, a random copolymer is envisaged. Increase of the aromatic content in the polymer chain resulted in decrease of the crystallinity. The butyl pendant groups contribute certainly to this morphology type by restricting of hydrogen bonding between polymer chains. An increase of glass transition temperature and $\tan \delta$ of PA6, in some extent, provided more thermal stability.

This innovative method is not only combined two challenging chemistries but contribute to vary some properties of PA6 too.

As a perspective, future works may focus on the removing of alkyl pendant groups on the polymer backbone by washing with an acid such as trifluoroacetic acid and investigating its thermal properties and comparing with starting polymers. Further studies will be based on the processability of this synthesis technique in an industrial producing standard.

Experimental and supporting information

Materials. ϵ -Caprolactam (CL) (BASF, 99 %) was recrystallized from dry cyclohexane prior to use. Brüggolen® C20 (17 % w/w of isocyanate in CL, N, N'-hexamethylenebis(2-oxo-1-azepanylcarboxamide) or hexamethylene-1,6-dicarbamoylcaprolactam in CL, Brüggemann Chemical), Brüggolen® C10 (~18 % w/w of sodium ϵ -caprolactamate in CL, Brüggemann Chemical). Ethyl 4-(butylamino)benzoate, ethyl 4-methylbenzoate, ethyl 4-nitrobenzoate, sodium tri acetoxyborohydride, sodium bicarbonate, ethyl acetate, magnesium sulphate, a solution of sodium bis(trimethylsilyl)amide (NaHMDS, 1.0 M in THF), lithium bis(trimethylsilyl)amide (LiHMDS, 1.0 M solution in THF), sodium ethoxide, sodium methoxide, potassium tert-butoxide, tetrahydrofuran, chloroform and diethylether were purchased from Sigma-Aldrich. 1,1,1,3,3,3-Hexafluoro-2-propanol (HFIP) (Acros Organics, \geq 99.7 %) was used without any further purification.

Measurements. ^1H NMR spectra of reactants were recorded by using a Bruker AC250 instrument at a proton frequency of 250 MHz at room temperature. Rate of polymerization was followed by temperature vs time monitoring using an ALMEMO2590 AHLBORN thermocouple. Differential scanning calorimetry (DSC) was performed on a Perkin-Elmer Diamond DSC with a heating rate of $10\text{ }^\circ\text{C}\cdot\text{min}^{-1}$ under nitrogen flow ($10\text{ mL}\cdot\text{min}^{-1}$). Thermogravimetric analysis (TGA) was performed on a Perkin-Elmer Diamond TA/TGA with a heating rate of $10\text{ }^\circ\text{C}\cdot\text{min}^{-1}$ under nitrogen flow. Dynamic mechanical thermal measurements were performed in a single-cantilever bending mode on an MKII dynamic mechanical thermal analyzer with a flat sample (prepared by heat pressing) at a heating rate $5\text{ }^\circ\text{C}\cdot\text{min}^{-1}$. The operating temperature range was $-10\text{ }^\circ\text{C}$ to $170\text{ }^\circ\text{C}$, and the frequency was 1 Hz. The storage modulus (E'), loss modulus (E''), and loss tangent ($\tan \delta$) for each sample were automatically recorded by a computer throughout the test.

Chain growth condensation polymerization of ethyl 4-(butylamino)benzoate²² at elevated reaction temperatures. A flask, equipped with a three-way stopcock, was purged with argon and then charged with dry THF (0.4 mL) and 1.0 M LiHMDS in THF (2.475 mmol). The flask was cooled to $0\text{ }^\circ\text{C}$ under an argon atmosphere with stirring for 10 min. Into the flask was added a solution of ethyl 4-nitro benzoate (0.04 mmol) in dry THF under dry

nitrogen, followed by a solution of ethyl 4-(butylamino)benzoate (2.25 mmol) in dry THF dropwise over ~60 min (when reddish color of the reaction mixture disappeared, the next drop of the solution was added) at 0 °C with stirring under dry nitrogen. The mixture was stirred at 0 °C for 2 h, and then the reaction was quenched with sat. NH₄Cl. The whole was extracted with CH₂Cl₂. The organic layer was washed with 1 M NaOH and dried over anhydrous MgSO₄. Concentration in vacuum gave the crude product as a yellow, viscous oil. Elevated temperature polymerization of this monomer was carried out in reflux system under inert atmosphere since this reaction was examined in THF having boiling point at 60 °C. ¹H NMR (CDCl₃) δ (ppm) = 7.7 (m, 1H), 7.0 (m, 1H), 6.7 (m, 1H), 6.5 (m, 1H), 4.5 (m, 2H), 3.8 (m, 2H), 1.6-1.2 (m, 2H), 0.8 (t, 3H). ¹³C NMR (CDCl₃) δ (ppm) = 168.7, 142.8, 137.8, 129.4, 128.9, 127.3, 126.8, 50.7, 31.8, 29.2, 27.4, 27.0, 22.9, 14.3.

Anionic ring-opening polymerization of ε-caprolactam with different activators. Polyamide 6 was prepared in bulk by anionic ring opening polymerization. ε-Caprolactam (CL) (8.35 g, 73.8 mmol) and sodium ε-caprolactamate (C10) (0.23 g, 1.7 mmol) were added in a glass reactor at 140 °C under nitrogen atmosphere. After hexamethylene-1,6-dicarbamoylcaprolactam (C20) (0.5 g, 1.3 mmol) (or 1.3 mmol of ethyl p-toluate; ethyl p-nitrobenzoate; 4-nitrobenzoyl chloride; 4-nitrobenzoyl caprolactam) was added to the molten mixture, the polymerization started. After reaction, the polymer obtained was crushed and refluxed in water and then dried in an oven overnight at 90 °C under vacuum before analysis. Conversion of the monomer was determined gravimetrically. ¹H NMR (CDCl₃) δ (ppm) = 6.0 (s, 1H), 3.1 (m, 2H), 2.0 (m, 2H), 1.25-1.75 (m, 6H). ¹³C NMR (CDCl₃) δ (ppm) = 176.5, 50.55, 40.25, 36.20, 28.09, 25.81, 24.85.

Percent monomer conversion = (polymer weight after extraction / polymer weight before extraction) × 100

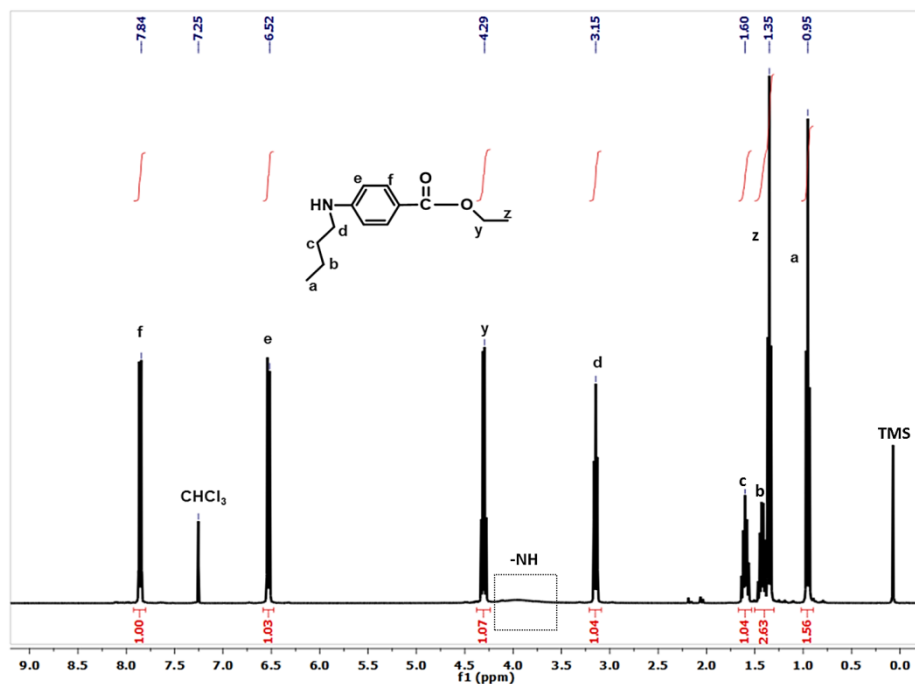
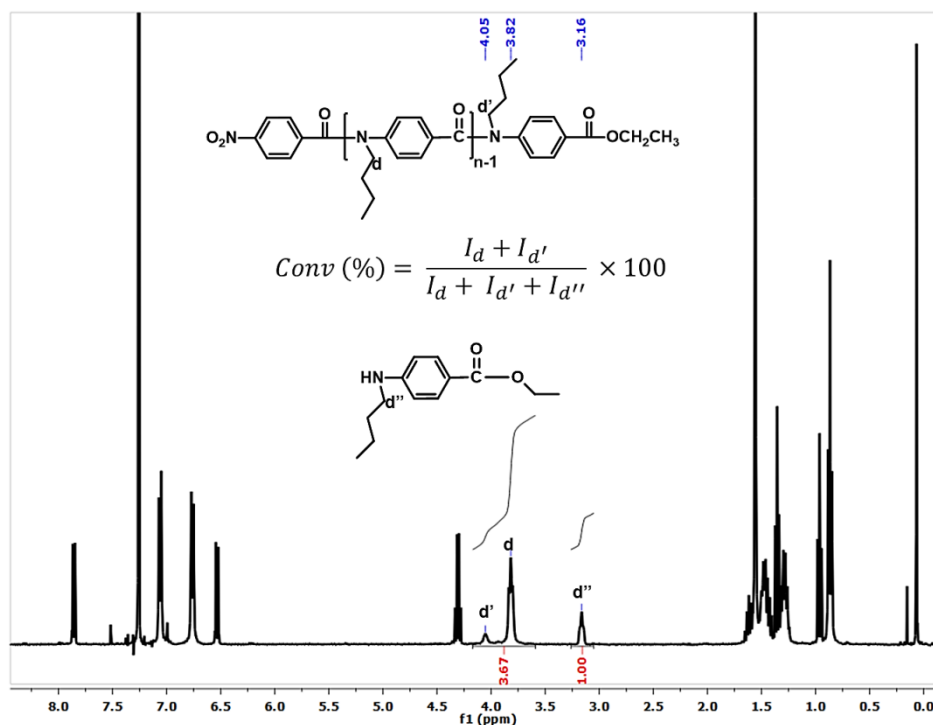
Anionic ring-opening polymerization of ε-caprolactam with different initiators. Polyamide 6 was prepared in bulk by anionic ring opening polymerization. ε-Caprolactam (CL) (8.35 g, 73.8 mmol) and sodium ε-caprolactamate (C10) (0.23 g, 1.7 mmol) (or 1.7 mmol of EtONa; MeONa; tBuOK) were added in a glass reactor at 140 °C under nitrogen atmosphere. After hexamethylene-1,6-dicarbamoylcaprolactam (C20) (0.5 g, 1.3 mmol) was

added to the molten mixture, the polymerization started. After reaction, the polymer obtained was crushed and refluxed in water and then dried in an oven overnight at 90 °C under vacuum before analysis. Conversion of the monomer was determined gravimetrically. ^1H NMR (CDCl_3) d (ppm) = 6.0 (s, 1H), 3.1 (m, 2H), 2.0 (m, 2H), 1.25-1.75 (m, 6H). ^{13}C NMR (CDCl_3) d (ppm) = 176.5, 50.55, 40.25, 36.20, 28.09, 25.81, 24.85.

Percent monomer conversion = (polymer weight after extraction / polymer weight before extraction) \times 100

Copolymerization of ϵ -caprolactam and ethyl 4-butylaminobenzoate (30%Ar-PA6 synthesis). A flask was purged with argon and then charged with THF (dry) and 1.0 M NaHMDS (2.3 ml, 2.30 mmol) in THF were added respectively. The flask was cooled to 0 °C under an argon atmosphere with stirring for 30 minutes. Into the flask ethyl 4-butylaminobenzoate (0.5g, 2.26 mmol) was added. Solution (1) was waited overnight for activation of all monomers. After overnight activation, AROP reactor heated it up to 140 °C under N_2 atmosphere. ϵ -caprolactam (CL) (1.14g, 10.1 mmol) was added with sodium ϵ -caprolactamate (C10) (0.06g, 0.44 mmol) and stirred till all are melted. The solution (1) was added to caprolactam mixture and copolymerization was started by adding of hexamethylene-1,6-dicarbamoylcaprolactam (C20) (0.13g, 0.33 mmol). Reaction was completed in 24h. Obtained copolymer was purified by reflux in THF for removing non-reactive monomers then it was filtered and dried in an oven at 100 °C for 24h. ^1H NMR (CDCl_3) d (ppm) = 7.6 (m, 1H), 6.6 (m, 1H), 6 (m, 1H), 3.07 (m, 4H), 2.06 (m, 2H), 1.45-1.38 (m, 6H), 1.18 (m, 4H), 0.8 (m, 3H). ^{13}C NMR (CDCl_3) d (ppm) = 177.3, 176.4, 151.9, 50.9, 43.7, 39.6, 36.2, 31.2, 30.2, 28.3, 25.8, 25.0, 22.5, 13.5.

Annexe: Supporting Information

Figure IV-S1. ^1H NMR of Ethyl 4-butylaminobenzoate.Figure IV-S2. ^1H NMR in CDCl_3 of crude polymer product after polymerization of ethyl 4-butylaminobenzoate at 0°C . Calculation of the conversion is shown in the inserted formula.

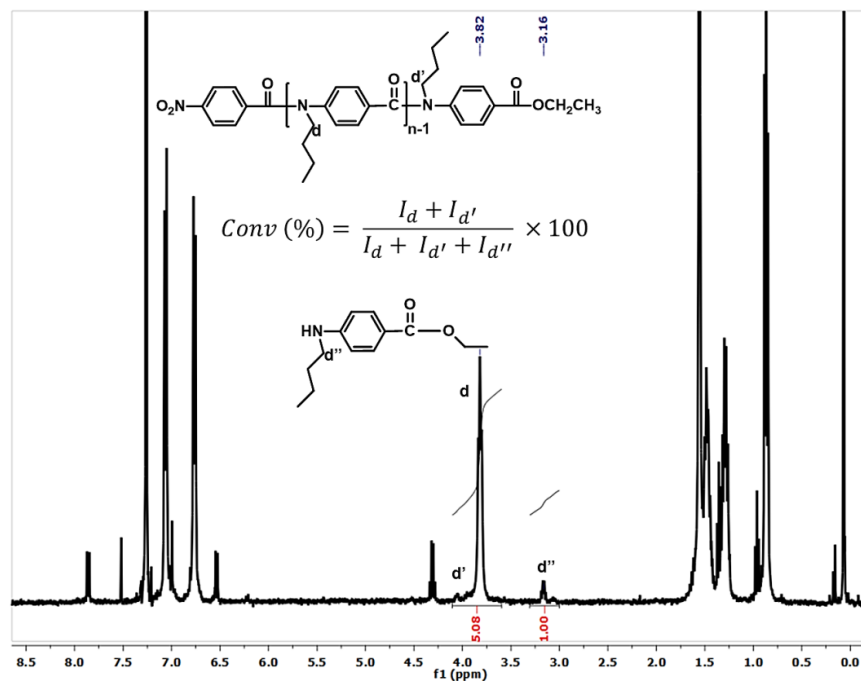


Figure IV-S3. ^1H NMR spectrum in CDCl_3 of crude polymer product after polymerization of ethyl 4-butylaminobenzoate at 25 °C. Calculation of the conversion is shown in the inserted formula.

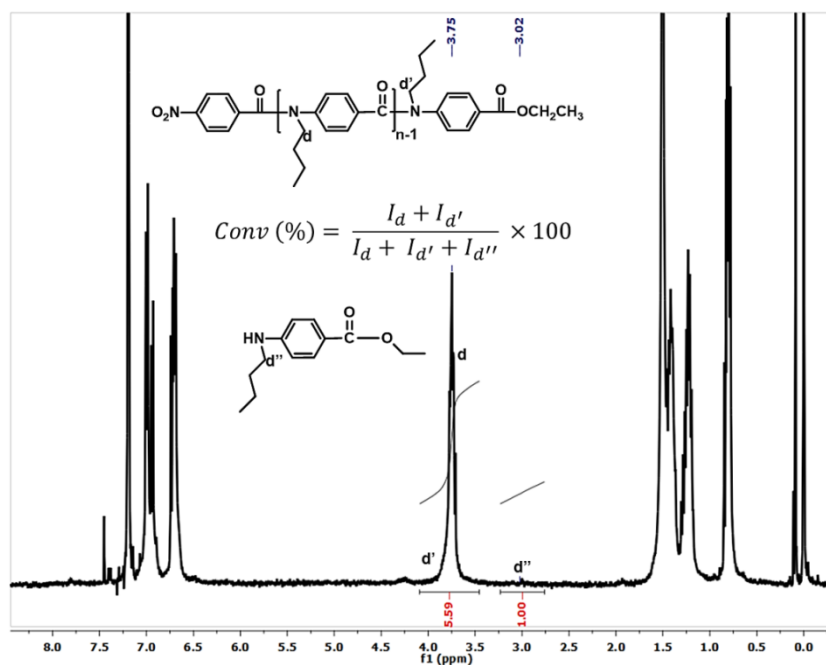


Figure IV-S4. ^1H NMR spectrum in CDCl_3 of crude polymer product after polymerization of ethyl 4-butylaminobenzoate at 50 °C. Calculation of the conversion is shown in the inserted formula.

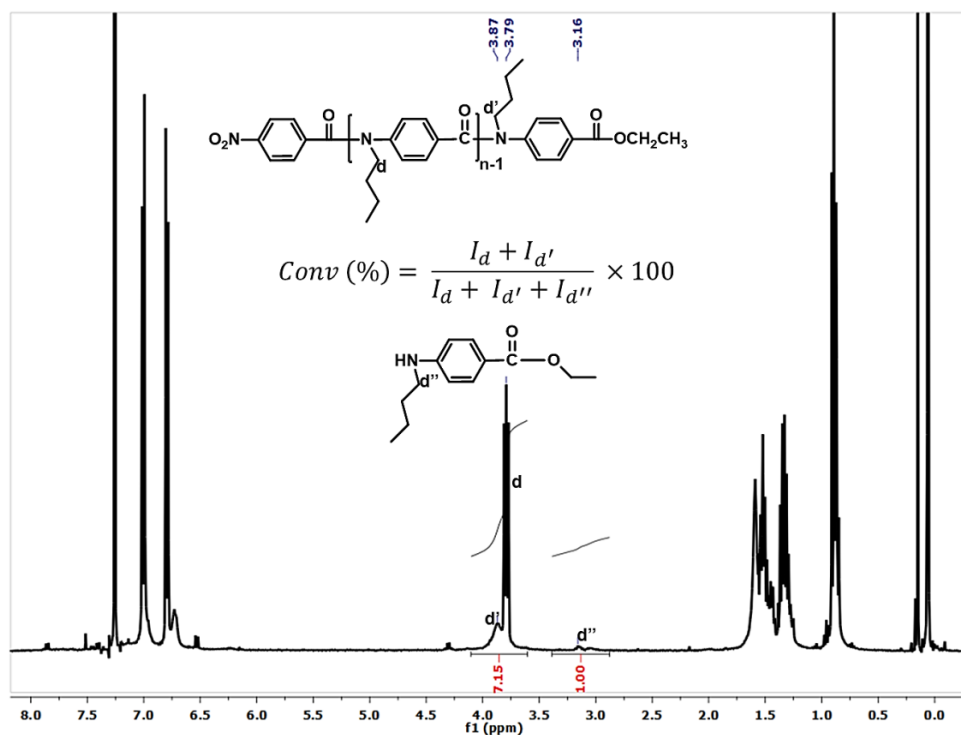


Figure IV-S5. ¹H NMR spectrum in CDCl₃ of crude polymer product after polymerization of ethyl 4-butylaminobenzoate at 100 °C. Calculation of the conversion is shown in the inserted formula.

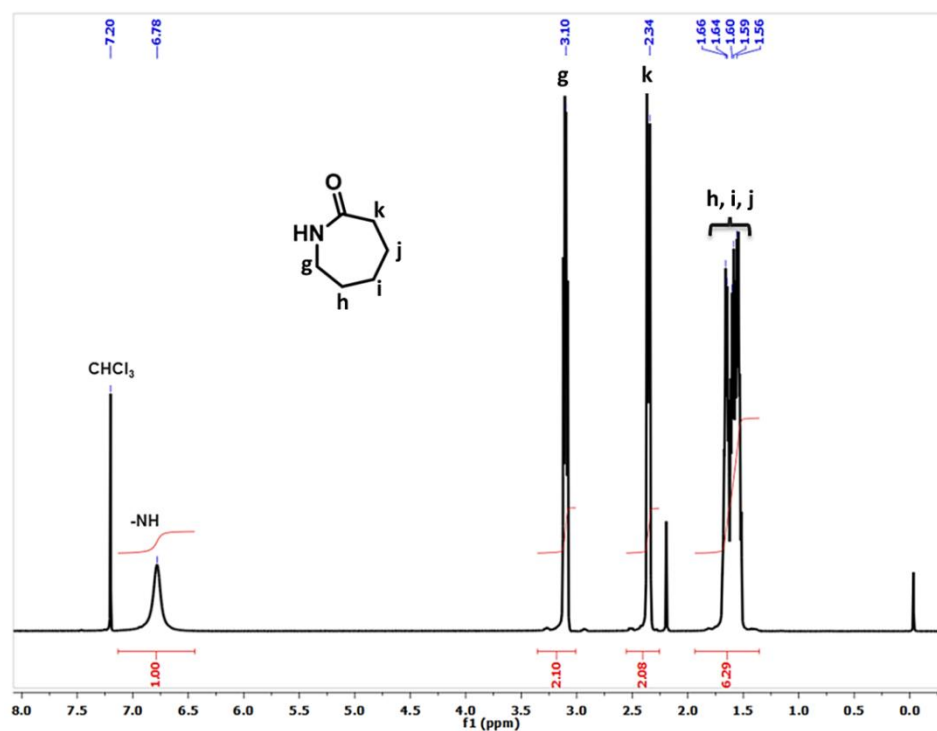


Figure IV-S6. ¹H spectrum NMR of ε-caprolactam (CL).

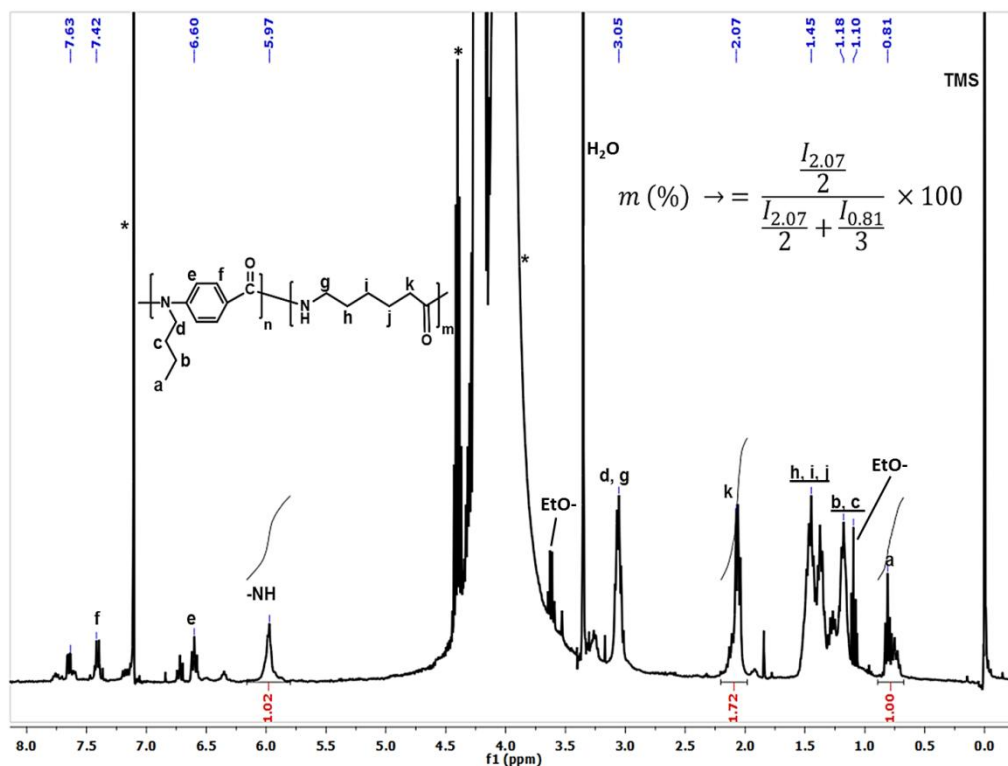


Figure IV-S7. ^1H NMR spectrum of 50%Ar-PA6 in $\text{CDCl}_3/\text{HFIP}$ solution. Peaks with asterisk were originated from solvents (CHCl_3 and HFIP).

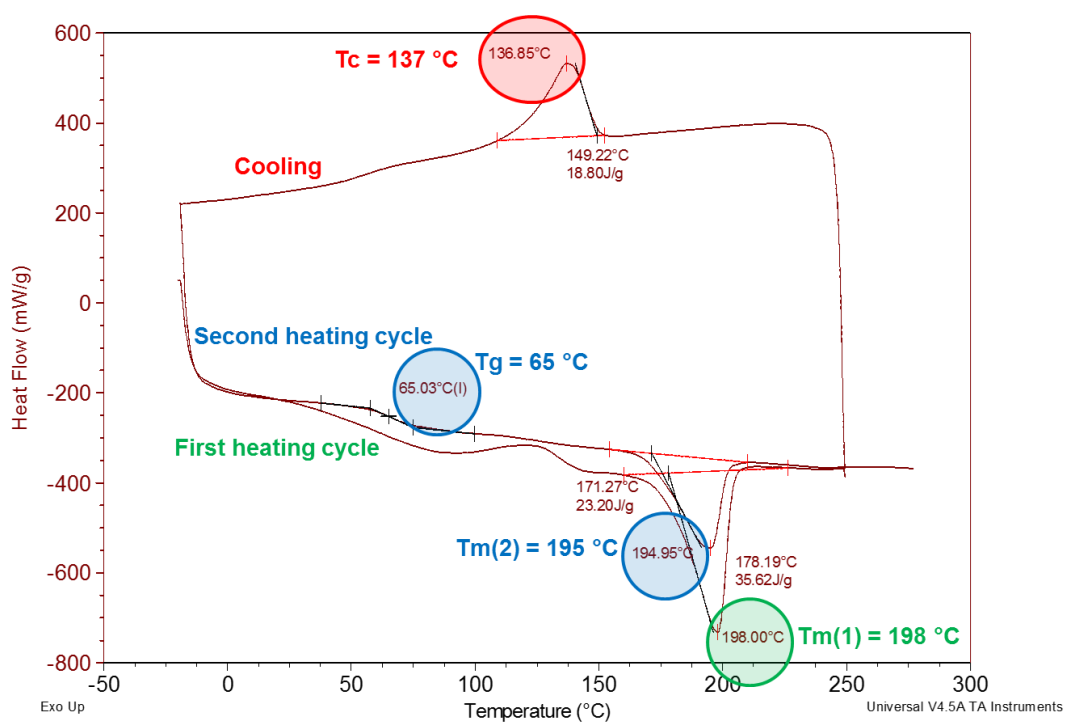


Figure IV-S8. DSC thermogram of 30%Ar-PA6.

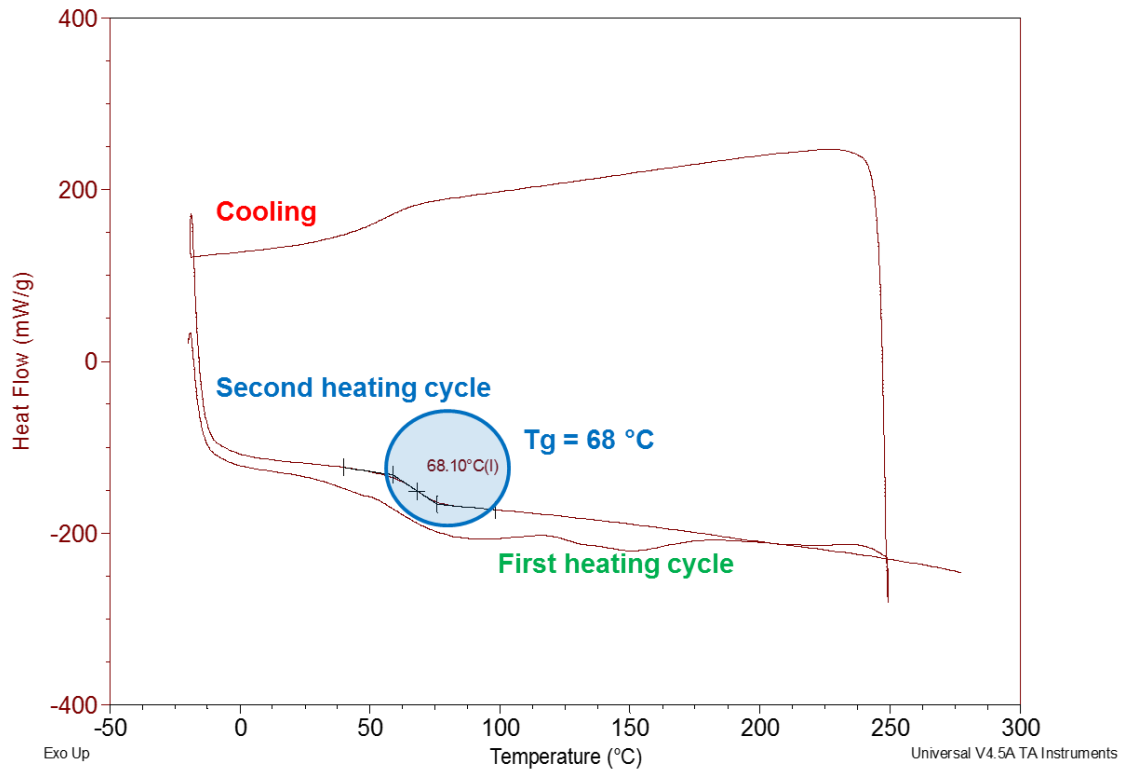


Figure IV-S9. DSC thermogram of 50%Ar-PA6.

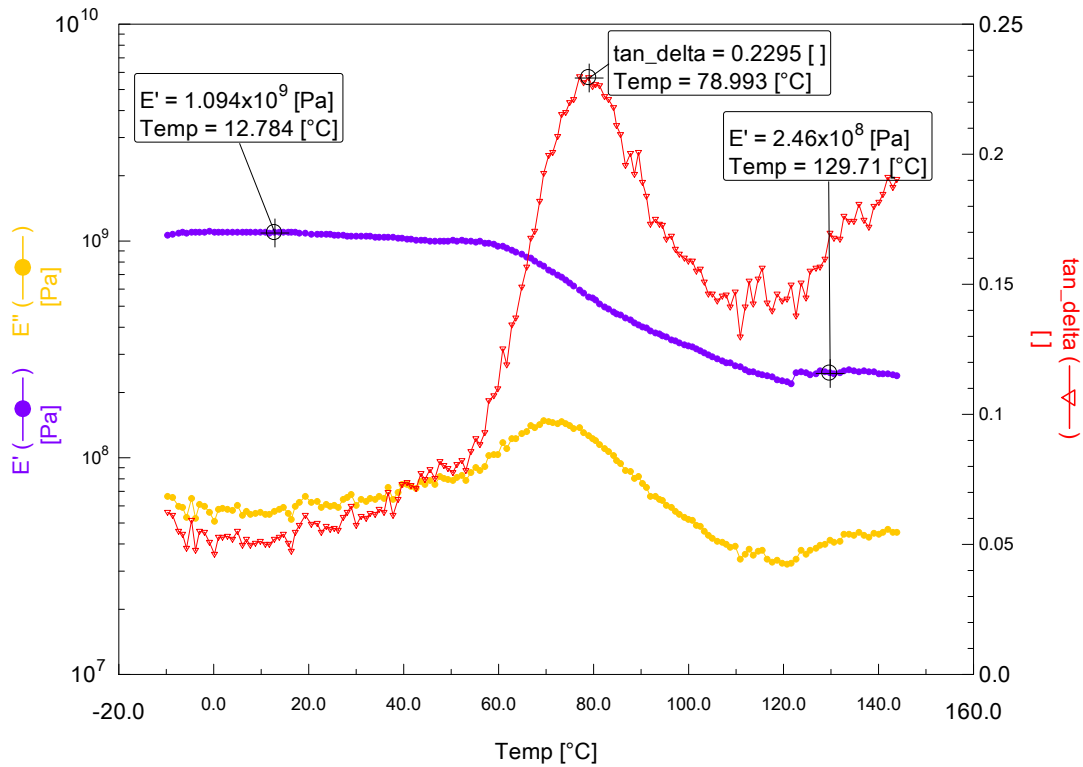


Figure IV-S10. DMA thermogram of 30%Ar-PA6.

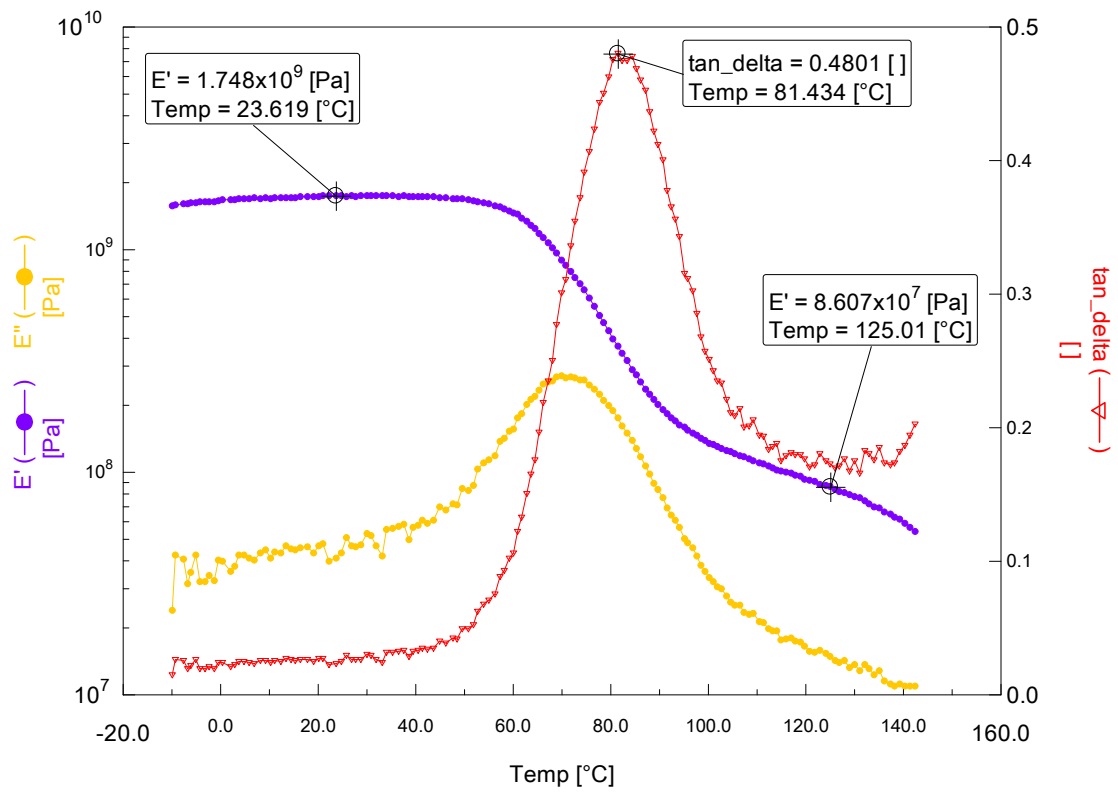


Figure IV-S11. DMA thermogram of 50%Ar-PA6.

References

1. M. Trigo-López, P. Estévez, N. San-José, A. Gómez-Valdemoro, F. C. García, F. Serna, J. L. de la Peña and J. M. García, *Recent Patents on Materials Science*, 2009, **2**, 190-208.
2. K. Marchildon, *Macromolecular Reaction Engineering*, 2011, **5**, 22-54.
3. P. Estévez, H. El-Kaoutit, F. C. García, F. Serna, J. L. de la Peña and J. M. García, *Journal of Polymer Science Part A: Polymer Chemistry*, 2010, **48**, 3823-3833.
4. H.-M. Wang, S.-H. Hsiao, G.-S. Liou and C.-H. Sun, *Journal of Polymer Science Part A: Polymer Chemistry*, 2010, **48**, 4775-4789.
5. H.-J. Yen, S.-M. Guo and G.-S. Liou, *Journal of Polymer Science Part A: Polymer Chemistry*, 2010, **48**, 5271-5281.
6. J. M. García, F. C. García, F. Serna and J. L. de la Peña, in *Handbook of Engineering and Specialty Thermoplastics*, John Wiley & Sons, Inc., 2011, pp. 141-181.
7. R. Puffr and V. Kubánek, *CRC Press, Boca Raton, FL*, 1991, **1**.
8. W. Memeger, *Macromolecules*, 1976, **9**, 195-199.
9. N. Yamazaki, F. Higashi and J. Kawabata, *Journal of Polymer Science: Polymer Chemistry Edition*, 1974, **12**, 2149-2154.
10. N. Yamazaki, M. Niwano, J. Kawabata and F. Higashi, *Tetrahedron*, 1975, **31**, 665-670.
11. N. Yamazaki, M. Matsumoto and F. Higashi, *Journal of Polymer Science: Polymer Chemistry Edition*, 1975, **13**, 1373-1380.
12. J. Preston and W. L. Hofferbert, *Journal of Polymer Science: Polymer Symposia*, 1978, **65**, 13-27.
13. F. Higashi, M. Goto, Y. Nakano and H. Kakinoki, *Journal of Polymer Science: Polymer Chemistry Edition*, 1980, **18**, 851-856.
14. F. Higashi, Y. Nakano, M. Goto and H. Kakinoki, *Journal of Polymer Science: Polymer Chemistry Edition*, 1980, **18**, 1099-1104.
15. F. Higashi and Y. Taguchi, *Journal of Polymer Science: Polymer Chemistry Edition*, 1980, **18**, 2875-2877.
16. W. Kawanobe, K. Yamaguchi, G. Rokicki, S. K. Mei, N. Yamazaki and S. Nakahama, *Journal of Polymer Science: Polymer Chemistry Edition*, 1984, **22**, 2371-2380.
17. R. R. Burch and L. E. Manring, *Macromolecules*, 1991, **24**, 1731-1735.
18. A. Yokoyama and T. Yokozawa, *Macromolecules*, 2007, **40**, 4093-4101.
19. T. Yokozawa and A. Yokoyama, *Progress in Polymer Science*, 2007, **32**, 147-172.
20. Y. Ohta, M. Karasawa, T. Niiyama, A. Yokoyama and T. Yokozawa, *Journal of Polymer Science Part A: Polymer Chemistry*, 2014, **52**, 360-365.
21. Y. Ohta, T. Niiyama, A. Yokoyama and T. Yokozawa, *Journal of Polymer Science Part A: Polymer Chemistry*, 2014, **52**, 1730-1736.
22. T. Ohishi, R. Sugi, A. Yokoyama and T. Yokozawa, *Journal of Polymer Science Part A: Polymer Chemistry*, 2006, **44**, 4990-5003.
23. J. M. García, F. C. García, F. Serna and J. L. de la Peña, *Progress in Polymer Science*, 2010, **35**, 623-686.
24. J. Stehlíček, J. Baldrian, R. Puffr, F. Lednický, J. Dybal and J. Kovářová, *European Polymer Journal*, 1997, **33**, 587-593.
25. R. S. Davé, R. L. Kruse, L. R. Stebbins and K. Udiipi, *Polymer*, 1997, **38**, 939-947.
26. T. Yokozawa, R. Sugi, T. Asai and A. Yokoyama, *Chemistry Letters*, 2004, **33**, 272-273.
27. Y. Ogata and J. Mibae, *The Journal of Organic Chemistry*, 1962, **27**, 2048-2052.

28. H. Sekiguchi, ed. K. J. S. Ivin, T., Elsevier, London, 1984, vol. 2, p. 809.
29. J. Sebenda, in *Comprehensive Polymer Science*, ed. G. B. Allen, J. C., Eds.; Eastmond, G. C.; Ledwith, A.; Russo, S.; Sigwalt, P., Pergamon Press; Oxford, UK, 1989, vol. 3, p. 511.
30. T. T. Konomi, H. , *J Polym Sci A-1*, 1971, **9**, 329.
31. K. Hashimoto, J. Yasuda and M. Kobayashi, *Journal of Polymer Science Part A: Polymer Chemistry*, 1999, **37**, 909-915.
32. K. Ueda, M. Hosoda, T. Matsuda and K. Tai, *Polym J*, 1998, **30**, 186-191.
33. C.-F. Huang, Y. Ohta, A. Yokoyama and T. Yokozawa, *Macromolecules*, 2011, **44**, 4140-4148.
34. H. Jia, A. Wildes and S. Titmuss, *Macromolecules*, 2011, **45**, 305-312.
35. Y. Ohta, Y. Kamijyo, S. Fujii, A. Yokoyama and T. Yokozawa, *Macromolecules*, 2011, **44**, 5112-5122.

*General Conclusion and
Perspectives*

General Conclusion and Perspectives

The first goal of this thesis was to demonstrate feasibility of different approaches throughout the synthesis of functionalized polyamide 6 exhibiting not only for improving current polyamide 6 characteristics but to shed light on future investigations as well.

In order to overcome the challenge for derivatizing of polyamide 6 by anionic ring-opening polymerization, we developed anionic ring-opening copolymerization of ϵ -caprolactam and α -amino- ϵ -caprolactam based comonomers with different attached groups. In the meantime, we merged this challenging anionic ring-opening polymerization of ϵ -caprolactam with chain-growth condensation polymerization of benzamide to gain aromatic-aliphatic polyamide, which was not possible with lactam polymerization so far, differently from conventional techniques such as polycondensation reaction.

As early mentioned in the introduction, even though polyamide 6 has attractive properties it needs improvements in thermal stability and hydrophobicity properties as we consider where mostly PA6 is used such as automotive and wind industry as a composite material.

In first part of the thesis, we focused on the set-up to introduce fluorinated groups into PA6 by AROP. One objective is to improve surface hydrophobicity of the PA6. Fluorinated derivative of α -amino- ϵ -caprolactam and caprolactam anionic ring-opening copolymerization was proposed to this issue. Obtained copolyamides showed expected increasing on their surface hydrophobicity according to contact angle measurements. However, the surface hydrophobicity improvement was limited with restricted amount of fluorinated units in the polyamide chains since increasing fluorinated comonomer amount consumed more initiator (sodium ϵ -caprolactamate) and slowed down the copolymerization. In spite of limited comonomer addition, obtained fluorinated polyamides revealed improved thermal stability owing to fluorine atoms presence in the polymer chain and their involving to the thermal degradation.

Another approach was the synthesis of reversible and irreversible crosslinked polyamide 6. Derivatives of α -amino- ϵ -caprolactam were also envisaged for this purpose. The first method was based on the synthesis of a bis-monomer from α -amino- ϵ -caprolactam and using it as a crosslinking agent. This method of crosslinking provided controlling of crystallinity and swelling which were shown to decrease with increasing content of

crosslinking agent. In further investigation, the production of controlled crosslinking by anionic bulk copolymerization of CL and N-functionalized α -amino- ϵ -caprolactam bis-monomers at low feed ratio, i.e. up to 2.8 mol%, was discussed in term of rate of polymerization (decreasing with increasing amount of crosslinker), thermal and rheological properties for an eventual processability in bulk at 140 °C.

The second crosslinking method was based on reversible crosslinking of polyamide 6 via thermo/photoresponsive groups, i.e. cinnamoyl functions. First, amidation reaction of cinnamoyl chloride and α -amino- ϵ -caprolactam was carried out. Then, copolymerization of obtained α -cinnamoylamido- ϵ -caprolactam with ϵ -caprolactam was examined in different quantities of (co)monomers. Since the anionic polymerization of ϵ -caprolactam requires high reaction temperature and cinnamoyl unit is thermoresponsive, crosslinking occurred during the copolymerization reaction. Crosslinked polyamide 6 were characterized by magic angle spinning NMR and their thermal stability was studied by thermo gravimetric analysis and differential scanning calorimetry. Thermal analysis of crosslinked polyamide 6 demonstrated higher thermal stability and glass transition temperature than neat polyamide 6. The decrosslinking was shown to occur in solution by UV irradiation between 200-280 nm. Re-crosslinking was then obtained by UV irradiation between 325-380 nm in solid state.

Reversible crosslinking approach can be attractive for self-healing and/or shape memory systems of PA6 since such kind of thermo or photo- responsive system has a potential as novel material in the stimuli or environmentally responsive (smart) materials.

Last part of this thesis was dedicated to demonstrate combination possibility of two challenging chemistries in one-step reaction; chain-growth condensation polymerization of ethyl 4-butylaminobenzoate and anionic ring-opening polymerization of ϵ -caprolactam. This approach has also provide for objective to new thermal and mechanical properties of PA6 by introducing aromatic units. Glass transition temperature of resulting polyamide was shifted from 53 °C to 68 °C. In the meantime, thermal stability was slightly increased. Crystallinity of aliphatic/aromatic random copolyamide was reduced by increasing aromatic repeating units bearing alkyl groups in polymer chains which restrict molecular packing and intermolecular hydrogen bonding. Coming study of this work will be to remove alkyl pendant groups via washing with trifluoroacetic acid after copolymerization in order to increase the crystallinity of aliphatic/aromatic random copolymers.

This thesis work was exploratory trying to open new methodologies. Researching areas were in very broad range and basically depending on improving and modifying current PA6 properties. Future work in line with BASF may focus on the processability of these achieved PA6 based copolymers in industrial level. Main parameters are slow polymerization rates, water uptake, and low conversions. These parameters will guide the selection and development of some systems and approaches.

Titre : Synthèse de polyamide 6 fonctionnalisés par polymérisation anionique par ouverture de cycle

Résumé : Les études présentées dans le cadre de cette thèse visent à copolymériser l' ϵ -caprolactame (CL) avec différents dérivés de l' α -amino- ϵ -caprolactame (qui possèdent une amine primaire fonctionnalisable) par polymérisation anionique par ouverture de cycle. En utilisant cette stratégie, nous décrivons; (i) la préparation de polyamides 6 fluorés thermiquement plus stables, et ayant une surface hydrophobe; (ii) la synthèse de polyamides 6 portant des groupes pendants cinnamoyl thermo et photosensibles. Une réticulation réversible est observée ainsi que l'amélioration des propriétés thermo-mécaniques; (iii) la copolymérisation anionique par ouverture de cycle de CL avec un bis-monomère issu de l' α -amino- ϵ -caprolactame comme contrôle de la réticulation du polyamide 6. Enfin, dans le cadre de notre intérêt continu pour la chimie du polyamide 6, nous avons mis en évidence la possible combinaison de la polymérisation anionique par ouverture de cycle de CL avec la polycondensation en chaîne de l'éthyl-4-butylaminobenzoate pour obtenir en une étape un polyamide aliphatique/aromatique.

Mots clés : polyamides, polyamide 6, ϵ -caprolactame, α -amino- ϵ -caprolactame, polymérisation anionique par ouverture de cycle, polycondensation en chaîne, polyamide aromatique, groupes cinnamoyl, polymères fluorés.

Title : Synthesis of functionalized polyamide 6 by anionic ring-opening polymerization

Abstract : The studies presented in this thesis aim to copolymerize ϵ -caprolactam (CL) with different derivatives of α -amino- ϵ -caprolactam (which has a functionalizable primary amine) via anionic ring-opening polymerization. By using this strategy, we describe: (i) the synthesis of thermally more stable fluorinated polyamide 6 having a hydrophobic surface; (ii) the synthesis of polyamides 6 bearing pendant cinnamoyl groups, which are thermo- and photoresponsive chromophore groups, and demonstrating their reversible crosslinking as well as improved thermo-mechanical properties; (iii) the copolymerization of CL with a crosslinker (*N*-functionalized α -amino- ϵ -caprolactam bis-monomers) into crosslinked polyamides 6. As part of our continuing interest in polyamide 6 chemistry, we developed the combination of anionic ring-opening polymerization of CL and chain-growth condensation polymerization of ethyl 4-butylaminobenzoate in order to obtain aliphatic/aromatic polyamides in one-step.

Keywords : polyamides, polyamide 6, ϵ -caprolactam, α -amino- ϵ -caprolactam, anionic ring-opening polymerization, chain-growth condensation polymerization, aromatic polyamide, cinnamoyl groups, fluorinated polymers.

Laboratoire de Chimie des Polymères
Organiques
16 avenue PeyBerland
F-33607 Pessac



Center for Education and Research on
Macromolecules
B-4000 Liège
Belgium

